MODEL BASED AND PARAMETRIC CONTROL FOR DRUG DELIVERY SYSTEMS

by

Pinky Dua

A Thesis submitted for the degree of Doctor of Philosophy of the University of London and for the Diploma of Membership of the Imperial College

Centre for Process Systems Engineering
Department of Chemical Engineering
Imperial College London

April 2005



ABSTRACT

Automation of drug delivery systems can significantly reduce the negative impact of side effects associated with therapy, minimize human intervention and thus improve the living standard of a patient. Automatic control techniques rely on developing a mathematical model of the patient which should be detailed enough to capture and reproduce the complex pharmacokinetic and pharmacodynamic effects of the drug, but on the other hand simple enough to design a controller for the optimal delivery of the drugs. In this work, models and model based control strategies for drug delivery systems are presented. Specific examples of drug delivery systems considered are insulin delivery for type 1 diabetes, automation in anesthesia and delivery of chemotherapeutic agents in cancer.

For people with type 1 diabetes, a model based parametric controller is derived that provides the optimal insulin delivery rate as an explicit function of the state of the patient. This is achieved by using parametric programming techniques. The key feature of the parametric controller is that it can simultaneously take into account the model of the patient and constraints on insulin delivery rate and state of the patient and yet can be implemented on a simple hardware. This is expected to provide significant improvement and advances in the development of portable insulin delivery devices and enhance patient safety and comfort levels. The implementation of the parametric controller via a microchip is demonstrated on a pilot plant reactor. A multi-objective controller that can take into account physician's performance criteria is also designed. The key issue here is that negative deviations from a target blood glucose level are more harmful to a patient's health than the positive deviations. This issue is addressed by formulating an asymmetric control objective function and by incorporating prioritization of constraints in a multi-objective control framework.

For people being operated under anesthesia, a compartmental model based upon the distribution of three drugs, isoflurane, sodium nitroprusside (SNP) and dopamine (DP), in the human body is presented. Based upon this model a detailed analysis of the effect of

these drugs on the key state variables of the patient is also presented. The model is then used for the simultaneous regulation of mean arterial pressure, cardiac output and unconsciousness of the patient. The importance of tight regulation of these variables is highlighted. Model based controllers are designed and their performance is analyzed. The developments reported in this work are expected to provide flexibility to the anesthesiologist to focus on critical issues, reduce drug overdose, result in patients spending less time in post-operative care unit and improve the safety of the patient.

For delivery of chemotherapeutic agents for cancer patients, optimal delivery schedules are derived. Two models are used for this purpose. The first model is based upon cell cycle non-specific drug whereas the second one considers cell cycle specific drug. The two models also differ in the way the tumour growth kinetics and toxicity to normal tissue are modelled. The optimal chemotherapy schedule obtained for the first model suggests a low drug administration in the initial period and infusing most of the drug towards the end of the therapy. The chemotherapy protocol for the second model suggests large doses of the drug at the beginning and end of the treatment period. The first problem is formulated and solved as a mixed integer dynamic optimization problem where integer variable is introduced to model the discontinuity in the cell loss term. Drug resistance is modelled via multiple time constraints. A dynamic optimization strategy is proposed for the solution of the second problem. The results depicting the variations in the tumour and normal cells are also analyzed extensively.

Acknowledgments

First and foremost, I would like to thank my supervisor Professor Stratos Pistikopoulos for encouraging me to work in a new, interesting and challenging field of drug delivery systems. His guidance, motivation, innovative ideas and above all enthusiasm have not only been instrumental in the successful completion of the project but have played a key role in shaping me as a researcher. I especially thank him for providing me with a platform where I had the freedom and opportunity to interact with researchers from various universities and companies. I would also like to express my gratitude to Professor Frank Doyle for his invaluable advice and guidance throughout the duration of the project. His thoughtful suggestions and comments have always inspired me.

Financial support from the Overseas Research Student Award Scheme (ORS) and the Industrial Consortium of the Centre for Process Systems Engineering is gratefully acknowledged.

Fruitful collaborations with MSc and undergraduate students, Alex Muller, Sofia Chrysafi, Anna-Maria Papageorgiou, David Damming, Jaidip Patel, Ali Jetha and Jimmy Lawal, were very helpful in the completion of the project.

Many thanks to Nikos Bozinis and Vassilis Sakizlis for interesting discussions and also for being a great source of help throughout the project. I would also like to thank Professor Lester Kershenbaum and Dr. Gary Frost for many useful suggestions. Technical and administrative support from Graham Stuart, Terrance Crombie, Malcolm Dix, Elios Jorisi, Senait Selassie is also gratefully acknowledged.

I would also like to thank all my friends and colleagues for their help and support throughout the course of the study and making the time more enjoyable. My sincere and special thanks go to Myrian Schenk who has always been a good friend and advisor in every possible way.

Last but not the least, this project would not have been realizable without the tremendous support from my family members. I would like to thank my parents and my sister for their encouragement, love, understanding and always being there for me. I sincerely thank my parents for always encouraging me to pursue higher studies. Above all, I would like to thank my husband, Vivek, for his constant love, understanding, support, guidance and motivation – without you this would not have been possible – thanks for being there.

Dedicated to my Parents
&
my lovely sister

TABLE OF CONTENTS

LIST OF TABLES xi

LIST OF FIGURES xii

1 INTRODUCTION AND PROJECT OBJECTIVES 1

1.1 Introduction 1

1.2 Project Objectives 2

1.2.1 Parametric and multi-objective control of insulin delivery for people with type 1 diabetes 3

1.2.2 Modelling and control strategies for surgery under anesthesia 3

1.2.3 Strategies for delivery of chemotherapeutic agents for cancer 4

1.2.4 Parametric control of a pilot plant reactor 5

2 LITERATURE REVIEW 7

2.1 Introduction 7

2.2 Modelling of Drug Delivery Systems 7

2.2.1 Common routes of drug administration 7

2.2.2 Pharmacokinetic modelling 8

2.2.3 Pharmacodynamic modelling 15

2.3 Modelling and Control of Diabetes 16

2.3.1 Modelling of diabetes 16

2.3.2 Control of diabetes 19

2.4 Surgery under Anesthesia 23

2.4.1 Modelling of anesthesia 24

2.4.2 Regulation of hemodynamic variables 25

2.4.3 Simultaneous regulation of hemodynamic variables and other states of anesthesia 28

2.5 Delivery of Chemotherapeutic Agents in Cancer 30

2.5.1 Cell cycle non-specific models 31

2.5.2 Cell cycle specific models 33

2.6 Parametric Programming and Control 35
2.6.1 Parametric programming 35
2.6.2 Model based and parametric control 38
Concluding Remarks 40

I CONTROL OF BLOOD GLUCOSE CONCENTRATION FOR PEOPLE WITH TYPE 1 DIABETES 41

3 BLOOD GLUCOSE CONTROL FOR TYPE 1 DIABETES 42
3.1 Introduction 42
3.2 Blood Glucose Control in the Normal Body 43
3.3 Introduction to Diabetes 45
3.3.1 Insulin 48
3.3.2 Routes of insulin delivery 49
3.3.3 Insulin delivery devices 49
3.3.4 Sensors for the measurement of blood glucose concentration 51
3.3.5 Closed loop glucose control 52
3.4 Model Predictive Control (MPC) 53
3.5 Parametric Programming and Control 55
3.6 Explicit Insulin Delivery Rate 57
3.6.1 Bergman model 58
3.6.2 Parametric controller for blood glucose regulation 59
3.7 Inter- and Intra-Patient Variability 67
Concluding Remarks 74

4 MULTI-OBJECTIVE CONTROL FOR TYPE 1 DIABETES 75
4.1 Introduction 75
4.2 Asymmetric Objective Function 76
4.3 Constraint Prioritization 80
Concluding Remarks 86

II DELIVERY OF DRUGS FOR SURGERY UNDER ANESTHESIA AND OPTIMAL CONTROL OF CANCER **88**

5 SURGERY UNDER ANESTHESIA **89**

5.1 Introduction 89

5.1.1 An introduction to anesthesia 91

5.1.2 Automation in anesthesia 97

5.2 Modelling Anesthesia 99

5.2.1 Pharmacokinetic modelling 100

5.2.2 Pharmacodynamic modelling 103

5.2.3 Baroreflex 109

5.3 Model Validation 109

5.4 Control of Anesthesia 116

5.5 Results 117

Concluding Remarks 120

6 OPTIMAL CONTROL OF CANCER **121**

6.1 Introduction 121

6.1.1 Chemotherapy for the treatment of cancer 122

6.1.2 Effectiveness of chemotherapy 126

6.1.3 Chemotherapeutic drugs 127

6.1.4 Problems related to chemotherapy 128

6.2 General Approaches to Modelling Cancer Chemotherapy 128

6.2.1 Tumour growth 128

6.2.2 Drug distribution and effect 131

6.3 Model Formulation 131

6.3.1 Cell cycle non-specific model 132

6.3.2 Cell cycle specific model 135

6.4 Simulation Results 138

6.4.1 Cell cycle non-specific model 138

6.4.2 Cell cycle specific model 140
6.5 Optimal Control for Cancer Chemotherapy 142
6.5.1 Cell cycle non-specific model 142
6.5.2 Cell cycle specific model 145
6.6 Optimization Results 147
6.6.1 Cell cycle non-specific model 147
6.6.2 Cell cycle specific model 150
Concluding Remarks 154

7 CONCLUSIONS AND FUTURE DIRECTIONS 156
7.1 Summary of Key Contributions 156
7.1.1 Blood glucose control for type 1 diabetes 156
7.1.2 Surgery under anesthesia 157
7.1.3 Delivery of chemotherapeutic agents in cancer 158
7.2 Key Contributions 160
7.3 Recommendations for Future Research Developments 161
7.3.1 Blood glucose control for diabetes 161
7.3.2 Surgery under anesthesia 163
7.3.3 Delivery of chemotherapeutic agents in cancer 165
7.3.4 Other drug delivery systems 165

PUBLICATION FROM THIS THESIS 167

REFERENCES 170

APPENDICES

A CLOSED LOOP BLOOD GLUCOSE CONTROL 185
A.1 Introduction 185
A.2 Insulin Pumps 185
A.3 Sensors for Blood Glucose Measurement 188

A.3.1 Medtronic MiniMed 188
A.3.2 Animas Corporation 192
A.3.3 Pendragon 192
A.3.4 Cygnus 193
A.4 Implementation of the Parametric Controller 194
A.4.1 FM400 chip 196
A.4.2 Experimental set-up 196
A.5 Performance of the Controller 198
Concluding Remarks 198

B ANALYSIS OF THE DETAILED MODEL FOR DIABETES 200
B.1 Introduction 200
B.2 Mathematical Modelling 201
B.2.1 Glucose submodel 202
B.2.2 Insulin submodel 205
B.3 Model Simulation and Analysis 207
Concluding Remarks 211

C PILOT PLANT PARSEX REACTOR 214
C.1 Introduction 214
C.2 Derivation of the Explicit Model Based Control Law 218
C.3 Results 219
C.4 Implementation of the Parametric Controller 220
Concluding Remarks 222

D MULTIPARAMETRIC QUADRATIC PROGRAMMING 223

E MULTIPARAMETRIC MIXED-INTEGER LINEAR PROGRAMMING 226

LIST OF TABLES

3.1 Hormones produced in the pancreas 44

3.2 Insulin preparations 50

4.1 Objectives and Priorities 83

5.1 Relation between BIS and Clinical Endpoints 93

5.2 Common Inhalation Anesthetics 94

5.3 Common Intravenous Anesthetics 96

5.4 Model Parameters 110

6.1 Parameter values for the cell cycle non-specific model 135

6.2 Parameter values for the cell cycle specific model (Breast cancer data) 138

6.3 Parameter values for the cell cycle specific model 148

B.1 Nomenclature 212

C.1 Startup and Shutdown Procedure 217

D.1 Solution Steps of the mp-QP Algorithm 225

E.1 Solution Steps of the mp-MILP Algorithm 228

LIST OF FIGURES

2.1 Drug Concentration and Effect Profiles 8

2.2 One Compartmental Model 10

2.3 Two Compartmental Model 11

2.4 Catenary Compartmental Model 12

2.5 Mammillary Compartmental Model 12

2.6 Physiological Based Model 14

2.7 An organ compartment consisting of the blood part and the tissue part 14

2.8 Drug Effect vs. Concentration 15

2.9 Parametric Programming: Optimization variables as a function of parameters 37

2.10 Model Based Control 39

2.11 On-line Optimization 39

2.12 On-line Optimization via Off-line Parametric Optimization 40

3.1 (a) Location of the pancreas in the human body and (b) the pancreas 43

3.2 Secretion of the hormones form the pancreatic islet cells into the blood vessel 44

3.3 Blood glucose control via interplay between insulin and glucagon 45

3.4 Structure of insulin 48

3.5 Closed Loop System for Blood Glucose Control 52

3.6 Model Predictive Control of Blood Glucose Concentration 55

3.7 Model Predictive Control of Blood Glucose Concentration via Parametric Programming 57

3.8 Schematic representation of Bergman minimal model 58

3.9 Critical regions for G=36. The trajectory depicts the values of I and X for a meal disturbance of 20 g and the corresponding insulin infusion rate shown in Figure 3.13 for Q/R=1000 62

3.10 Critical regions for I=-5. The trajectory depicts the values of G and X for a meal disturbance of 20 g and the corresponding insulin infusion rate shown in Figure 3.13 for Q/R=1000 62

3.11 Critical regions for X=0.02. The trajectory depicts the values of G and I for a meal disturbance of 20 g and the corresponding insulin infusion rate shown in Figure 3.13 for Q/R=1000 63

3.12 Glucose concentration profiles for Fisher meal disturbances of 20 g, 50 g and 40 g and for Q/R equal to 10 (red line), 100 (green line) and 1000 (blue line) 64

3.13 Insulin infusion rate profiles for Fisher meal disturbances of 20 g, 50 g and 40 g and for Q/R equal to 10 (red line), 100 (green line) and 1000 (blue line) 64

3.14 Rate of Gastric Emptying as a Function of Time 65

3.15 Glucose concentration profile for 20 g Lehmann and Deutsch meal disturbance and for Q/R = 1000 66

3.16 Insulin infusion profile for 20 g Lehmann and Deutsch meal disturbance and for Q/R = 1000 66

3.17 Critical regions of G=36: feasible case. The trajectory depicts the values of I and X for a meal disturbance of 25 g and the insulin infusion rate corresponding to the feasible control law obtained for A and B given in (3.12) 69

3.18 Critical regions for I=-5: feasible case. The trajectory depicts the values of G and X for a meal disturbance of 25 g and the insulin infusion rate corresponding to the feasible control law obtained for A and B given in (3.12) 70

3.19 Critical regions for X=0.02: feasible case. The trajectory depicts the values of G and I for a meal disturbance of 25 g and the insulin infusion rate corresponding to the feasible control law obtained for A and B given in (3.12) 70

3.20 Critical regions of G=36: nominal case. The trajectory depicts the values of I and X for a meal disturbance of 25 g and the insulin infusion rate corresponding to the nominal control law obtained for A and B given in (3.10) and for $54 \leq G+G_b \leq 270$ 71

3.21 Critical regions of I=-5: nominal case. The trajectory depicts the values of G and X for a meal disturbance of 25 g and the insulin infusion rate corresponding to the nominal control law obtained for A and B given in (3.10) and for $54 \leq G+G_b \leq 270$ 71

3.22 Critical regions of X=0.02: nominal case. The trajectory depicts the values of G and I for a meal disturbance of 25 g and the insulin infusion rate corresponding to the nominal control law obtained for A and B given in (3.10) and for $54 \leq G+G_b \leq 270$ 72

3.23 Comparison of the feasible and the nominal control law. Feasible control law (blue line) ensures that the constraint $54 \leq G+G_b$ is not violated whereas the state of hypoglycaemia is reached for the nominal control law (red line) 72

3.24 Performance of feasible control law: Glucose concentration profiles for Fisher meal disturbances of 20 g, 50 g and 40 g, Q/R=10 and for various values of uncertainty in the model parameters 73

3.25 Performance of feasible control law: Insulin infusion rate profile for Fisher meal disturbances of 20 g, 50 g and 40 g, Q/R=10 and for various values of uncertainty in the model parameters 73

4.1 Sinusoidal Disturbance 79

4.2 Glucose concentration profile for a Symmetric Objective Function 80

4.3 Glucose concentration profile for Asymmetric Objective Function 81

4.4 Glucose concentration profile for Prioritized Constraints 84

4.5 Profile of 0-1 Objective Variables, O_1 to O_5 84

4.6 Profile of 0-1 Objective Variables, O_6 to O_9 85

4.7 Profile of 0-1 Priority Variables P_1 to P_5 85

4.8 Profile of 0-1 Priority Variables P_6 to P_9 86

5.1 Demonstration of Pain Relief via Anesthetics in Ancient Times 90

5.2 Anesthesiologist in Modern Operation Theatre 90

5.3 Triad of Anesthesia 92

5.4 Anesthesia Control System 98

5.5 Compartmental Model 99

5.6 Electrical analogy of the circulatory system and its application in this study 107

5.7 MAP response to an uptake of 1% vol. of isoflurane 111

5.8 BIS response to an uptake of 1% vol. of isoflurane 111

5.9 BIS response to an uptake of 0.5% vol. of isoflurane 112

5.10 DP infusion in response to a drop in MAP 112
5.11 MAP response to a continuous injection of 1 μg/kg/min of SNP after 10 minutes 113
5.12 MAP response to a continuous injection of 10 μg/kg/min of SNP after 10 minutes 113
5.13 Simulation of the regulation of MAP during anesthesia 114
5.14 Simulation of the regulation of BIS during anesthesia 115
5.15 Profile of BIS for linear and nonlinear models over time 117
5.16 Profile of MAP for linear and nonlinear models over time 118
5.17 MPC performance for anesthesia for a set point of $[20\ -10\ 1]^T$ deviation from the nominal point 119
5.18 Parametric controller: State Profiles 120
6.1 Stages of carcinogenesis 122
6.2 The cell cycle 124
6.3 Functional compartments within tumours 125
6.4 Tumour growth equations 131
6.5 Two compartment model 136
6.6 The evolution with time of tumour cell population, when the maximum dose of the drug is administered at the beginning of the therapy 139
6.7 The evolution with time of tumour cell population, when the maximum dose of the drug is administered towards the end of the therapy 140
6.8 The evolution with time of proliferating cell population, when two doses of the drug are administered 141
6.9 The evolution with time of resting cell population, when two doses of the drug are administered 141
6.10 The evolution with time of normal cell population, when two doses of the drug are administered 141
6.11 Optimal chemotherapy protocol for the cell cycle non-specific case 148
6.12 Predicted tumour growth using the optimal treatment protocol 149
6.13 Detailed predicted tumour growth using the optimal treatment protocol 149
6.14 Drug concentration profile that corresponds to the optimal treatment protocol 150

6.15 Optimal chemotherapy protocol for the cell cycle specific case 151
6.16 Predicted tumour growth using the optimal treatment protocol-Objective Function (proliferating and resting cells) 152
6.17 Predicted growth of the normal cell population using the optimal treatment protocol 152
6.18 Predicted growth of the proliferating compartment using the optimal treatment protocol 153
6.19 Predicted growth of the resting compartment using the optimal treatment protocol 153
6.20 Drug concentration profile that corresponds to the optimal treatment protocol 154

A.1 Closed loop control system 186
A.2 Different insulin pump models 187
A.3 CGMS sensor 188
A.4 Mechanism of the CGMS 189
A.5 CGMS monitor 189
A.6 Blood Glucose Concentration obtained by CGMS 190
A.7 Guardian System 191
A.8 Sensor Augmented System 191
A.9 Pendra Sensor 193
A.10 Impedence Spectroscopy principle of the Pendra Sensor 193
A.11 Cygnus GlucoWatch 194
A.12 Cygnus GlucoWatch Mechanism 194
A.13 Sensor Electrode Configuration 195
A.14 FM400 Chip 196
A.15 Calibration Curve for Blood Glucose Deviation 197
A.16 Experimental Set-up 197
A.17 Controller Performance 198
B.1 Detailed compartmental model for people with type 1 diabetes 201
B.2 Glucose compartmental concentration without insulin and meal disturbance inputs 208

B.3 Liver glucose concentration for different insulin infusion rates 208
B.4 Liver and heart and lungs glucose concentrations under meal disturbance 209
B.5 Glucose concentration variation under insulin and meal disturbance inputs 210
B.6 Glucose concentration variation for insulin unit step change after 10 minutes and 20 units glucose step change after 40 minutes 210
B.7 Glucose concentration variation under insulin and glucose step disturbance at varying time gaps 211
C.1 Pilot Plant PARSEX Reactor 215
C.2 Schematic diagram of the PARSEX Reactor 216
C.3 Critical Regions stored on a microchip and also on a computer 220
C.4 The microchip containing Parametric Controller 221
C.5 Current Control Software 221
C.6 Performance of the Parametric and PI Controller in the pilot plant 222

Chapter 1

Introduction and Project Objectives

1.1 Introduction

An effective treatment of disease does not always rely on stronger drugs and can often be achieved by improved drug delivery systems. An integrated approach involving biological sciences, engineering technology and mathematical analysis is reconfirming our belief that disease such as cancer and those related to heart will ultimately yield to technological advances, emerging from the integrated approach. This is a multidisciplinary area where engineers can play a unique role and provide significant contributions.

The effectiveness of a drug is determined by its concentration and the duration for which it is present at the site of action. Past practices for determining the drug dosage were based on clinical experiments where the drug dose was increased and its effect and toxicity were estimated as a function of the dosage. This still remains to be the approach for the approval of new drugs for clinical use, but a much more rational approach based upon the distribution of the drug in the body and its concentration in various tissues has emerged and is providing a systematic framework for determining optimal drug dosages and is even assisting in discovery of new drugs.

Automation of drug delivery systems relies on developing models that can accurately describe the transport and concentration aspects as well as the effect aspects of drugs. This involves incorporating absorption, distribution, metabolism, elimination and toxicity issues for various tissues and often results in complex mathematical models. An advantage of these models is that they can be used to carry out detailed and extensive analysis for various tissue parts of the human body. However, the major disadvantage of using the detailed models is that due to extensive computational

requirements they are not suitable for on-line control of drug infusion rates. The control and automation relevant models aim to be computationally efficient and yet be able to incorporate the complexities involved in the system by, for example, developing input-output relationships. A disadvantage of this approach is that the insight of the details, for example, drug concentration profile in the major tissues of the body, is lost. Despite the simplification of the model, on-line implementation of a drug infusion rate controller can become impractical due to the presence of constraints on drug infusion rates and state of the patient where the state includes drug concentration, effect and toxicity. Controllers that do not take into account the constraints do not give good performance and may lead to unsafe situations.

There are some more interesting challenges involved in the modelling and control of biological systems. The parameters involved in the modelling of drug delivery and distribution may change within and amongst the patients. Also, many of the drug delivery problems are multi-objective in nature. The objective in such a case is not only to take the patient state to the desired value, subject to satisfaction of the constraints, but to also take into account that the trajectory of the state profile is such that it is able to place more emphasis on satisfaction of some constraints than on the satisfaction of the other constraints. Such criteria are usually specified by the physician based upon the side effects observed due to violation of certain constraints, such as on drug concentration, in clinical settings.

1.2 Project Objectives

The main aim of this work is to develop models and model based control techniques for drug delivery systems, which would ensure:

- Fast calculations of the optimal drug dosage without an online computer while taking into account the patient model and constraints such as on drug dosage
- Flexibility to adapt to changing patient characteristics
- Incorporation of the physician's performance criteria
- Safety of the patients
- Reduced side effects by optimizing the drug infusion rates.

The objectives of this thesis are as follows:

1.2.1 Parametric and Multi-objective Control of Insulin Delivery for people with Type 1 Diabetes

Diabetes is a disease that affects the body's ability to regulate glucose. Type 1 diabetes or insulin dependent diabetes is characterized by insufficient secretion of insulin from the pancreas, which means that to maintain blood glucose concentration at normal levels, the patient is totally dependent on external source of insulin, which needs to be infused at an appropriate rate. This problem can be formulated as a model predictive control problem where the objective is to reach the desired target blood glucose concentration subject to constraints on insulin delivery rate and glucose concentration. An objective of this work is to derive model based parametric controllers that will provide the optimal insulin delivery rate as an explicit function of the state of the patient. These explicit functions can then be stored on a microchip allowing the implementation of model based blood glucose controllers on a portable device. Another objective of this work is to be able to take into account variations in inter- and intra-patient model parameters. These issues are addressed in Chapter 3 whereas Chapter 4 presents a multi-objective controller where physician's performance criteria, pertaining to the fact that negative deviations from target blood glucose concentration are more harmful than positive deviations, is equated to the engineering performance criteria. This problem is solved by using asymmetric objective function approach and also by using a constraint prioritization methodology.

1.2.2 Modelling and Control Strategies for Surgery under Anesthesia

Safe and adequate anesthesia is characterized by analgesia, muscle relaxation and hypnosis while maintaining vital functions such as mean arterial pressure (MAP), heart rate and cardiac output (CO) within certain desired ranges. Usually this task is based upon manual, qualitative and rule based methodologies, which may result in non optimal drug uptake and therefore increased wake-up time and fatal situations. The main objective of this work is to develop model and model based automatic controllers for the regulation of vital functions that will lead to reduced drug

consumption, less time spent in post-operative care unit and enhanced safety for the patients being operated under anesthesia. In Chapter 5, a model for the infusion of three drugs, isoflurane, sodium nitroprusside (SNP) and dopamine (DP) for the simultaneous regulation of MAP, CO and hypnosis is presented. For modelling purposes the human body is considered to be consisting of five major interconnected compartments and the model is based upon the pharmacokinetic (PK) and pharmacodynamic (PD) aspects of the drugs on these compartments. The PK/PD parameters for the drugs are based upon the data reported in the medical literature. The model is then validated by carrying out a number of dynamic simulations to compare the effect of various drug infusion rates, on the patient variables, with the data reported in open literature. The model is then used for designing controllers so as to compute the optimal drug infusion rates. A model based control problem is formulated where the objective is to minimize the deviations of the patient variables from the desired setpoints and the constraints are given by the bounds on drug infusion rates and patient variables. The derivation of the controller requires solving this optimization problem, for the given states of patient, at regular time intervals. A parametric programming approach for model based control, which does not require solving an optimization problem at regular time intervals, is also presented. This approach provides the optimal drug infusion rate as a set of explicit functions of the state of the patient and the corresponding polyhedral regions in the space of the state variables. This reduces implementation of the controller to simple function evaluations.

1.2.3 Strategies for the Delivery of Chemotherapeutic Agents for Cancer

Cancer is a disease that can be characterized by uncontrolled and unregulated cell growth that may result from gene mutation and may lead to the death of the patient. An effective chemotherapy schedule aims to minimize the tumour size at the end of a final time period. For the growth of the tumour size there are two main models: cell cycle non-specific and cell cycle specific that have been extensively used in literature. The aim of this work is to develop optimal chemotherapy schedules, given these models, so as to minimize the tumour size while incorporating constraints on tumour size reduction during the course of chemotherapy, toxicity of the drug and its effect

on normal cells. Chapter 6 presents a mixed integer dynamic optimization approach where an integer variable is introduced to describe the discontinuity in the cell cycle non-specific model. An optimal control approach for cell cycle specific model is also presented and optimal chemotherapy schedules are derived and behaviour of the tumour and normal cells is also analyzed.

1.2.4 Parametric Control of a Pilot Plant Reactor

An aim of this work is to demonstrate the capability of parametric controller in real life. An experimental study is reported in Appendix C in which the parametric controller is implemented on a pilot plant scale partially simulated exothermic reactor (PARSEX). This demonstrates that the model based parametric controller can be implemented without using an on-line solver and minimum computational power. The encouraging results obtained from this work pave the way for the development of portable drug delivery devices, enhancing the safety, convenience and life style of the patients.

To summarize, in this thesis, models and model based controllers for three drug delivery systems, insulin delivery for people with type 1 diabetes, surgery under anesthesia and optimal control of cancer are developed. A successful implementation of model based parametric control of a pilot plant reactor on a simple computational hardware is also demonstrated. The developments reported in this thesis are expected to be of great benefit not only to the patients, but also provide the physician and general caretakers such as nurse and family members of the patients with an advisory system for monitoring the state of the patient.

The rest of the thesis is organized as follows. Chapter 2 presents a literature review of modelling and control of drug delivery systems and model based parametric control. In Part I of the thesis the focus is on delivery of insulin for people with type 1 diabetes. Optimal insulin delivery rates for fixed and varying model parameters are derived in Chapter 3, while Chapter 4 is concerned with the asymmetry in the objective function and prioritization of the multiple objectives. In Appendix A development of a prototype closed loop glucose control system is presented and the system is tested with simulation experiments. Appendix B presents an extensive

analysis of a detailed physiologically based compartmental model for diabetes. Implementation of parametric control of a pilot plant reactor via a microchip is demonstrated in Appendix C. Part II of the thesis is concerned with the other two drug delivery systems. In Chapter 5 a compartmental model and model based controller for patients being operated under anesthesia are developed. In Chapter 6 derivation of the optimal cancer chemotherapy schedule is presented. Two models, cell cycle specific and cell cycle non-specific are considered for this purpose. Finally conclusions and future directions are presented in Chapter 7.

Chapter 2

Literature Review

2.1 Introduction

This chapter presents a literature review in the field of modelling and control of drug delivery systems. Section 2.2 presents an overview of modelling the pharmacokinetic and pharmacodynamic aspects of the drugs. Insulin delivery for type 1 diabetes, surgery under anesthesia and delivery of chemotherapeutic agents in cancer are discussed in detail in sections 2.3, 2.4 and 2.5 respectively. A review of parametric programming and model based control is presented in section 2.6.

2.2 Modelling of Drug Delivery Systems

2.2.1 Common routes of drug administration

Many routes of drug administration have evolved over the centuries. Amongst these routes although the oral delivery is the most common and simple, it is not suitable and effective for all the diseases. In such cases, other delivery modes, such as intravenous, intramuscular and subcutaneous injections, are used but these methods have the disadvantages of being uncomfortable to the patients and there is a risk of infection. Ophthalmic and topical routes are less common and have the disadvantages including requiring frequent administration, for the ophthalmic route, and being limited to drugs that are locally active, for the topical route. Finally, controlled release implants can release drugs over long periods of time but require surgery (Saltzman, 2001).

Clinical trials on healthy volunteers and patients are carried out to calculate an average amount of a drug based upon the body's ability to absorb, distribute and eliminate the drug. This amount is usually known as the standard dosage. For a given drug dose, a pharmacokinetic (PK) model can be used to predict the drug

concentration profile over a given time and a pharmacodynamic (PD) model can be used to describe the effect of the drug as function of the drug concentration (Holford and Benet, 1998). A combination of the two models then allows describing effect of the drug as function of time which can be used to compute optimal amount of the drug dosage (see Figure 2.1). In this section, a review of PK and PD models is presented.

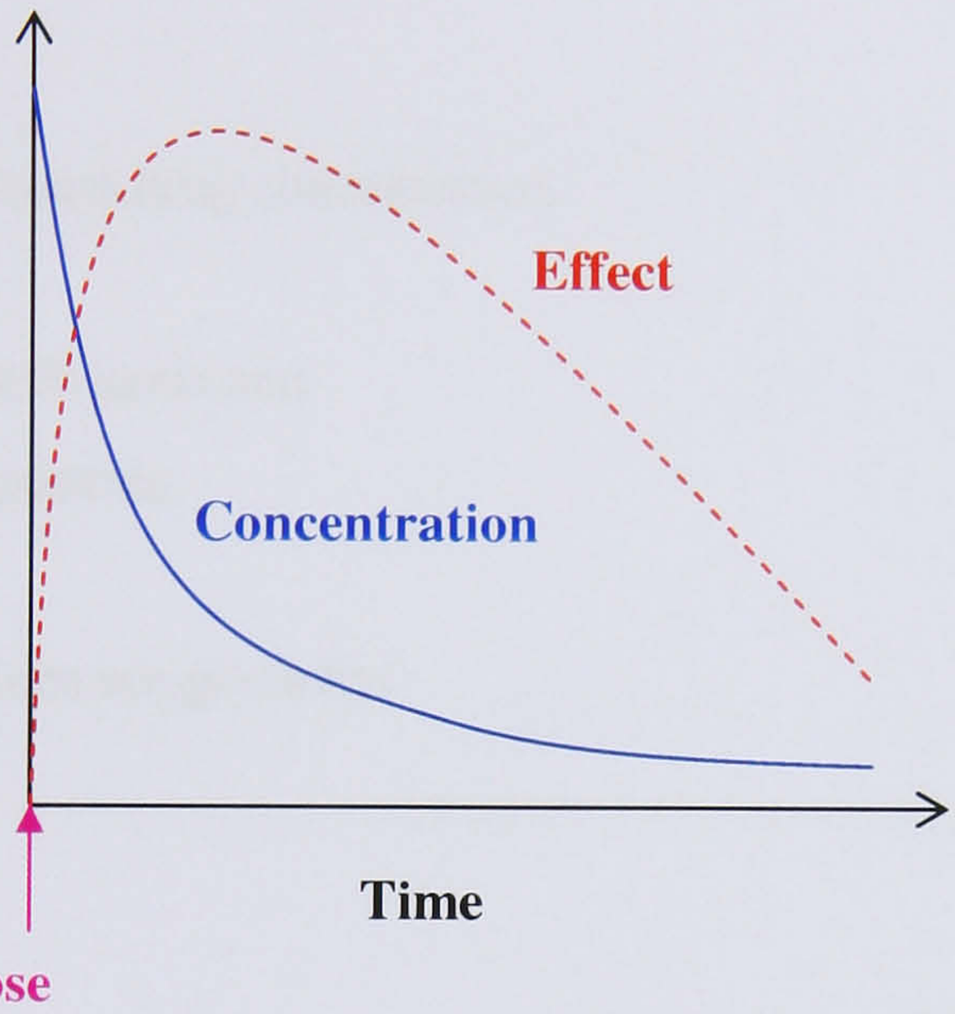


Figure 2.1 Drug Concentration and Effect Profiles

2.2.2 Pharmacokinetic Models

The three major types of pharmacokinetic models are: empirical, compartmental and physiological (Tucker, 1990). Empirical models are black box type of models that provide an input-output type of relationship where inputs are the drug dosages and the outputs are the drug concentrations. Compartmental models rely on a minimum number of compartments that can adequately describe the observed data. Physiological models are the most realistic since the drug kinetics, biochemistry, physiology and anatomy are taken into account. Although one type of model has some advantage over the other, all the three types of models are used extensively, share some common features and in principle are empirical in nature.

Empirical Models

Four types of relationships that have been observed to adequately fit the data are exponentials, power functions, gamma functions and Weibull functions. The exponential functions are given by:

$$C(t) = \sum C_i . e^{-\lambda_i t}$$

where

$C(t)$ is the plasma drug concentration

t is the time

C_i are the coefficients and

λ_i are the exponents.

Power functions are given by:

$$C(t) = At^{-a}$$

Gamma functions by:

$$C(t) = At^{-a} . e^{-bt}$$

and Weibull functions by:

$$C(t) = Bt^{s-1} . e^{-\lambda t} .$$

These functions give good curve fit of the data for different drugs, for example, for some cases gamma functions give a comparable or better fit than the sum of exponentials.

Compartmental Models

The simplest pharmacokinetic model consists of a single compartment representing the systemic circulation (Figure 2.2). The elimination of the drug from the compartment is usually assumed to follow first order kinetics:

$$\frac{dC(t)}{dt} = -k.C(t)$$

where k is the rate constant and is related to the half-life, $\tau_{1/2}$, for drug residence within the compartment by:

$$\tau_{1/2} = \frac{\ln(2)}{k}.$$

The half-life of the clearance can then be used to calculate the intervals of drug doses to keep the drug plasma concentration above the desired level.

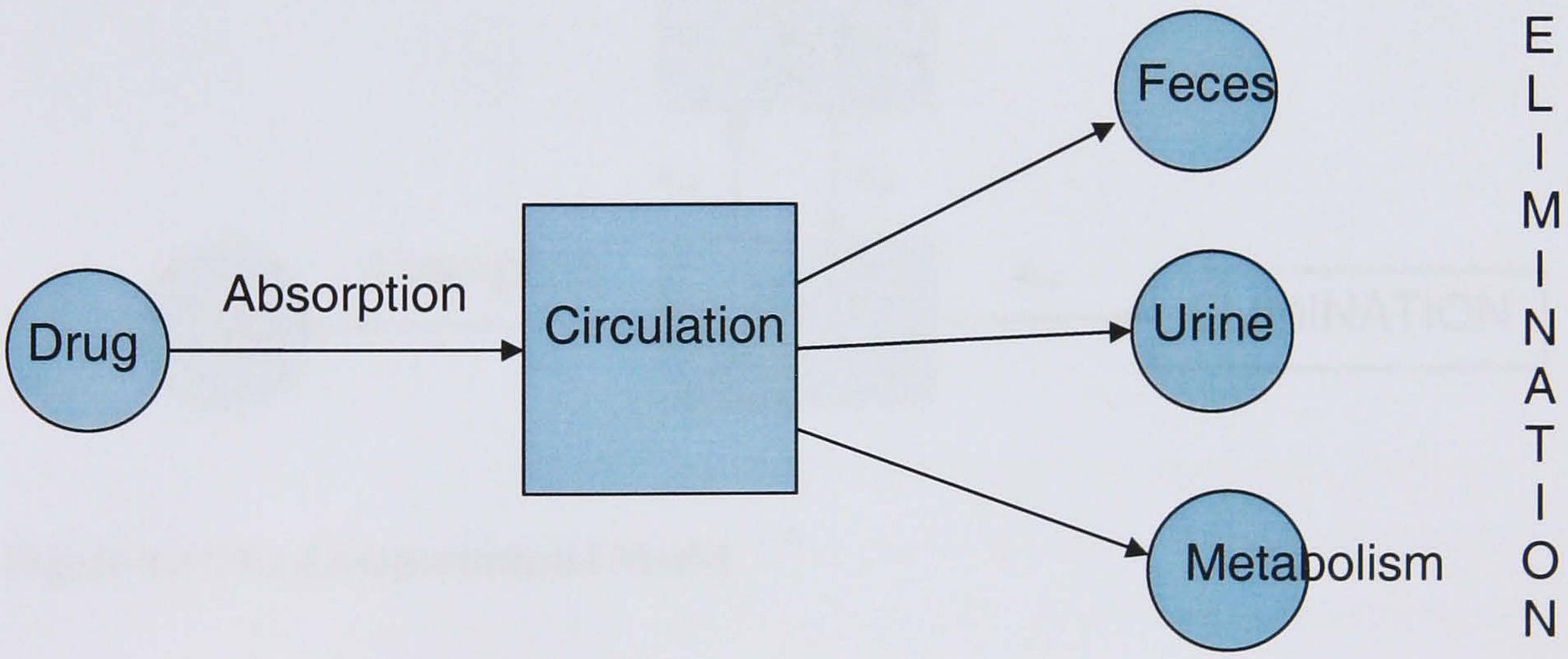


Figure 2.2 One Compartmental Model

Figure 2.3 shows the two compartment model where the body is considered to have a central compartment representing the blood and well perfused tissues and a peripheral compartment representing less well perfused tissues. The elimination is usually

assumed to occur from the central compartment. The differential equations governing the system are given by:

$$\frac{dC_1}{dt} = -(k_{10} + k_{12})C_1 + k_{21}C_2$$

$$\frac{dC_2}{dt} = -k_{21}C_2 + k_{12}C_1$$

the solution of which is given by sum of two exponentials. This type of model is frequently used for cases when the disappearance of the drug from the body follows a bi-exponential decay. The elimination from the central compartment takes place in two steps: the first step is fast and corresponds to the distribution of the drug from the central to the peripheral compartment and the second step is slow, corresponding to the elimination from the central compartment.

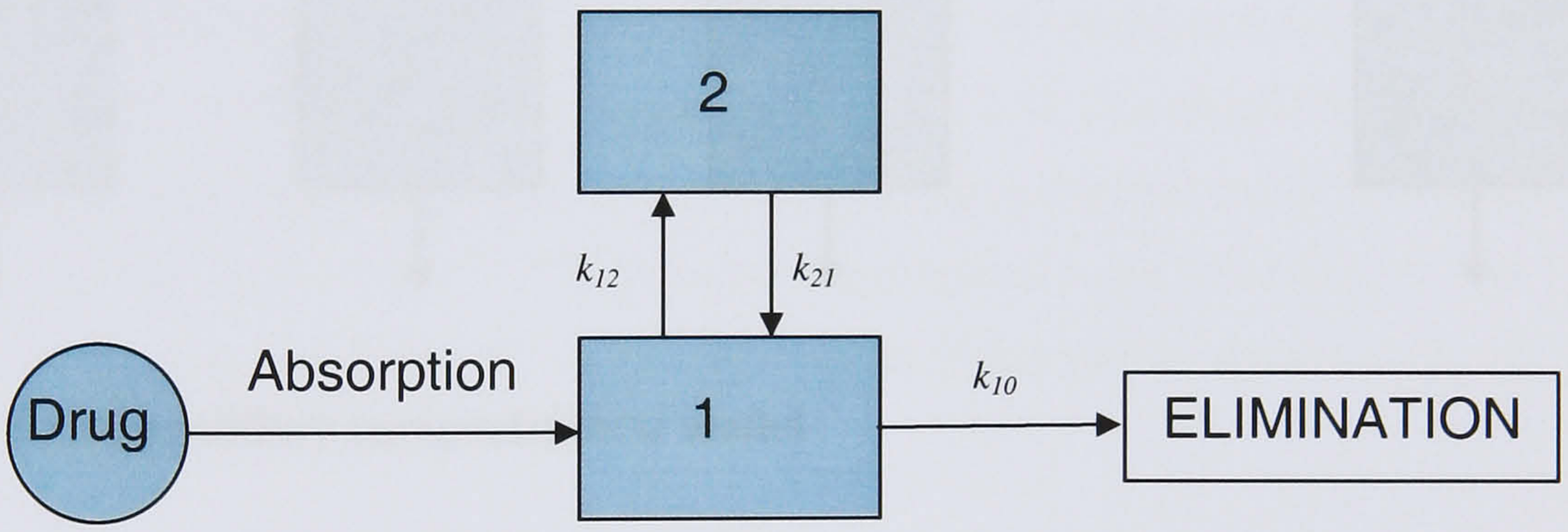


Figure 2.3 Two Compartmental Model

There are two major types of general multi-compartmental models: catenary compartmental model and the mamillary compartmental model. The catenary compartmental model consists of an inter-connected chain of compartments (Figure 2.4) whereas the mammillary model (Figure 2.5) consists of a central compartment linked with a number of peripheral compartments.

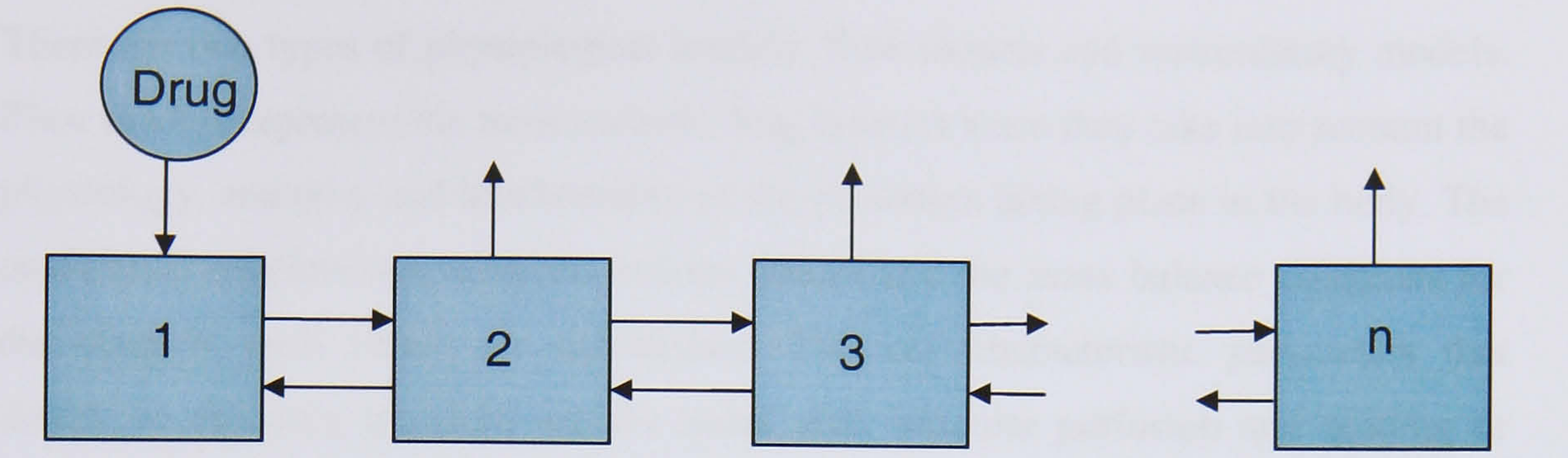


Figure 2.4 Catenary compartmental model

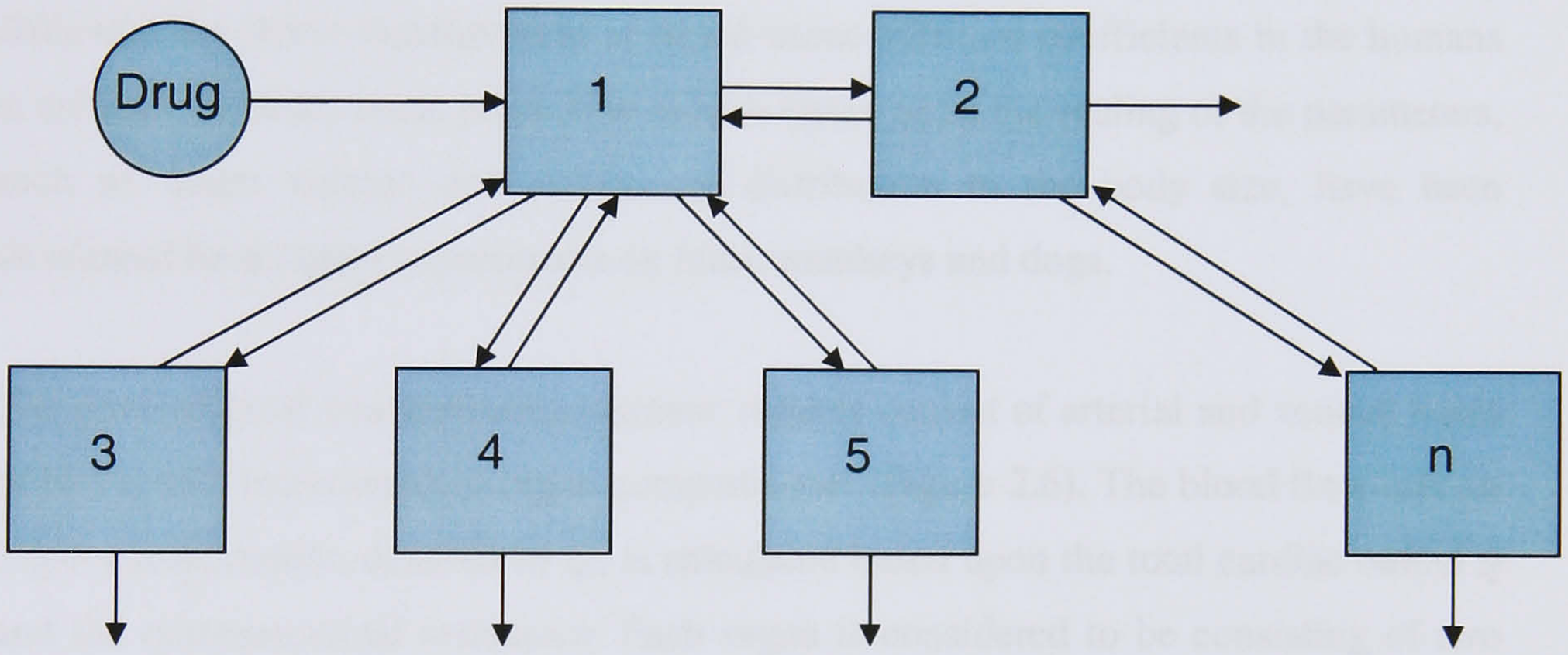


Figure 2.5 Mammillary compartmental model

There are two major drawbacks of the compartmental modelling techniques. First, it is difficult to relate a compartment to the real physiological space in the human body. Second problem is concerned with identifiability. The number of compartments is usually decided based upon the number of exponential terms required to adequately describe the plasma drug concentration profile with time. This however does not result in a unique solution of the estimation of the parameters. Despite these drawbacks, there are cases where compartmental models provide useful information for designing drug dosages.

Physiological Models

There are two types of physiological models: flow models and recirculatory models. Flow models represent the most realistic drug kinetics since they take into account the physiology, anatomy and biochemistry of the processes taking place in the body. The anatomical relationships between various tissues and the mass balance equations for the drug in each tissue are established. The key characteristic parameters that determine the drug transport are the tissue size, vascular perfusion and binding or partitioning of the drug between blood components and those in the tissues. A key feature of the physiological flow models is that they use the information and data on blood flows and blood-tissue partition coefficients rather than fit the model to the observed drug concentration profile as in the empirical and compartmental models. Although the direct measurement of blood-tissue partition coefficients in the humans is difficult, in many cases good flow models based upon the scaling of the parameters, such as tissue volume and volume of distribution to the body size, have been developed based upon experiments on mice, monkeys and dogs.

The physiological based pharmacokinetic models consist of arterial and venous pools of blood and interconnected organ compartments (Figure 2.6). The blood flow into an organ compartment, denoted by q_i, is calculated based upon the total cardiac output q and the compartmental resistance. Each organ is considered to be consisting of two compartments corresponding to the blood part and the tissue part as shown in Figure 2.7.

The recirculatory models consider the body as a dynamic control system with a simple positive feedback arrangement where the drug disposition results because of the repetitive circulation.

There are two major disadvantages of physiological models. The first issue is concerned with the identification of the model parameters that can adequately describe the detailed physiological phenomenon. The second disadvantage stems from the complexity of the model that can sometimes render it not of much use for design of model based controller.

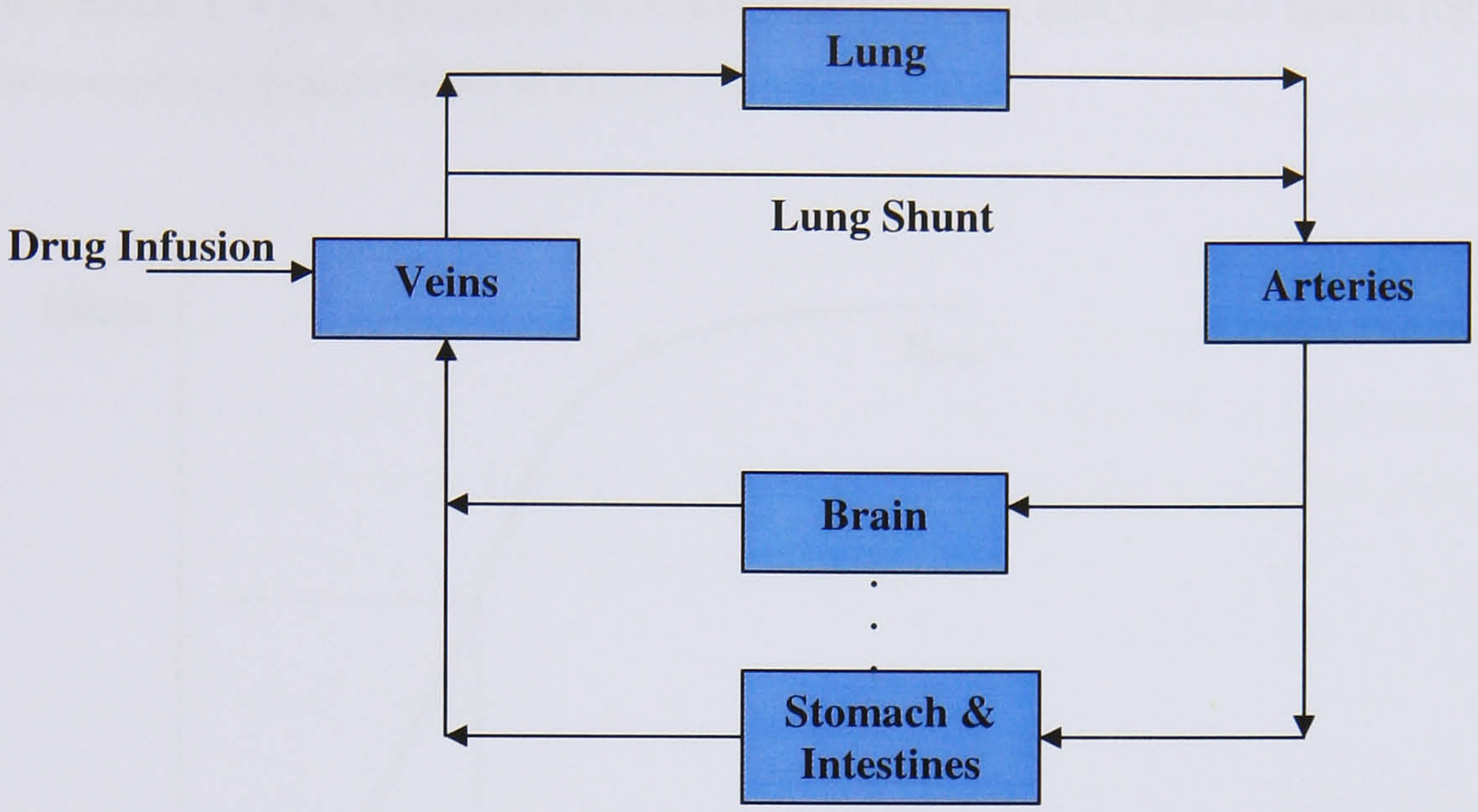


Figure 2.6 Physiological based model

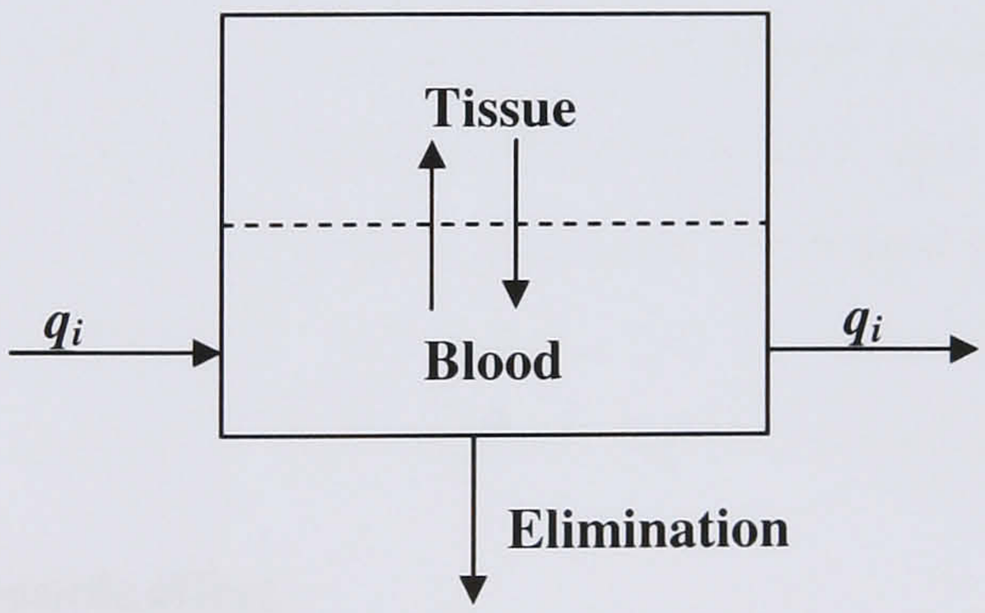


Figure 2.7 An organ compartment consisting of the blood part and the tissue part

2.2.3 Pharmacodynamic Modelling

Pharmacodynamic models provide the profile of the drug effect as a function of drug concentration at a site. This profile is usually depicted as the effect plotted against log of drug concentration as shown in Figure 2.8.

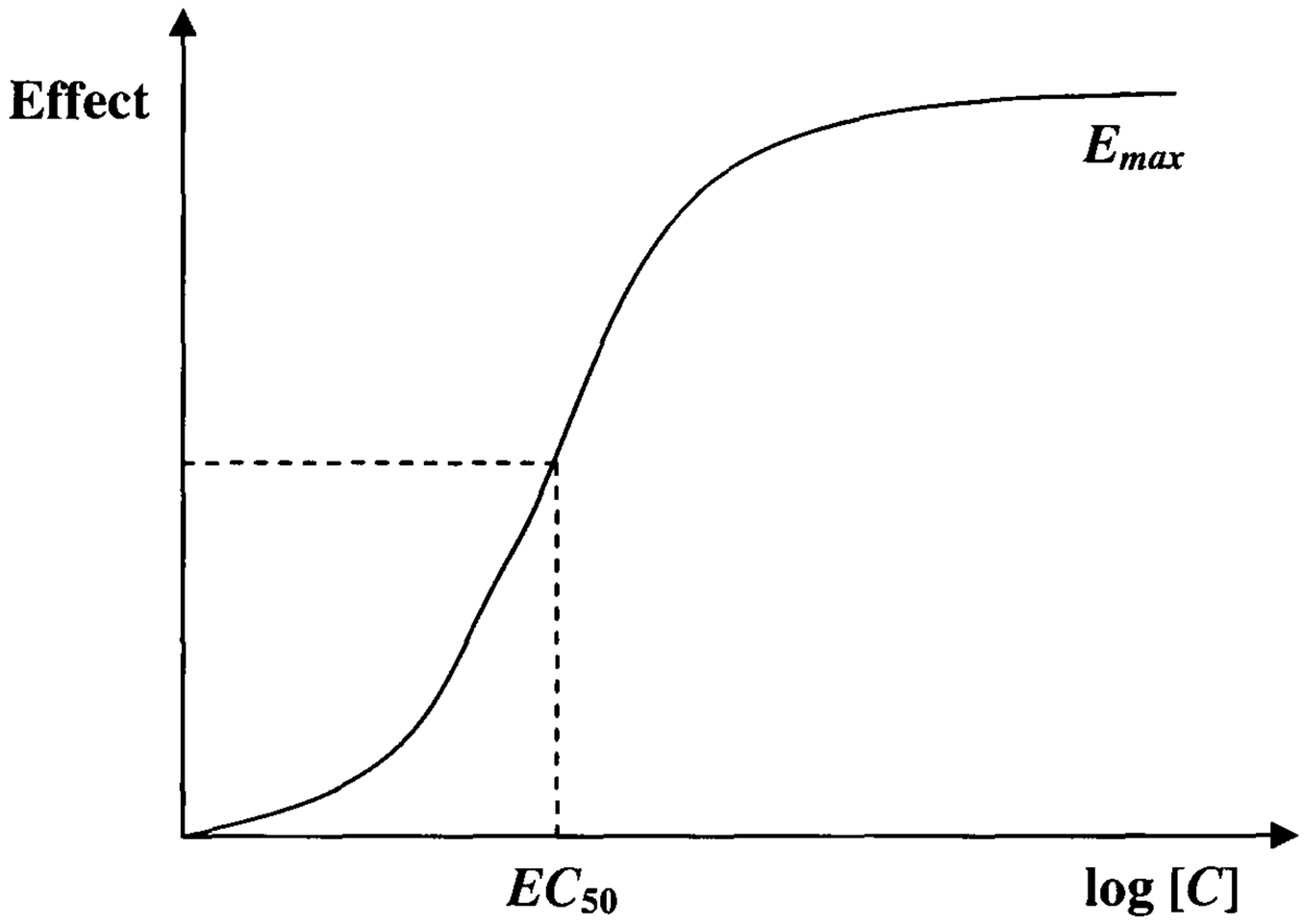


Figure 2.8 Drug Effect vs. Concentration

This is a sigmoid curve where the effect, E, and the concentration, $[C]$, are related as follows:

$$E = \frac{E_{\max} \cdot [C]^{\gamma}}{EC_{50}^{\gamma} + [C]^{\gamma}}$$

where

E_{max} is the maximum possible effect

EC_{50} is the concentration at half maximal effect and

γ is a measure of the steepness of the curve.

2.3 Modelling and Control of Diabetes

Diabetes is characterized by relative or absolute insufficiency of insulin to regulate blood glucose concentration. Type 1 diabetes is characterized by the destruction of β-cells in the pancreas and therefore, a person with type 1 diabetes requires exogenous insulin to be infused at an appropriate rate to maintain the blood glucose concentration. Regulation of blood glucose concentration is vital, otherwise it may lead to hypo- or hyper-glycemic conditions, which can have short-term and long-term effects on an individual's health. This regulation can be achieved by developing models that can accurately represent the glucose-insulin dynamics and then using these models for developing model based controllers.

2.3.1 Modelling of Diabetes

Bolie (1961) developed a two state linear model consisting of two differential equations, representing glucose and insulin concentrations. In his analysis, the liver, pancreas and peripheral tissues were considered to be acting through a single compartment. The major limitations of the work were that the function of kidney was not considered and intravascular-extravascular differences in concentration were not taken into account. Ackerman *et al.* (1965) developed a similar model where insulin system was described by linear equations. The model was used for the interpretation of the curves corresponding to blood glucose and blood insulin concentrations. Simulation studies for various intestinal absorption and oral doses were also presented. It was observed that in most of the cases the model prediction matched quite well with the experimental data points, but in some cases many more experiments must be carried out to reach a satisfactory interpretation.

A circulation and organs model for insulin dynamics based upon physiological parameters was presented by Tiran *et al.* (1979). The model incorporates physiological parameters including plasma flowrates, circulatory paths, intra- and extravascular insulin spaces and specific tissue and organs, concerned with the disappearance of insulin. The model consistently predicted the total insulin degradation rates as well as peripheral insulin concentrations, based upon experiments on diabetic dogs when subjected to different routes, portal and peripheral, and wave

forms of insulin infusions. The model was also used to compute insulin degradation in the liver, kidney and peripheral tissues and it was observed that degradation in the periphery dominates when insulin is infused peripherally.

Bergman *et al.* (1981) developed a 'minimal model' to quantify both pancreatic responsiveness and insulin sensitivity. The individual contributions of insulin secretion and action were measured in 18 lean and obese subjects by analyzing the dynamics of plasma glucose and insulin during the intravenous glucose tolerance test. It was observed that intolerant subjects had impaired ability to normalize the concentration under hyperglycemic conditions in the absence of an acute insulin response. The mathematical equations describing the model are discussed in Chapter 3.

Cobelli *et al.* (1982) presented a nonlinear model representing the major crucial processes of glucose, insulin and glucagon dynamics and their interrelationships. The model consists of a metabolic plant: glucose and a two hormone controller, insulin and glucagon. The glucose subsystem is described by a one compartment model of distribution and metabolism, the insulin subsystem by five compartment model and the glucagon subsystem by a one compartment model. The interaction between the three subsystems takes place via the control signals from the glucose subsystem to the hormonal controllers and vice versa. A brief outline of carbohydrate metabolism regulation was also presented.

Pancreatic beta cell and liver represent the secreting and the major degrading site of insulin respectively. Pacini and Cobelli (1990) presented a model to quantitatively represent this mechanism. The model provides the time course of beta cell insulin secretion, the sensitivity of the islets to the glucose stimulation and insulin extraction by the liver. Although the model can adequately quantify individual components of glucose intolerance in many cases such as diabetes and aging, the application of the model was demonstrated for the observed elevated insulin peripheral levels in liver cirrhosis and obesity.

A review of models for subcutaneous insulin delivery was presented by Nucci and Cobelli (2000). The key issue in the modelling of subcutaneous insulin delivery is to

be able to take into account the distribution in the subcutaneous depot and transfer to plasma. It was shown that most of the models are suitable for regular insulin preparations but only some can adequately take into account intermediate acting and new insulin analogues. Dalla Man *et al.* (2004) presented a study for measuring the insulin sensitivity during a meal or an oral glucose tolerance test. Two methods, "tracer" and "non-tracer" were compared and it was observed that the non-tracer method based on the oral minimal model can be used as a reliable tool for the measurement.

Boroujerdi *et al.* (1995) included the glucose transporter mechanism saturation by extending the compartmental model of glucose kinetics by Cobelli *et al.* (1984). Five compartments were considered: a plasma compartment, two interstitial compartments, representing insulin-dependent glucose uptake, and insulin-independent tissues, respectively, and a glucose transporter limited metabolism compartment for each interstitial space. Simulation of the model and estimation of glucose utilization flux indicated that in people with uncontrolled diabetes high plasma glucose concentration can be attributed to high glucose production rate by liver. This is due to relative saturation of the available pool of glucose transporter resulting in reduced glucose metabolic clearance rate.

A model to predict the effect of changes in the subcutaneous insulin dosages and physiological fluctuations on the insulin levels and glucose control was presented by Puckett and Lightfoot (1995). Parameter and sensitivity analysis results were used to analyze insulin kinetics and its effect on glucose dynamics. It was suggested that improved control for large inter- and intra-patient variations can be achieved by more frequent sampling and control action. The importance of the sensitivity coefficient for absorption and the effect of the overlapping insulin injections were also highlighted.

Guyton *et al.* (1978) used extensive data from other workers and more than 100 intravenous glucose tolerance tests, including variable dosages and durations of infusions, to develop a mathematical model of glucose metabolism in normal subjects. The model utilized the physiologic knowledge about glucose-insulin homeostasis in liver, brain, pancreas, kidney, peripheral tissues and central vascular organs. The main emphasis of the model was on the fast phase of insulin response to vascular glucose. It

was observed that during the fast phase the amount of insulin released rather than the insulin release rate is regulated by the glucose level.

Based on the work of Guyton *et al.* (1978), Sorensen (1985) presented a physiologically based compartment model for glucose and insulin dynamics. This model is described in detail in Appendix B. Parker (1999) extended this model for people with type 1 diabetes by incorporating the meal model of Lehmann and Deutsch (1992).

Lehmann and Deutsch (1992) presented a model to simulate the steady state glycemic profiles, following a change in either the insulin infusion or diet, and plasma insulin responses. The model can simulate the glycemic profiles and responses independent of the initial values used for the simulation. The model involves a single glucose pool where glucose enters via intestinal absorption and hepatic glucose production and is removed by insulin independent utilization in red blood cells, central nervous system and insulin dependent utilization in the liver and periphery. The rate of gastric emptying is controlled so that the glucose supply to the gut follows a trapezoidal profile. The duration of the period during which the glucose supply remains constant is determined by the amount of the carbohydrate intake.

2.3.2 Control of Diabetes

BIOSTATOR is one of the first feedback controller systems, developed by Miles Laboratories, for maintaining the blood glucose concentration at the desired level (Clemens, 1979). It consists of an on-line glucose analyzer, a controller for the calculation of insulin and dextrose infusion and a multi-channel infusion system and the response time of the whole system is less than 90 seconds. The glucose analyzer was based on an electrochemical sensor with immobilized glucose oxidase and measures hydrogen peroxide produced to infer the glucose concentration. The analyzer could be calibrated without disconnecting the catheter from the patient.

Salzsieder *et al.* (1990) developed a diabetes management system comprising of the tools for evaluation of therapeutic data and for simulation of the model. The model was represented by a third order differential equation system and was adapted for

humans based upon the parameters obtained from validation in diabetic dogs. This model was then used for the development of a control system based upon the modification of the BIOSTATOR algorithm.

Swan (1982) used optimal control theory for the computation of the optimal insulin infusion rates. One of the findings of this work was that the solution of the optimal control problem indicates a minimum amount of insulin that should be infused continuously to people with diabetes. It was also concluded that the feedback control exists and the control is given by a linear combination of the insulin and glucose concentration. Although only a particular set of parameters were used, the possibility of predicting the optimal outcome for a variety of situations was suggested.

Ollerton (1989) designed the controller based on an integrated square error cost function incorporating the deviation from same desired blood glucose concentration. The three compartmental model of Bergman *et al.* (1981) was used for the design of the controllers. The control algorithms were tested for the case of 180 min and 10 min glucose sampling times and in the absence and presence of glucose infusion; for a sampling time of 180 min a continuous form of the model and cost function was used whereas the discrete form was used for a sampling time of 10 min. The difficulties involved in the identification of individual model parameters for each patient and analysis of plasma glucose and insulin levels were also highlighted.

Furler *et al.* (1985) carried out a theoretical study to examine the effect of the sampling frequencies and the control algorithm parameters on the control of blood glucose. It was observed that as the sampling interval increased from 1 to 4 hr and as the sensitivity of the control algorithm increased there was a decrease in the stability. The choice of control algorithm sensitivity was found to be compromise between two opposing objectives: high sensitivity accelerates glycemic control and low sensitivity reduces the chances of instability. Based upon these developments the possibility of the use of a closed loop or semi closed loop system was proposed.

Fisher and Teo (1989) investigated two cases: development of an insulin infusion protocol for a hyperglycemic patient and identifying a program of single insulin injections following a meal. Three insulin infusion programs: sub-optimal feedback

control, impulse control and constant infusion were examined and impulse control was found to superior in reducing high blood glucose levels. It was also suggested that a coordinated program of single injections is an ideal choice for controlling blood glucose concentration after meals.

Fisher (1991) designed the controller for the Bergman model (Bergman *et al.*, 1981) based on integral squared error objective function so as to minimize the set point deviations. In the absence of a meal, a combination of injections and constant infusion was found to provide an effective control for a patient in the state of hyperglycemia. In the presence of meal, giving an injection coinciding with the meal was also suggested.

Sorensen (1985) designed an internal model controller for an approximation of a 19 state, physiologically based, nonlinear compartmental model. The performance of the controller deteriorated in the presence of meal disturbances and variations in the model parameters.

Kienitz and Yoneyama (1993) used H_∞ control technique to design a robust controller. A low-order model containing patient-dependent parameters was used to describe glucose and insulin dynamics. The controller design relied on the nominal patient model and a set of frequency-dependent weighting functions, tuned to capture the entire expected patient population, based on the variations in parameter values. The controller was robust to small uncertainties but required retuning for the case of large patient variations.

Doyle *et al.* (1995) proposed a nonlinear feedforward-feedback controller synthesized using feedback linearization. Modelling and experimental techniques for controlling blood glucose were explored. It was observed that low order models may not adequately describe the real process and may contain modelling errors and process-model mismatch. The design and development of glucose responsive, gel-based polymeric devices for insulin delivery was also explored. It was envisaged that the insulin entrapped in the polymeric device would lower the blood glucose levels to the normal range and then return to its original equilibrium configuration.

Trajanoski *et al.* (1998) presented a neural predictive control strategy, using neural networks for the identification and nonlinear model predictive control for blood glucose control. The controller enabled stable control in the presence of large noise levels and for unknown or variable time delays.

The Automated Insulin Dosage Advisor (AIDA) is based on the work of Lehmann and Deutsch (1992). The control objective is to minimize the square of blood glucose concentration from the target value over a fixed period of time by utilizing subcutaneous insulin injections. This system can be used to carry out simulation experiments for common clinical situations and can be used as an educational tool for patients, their relatives, students and medical staff. Various ideas to identify possible changes in the treatment regimen can also be tested.

Parker *et al.* (1999) demonstrated the use of a model predictive controller with state estimation for regulating blood glucose. The controller was designed by linearizing a 19-state nonlinear physiologically based model. Unconstrained model predictive control was used and optimum results were not obtained when constraints were encountered. Parker *et al.* (2000) developed H_∞ controllers for the linearized 19-state model. The H_∞ controller gave comparable performance to the model predictive control but the controller performance deteriorated in the presence of uncertainty. The performance of model predictive controller was superior to H_∞ controller in terms of tracking the blood glucose concentration.

Lynch and Bequette (2001) designed a constrained state space model predictive controller for the 3-state Bergman model and carried out simulation study on the 19-state model of Sorensen (1985). The performance of the controller on the 19-state model when subjected to meal disturbance of 50 g was observed. It indicated that the dynamics of the 19-state model are slower than the 3-state model. Lynch and Bequette (2002) used the Bergman model to design the controllers to regulate the system based on the subcutaneous glucose measurement. This approach was based on the subcutaneous insulin delivery rather than intravenous delivery.

A critical review of control algorithms for intravenous and subcutaneous routes of insulin delivery is presented in Parker *et al.* (2001) and Bellazzi *et al.* (2001) respectively. Recently Hovorka *et al.* (2004) analyzed the performance of nonlinear model predictive control during fasting conditions. The controller employed the Bayesian parameter estimation to determine time-varying model parameters. This study involved 15 clinical experiments and used intravenous glucose sampling and subcutaneous insulin infusions. Nonlinear MPC was identified as a promising candidate for control of glucose concentration during fasting conditions in people with type 1 diabetes.

A detailed theoretical analysis involving a comparison of various control algorithms was presented by Hernjak and Doyle III (2005). Linear model based controller was found to be an ideal choice; while nonlinear MPC does not add any significant benefit, the use of low-complexity control algorithms such as proportional derivative and proportional integral derivative was discouraged if high levels of performance is desired.

2.4 Surgery under Anesthesia

Anesthesiologists maintain patient's vital states, including mean arterial pressure (MAP), cardiac output (CO), carbon dioxide and oxygen levels, blood acidity, fluids levels, heart contractibility and renal function, within acceptable ranges by infusing intravenous drugs and/or introducing inhalation anesthetics. Not all these states can be measured directly and must be inferred by the physician. Intravenous drugs, such as dopamine (DP), sodium nitroprusside (SNP) or prasosin, are typically infused manually using drip intravenous lines, or by using programmable pumps for specified infusion rate profiles. Inhalation anesthetic agents such as ether, halothane, desflurane or isoflurane are introduced via the respiratory system into the patient's lungs, where they enter the circulatory system. The uptake is regulated by adjusting the inlet concentration of agents in the respiratory system and the pulmonary ventilation. Model based control strategies for the automation of regulation of the patient state rely on an accurate model describing the dynamic response of the patient during anesthesia.

2.4.1 Modelling of Anesthesia

Zwart *et al.* (1972) developed a model for the uptake and distribution of halothane. The model comprises of two loops, one for the uptake and distribution of halothane and the other for blood circulation. Twelve compartments, consisting of nine for the different organs or group of organs, two for the arterial and venous blood pool and one for the lungs are used to describe the pharmacokinetic and pharmacodynamic aspects of the drug. The influence of halothane on CO and MAP was modelled by applying the Ohm's law to the circulatory system. However, this work did not take into account the body's control mechanisms, the so-called baroreceptor reflex or baroreflex, which describes the reaction of the central nervous system to changes in MAP. This reflex maintains MAP in short term by stretch sensors at the carotid sinus and aortic arch. Slight changes in those sensors initiate baroreflex response, which acts as a negative feedback loop modifying the level of inhibition on the sympathetic vasodilator system. This can result in: (i) contraction of smooth muscles surrounding the arteries, modifying the vascular resistance, (ii) stimulation of the heart muscle causing an increase in heart rate and its contractibility and (iii) modification of the venous compliance affecting the holding capacity of the veins and therefore, the venous return of the heart.

Yasuda *et al.* (1989, 1991) developed a model for the uptake of isoflurane, an inhalation anesthetic. It consists of four peripheral compartments and one central compartment corresponding to the lungs, where the uptake of isoflurane takes place. This work also involved the determination of many parameters such as the partition coefficients, the regional blood flows and the kinetic constants governing the distribution of isoflurane.

Yu *et al.* (1990) developed a model for the hemodynamic responses to the intravenous agents, DP and SNP, for the case of an acute heart failure. SNP is a vasodilator which dilates the arteries, decreases the systemic resistance and lowers MAP. DP is used in anesthesia as an inotropic agent to enhance the cardiac performance by improving the heart contractibility. The model consists of two main parts: first, for the distribution of the drugs described with an electric analog model with baroreflex feedback and second consisting of equations governing the action of the drugs, to simulate the drug

response. Despite some shortcomings such as, the parameters of the baroreflex were assumed constant whereas they may change with the depth of anesthesia, the model showed good agreement with experimental and clinical data.

2.4.2 Regulation of Hemodynamic Variables

Slate *et al.* (1979) used a fixed-gain, non-adaptive PID controller with empirical rules for the regulation of MAP by infusing SNP. Since then, more complex control strategies have been developed to overcome the limitations of non-adaptive schemes. Isaka and Sebald (1993) provide a comprehensive review of different control strategies for the regulation of blood pressure. Mansour and Linkens (1989) proposed a pole-placement self-tuning control scheme for hypertensive patients following open-heart surgery. The model used in this work was proposed by Slate *et al.* (1979) and was used for the control of arterial pressure through administration of SNP and was extended to involve a recirculation term and two threshold-switchable reflex loops due to angiotensin and epinephrine. These reflex control loops were added to maintain circulatory system homeostasis despite disturbances in the circulatory system. The model also includes drug saturation effects, time-varying patient gains as well as drug concentration changes. The extensive simulation results obtained from a clinically validated hypertensive model confirmed that a pole-placement self tuner is adequate for controlling blood pressure, particularly when the recirculation term is included, or time delay is expected to change. The drawback of this control scheme is that it doesn't impose constraints on the infusion rate to ensure the patient's safety.

Behbehani and Cross (1991) used an integrating self tuning (IST) control strategy to regulate MAP, using SNP as an input. The controller adapts to variations that may occur in the patient's response to SNP and simultaneously optimizes the amount of drug infused. Furthermore, the controller was designed to eliminate the output bias. The controller optimizes the amount of drug infused by restricting the infusion variations during the transient phase of the control. This strategy is of particular interest in situations where the total amount of infused SNP should be minimized, such as for the treatment of pregnant women with toxemia and for patients with severe chronic hypertension. The proposed control strategy has two main advantages: first, it is based on theoretical derivation and not on a heuristic one; thus, it can be

applied under a broad range of physiological variations. Secondly, since the controller optimizes the amount of drug infused, it is particularly advantageous in situations where expensive or potentially toxic drugs are employed. However, a significant drawback of the specific control scheme is that it requires prior knowledge of the time delay.

Yu *et al.* (1992) presented a new control strategy called Multiple-Model Adaptive Predictive Control to regulate both hemodynamic variables, MAP and CO, by using SNP and DP respectively, in case of congestive heart failure subjects. The controller described in this work used a novel combination of the Multiple Model Adaptive Control (MMAC) and the Model Predictive Control (MPC) to adapt to the nonlinear and time-varying nature of the patients response. To avoid extensive computations associated with this design, only six models with the highest probabilities were considered in the calculation of the drug infusion rates. The control scheme described in this work required a set of models to predict the patient response for a finite time in the future. Although extremely accurate models are desired, complex models tend to be impractical, since a large number of parameters have to be estimated in this case. The controller described in this work assumed that the patient response can be represented by a linear small-signal first-order transfer function matrix. The first order behaviour associated with each element of the matrix was derived from previous studies by different investigators. Although it is known that changes in MAP can affect CO and vice versa, in this work SNP-MAP and DP-CO loops are not considered to be dependent. However, the coupling between these two loops, while not explicitly stated in the model, is manifested by changes in parameter values. During trials on animals, the controller performance was shown to be robust with respect to excessive switching between models and nonconvergence to a single dominant model.

Gopinath *et al.* (1995) presented a multirate MPC for MAP and CO regulation by combined infusion of SNP and DP, based on the comprehensive nonlinear model of the system introduced by Yu *et al.* (1990). The MPC algorithm is based on nonlinear quadratic dynamic matrix control. To reduce computational time, a selective linearization technique was implemented which linearized the model on the basis of trends in the plant-model mismatch. Restrictions on initial DP infusion rate, to avoid

extremely slow onset further complicate the problem. A novel rule-based override (RBO) to the MPC controller was introduced, which uses a set of heuristics to initialize DP infusion rate. The simulations performed showed that the use of a selectively linearized model in the prediction phase results in significant computational savings. Also, the algorithm implementation succeeded in handling the constraints which were imposed.

Held and Roy (1995) introduced a multiple drug hemodynamic control strategy based on a supervisory-fuzzy rule-based adaptive control technique to regulate the two hemodynamic variables, MAP and CO, via administration of SNP and DP. A control device that uses an expert system approach for the two inputs - two outputs system was developed. The control structure had a dual mode, i.e. it had two levels: a critical condition (coarse) control mode and a noncritical (fine) condition control mode. The system switched from one to the other when threshold conditions were met. Different "controller parameter sets" were given to the system which lead to different controller outputs. The noncritical control mode is a fuzzy logic controller. The system includes heuristics, typically considered by anesthesiologists, like "forbidden dosage range" for SNP. An adaptive controller incorporated a wide range of sensitivities to SNP observed in different patients, as well as with the time varying sensitivity observed in a single individual. The simulations showed that the control scheme was able to adequately keep the two hemodynamic variables within prescribed ranges.

Frei *et al.* (1997) studied models to be used for the design of automatic controllers for MAP during anesthesia. They reintroduced a physiology-based model of Zwart *et al.* (1972) describing the distribution and the effect of halothane with slightly modified parameters to be applicable in case of other volatile anesthetics (such as isoflurane). The model consists of two parts: one for the uptake and distribution of drugs and one for the circulation of the blood flows. To describe the drug distribution in the body a compartmental model was proposed. The resulting nonlinear model is then linearized around an equilibrium point for the purpose of controller design.

Gentilini *et al.* (2002) presented a paradigm for the closed-loop administration of analgesics during general anesthesia. The manipulated variable in this case was the infusion rate of alfentanil, an opiate and the controlled outputs were MAP as well as

the drug concentration in the plasma. In this case explicit Model Predictive Control that allows handling of input and output constraints, as well as the prioritization of the different constraints imposed and provides control variables as an explicit function of the state variables was used. This formulation reduces computational time since no on-line optimization routine was required. The control system, after validation in clinical practice, was found to be able to achieve multiple clinical goals.

Rao *et al.* (2003) developed a new, model-based control methodology for automated regulation of MAP and CO in critical care subjects by infusion of SNP and DP. The control algorithm used a multiple-model adaptive approach in a model predictive control framework to account for variability and explicitly handle drug rate constraints. The problem was a model predictive control problem which used a weighted model bank as a prediction model. The weights for each model were calculated through the recursive Bayesian algorithm. Each MIMO model in the bank incorporated four SISO pairs, i.e., SNP-MAP, SNP-CO, DP-MAP and DP-CO loops. The on-line optimization included soft constraints on the outputs as penalty functions, allowing the physician to specify ranges on MAP and CO. The controller derives its adaptability from the Bayesian weighting scheme that is computationally inexpensive and effective in building a higher order prediction model from basic blocks of first-order models.

2.4.3 Simultaneous Regulation of Hemodynamic Variables and other States of Anesthesia

Linkens and Mahfouf (1994) presented the application of Generalized Predictive Control (GPC) for the control of muscle relaxation through administration of atracurium. A compartmental model for the distribution and the metabolism of this muscle relaxant was presented. Multivariable GPC was also applied for the control of muscle relaxation and unconsciousness. Measurement of muscle relaxation was obtained via signal processing of evoked electromyography (EMG) responses, while the level of unconsciousness was inferred from measurements of MAP. The two drugs considered in the model are: atracurium for producing muscle relaxation and isoflurane for inducting anesthesia. By combining the effects of the two agents, a nonlinear multivariable system was obtained. It was concluded that the use of

prespecified set-points, in single or multi-loop systems, can considerably contribute to the improvement of the closed-loop characteristics of these systems. SISO GPC was robust when mismatch conditions between the actual and the assumed set points were considered.

Abbod and Linkens (1998) presented an anesthesia simulator for monitoring and control of depth of anesthesia during surgical operations, using propofol for unconsciousness and fentanyl for analgesia. The patient was simulated using a three compartment mathematical model describing the effects of drug infusions. A hierarchical structure using cardiovascular indicators (heart rate and blood pressure) and Mid Latency Auditory Evoked Potential (MLAEP) signals was implemented to monitor the Depth of Anesthesia (DOA) where the evoked brain signals were analyzed by using multi-resolution wavelet analysis. The two measures, cardiovascular system status and MLAEPs, were derived and then used together to assess DOA. Based on the DOA, a target concentration was decided and a rule-based fuzzy logic controller feeds the set-point to a Target Controller Infusion algorithm (TCI). The system provides a closed-loop architecture that can automatically provide the drug profile necessary to maintain the patient at a safe level of anesthesia. Consequently, the overall system can be used as an anesthesia simulator designed for guidance on the target of propofol concentration to be used. The anesthesiologist controls the final target concentration for the TCI system, thereby maintaining overall control of the system.

Zhang *et al.* (1998) presented a model incorporating the interaction between propofol and fentanyl and a method to incorporate this model into an Automatic Anesthesia Management System (AAMS). The model includes the pharmacokinetics and pharmacodynamics of each of the two drugs used, as well as a part describing the effects resulting from their interaction. The depth of anesthesia was determined by an Artificial Neural Network (ANN) algorithm, which uses as input the propofol concentration as well as the Mid Latency Auditory Evoked Potentials. The depth of anesthesia derived from the ANN algorithm was then regulated by means of a fuzzy-logic based controller for the decrement and by a confidence level estimator for the scheduled increment of propofol set-point.

E.Mortier *et al.* (1998) used an adaptive, closed-loop feedback control scheme to control the patients' Bispectral Index (BIS) via administration of propofol. This feedback control system was found to be adequate and safe for patients undergoing spinal anesthesia.

Gentilini *et al.* (2001) presented an autonomous, multitask anesthesia control system, incorporating three separate control schemes: one for regulating MAP, one for controlling hypnosis through the BIS and finally a supervisory function to connect the different controllers. For the design of both MAP and BIS controllers, physiology-based compartmental models were used. Control of MAP was performed by means of three observer-based state feedback (OBSF) controllers. The control strategy adopted for control of BIS was a cascaded Internal Model Control, where the master controller regulates BIS and slave controller regulates end tidal concentrations.

2.5 Delivery of Chemotherapeutic Agents in Cancer

Cancer can be characterized by uncontrolled growth and spread of abnormal cells which if not controlled can lead to the death of the patient. Cancer develops from a single cell that has undergone mutations in its DNA and instead of maturing normally and dying, cancerous cells reproduce without restraint. Chemotherapy which is one of the most commonly used treatments of cancer, relies on using anticancer agents which destroy cancer cells by preventing them from growing or multiplying. Chemotherapy can also harm healthy cells especially those that divide quickly. The main objective of using mathematical models for cancer chemotherapy is to verify the optimality of existing chemotherapy administration protocols and to propose alternative, improved regimens. The overall procedure of the model development is very difficult, since the mathematical representation of such a process involves several biological and chemical mechanisms that are extremely complex and often not completely understood.

There are two general approaches to model cancer chemotherapy. The first considers the tumour as a homogeneous entity in terms of the cells that it contains and provides a lumped parameter model. All the cells are of the same type and the spatial structure of the tumour is neglected. The advantage of this model is that it can be easily used

for control purposes, since in most cases it involves low order equations with monotonic behaviour in terms of cell growth. On the other hand, these models tend to be unrealistic, since the assumption of homogeneous tumour is not always the case. For example, it is not trivial to describe the behaviour of cycle specific drugs. Commonly used lumped parameter modelling equations are the logistic, the exponential and the Gompertz equation.

The other approach is concerned with the effect of cycle specific drugs. The cell cycle is divided into different stages and each stage is modelled with a differential equation. This type of model is more detailed and precise when cycle specific drugs are used for chemotherapy. However, it is more complex than the previous one, from mathematical point of view. Another drawback of this modelling approach is that it is difficult to determine the exact number of cells that appear at each stage or change from one stage to another over a period of time. Still, if the model parameters are well estimated, this type of model provides a good representation of the problem. (Swan, 1987; Bajzer *et al.*, 1996; Parker and Doyle, 2001).

2.5.1 Cell Cycle non-Specific Models

Martin (1992) and Martin and Teo (1992) used Gompertz equation to model tumour growth to apply optimal control for deriving chemotherapy schedule. The drugs considered were cycle non-specific and the kill rate was not dependent upon the size of the tumour. The toxicity of the drug was considered to be equal to the drug concentration multiplied by the time of exposure to the drug. As a result, the cell loss was an affine function of the drug concentration. Some constraints were placed to define the acceptable levels of toxicity. The anti-cancer agent was delivered continuously to the tumour site by infusion. It was assumed that there was an instantaneous mixing of the drug with the plasma and an immediate delivery of the drug to the tumour site. In order to avoid drug resistance, one additional constraint was posed which forces the tumour size to decrease at, or faster than, a given rate. The optimal control problem in this case was formulated as the minimization of the final tumour population. The problem was solved by using control vector parameterization.

Costa *et al.* (1994) developed a model of tumour cell growth for cycle non-specific chemotherapy. The aim was to derive an optimal treatment when a rate-of-kill term of saturation type was considered. The control variable was the concentration of the drug in the environment. Drug resistance and toxicity were also taken into account. The optimal chemotherapy problem was examined in three cases. The first model was independent of tumour growth rates, the second assumed the Malthusian (exponential) case and the third used the logistic equation. The tumour undergoes homogeneous growth, i.e. it does not depend on the cell position within the tumour. Drug resistant and sensitive cells were both modelled. The kill rate of the drug was considered as a function of the size of the sensitive cells population. The kill rate should tend to a maximum value if the drug concentration increases without any bounds and should be zero if no drug is present (saturation effect of the drug). The results derived from this study showed that the optimal solution is strongly influenced by the parameters of the model.

In a following study, Costa *et al.*, (1995) modelled the kinetics of the drug, when the mixing of the drug in the plasma is not instantaneous and the delivery to the tumour site includes delay. A pharmacokinetic equation was added to describe the relation between drug concentration at the tumour site and delivered drug concentration (first-order kinetics). Two tumour growth models were used: the Malthusian (exponential) model and a more general model. The tumour was considered to undergo homogeneous growth and consists of both sensitive and drug-resistant cells. The kill rate in both cases was assumed to be linear. The optimal control problem provided injected drug concentration profiles. The results for the two growth models were different and seemed to be in accordance with clinical evidence.

Barbolosi *et al.* (2001) formulated an optimization problem in which the value of the tumour cells at the end of a fixed time period was minimized, while toxicity was limited by always maintaining a lower bound on the white blood cell count. The tumour was considered homogeneous, not only throughout its growth but also after being perturbed by an anticancer drug. A cell-kill hypothesis was presented that suggested that the cell loss function depends on the drug concentration at the tumour site. Plasma and active drug concentrations were distinguished by considering the dynamic relationship between the kinetic behaviour of the administered drug and its

corresponding concentration profile at the cell level. A compartmental model was used for this purpose. The constraints, maximum allowed concentration and maximum allowed drug exposure were imposed and the problem was solved by using MATLAB. The data used for the solution were artificially chosen to provide a generic treatment of a solid tumour by an anticancer drug. A modification of the toxicity constraint, in order to include the white blood cell constraint, results in a new model. The optimization problem in this case was to minimize tumour burden while limiting toxicity at the level of WBC (white blood cell) count. Iliadis and Barbolosi (2000) considered a similar case where the chemotherapy protocols were optimized by using simulations.

2.5.2 Cell Cycle Specific Models

An optimal control problem was considered by Pereira *et al.* (1990), which allows the computation of an optimal dosage schedule for several drugs. The model considers the possibility that each cell spends different periods of time in the various phases and each phase was divided into several compartments. The cell cycle was described by four to five phases. The objective of the optimal control problem was to find a combination chemotherapy that minimizes a cost function where the cost function takes into consideration the toxicity and tumour growth. An algorithm based on model reference adaptive scheme was used to estimate the model parameters. Drug resistance, toxicity effects to normal tissue and drug interactions, if incorporated in the model would increase its reliability.

Panetta and Adam (1995) developed a model for cycle specific chemotherapy. It combined the four stages of the cell cycle into one, so that the resulting model has two-compartments: a cycling and a resting one. The resting cells are not affected by drugs. Two chemotherapeutic effects were investigated; the pulsed therapy and a piecewise-continuous therapy. The tumour growth is described by first order kinetics. Spatial or age effects were taken into account. The model also included an equation that describes the effects of the drugs on normal tissue, such as bone marrow. Two cases were considered: the first assumed that normal tissue has limited growth compared to the tumour growth and the second one assumed the logistic growth law, for both the piecewise and the pulsed therapy. The ranges of the model parameters

were calculated, in terms of dose and period, needed to prevent further growth of the tumour. The optimal period needed for maximum tumour reduction was calculated, using growth factors and chemotherapeutic regimens. This work showed that the piecewise model is the more realistic one, but mathematically is more difficult to investigate. One of the limitations of this model is that it does not take into account the variations in the parameters.

Panetta (1997) developed a model that describes the effects of cell cycle specific drugs and used clinical data from medical literature to estimate the parameters for breast and ovarian cancer. The cell cycle was divided in two compartments: the proliferating cell mass and the quiescent cell mass. The proliferating cells are sensitive to treatment, whereas the quiescent cells are resistant to treatment. Normal tissue was also modelled and the parameters that relate to bone marrow toxicity were estimated. This work examined the effects of Taxol (Paclitaxel) on breast and ovarian cancer by using data from various clinical studies. The objective was to destroy cancer while protecting the bone marrow cell growth. Paclitaxel is a cell cycle specific drug that is used in cancer chemotherapy as a single agent. It is most cytotoxic to cells in mitosis, less toxic in pre- and post-mitosis phases and non-toxic in resting phase. Toxicity to normal tissue is very limiting, especially in the case of bone marrow.

A mathematical model for treatment with the antimitotic agent curacin A was developed by Kozusko *et al.* (2001). Antimitotic agent curacin A is an experimental drug currently under investigation. Curacin A interferes with the cells' microtubule dynamics and prevents completion of mitosis. Other antimitotic drugs are Paclitaxel and Vinblastine. The model describes the effects of curacin A in vitro. Several assumptions were made in the development of the in vitro growth model: such as, the in vitro growth medium is constant, thus the cells are growing at a fixed rate and there are no quiescent cells. Growth studies were used to determine effects on the cell cycle and cell viability. Numerical solution of the differential equations predicted the minimum concentration to prevent growth.

Kimmel and Swierniak (2003) applied optimal control theory to models of cell cycle dynamics where the cell cycle is divided into subphases. Three types of perturbation

of the cell cycle were considered: cell killing, cell arrest and alteration of the Transit Time. Three cases were examined: the first considered a cell cycle non-specific agent and the cell cycle is modelled as a single compartment. The second assumed the use of a killing agent that is cycle specific, so the cell cycle was divided into two compartments: the sensitive cells and the resistant cells. The third one modelled the effect of a blocking agent, which acts in DNA synthesis phase, and the effect of a killing agent, which is cycle specific and acts in pre-mitotic and mitotic phase. In vitro experimental models were used for the parameter estimation. The optimal control problem was formulated as the maximization of the number of cancer cells, which the agent kills, while keeping the toxicity to the normal tissues within acceptable limits. Swierniak *et al.* (2003) and Ledzewicz and Schattler (2000) examined similar cases.

2.6 Parametric Programming and Control

2.6.1 Parametric Programming

Parametric programming is a generic mathematical technique that for a given objective function to optimize, a vector of optimization variables and a vector of parameters, provides the optimization variables as a set of functions of the parameters and the corresponding regions in the space of parameters, called critical regions, without exhaustively enumerating the entire space of the parameters.

Consider the following general parametric programming problem:

$$z(\theta) = \min_{x,y} f(x, y, \theta)$$
$$\text{s.t.} \quad g(x, y, \theta) \leq 0 \tag{2.1}$$

where,

x is the vector of continuous variables

y is the vector of 0-1 binary variables

$\theta \in \Theta$ is the vector of parameters bounded between certain lower and upper bounds.

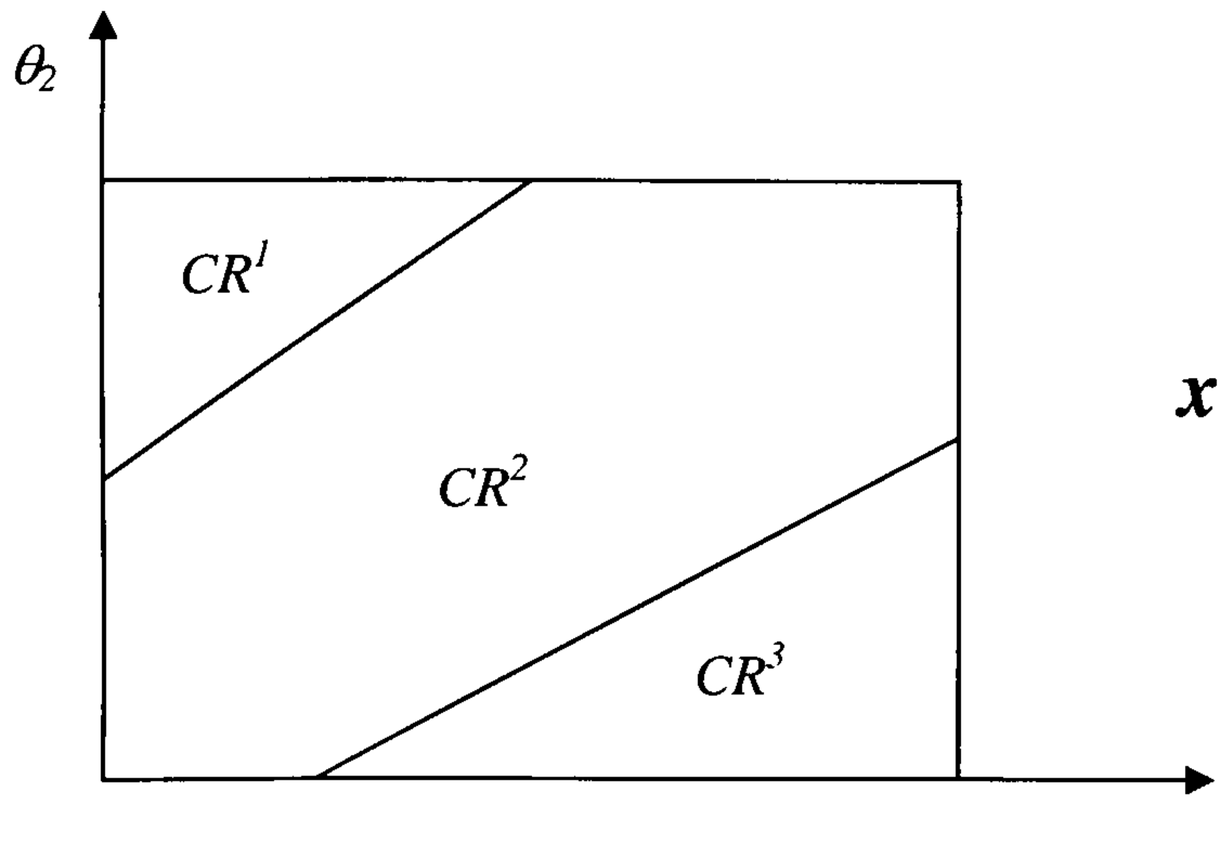
The solution of (2.1) for the case when no y is present in the formulation is given by:

$$x(\theta) = \begin{cases} x^1(\theta) & \text{if} \quad \theta \in CR^1 \\ x^2(\theta) & \text{if} \quad \theta \in CR^2 \\ \vdots & \\ x^i(\theta) & \text{if} \quad \theta \in CR^i \\ \vdots & \\ x^N(\theta) & \text{if} \quad \theta \in CR^N \end{cases}$$

such that $CR^i \bigcap CR^j = \varnothing$, $i \neq j$, $\forall i, j = 1,\ldots,N$ and $CR^i \subseteq \Theta, \forall i = 1,\ldots,N$ where a CR^i denotes a critical region. A graphical interpretation of the solution of (2.1) is depicted in Figure 2.9 where $x(\theta)$ is obtained by solving only three optimization problems. Substituting $x(\theta)$ into f provides the $z(\theta)$, the parametric profile of the objective function.

The procedure for obtaining $x^i(\theta)$ and CR^i depends upon whether f and g are linear, quadratic, nonlinear, convex, differentiable or not, and also on whether or not y is present in the formulation. A number of algorithms have been proposed for the solution of (2.1) and have been tested on a number of applications. For the case when no y is present and f and g are linear in x and θ, (2.1) reduces to a multiparametric linear program (mp-LP). Algorithms for mp-LPs based upon the Simplex algorithm when θ is present on the right hand side of the constraints and in the coefficients of the objective function are given in Gal (1995). Bansal *et al.* (2000) presented an mp-LP approach for the solution of flexibility analysis problems in the field of process design under uncertainty. An algorithm for multiparametric quadratic programs (mp-QP) with convex and quadratic f and linear g has been proposed by Dua *et al.* (2002). The basic idea of this algorithm is to iteratively identify a set of unique active constraints and the corresponding critical regions by writing the Karush-Kuhn Tucker optimality conditions of the mp-QPs. This algorithm is described in Appendix D and can be used for the solution of model based control problems to obtain control variables as an explicit function of the state variables (Pistikopoulos *et al.*, 2002). The algorithms for mp-LPs and mp-QPs provide exact solutions to the problem, whereas for the case when f and g are general nonlinear functions, the algorithms provide an approximation of the solution within a pre-specified tolerance. The approximation of

the parametric solution for the case when f and g are continuous and convex is based upon the continuity and convexity properties of $z(\theta)$ given in Fiacco (1983).



$$\boldsymbol{x}(\theta)=\begin{cases}\boldsymbol{x}^1(\theta) & \textbf{if} \quad \theta\in \boldsymbol{CR}^1\\ \boldsymbol{x}^2(\theta) & \textbf{if} \quad \theta\in \boldsymbol{CR}^2\\ \boldsymbol{x}^3(\theta) & \textbf{if} \quad \theta\in \boldsymbol{CR}^3\end{cases}$$

Figure 2.9 Parametric Programming: Optimization variables as a function of parameters

Ohtake and Nishida (1985) and Pertsinidis (1992) developed algorithms for parametric mixed integer linear programs (p-MILP), where f and g are linear in x and y and θ is a scalar, based upon branch and bound (B&B) techniques and introducing cuts, respectively. Pertsinidis (1992) used the p-MILP algorithm for the solution of multi-objective optimization problems involving simultaneous minimization of cost and environmental index.

Acevedo and Pistikopoulos (1997) and Dua and Pistikopoulos (2000) presented algorithms for solution of multiparametric mixed integer linear programs (mp-MILP) by solving mp-LPs at the nodes of a B&B tree and solving mp-LPs for fixed integer solutions, respectively. Dua and Pistikopoulos (1998) and Pistikopoulos and Dua (1998) used mp-MILP algorithm for the solution of material design problem under property prediction uncertainty and planning problem under product demand uncertainty. An algorithm for mp-MILPs is presented in Appendix E. An algorithm for the solution of multiparametric mixed integer quadratic programs (mp-MIQP) proposed by Dua *et al.* (2002) provides an envelope of the solutions by identifying integer solutions, by introducing integer and parametric cuts, and solving mp-QPs for fixed integer solutions.

Pertsinidis (1992) and Acevedo and Pistikopoulos (1996) presented an algorithm for the solution of parametric mixed integer nonlinear programs (p-MINLP), where f and g are convex in x and linear in y and θ is a scalar, based upon an outer-approximation approach. A generalized Benders decomposition (GBD) approach was developed by Papalexandri and Dimkou (1998) for the solution of p-MINLPs and applied for the solution of multiobjective optimization problems. Algorithms for multiparametric mixed integer nonlinear programming (mp-MINLP) have been developed by Dua and Pistikopoulos (1999), Banerjee and Ierapetritou (2003) and Acevedo and Salgueiro (2003). The algorithm of Dua and Pistikopoulos (1999) is based upon outer approximation principles and utilizes the fact that a linear underestimator of a convex function has its maximum distance from the function at the end points of the critical region. A B&B algorithm for parametric concave programs was presented by Benson (1982). Algorithms for multiparametric global optimization problem are relatively new (Dua *et al.*, 2004) and rely on obtaining multiparametric overestimators and underestimators that converge by using a B&B framework. Sakizlis (2003) developed two algorithms for multiparametric dynamic optimization problems based upon control vector parameterization and based upon the optimality conditions respectively.

2.6.2 Model Based and Parametric Control

Model based control techniques provide a sequence of control actions over a future time horizon that optimizes the controller performance based upon the predicted state of the system. This concept is illustrated in Figure 2.10 where k is the current time interval and N is the prediction horizon. At the next time interval, k+1, the optimization problem is solved and this sequence is repeated so as to bring the state of the system to the desired level.

A key disadvantage of model based control techniques is that they require solving an optimization problem at regular time intervals so as to optimize the controller performance (Figure 2.11). The main advantage on the other hand is that constraints on state and control variables can be taken into account. Pistikopoulos *et al.* (2002) and Bemporad *et al.* (2002) presented a parametric programming approach where control variables were treated as optimization variables and state variables as parameters. The model based parametric controller thus derived has the advantages of

model based controller, does not require on-line optimization solvers and require simple function evaluations (Figure 2.12) that can be implemented on a microchip.

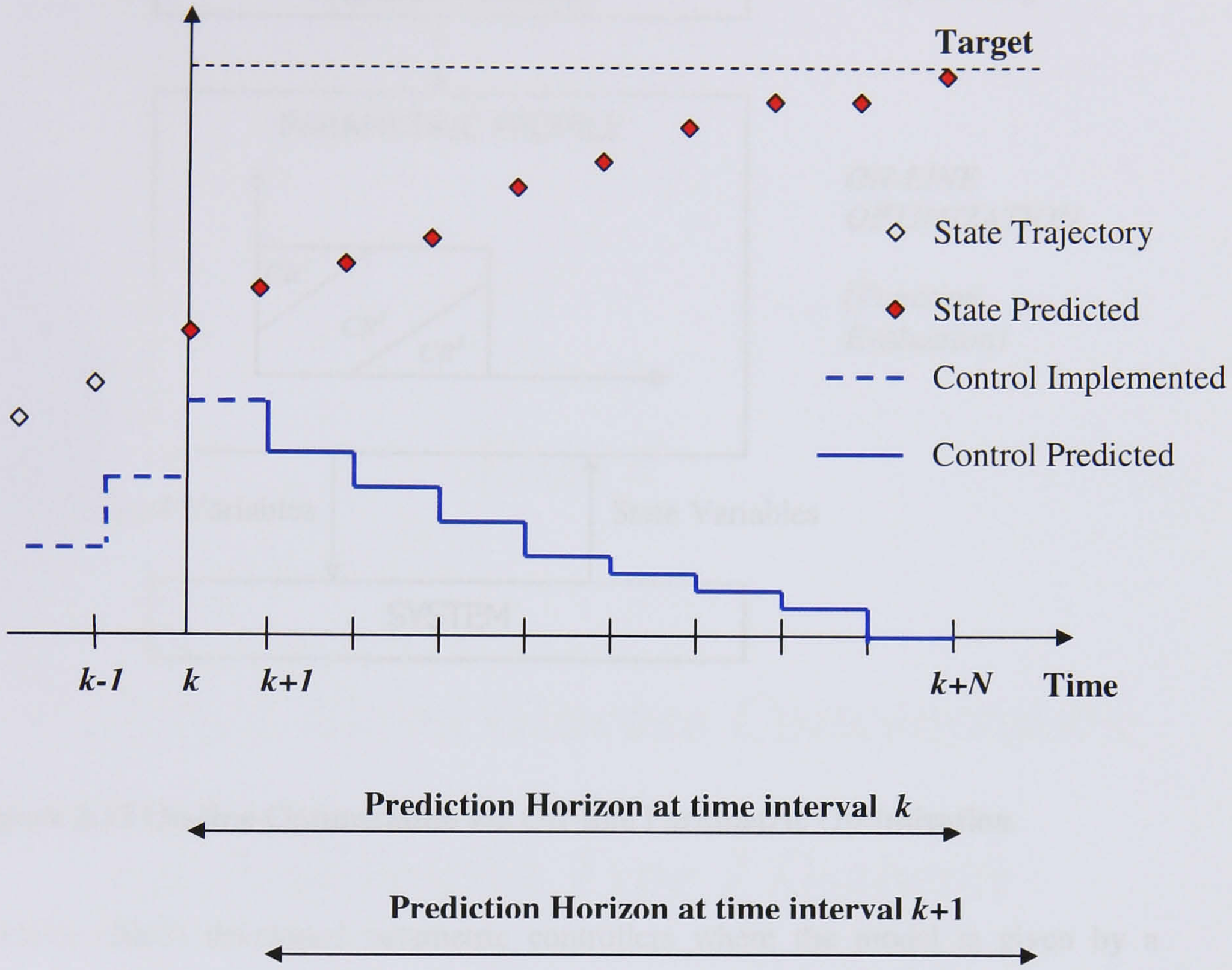


Figure 2.10 Model Based Control

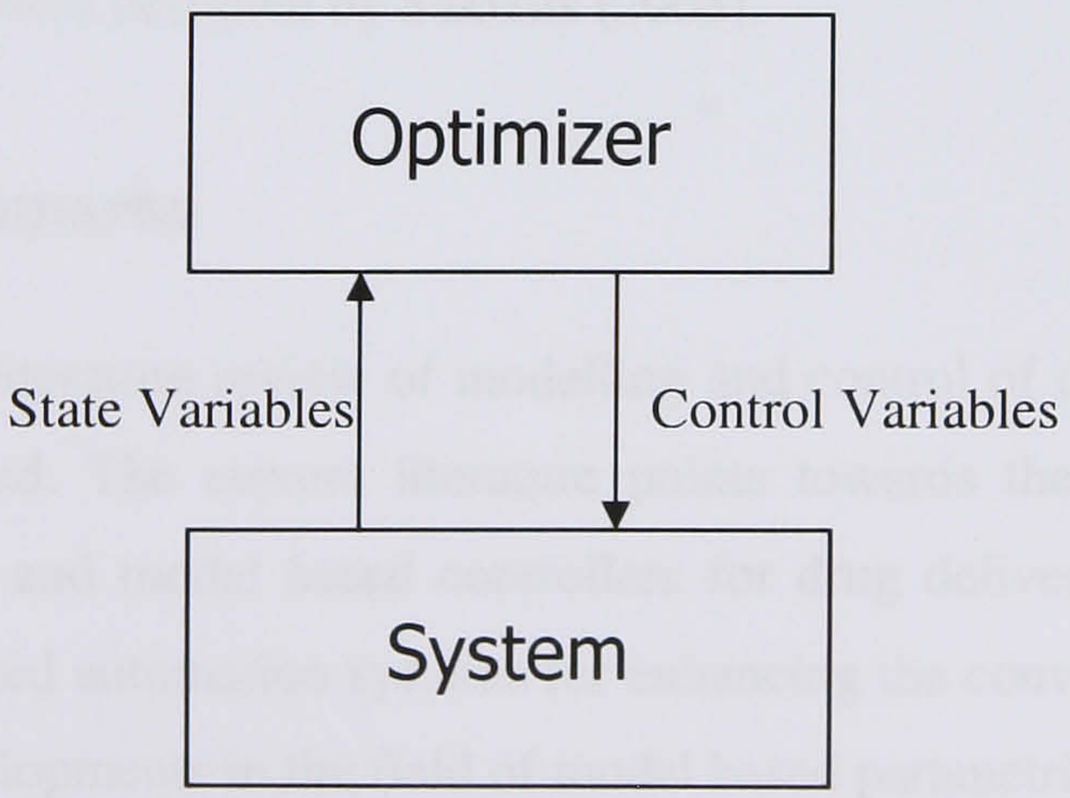


Figure 2.11 On-line Optimization

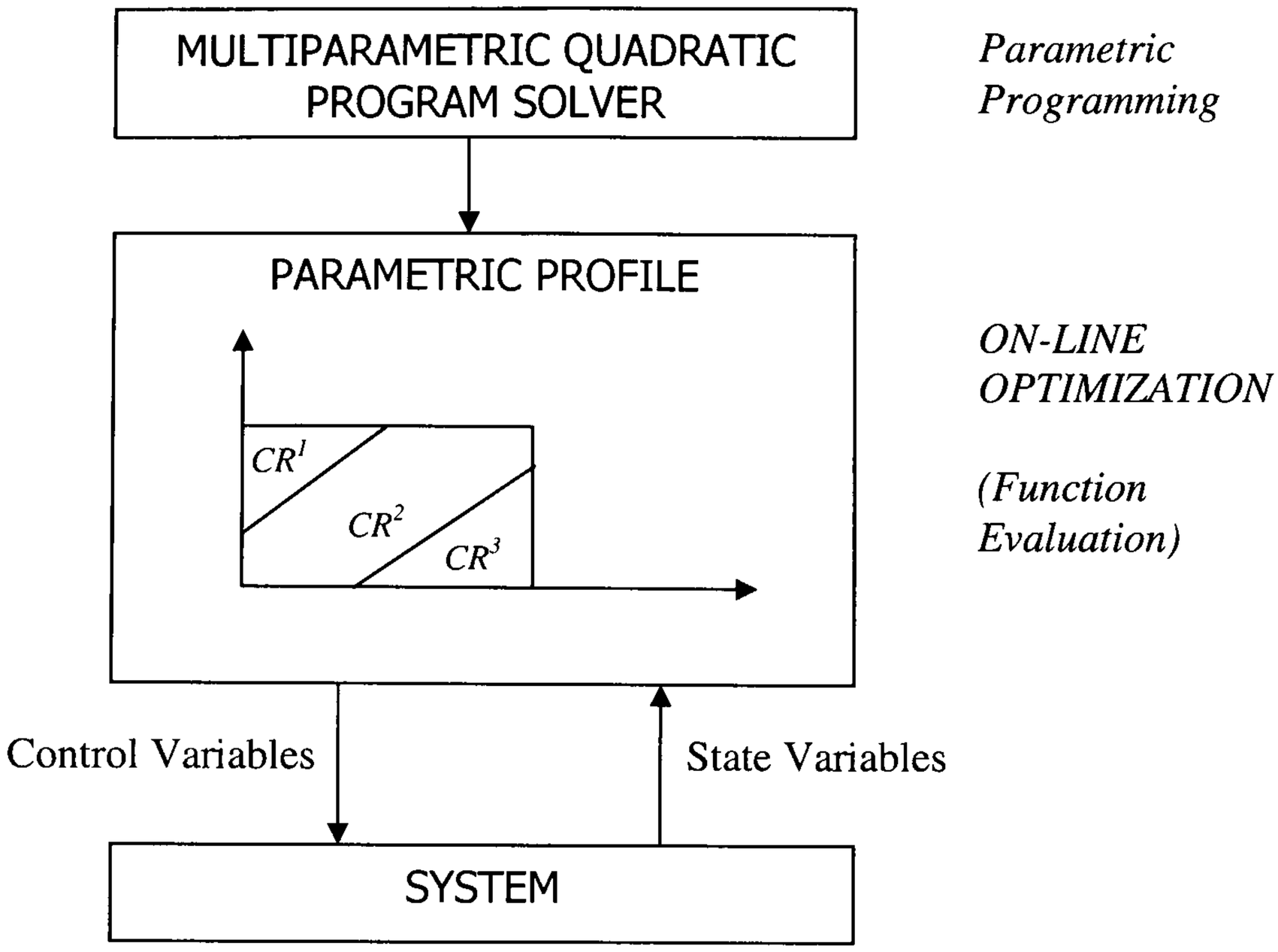


Figure 2.12 On-line Optimization via Off-line Parametric Optimization

Sakizlis (2003) developed parametric controllers where the model is given by a continuous time formulation, unlike the discrete time intervals described in the last paragraph. An algorithm for robust parametric controllers that can take into account disturbances in the system was also presented by Sakizlis *et al.* (2004). Parametric controllers for hybrid systems, that also involve logical conditions modelled via 0-1 binary variables, were designed by Sakizlis (2003).

Concluding Remarks

In this chapter a literature review of modelling and control of drug delivery systems has been presented. The current literature points towards the need of developing advanced models and model based controllers for drug delivery systems. This will lead to sophisticated automation systems for enhancing the convenience and safety of the patients. Developments in the field of model based parametric controllers that will play a crucial role in the automation were also reviewed. The next chapter addresses control of blood glucose concentration for people with type 1 diabetes.

Part I

Control of Blood Glucose Concentration for People with Type 1 Diabetes

Chapter 3

Blood Glucose Control for Type 1 Diabetes

An advanced model based control technique for regulating the blood glucose for patients with Type 1 diabetes is presented. The optimal insulin delivery rate is obtained off-line as an explicit function of the current blood glucose concentration of the patient by using novel parametric programming algorithms. The implementation of the optimal insulin delivery rate therefore requires simple function evaluation and minimal on-line computations. The proposed framework also addresses the uncertainty in the model due to inter- and intra-patient variability. This is expected to simplify the insulin delivery mechanism, thereby enhancing the quality of life of the patient.

3.1 Introduction

Diabetes is a chronic disease characterized by inadequate control of blood glucose concentration in the body. People with diabetes rely on exogenous insulin to be infused at appropriate rates to keep the blood glucose levels within certain desired levels. This chapter presents a model based parametric control approach for blood glucose regulation - the rest of the chapter is organized as follows. In the next section an introduction to the blood glucose control in the normal body is provided. Section 3.3 gives an introduction to diabetes and reviews the current technology available for the treatment of diabetes. Model based control is discussed in section 3.4. The parametric programming approach is discussed in section 3.5 and section 3.6 presents the derivation of the explicit insulin delivery rate for a patient model taken from the literature. The issue of uncertainty is addressed in section 3.7 and finally concluding remarks are presented.

3.2. Blood Glucose Control in the Normal Body

The blood glucose level in the body is controlled by pancreas. The pancreas is an organ that is located behind the stomach next to the duodenum (see Figure 3.1). The size of the pancreas is similar to that of a banana and has a slight curve on it, and is about the same length, width and thickness.

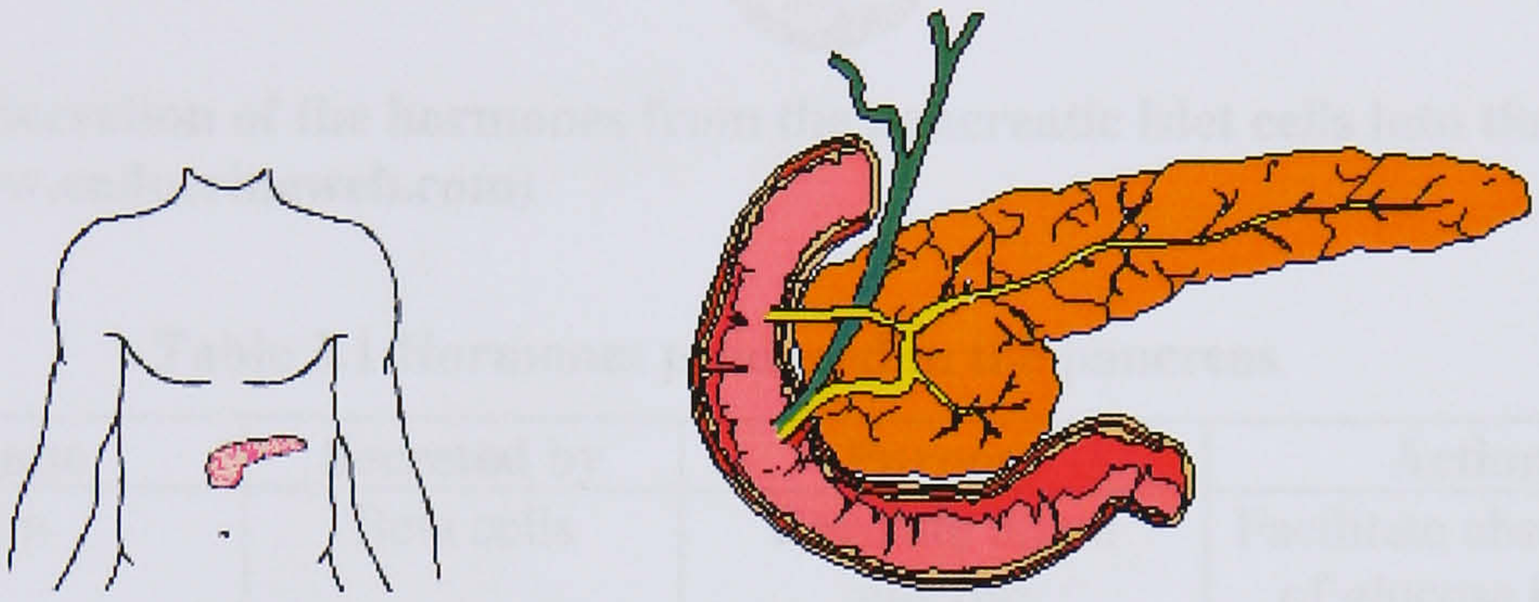


Figure 3.1 (a) Location of the pancreas in the human body and (b) the pancreas (www.endocrineweb.com)

The pancreas is responsible for carrying out two main functions: (i) to produce pancreatic endocrine hormones and (ii) to produce pancreatic digestive enzymes. The digestive enzymes are produced in the cells which constitute about 90% of the total cell mass of the pancreas. These enzymes break down the proteins, fats and carbohydrates, in the food that we eat, to smaller molecules that facilitates their absorption into the intestines. These enzymes enter the intestine through a tube called the 'pancreatic duct' that runs through the middle of the pancreas. The pancreatic hormones are responsible for maintaining the sugar and salt balance in the body. These are produced by the endocrine cells which are about 5% of the total pancreatic mass. These cells are clustered in groups within the pancreas and are also known as the 'Pancreatic Islets' or the 'Islets of Langerhans' because they look like little islands of cells under a microscope. In the pancreatic islets are the cells, called the pancreatic islet cells that are responsible for producing specific hormones. Unlike the digestive pancreas that secrete enzymes into the ducts, pancreatic islets secrete the hormones into the bloodstream (see Figure 3.2). This allows the endocrine hormones to reach

cells that are even far away. The hormones which are secreted in the pancreas and their functions are given in Table 3.1.



Figure 3.2 Secretion of the hormones from the pancreatic islet cells into the blood vessels (www.endocrineweb.com)

Table 3.1 Hormones produced in the pancreas

Hormone	Secreted by	Purpose	Action
Insulin	Beta cells	Regulate blood glucose	Facilitate absorption of glucose in the cells
Amylin	Beta cells	Tend to supplement that of insulin	Inhibit secretion of glucagon
Glucagon	Alpha cells	Assist insulin in blood glucose regulation	Facilitate release of glucose from the cells
Somatostatin	Delta cells	Regulate the production and excretion of other endocrine hormones	Slow down the production of endocrine hormones
Gastrin	Gastrin cells	Assist in digestion in the stomach	Induce stomach to produce acid
Vasoactive Intestinal Peptide	D1 cells	Help control water absorption and secretion from the intestines	Causes intestinal cells to secrete water and salts into the intestines
Pancreatic Polypeptide	Gamma cells	Unknown	Unknown

The interplay between insulin and glucagon maintains the blood glucose concentration in the body: insulin lowers the blood glucose concentration whereas glucagon increases it (see Figure 3.3). After a meal, the carbohydrates are absorbed from the intestines into the blood resulting in an increased blood glucose concentration. This stimulates the production of insulin which prevents the blood glucose concentration

from increasing substantially, by activating the receptors that allow the absorption of glucose in the cells. In contrast, in between meals or in the state of sleep, the body is essentially starved of glucose. This stimulates the α-cells of the pancreas to produce glucagon, which breaks the glycogen molecules to glucose and prevents the glucose concentration from decreasing substantially. These opposite effects of insulin and glucagon help regulate the blood glucose concentration.

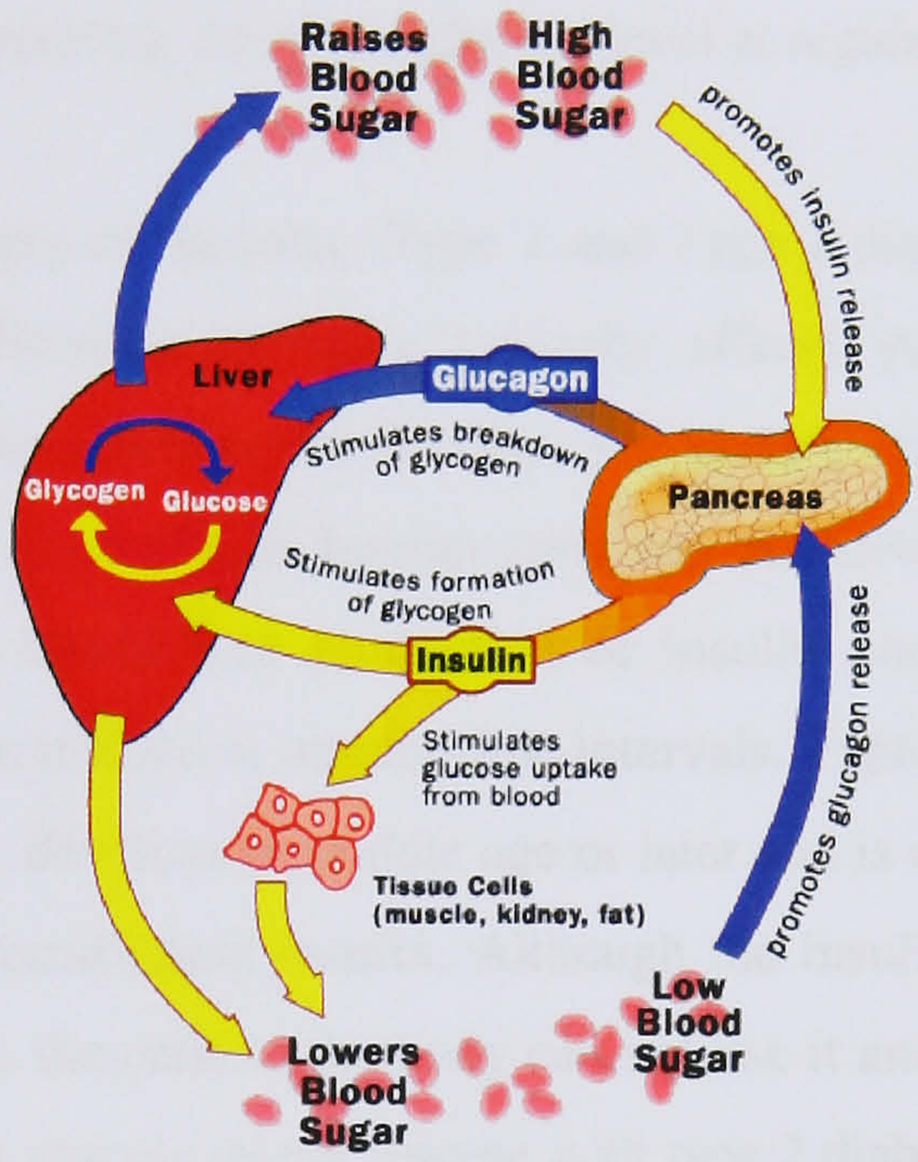


Figure 3.3 Blood glucose control via interplay between insulin and glucagon (www.howstuffworks.com)

3.3 Introduction to Diabetes

Diabetes is a chronic disease that is characterized by relative or absolute insufficiency of insulin to regulate the blood glucose concentration. Approximately 177 million people have diabetes worldwide and this number is expected to increase to 300 million by the year 2025 (www.who.int/mediacentre/factsheets/fs236/en/). According to the Diabetes Control and Complications Trial (DCCT) (DCCT, 1993), blood glucose concentration should be controlled within the range 60-120 mg/dL.

The two main tests used to diagnose diabetes are (i) the direct measurement of the blood glucose levels after an overnight fast, known as the fasting blood glucose test and (ii) measurement of the body's ability to appropriately handle the excess glucose, known as the Oral Glucose Tolerance Test (OGTT). The fasting blood glucose test is based upon testing the blood glucose level after an overnight fast i.e. not eating anything after midnight. If a value above 140 mg/dL is observed on atleast two occasions, the person is considered to be suffering from diabetes. OGTT is performed after the person has fasted for 10-16 hours and subsequently giving the person a dose of glucose and then measuring the blood glucose level at regular time intervals.

There are two main types of diabetes: Type 1 and Type 2 diabetes. Type 1 diabetes, also known as juvenile-onset diabetes, typically affects younger individuals and usually occurs due to an autoimmune disorder. The body's immune system perceives the insulin producing islet cells as foreign cells and produces antibodies to destroy them. This results in insufficient production of insulin and the patient relies on exogenous insulin to be infused at regular time intervals. Type 2 diabetes, also known as adult onset diabetes, develops in middle age or later and is characterized by insulin resistance rather than insufficient insulin. Although the insulin levels are normal or higher than the normal, the cells in the body can not use it and fail to absorb glucose leading to higher blood glucose levels. People with type 2 diabetes initially respond to oral drugs but may need insulin infusions at a later stage. The focus of this work is on type 1 diabetes.

The current treatment for people with type 1 diabetes involves 3-4 daily glucose measurements, normally coinciding with the meal times, usually by an invasive method of finger prick, followed by an equivalent number of subcutaneous insulin injections. If insulin is supplied in excess, the blood glucose concentration falls below the normal value (<60 mg/dL) and this state is known as *hypoglycemia*, whereas if insulin is not supplied sufficiently, the concentration rises above the normal value (>120 mg/dL) and this state is known as *hyperglycemia.* Both these situations can be harmful to an individual's health, in very different ways. Hypoglycemia has short term effects which can lead to diabetic coma and possibly death, while hyperglycemia has

long term impact that has been linked to nephropathy, retinopathy and other tissue damage.

The effectiveness of the treatment is usually assessed by two main methods: (i) regular measurements of blood glucose and (ii) measurement of glycosylated hemoglobin. The main objective of the therapy is to keep the fasting blood glucose level below 140 mg/dL and within the 60-120 mg/dL range. Usually the blood glucose measurements are done and recorded 4 times a day, before each meal and at bed time, to assess how well the blood glucose levels are controlled. This information is then used to adjust the amount of insulin and the diet of the patient. The physicians are also very keen on assessing the level of the blood glucose overnight and therefore want the patients to test and keep a record of their blood glucose levels at 2 a.m. It is desirable that the blood glucose levels remain more than 65 mg/dL to avoid overnight hypoglycemia. The second method for the assessment of the effectiveness of the therapy relies on the measurement of glycosylated hemoglobin and is known as Hemoglobin A1c (HbA1c) test. Unlike the first assessment method, this test has to be carried out in the physician's laboratory. HbA1c gives a good indication of how the patient's blood glucose levels have been for the past 2-3 months. It has been shown that the HbA1c values in the desired range of 6.5-7.5 result in less diabetic complications later in life.

The current medical practice for the treatment of type 1 diabetes, which involves invasive methods of glucose measurement and insulin infusion, is not only inconvenient and painful but also unreliable due to the approximation involved in the amount and type of insulin delivered. A significant amount of research is being carried out to overcome the shortcomings of the current medical practice. The main research issues that are being investigated are concerned with: type of insulin, the site and mode of insulin delivery, glucose sensors and control algorithms for computing the optimal amount of insulin to be delivered. These issues are discussed in the following paragraphs. An introduction to the insulin and different types of insulin is presented in the next section.

3.3.1 Insulin

Insulin has the empirical formula $C_{254}H_{377}N_{65}O_{75}S_6$ and its structure is shown in Figure 3.4 where Carbon, Oxygen, Nitrogen and Sulphur are denoted by red, green, blue and pink respectively.

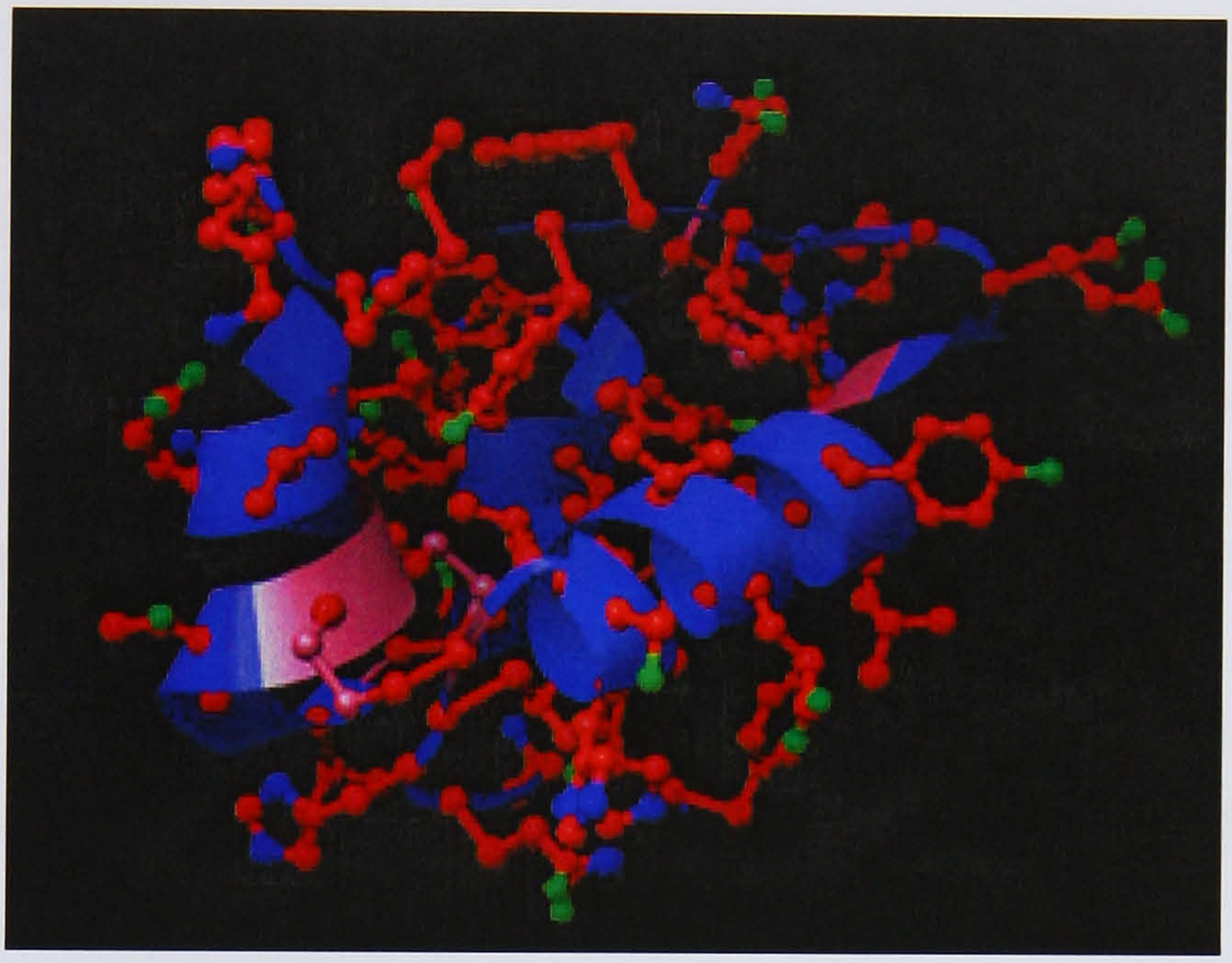


Figure 3.4 Structure of insulin

Commercially available insulin which is used by people with diabetes is taken from animals or manufactured in the labs so as to be similar to the human insulin. There are more than 20 types of insulin that are available and can be classified based upon: (i) onset which indicates how fast the insulin starts working, (ii) peak time which is concerned with the time it has the maximum effect and (iii) duration indicating the time it lasts in the body.

These characteristics together with an individual's lifestyle, physician's experience and the person's blood glucose levels are the key factors in deciding the type of insulin to be used. The insulin preparations produced in the labs are based upon the recombinant DNA technology that allows the lab cultivated bacteria or yeast to produce the human insulin. Recently, a number of insulin analogues which slightly differ from the human insulin, by one or two amino acids, have been produced that

have different onset and peak time characteristics. A list of common insulin preparations is given in Table 3.2. Next section gives a brief overview of the major insulin delivery routes and their main advantages and disadvantages.

3.3.2 Routes of Insulin Delivery

There are four major sites for invasive insulin delivery (Nalecz *et al.*, 1987): subcutaneous, intramuscular, intravenous and intraperitoneal. While the subcutaneous site is the simplest and safest in the long term, the absorption of insulin from the subcutaneous tissue is delayed. The intramuscular site is usually preferred for people affected by brittle diabetes, who have a subcutaneous barrier to insulin absorption, but may result in muscle fibrosis and disconnection of cannula. The intravenous site on the other hand results in faster delivery of insulin and therefore is ideal for controlling the glucose concentration. The most physiologic mode of insulin delivery is achieved through the intraperitoneal site, though the major disadvantage is its difficult access. A review of the currently used insulin delivery devices and those being developed is given in the next section.

3.3.3 Insulin Delivery Devices

Insulin syringes are the commonly used method for delivering insulin through the skin and into the fatty tissue below the skin. These syringes are available in different sizes for different insulin strengths and dosages and have needles with a special coating to reduce the pain as the needles enter the skin. New technological advances have brought in devices that aim to deliver precise amounts of insulin with minimal pain. Insulin pens look just like pens and have a fine short needle to deliver insulin under the skin. They are available as disposable or having refillable cartridges of insulin. The delivery mechanism involves turning a dial to select the amount of insulin and then pressing a plunger to deliver the insulin. Jet injectors take a step further in increasing the patient comfort level by using high pressure air to deliver insulin through the skin by using a head that has the diameter of the fraction of that of the syringe needle. Unlike insulin syringes which result in a pool of insulin under the skin,



Table 3.2 Insulin preparations

Type of Insulin	Examples	Onset of Action	Peak of Action	Duration of Action
Rapid-acting	Humalog (lispro) Eli Lily	15 minutes	30-90 minutes	3-5 hours
	NovoLog (aspart) Novo Nordisk	15 minutes	40-50 minutes	3-5 hours
Short-acting (Regular)	Humulin R Eli Lily Novolin R Novo Nordisk	30-60 minutes	50-120 minutes	5-8 hours
Intermediate-acting (NPH)	Humulin N Eli Lily Novolin N Novo Nordisk	1-3 hours	8 hours	20 hours
	Humulin L Eli Lily Novolin L Novo Nordisk	1-2.5 hours	7-15 hours	18-24 hours
Intermediate and short-acting mixtures	Humulin 50/50 Humulin 70/30 Humalog Mix 75/25 Humalog Mix 50/50 Eli Lily Novolin 70/30 Novolog Mix 70/30 Novo Nordisk	The onset, peak and duration of action of these mixtures would reflect a composite of the intermediate and short or rapid-acting components, with one peak of action		
Long-acting	Ultralente Eli Lily	4-8 hours	8-12 hours	36 hours
	Lantus (glargine) Aventis	1 hour	None	24 hours

the jet injectors produce a mist of insulin which gets absorbed more quickly and this effect should be taken into account while calculating the amount of insulin dosage. Insulin pumps are worn outside of the body and deliver precise amount of insulin through a catheter that is located under the skin of the abdomen and connected to the pump through a flexible tubing. The pump is programmed to continuously give a small dosage of insulin that is supplemented with extra dosages at around the meal times.

New methods of delivery currently being developed include transdermal, pulmonary and oral modes. The transdermal mode will rely on an insulin patch placed on the skin to continuously give a small dose of insulin. These patches will have the flexibility of releasing larger dosage around the meal times. The pulmonary mode will give the rapid acting insulin as a dry powder that will be inhaled and absorbed from the lungs into the blood stream. Oral modes of delivery would be the simplest but would require insulin to be protected from the digestive enzymes in the gut. The current protective mechanisms being developed include complexing insulin to liposomes and coating it with impermeable polymers. The next section presents a brief overview of the sensors for the measurement of the blood glucose concentration.

3.3.4 Sensors for the Measurement of Blood Glucose Concentration

New sensor technologies are being developed to continuously monitor the glucose concentration (Pickup *et al.*, 1999). Amperometric enzyme electrode sensors infer the glucose concentration by measuring the catalyzed production of hydrogen peroxide. The issues that are being addressed are invasiveness and error due to other substances and biocompatibility for totally implantable sensors. While the issue of biocompatibility can be avoided by using tissue sampling techniques such as microdialysis and reverse iontophoresis, expected problems under investigation are prolonged time for sample collection, quality of the sample collected and skin infection. Another way of dealing with the issue of biocompatibility is the development of non-invasive sensors. These are based on the principles of near infrared spectroscopy, light scattering and photoacoustic spectroscopy. A detailed review of the current sensor technology is presented in Appendix A.

3.3.5 Closed Loop Glucose Control

Ultimately the objective is to develop a closed loop glucose control system (Clemens, 1979; Jaremko and Rorstad, 1989; Bellazi *et al.*, 2001; Parker *et al.*, 2001) consisting of three components: (i) glucose sensor (ii) control algorithm and (iii) a mechanical pump – see Figure 3.5. In this system, the glucose concentration will be measured by the glucose sensor and based on the measurement; the control algorithm will compute the optimal insulin delivery rate. The mechanical pump will then infuse the computed amount of insulin.

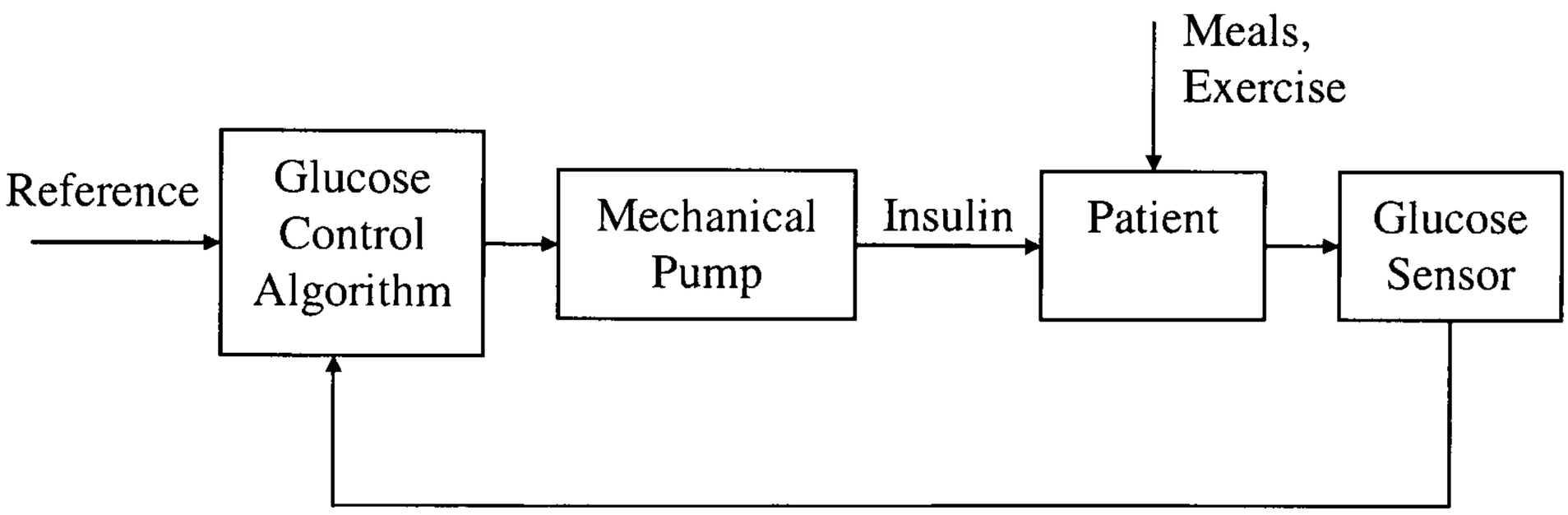


Figure 3.5 Closed loop system for blood glucose control

The control algorithms reported in the open literature can be considered to differ from each other in their ability to handle constraints, the complexity of the considered mathematical model (Bergman *et al.*, 1981; Lehmann and Deutsch, 1992; Sorensen, 1985; Nucci and Cobelli, 2000) and ease of computer implementation. While the traditional Proportional Integral (PI) control algorithm (Clemens, 1979) is easy to implement, it does not take into account constraints, i.e. the bounds on the insulin delivery rate of the mechanical pump and the hypoglycemic and hyperglycemic states of the patient. Model based control algorithms on the other hand can take into account the detailed model of the patient and simultaneously consider the constraints. These algorithms have been applied and tested on a variety of biomedical systems including the control of mean arterial pressure under anesthesia (Mahfouf *et al.*, 2003; Rao *et al.*, 2001; Gentilini *et al.*, 2001). The main limitation of the model based control

algorithms is their extensive on-line computational requirement. An introduction to model based control is presented in the next section.

3.4 Model Predictive Control (MPC)

Model based control techniques are based on the so-called receding horizon philosophy. At each sampling time, an optimal control problem is solved starting at the current state over a finite horizon. The optimal control problem consists of an objective function to be optimized, model of the system and a set of constraints on the state and control variables. The solution of this problem provides an optimal profile of the control variables over a finite time interval so as to drive the current state of the system to the target value. Only the first control action is implemented and at the next time step, a new set of measurements becomes available and the optimal control problem is resolved starting from the new state and over a shifted horizon, leading to a moving horizon policy (Garcia *et al.*, 1989).

Linear model predictive control (MPC) is one such technique that has been successfully used in a variety of control applications including process and biomedical systems. The solution of linear MPC relies on a linear dynamic model, incorporates all the input and output constraints, and optimizes a quadratic performance index. Consider the following mathematical model of the patient,

$$x_{t+1} = Ax_t + Bu_t \tag{3.1}$$

subject to the following constraints:

$$x_{\min} \le x_t \le x_{\max}$$
$$u_{\min} \le u_t \le u_{\max} \tag{3.2}$$

where:

$x_t \in R^n$ is the vector of the state variables and

$u_t \in R^m$ is the vector of the input variables

and the subscripts *min* and *max* denote lower and upper bounds respectively. Typically, x_t represents the deviation of the glucose concentration from the target value and u_t represents the insulin delivery rate, at time interval t. The MPC problem can then be posed as the following optimization problem:

$$\min_U J(U, x(t)) = x_{t+N_y|t}^T P x_{t+N_y|t} + \sum_{k=0}^{N_y-1} \left[x_{t+k|t}^T Q x_{t+k|t} + u_{t+k}^T R u_{t+k} \right]$$

$$s.t. \quad x_{\min} \le x_{t+k|t} \le x_{\max}, k = 1,....., N_c$$

$$u_{\min} \le u_{t+k} \le u_{\max}, \quad k = 1,....., N_c \qquad (3.3)$$

$$x_{t+k+1|t} = A x_{t+k|t} + B u_{t+k}, k \ge 0$$

$$u_{t+k} = K x_{t+k|t}, N_u \le k \le N_y$$

where $U = \left[u_t^T, ..., u_{t+N_u-1}^T \right]^T$ and the superscript T denotes transpose of the vector. The tuning parameters are: Q and R, that are constant, symmetric and positive definite matrices, P is given by the solution of the Riccati equation, N_y, N_u and N_c are the prediction, control and constraint horizons respectively and K is some feedback gain. Problem (3.3) is solved repetitively at each time t for the current state x_t and the vector of predicted state variables, $x_{t+1|t},.....,x_{t+Ny|t}$ at time $t+1,....,t+N_y$ respectively and corresponding control actions $u_t,....,u_{t+Ny-1}$ are obtained.

A schematic of the model predictive control for the regulation of blood glucose control is given in Figure 3.6. In the presence of the meal disturbance, the objective is to take the current blood glucose concentration to a target value by optimally manipulating the insulin infusion rate. This is achieved by minimizing the square of the deviation of the current and the future values of the blood glucose concentrations from the target value where the future values are predicted based on the model of the patient. At the current instant of time, only the first optimal insulin infusion rate is implemented and the MPC problem is resolved at the next time interval when new

glucose measurement becomes available. A key feature of this approach is that it can take into account the bounds on the insulin infusion rate and blood glucose concentration.

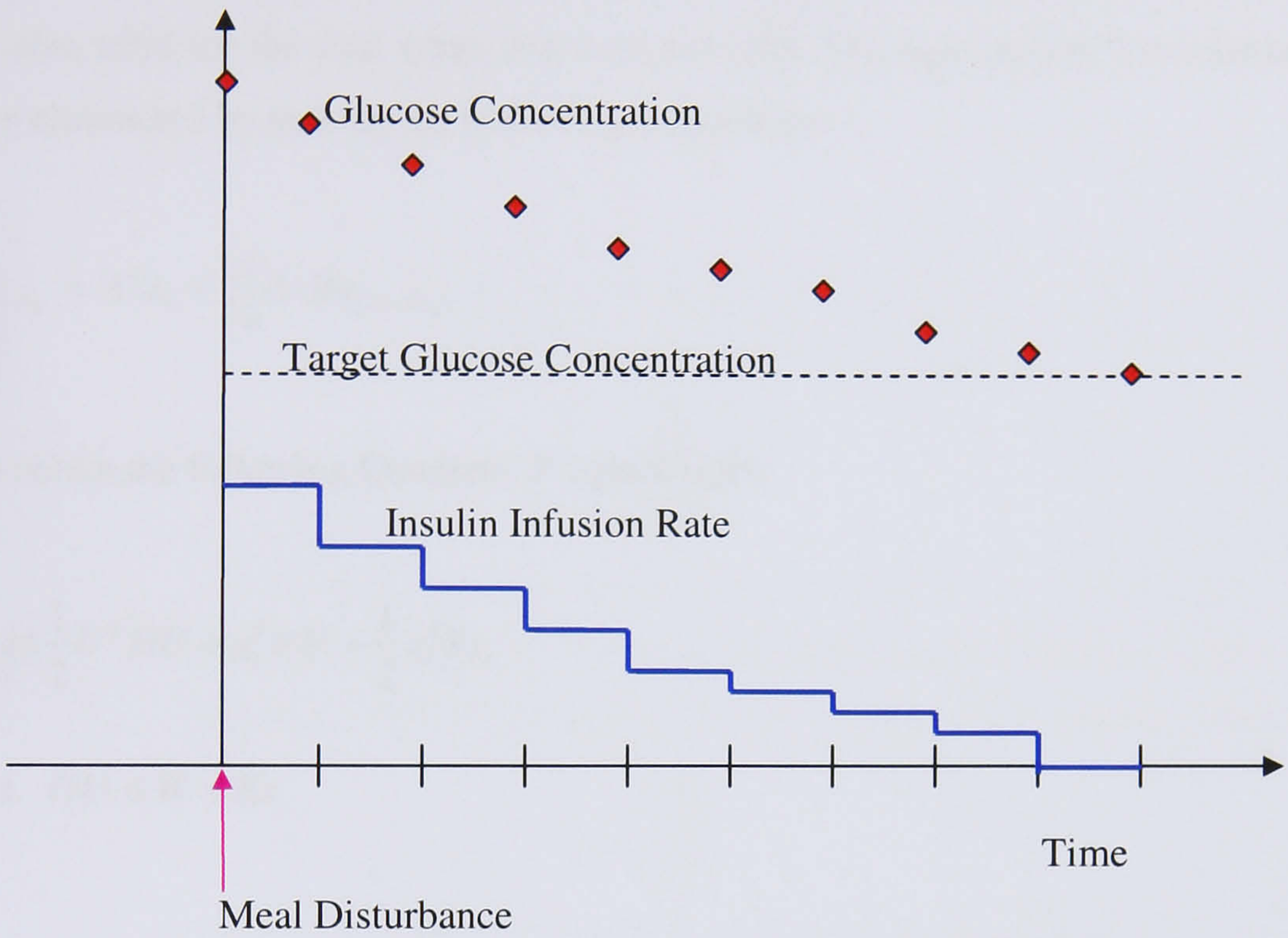


Figure 3.6 Model Predictive Control of Blood Glucose Concentration

The main drawback of MPC is that it requires solving an optimal control problem, at regular time intervals, that requires an online computer. The next section presents a parametric programming approach that does not require an online computer, can be implemented on a microchip and yet gives the same performance as MPC.

3.5 Parametric Programming and Control

Parametric programming is a technique which is usually used in an optimization framework where given an objective function, a set of constraints and a vector of parameters, an optimal value of the optimization variables is obtained as a set of functions of the parameters and the corresponding regions in the space of parameters where these functions are valid. This is a generic mathematical technique that can be

used in the MPC framework to obtain U as a function of x_t by treating U as optimization variables and x_t as parameters as described next (Pistikopoulos *et al.*, 2002; Bemporad *et al.*, 2002).

For simplicity in presentation assume that $N_y = N_u = N_c$, however, the theory presented is also valid for the case when this does not hold. The equalities in formulation (3.3) are eliminated by making the following substitution:

$$x_{t+k|t} = A^k x_t + \sum_{j=0}^{k-1} A^j B u_{t+k-1-j} \tag{3.4}$$

to obtain the following Quadratic Program (QP):

$$\begin{aligned} &\min_U \frac{1}{2} U^T H U + x_t^T F U + \frac{1}{2} x_t^T Y x_t \\ &s.t. \quad GU \le W + Ex_t \end{aligned} \tag{3.5}$$

where, $U = \left[u_t^T, ..., u_{t+N_u-1}^T \right]^T \in R^s$, is the vector of optimization variables, $s = mN_u$, H is a constant, symmetric and positive definite matrix and H, F, Y, G, W, E are obtained from Q, R and (3.1) and (3.2).

The QP problem in (3.5) can now be reformulated as a multi-parametric quadratic program (mp-QP) (Dua *et al.*, 2002):

$$\begin{aligned} &V_z(x) = \min_z \frac{1}{2} z^T H z \\ &s.t. \quad Gz \le W + Sx_t \end{aligned} \tag{3.6}$$

where, $z = U + H^{-1} F^T x_t, z \in R^s$, and $S = E + GH^{-1} F^T$.

This mp-QP is solved by treating z as the vector of optimization variables and x_t as the vector of parameters to obtain z as a set of explicit functions of x_t. U is then obtained as a set of explicit functions of x_t by using $U = z - H^{-1}F^T x_t$. Each of these functions is valid in a polyhedral region, known as the critical region, in the space of state variables x_t – see Appendix D for an algorithm for the solution of mp-QPs to obtain U as a function x_t. An overview of the parametric programming approach for the model predictive control of blood glucose concentration is summarized in Figure 3.7.

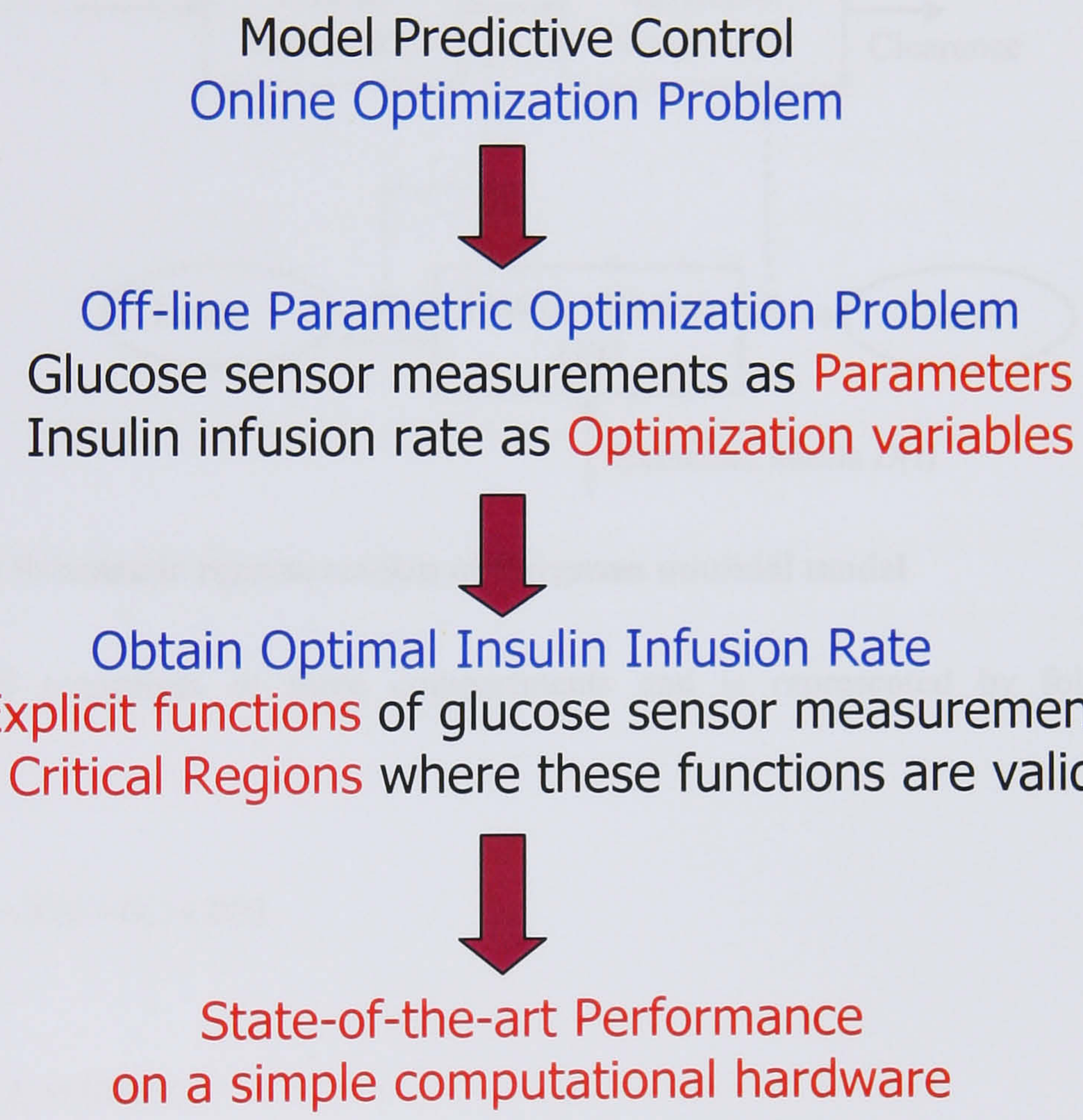


Figure 3.7 Model Predictive Control of Blood Glucose Concentration via Parametric Programming

3.6 Explicit Insulin Delivery Rate

In this section the derivation of the optimal insulin delivery rate as a function of the blood glucose concentration measurement is presented. For this purpose, a model of people with type 1 diabetes is taken from the literature and is described next.

3.6.1 Bergman Model

The widely used Bergman model (Bergman *et al.*, 1981) is selected for the controller design. The schematic representation of this model is shown in Figure 3.8. This representation captures the glucose-insulin response of the patient by using minimum number of compartments.

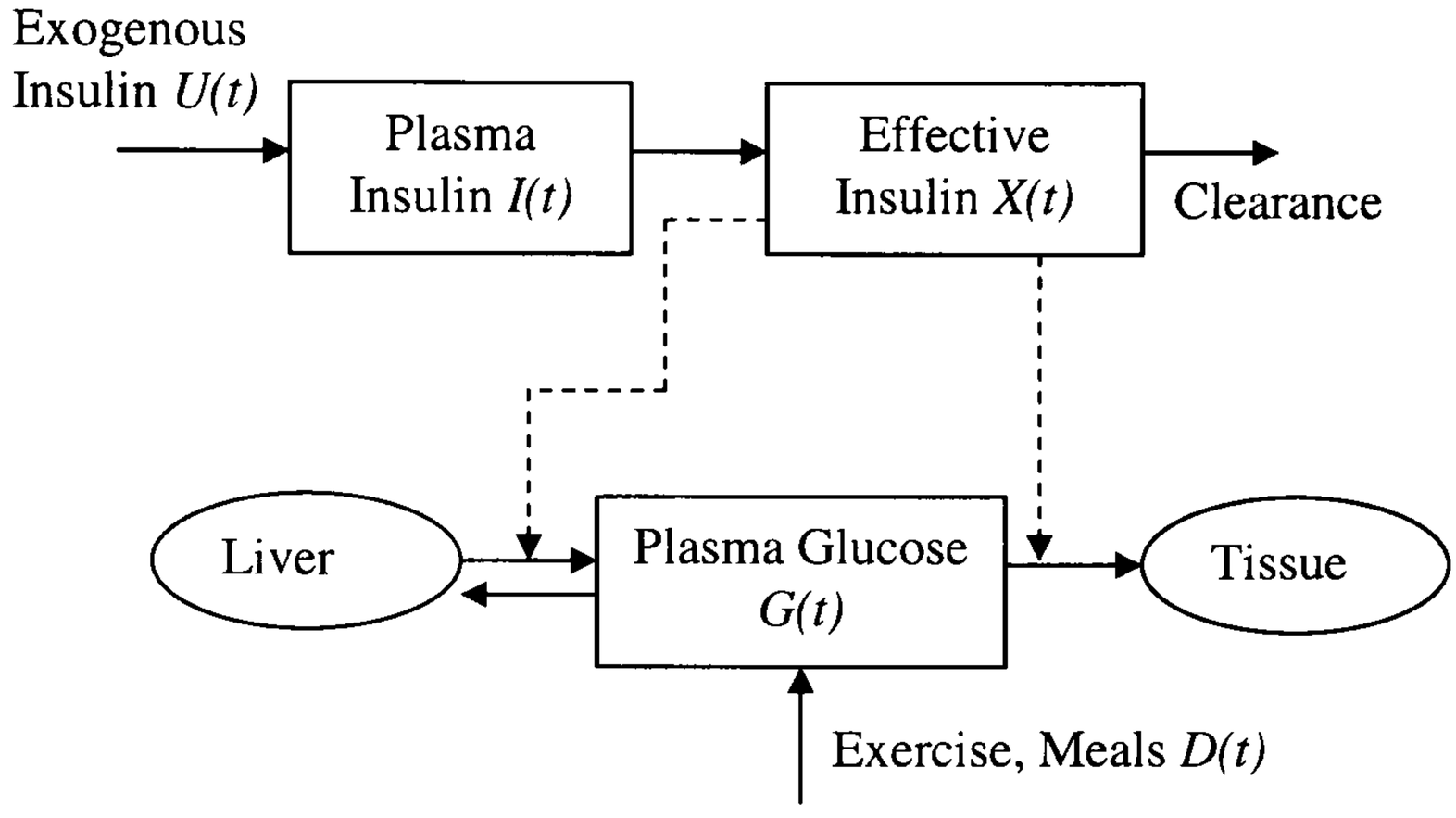


Figure 3.8 Schematic representation of Bergman minimal model

The model comprises of three compartments and is represented by following equations,

$$\frac{dG}{dt} = -P_1 G - X(G + G_b) + D(t) \tag{3.7}$$

$$\frac{dI}{dt} = -n(I + I_b) + U(t)/V_1 \tag{3.8}$$

$$\frac{dX}{dt} = -P_2 X + P_3 I \tag{3.9}$$

where:

G is the plasma glucose concentration above basal value (mg/dL)

I is the plasma insulin concentration above basal value (mU/L)

X is proportional to plasma insulin concentration in the remote compartment (min^{-1})

D is the meal glucose disturbance (mg/dL min^{-1})

U is the exogenous insulin infusion rate (mU/min)

G_b is the basal value of glucose concentration (mg/dL)

I_b is the basal value of insulin concentration (mU/L)

V_I is the insulin distribution volume (L), and

n is the fractional disappearance rate of insulin (min^{-1}).

The plasma insulin compartment is represented by (3.8) where exogenous insulin is supplied. The output from this compartment goes to the effective insulin compartment, which is represented by (3.9), where insulin is active in accelerating the glucose disappearance into the periphery and liver as shown in Figure 3.8 and represented by (3.7).

3.6.2 Parametric Controller for Blood Glucose Regulation

The states in this model are $x_t = [G\ I\ X]^T$, $u_t = U(t)$ is the control variable and G_b and I_b are the basal values of glucose and insulin concentration. The parameter values that are considered are (Fisher, 1991):

$P_1 = 0\ min^{-1}$

$P_2 = 0.025\ min^{-1}$

$P_3 = 0.000013\ L/mUmin^2$

$V_I = 12$ L, and

$n = 5/54$ min.

For normal subjects the mean values of the parameters P_1, P_2 and P_3 are 0.028, 0.025 and 0.000013 respectively. The available clinical data indicates that for patients with diabetes the value of P_1 is well below the normal value and is difficult to quantify; as a theoretical case $P_1 = 0$ is therefore considered (Fisher, 1991).

The model, (3.7)-(3.9) is linearized about the steady-state values of:

$G_b = 4.5$ mmol/L (81 mg/dL)

$I_b = 15$ mU/L, and

$U_b = 16.66667$ mU/min,

to obtain the form similar to that given in (3.1):

$$x_{t+1} = Ax_t + Bu_t + B_d d_t$$

$$y_t = Cx_t$$

where the term d_t represents the input disturbance glucose meal and y is the blood glucose measurement. The sampling time considered is 5 minutes, which is reasonable for the current glucose sensor technology (Reach and Wilson, 1992). The discrete state-space matrices A, B, C and B_d are calculated as follows by using gPROMS:

$$A = \begin{bmatrix} 1 & -0.000604 & -21.1506 \\ 0 & 0.6294 & 0 \\ 0 & 0.00004875 & 0.8825 \end{bmatrix}$$

$$B = \begin{bmatrix} -0.000088 \\ 0.3335 \\ 0.0000112 \end{bmatrix} \qquad (3.10)$$

$$C = \begin{bmatrix} 1 & 0 & 0 \end{bmatrix}$$

$$B_d = \begin{bmatrix} 5 \\ 0 \\ 0 \end{bmatrix}$$

The constraints imposed are glucose concentration between 60-120 mg/dL, which is the desired blood glucose concentration range, and insulin infusion rate between 0-100 mU/min, which is suitable for the insulin pumps, i.e., $60 \leq G+G_b \leq 120$ and $0 \leq U+U_b \leq 100$.

The prediction horizon was tuned and it was observed that $N_y = 5$ gives a good controller performance; and three different Q/R ratios: 10, 100 and 1000 are considered for deriving the control law – this results in partitioning of the state-space into 54, 60 and 59 polyhedral or critical regions respectively. Associated with each Critical Region (CR) is a control law that is an affine function of the state of the patient. For example, one of the CRs is given by the following state inequalities:

$$-5 \le I \le 25$$
$$0.0478972G - 0.0002712I - X \le 0.104055$$
$$0.0261386G - 0.0004641I - X \le 0.0576751$$
$$-0.00808846G + 0.00119685I + X \le 0$$
$$-0.00660123G + 0.00130239I + X \le 0$$
$$0.00609435G - 0.00134362I - X \le 0$$

where the insulin infusion rate as a function of the state variables for the next five time intervals is given as follows:

$$U(1) = 30.139G - 0.44597I - 3726.2X$$
$$U(2) = 24.874G - 0.40326I - 3280.4X$$
$$U(3) = 20.16G - 0.35946I - 2842.8X$$
$$U(4) = 16.002G - 0.31571I - 2424.1X$$
$$U(5) = 0$$

Figures 3.9-3.11 show the partition of the state space into CRs for fixed values of G, I and X. The implementation of the controller therefore requires identification of the CR corresponding to the current state of the patient and then computing the optimal amount of insulin delivery rate. Similar to MPC, if at any time instant the current state is infeasible, i.e. does not lie within any of the CRs, then the last control action is implemented.

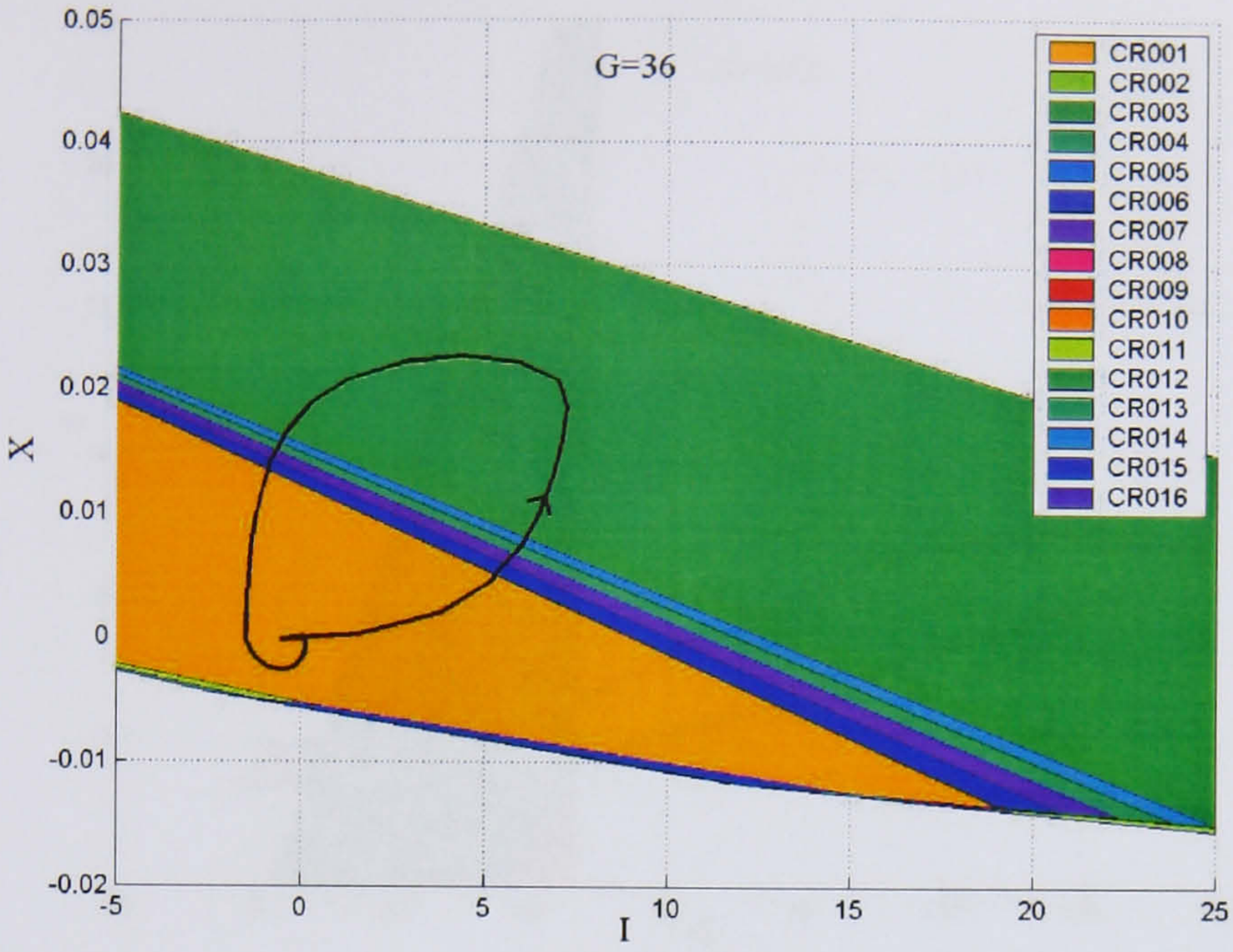


Figure 3.9 Critical regions for G = 36. The trajectory depicts the values of I and X for a meal disturbance of 20 g and the corresponding insulin infusion rate shown in Fig. 3.13 for Q/R = 1000

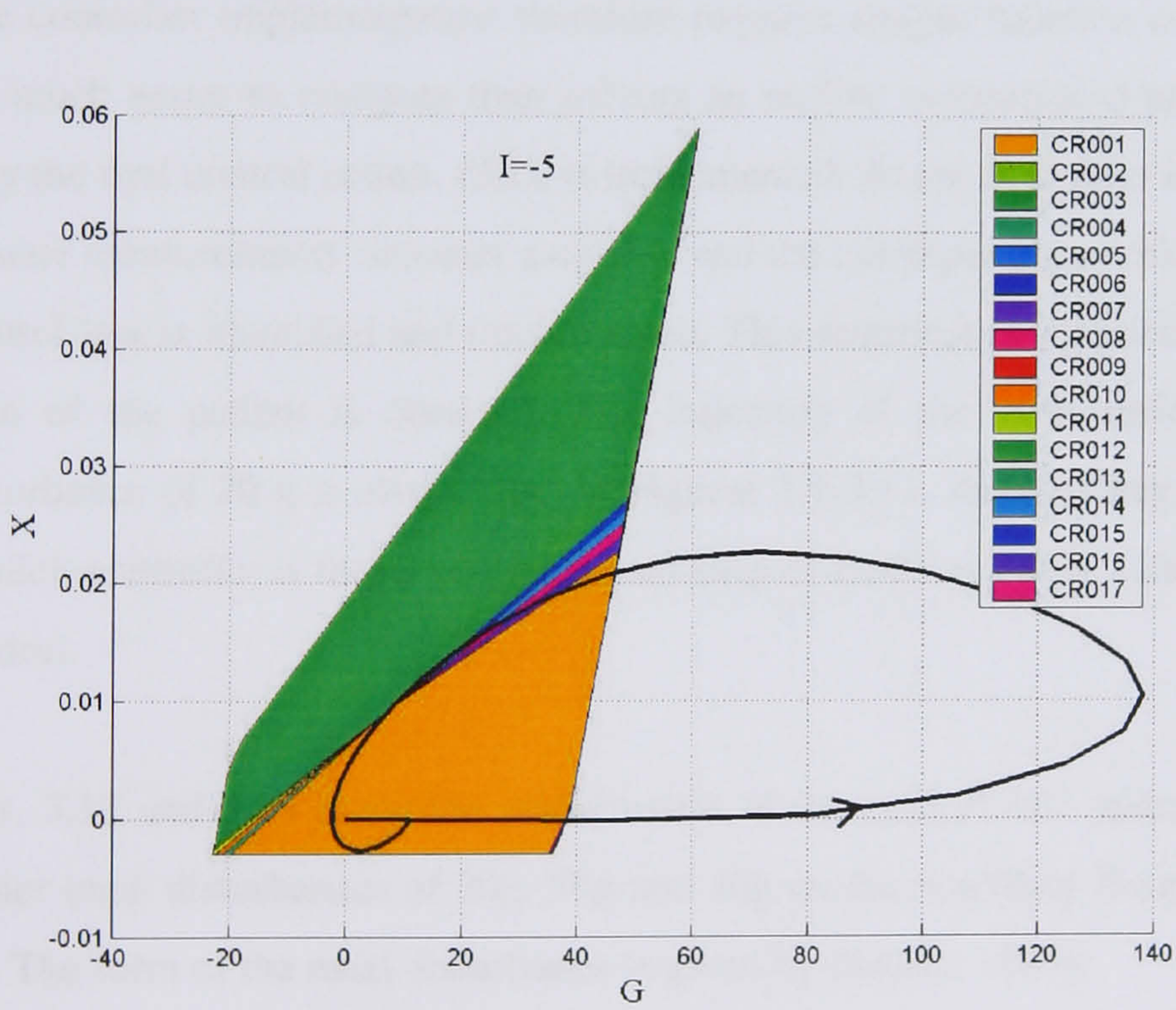


Figure 3.10 Critical regions for I = -5. The trajectory depicts the values of G and X for a meal disturbance of 20 g and the corresponding insulin infusion rate shown in Fig. 3.13 for Q/R = 1000

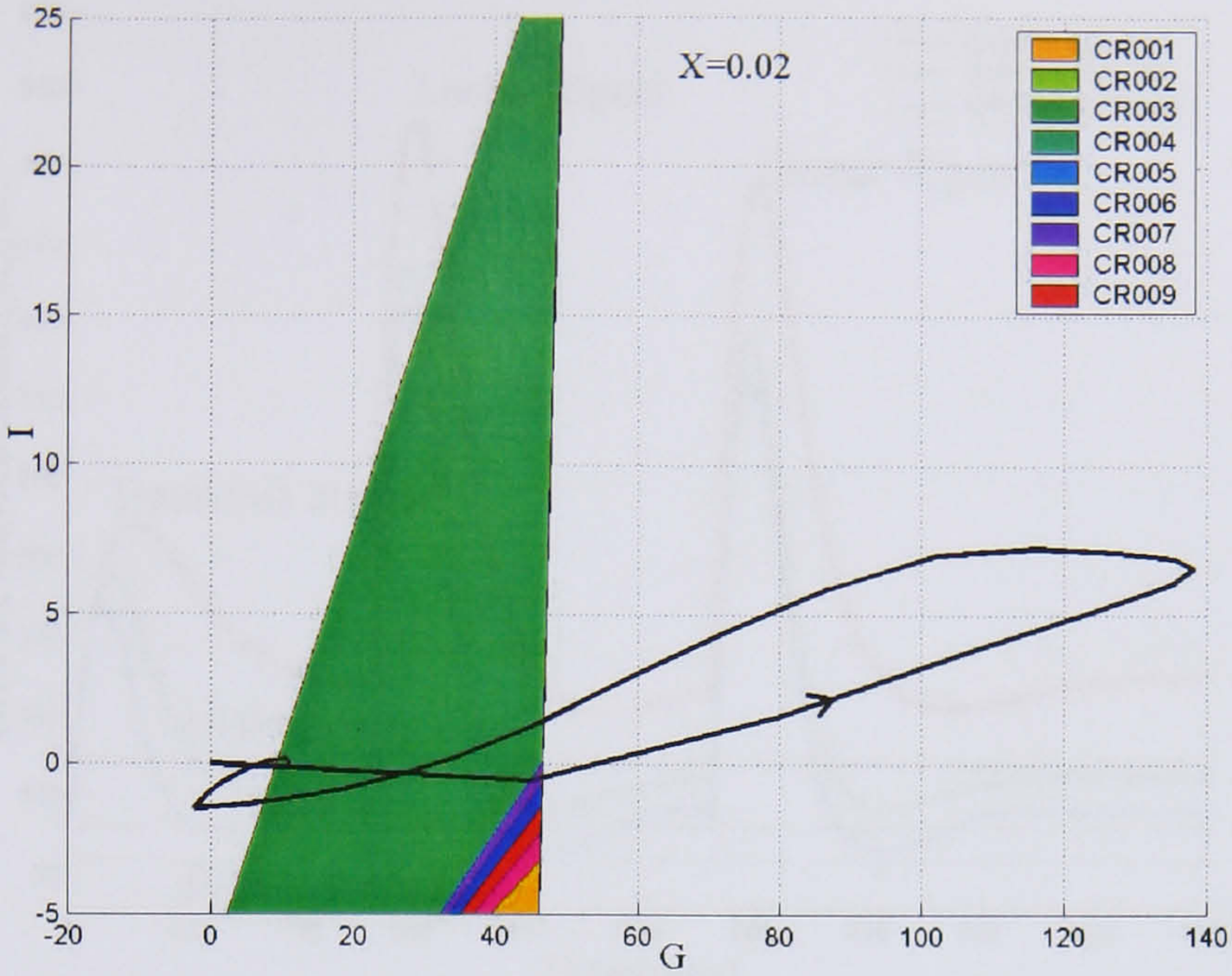


Figure 3.11 Critical regions for X = 0.02. The trajectory depicts the values of G and I for a meal disturbance of 20 g and the corresponding insulin infusion rate shown in Fig. 3.13 for Q/R = 1000

The controller implementation therefore requires simple function evaluations, which are much easier to compute than solving an on-line optimization problem. Note that only the first control action, $U(1)$, is implemented. At the next time interval, a new set of state measurements becomes available and the corresponding critical region and the control law is identified and implemented. This sequence is repeated until the desired state of the patient is obtained. The trajectory of the state variables for a meal disturbance of 20 g is also shown in Figures 3.9-3.11. Another key advantage of the explicit controller is that a complete road-map of all the possible solutions is available a priori.

Figs. 3.12 and 3.13 show the performance of the control law under the presence of Fisher meal disturbances of 20g, 50g and 40g on the nonlinear Bergman model (7) – (9). The form of the meal disturbance is given by (Fisher, 1990):

$$D(t) = \beta.\exp(-0.05t)$$

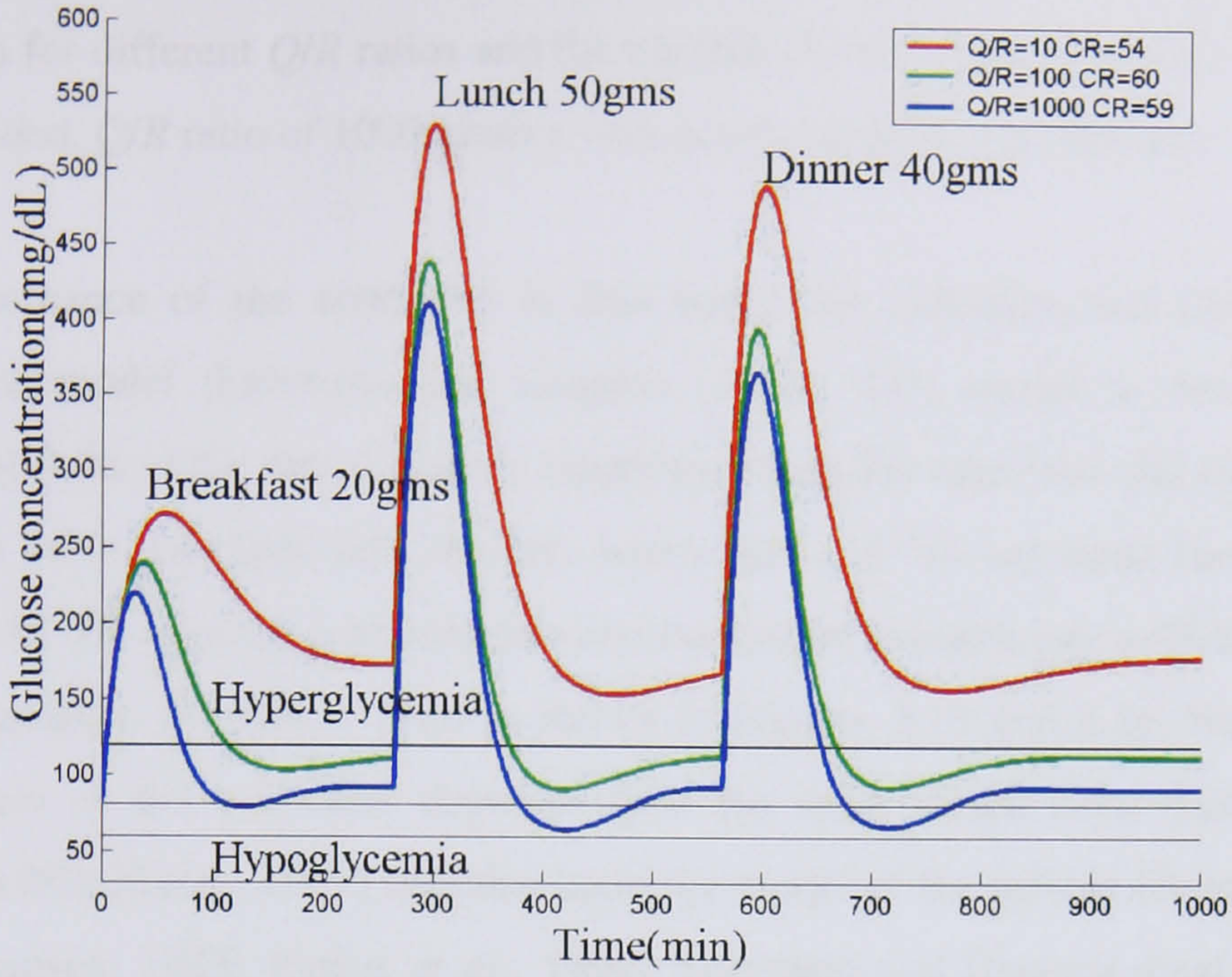


Figure 3.12 Glucose concentration profiles for Fisher meal disturbances of 20g, 50 g and 40 g and for Q/R equal to 10 (red line), 100 (green line) and 1000 (blue line)

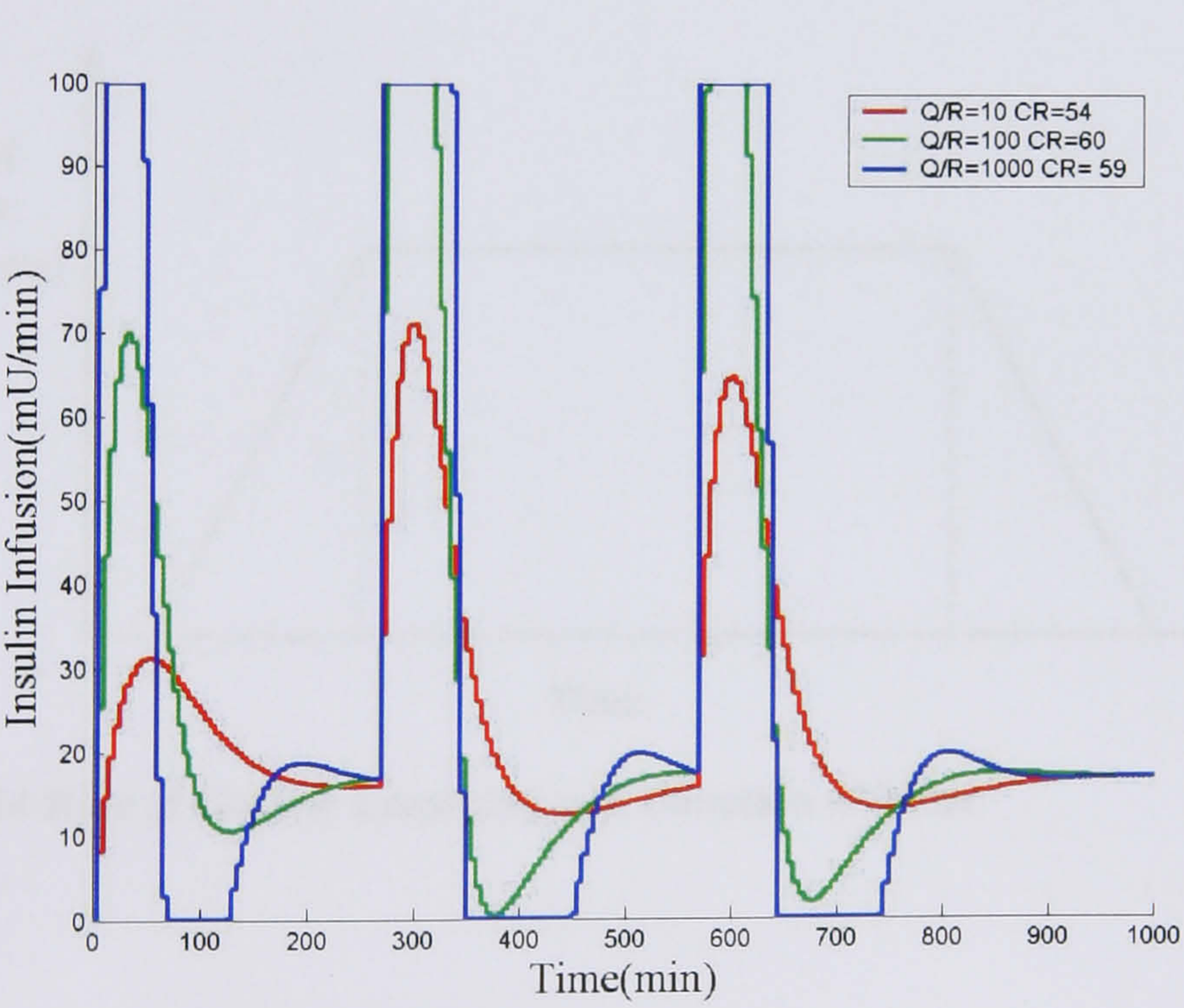


Figure 3.13 Insulin infusion rate profiles for Fisher meal disturbances of 20g, 50 g and 40 g and for Q/R equal to 10 (red line), 100 (green line) and 1000 (blue line)

where β depends upon the amount of disturbance (Fisher, 1991). The performances are shown for different *Q/R* ratios and the number of critical regions (CR) obtained is also provided. *Q/R* ratio of 1000 gives a very good controller performance.

The performance of the controller is also tested for Lehmann and Deutsch meal disturbance model (Lehmann and Deutsch, 1992). This model is based upon a trapezoidal form of the rate of gastric emptying where the rate rises and saturates to a maximum value and then falls to zero, where rise and fall are ramp functions (see Figure 3.14). The glucose concentration and the insulin infusion rate profiles for a 20g meal disturbance for Q/R = 1000 is shown in Figures 3.15 and 3.16. Note that the performance of the controller depends upon the meal model used (Lehmann and Deutsch, 1992; Fisher, 1991) and also upon the model of the patient (Bergman *et al.*, 1981; Sorensen, 1985; Parker *et al.*, 1999). Lehmann and Deutsch meal model has much slower initial dynamics than the Fisher meal disturbance model and therefore results in smaller glucose excursions – see Figures 3.12 and 3.14.

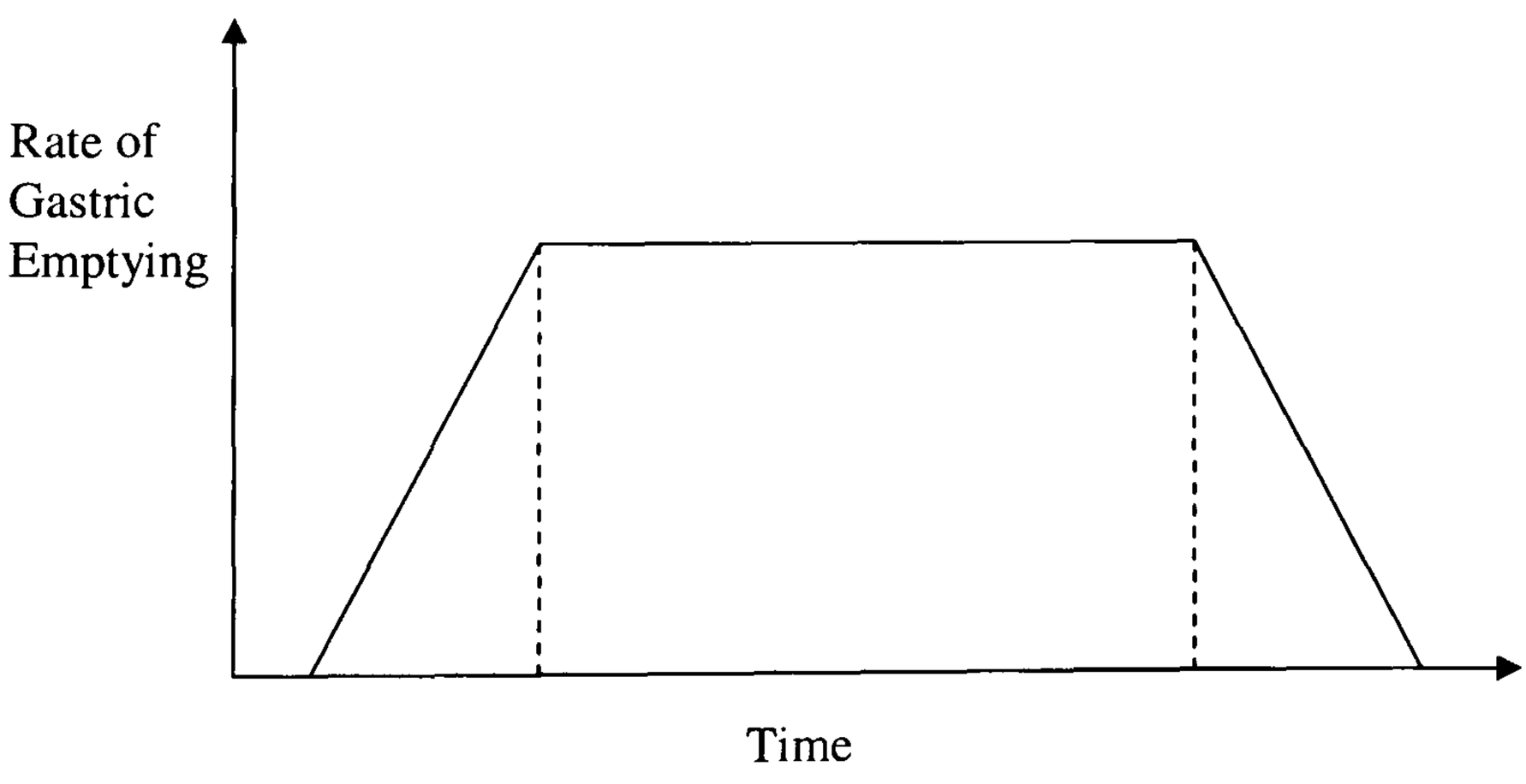


Figure 3.14 Rate of Gastric Emptying as a Function of Time

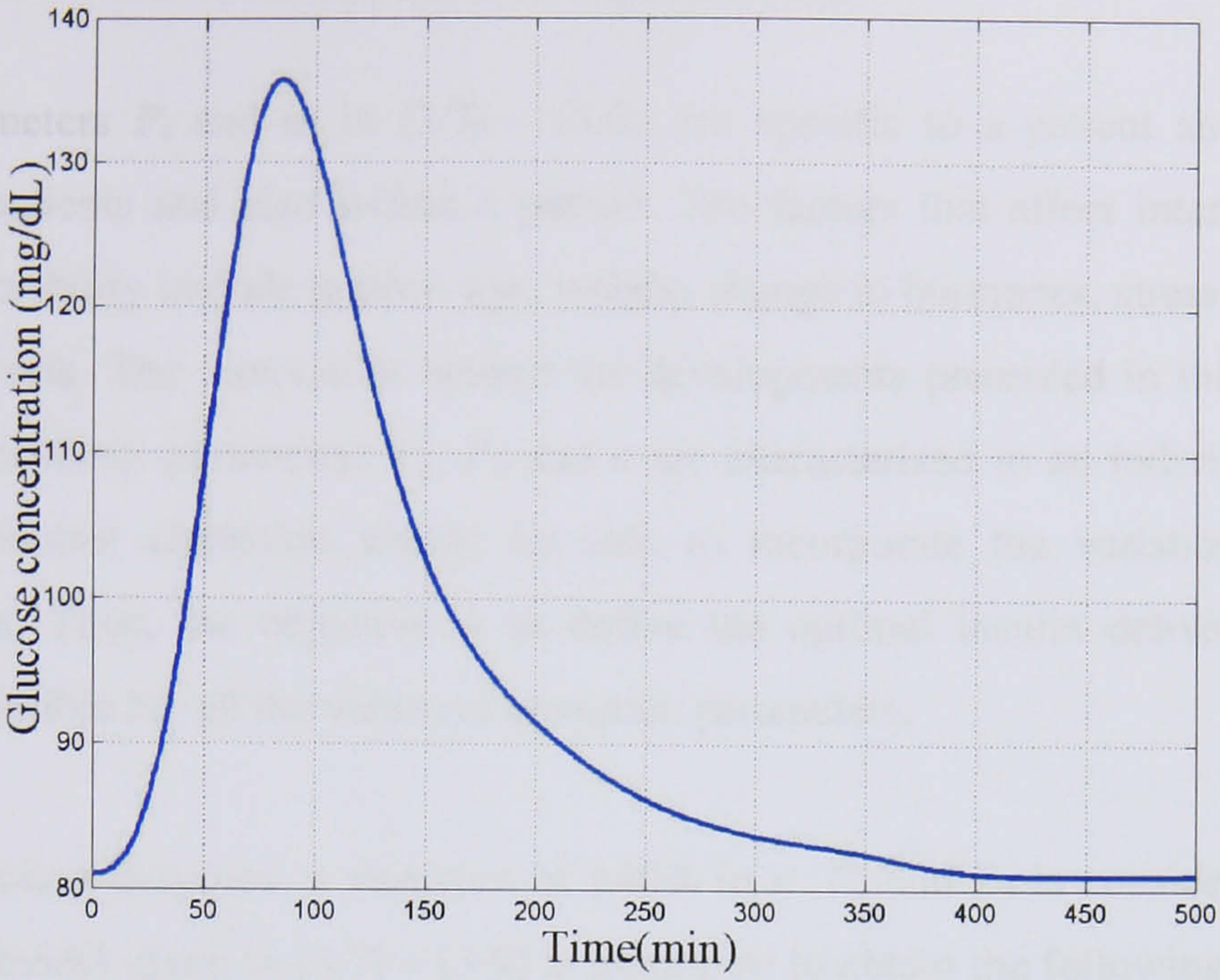


Figure 3.15 Glucose concentration profile for 20 g Lehmann and Deutsch meal disturbance and for Q/R = 1000

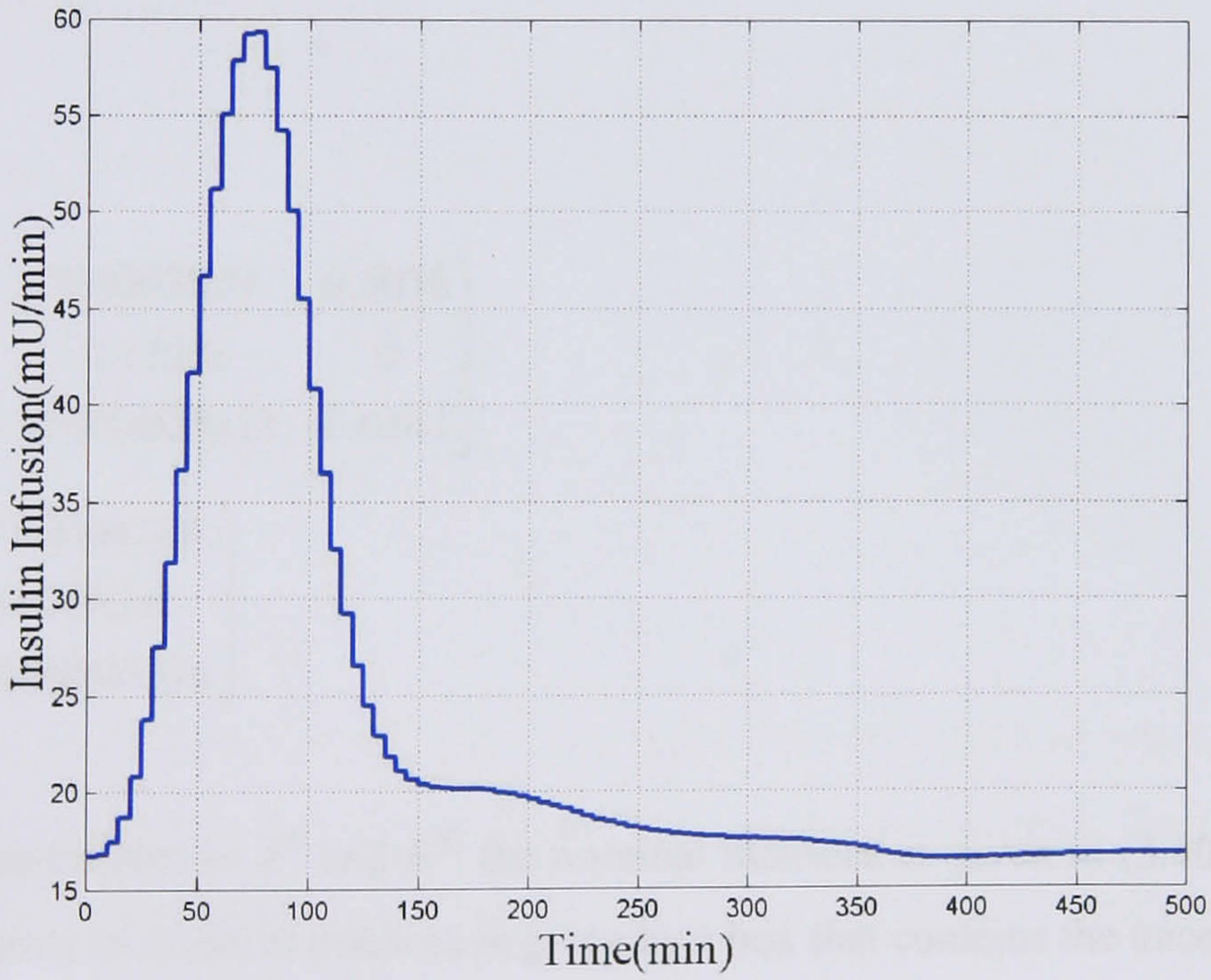


Figure 3.16 Insulin infusion profile for 20 g Lehmann and Deutsch meal disturbance and for Q/R = 1000

3.7 Inter- and Intra-Patient Variability

The parameters P_i and n, in (3.7) – (3.9), are specific to a patient and may vary between patients and also within a patient. The factors that affect inter- and intra-patient variability include gender, age, weight, change in hormones, stress, illness and activity levels. The motivation behind the developments presented in this section is that the uncertain parameters P_2, P_3 and n are characterized to an individual patient and the control algorithm should be able to incorporate the variations in these parameters. Thus, the objective is to derive the optimal insulin delivery rate that remains feasible for all the values of uncertain parameters.

For illustration purposes, a variation of ±40% in n, P_2 and P_3 is considered and the Bergman model given in (3.7) – (3.9) is linearized to obtain the following state space equation:

$$x_{t+k+1} = \left(A^N \pm \Delta A\right)x_{t+k} + \left(B^N \pm \Delta B\right)u_{t+k} + B_d d_{t+k},\ k = 0,\ldots,5$$

where

$$\Delta A = \pm\begin{bmatrix} 0 & 0.0002899 & 0.5076 \\ 0 & 0.12588 & 0 \\ 0 & 0.000025311 & 0.0441 \end{bmatrix}$$

$$\Delta B = \pm\begin{bmatrix} 0.00004224 \\ 0.029348 \\ 0.000005376 \end{bmatrix}$$

are the uncertainties in A^N and B^N, the nominal matrices as given in (3.10). Note that the uncertainty in A and B matrices is given by a box that contains the uncertainty in n, P_2 and P_3.

The maximum range of the A and B matrices for which feasibility is guaranteed (i.e. control strategy remains feasible) are obtained by solving the following problem:

$$\max_{\delta} \delta$$

$$s.t. \ \max_{A,B} \min_{z} \max_{j \in J} G_j z - W_j - S_j x_t \leq 0$$

$$A^N - \delta\Delta A \leq A \leq A^N + \delta\Delta A \tag{3.11}$$

$$B^N - \delta\Delta B \leq B \leq B^N + \delta\Delta B$$

where δ is a positive scalar variable, $Gz - W - Sx_t \leq 0$ correspond to the inequalities in (3.6) and G_j, W_j and S_j is the jth row of G, W and S respectively. This problem can be solved by, for example, using the algorithm described in (Grossmann and Floudas, 1987). Note that G, W and S in (3.6) are constant matrices, whereas in (3.11) they are nonlinear functions of the uncertain parameters, A and B and therefore the solution of (3.11) may not necessarily lie at a vertex of the uncertainty space. Equation (3.11) is solved for a meal disturbance of 25 g and blood glucose concentration bounded between 3 mmol/L and 15 mmol/L i.e. 54 mg/dL $\leq G+G_b \leq$ 270 mg/dL. The solution is given by $\delta = 0.859$,

$$A = \begin{bmatrix} 1 & -0.0008530 & -21.587 \\ 0 & 0.738 & 0 \\ 0 & 0.000070417 & 0.920 \end{bmatrix}$$

$$B = \begin{bmatrix} -0.0001243 \\ 0.359 \\ 0.000016 \end{bmatrix}. \tag{3.12}$$

The optimal explicit insulin delivery rate is then obtained for these values of A and B matrices by using parametric programming and 32 CRs are obtained. This control law is guaranteed to be feasible for all the values of A and B matrices where:

$A^N - \delta\Delta A \leq A \leq A^N + \delta\Delta A$

$B^N - \delta\Delta B \leq B \leq B^N + \delta\Delta B$, and

$\delta = 0.859$.

The partition of the space of state variables for fixed values of G, I and X and the profile of the state variables for a meal disturbance of 25g are shown in Figs. 3.17-3.19.

For comparison purposes, the explicit insulin delivery for the nominal values, A^N and B^N, of A and B matrices for $54 \leq G+G_b \leq 270$ is also derived resulting in 26 CRs. For fixed value of G, I and X the CRs are depicted in Figs. 3.20-3.22.

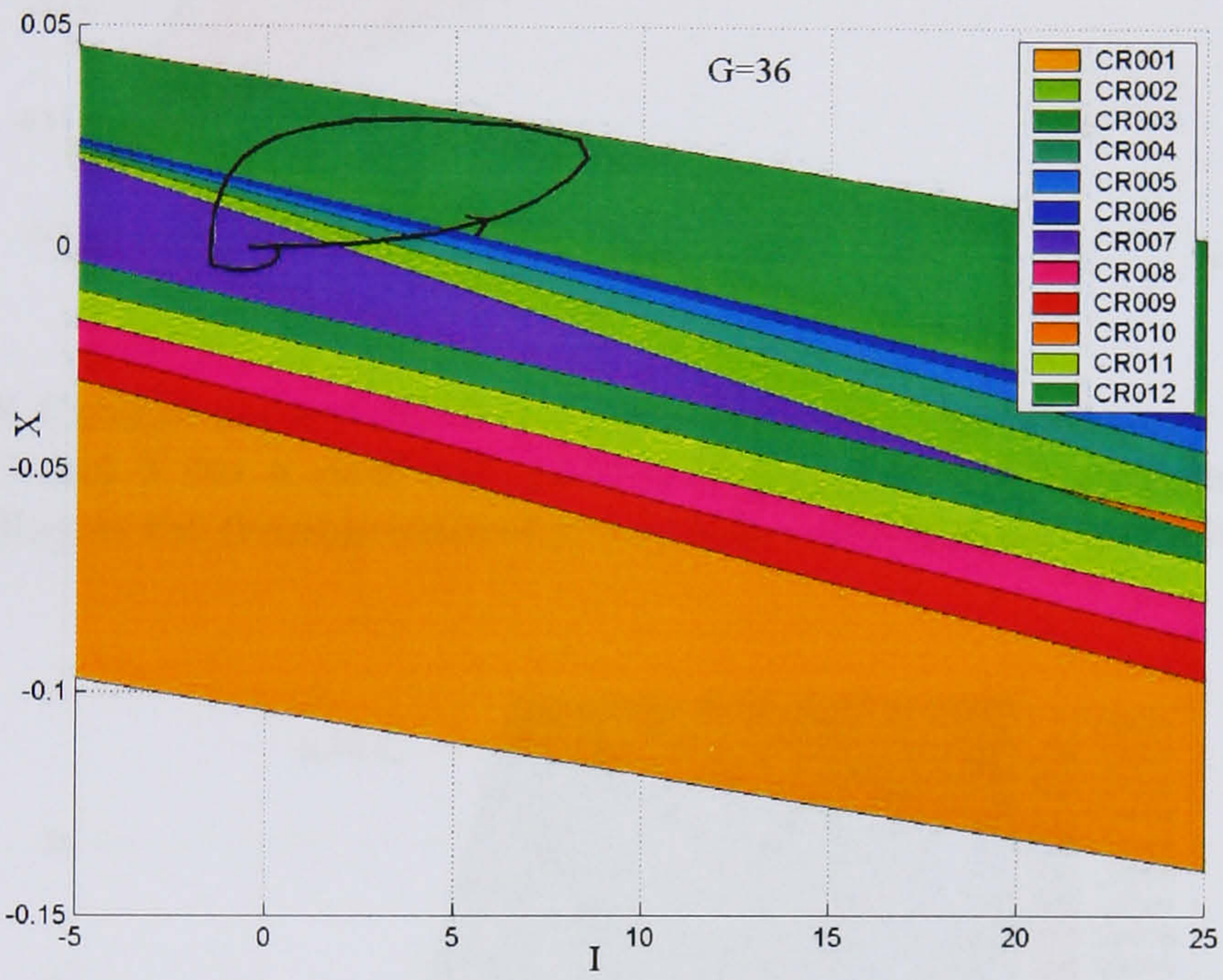


Figure 3.17 Critical regions for G = 36: feasible case. The trajectory depicts the values of I and X for a meal disturbance of 25 g and the insulin infusion rate corresponding to the feasible control law obtained for A and B given in (3.12)

Fig. 3.23 shows the comparison of the performance of the feasible control law (blue line) and the nominal control law (red line) for a meal disturbance of 25 g on the Bergman model with non-nominal model parameters:

$P_2 = 0.02$

$P_3 = 0.0000156$, and

$n = 0.07407$.

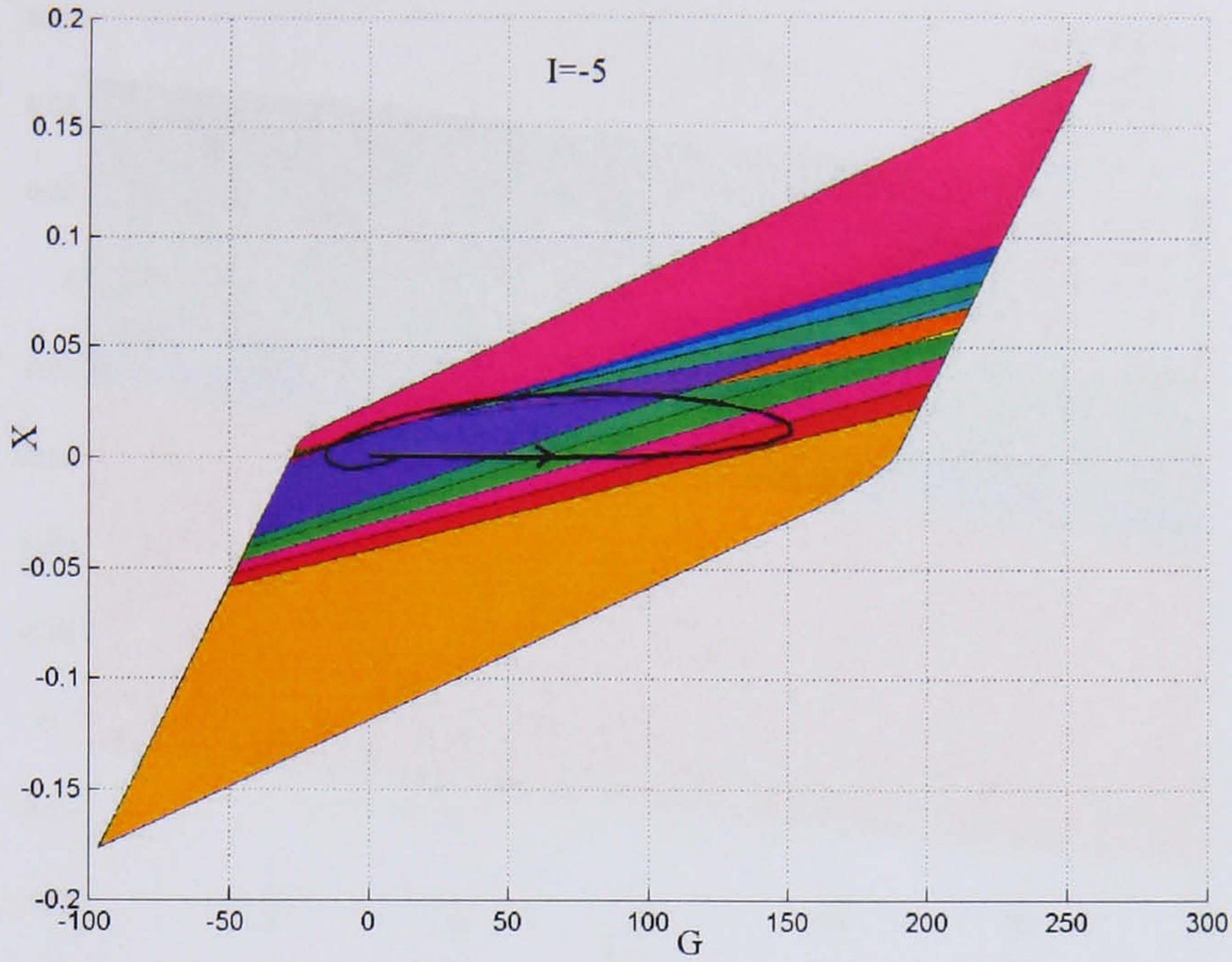


Figure 3.18 Critical regions for I = -5: feasible case. The trajectory depicts the values of G and X for a meal disturbance of 25 g and the insulin infusion rate corresponding to the feasible control law obtained for A and B given in (3.12)

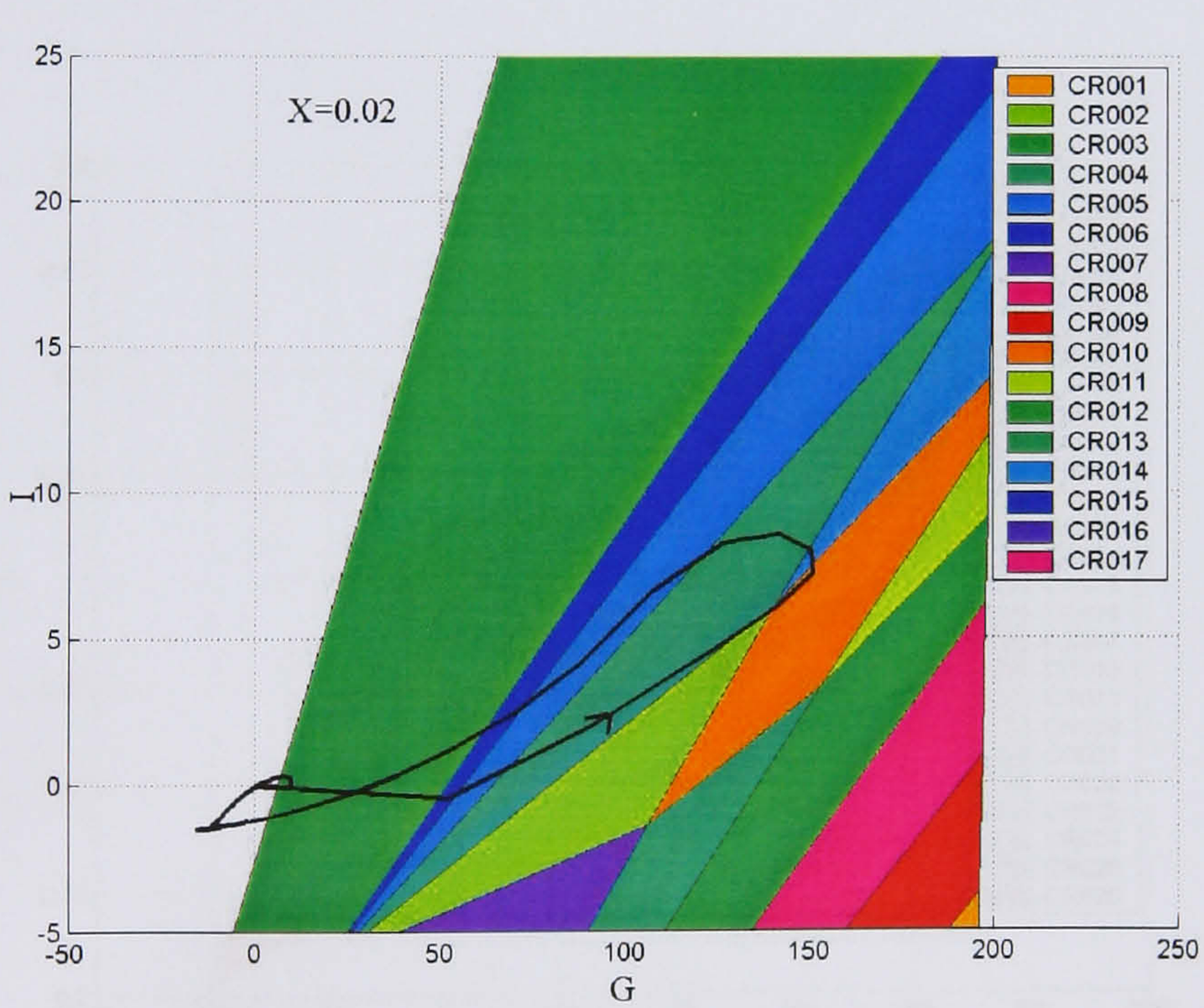


Figure 3.19 Critical regions for X = 0.02: feasible case. The trajectory depicts the values of G and I for a meal disturbance of 25 g and the insulin infusion rate corresponding to the feasible control law obtained for A and B given in (3.12)

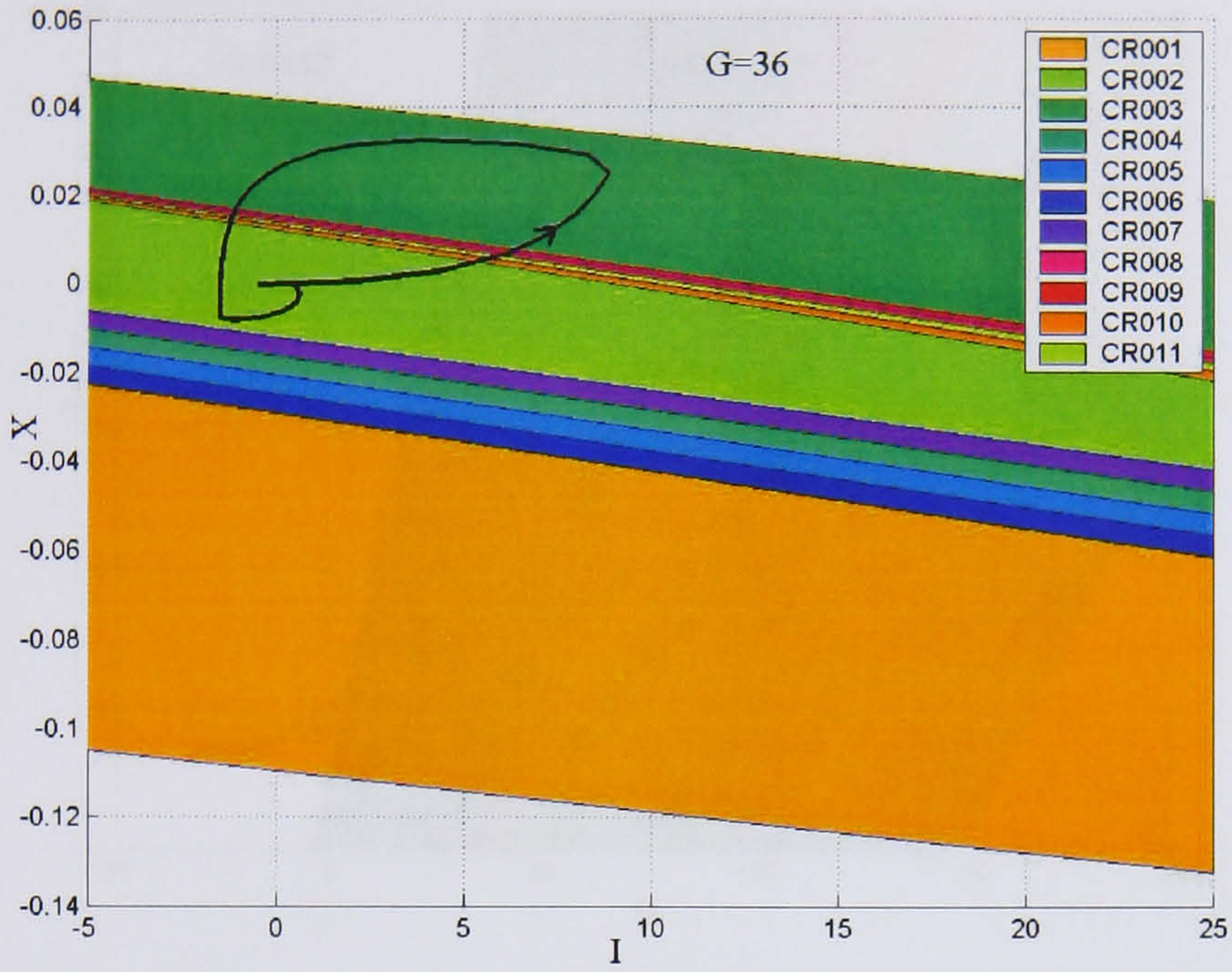


Figure 3.20 Critical regions for G = 36: nominal case. The trajectory depicts the values of I and X for a meal disturbance of 25 g and the insulin infusion rate corresponding to the nominal control law obtained for A and B given in (3.10) and for $54 \leq G+G_b \leq 270$

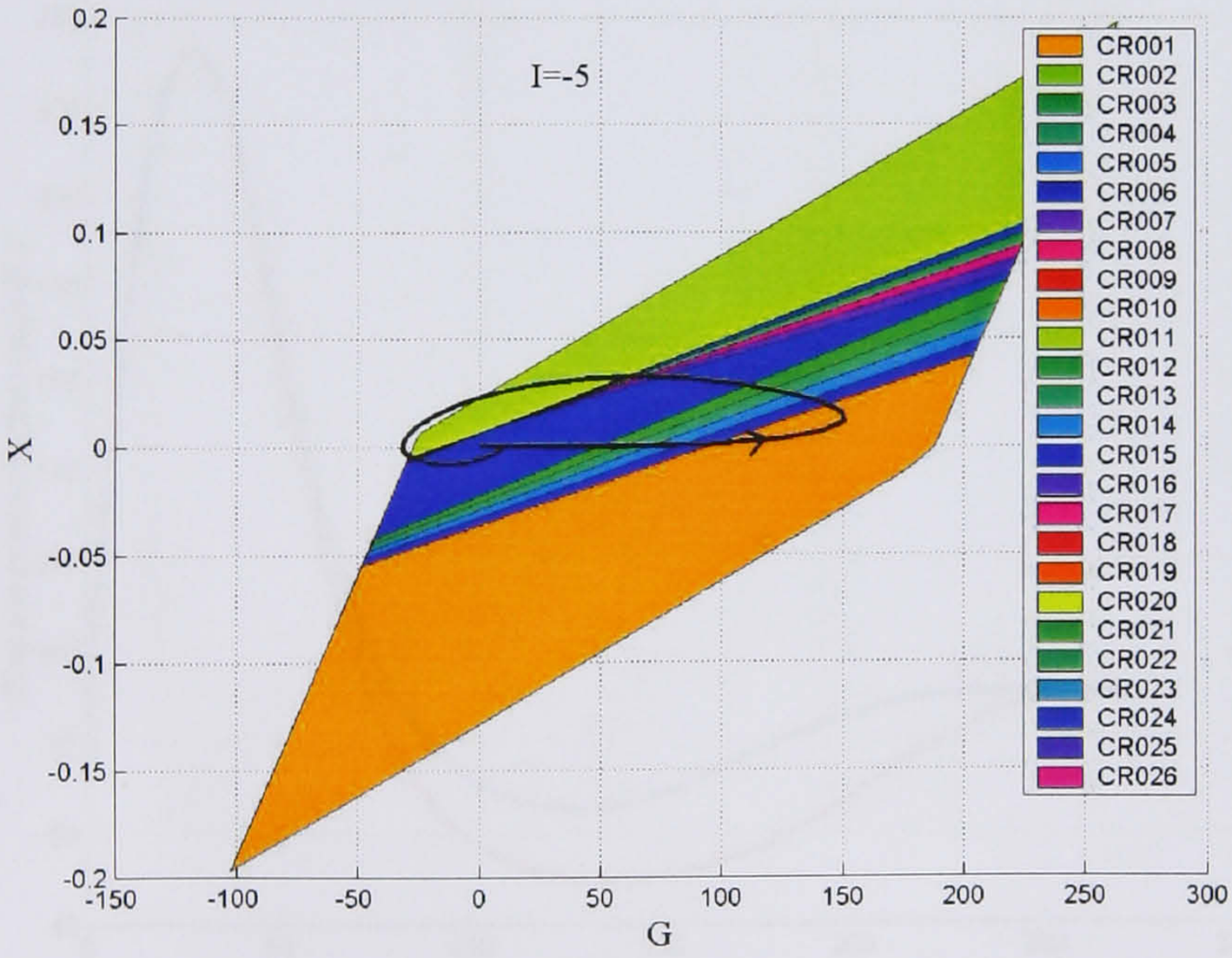


Figure 3.21 Critical regions for I = -5: nominal case. The trajectory depicts the values of G and X for a meal disturbance of 25 g and the insulin infusion rate corresponding to the nominal control law obtained for A and B given in (3.10) and for $54 \leq G+G_b \leq 270$

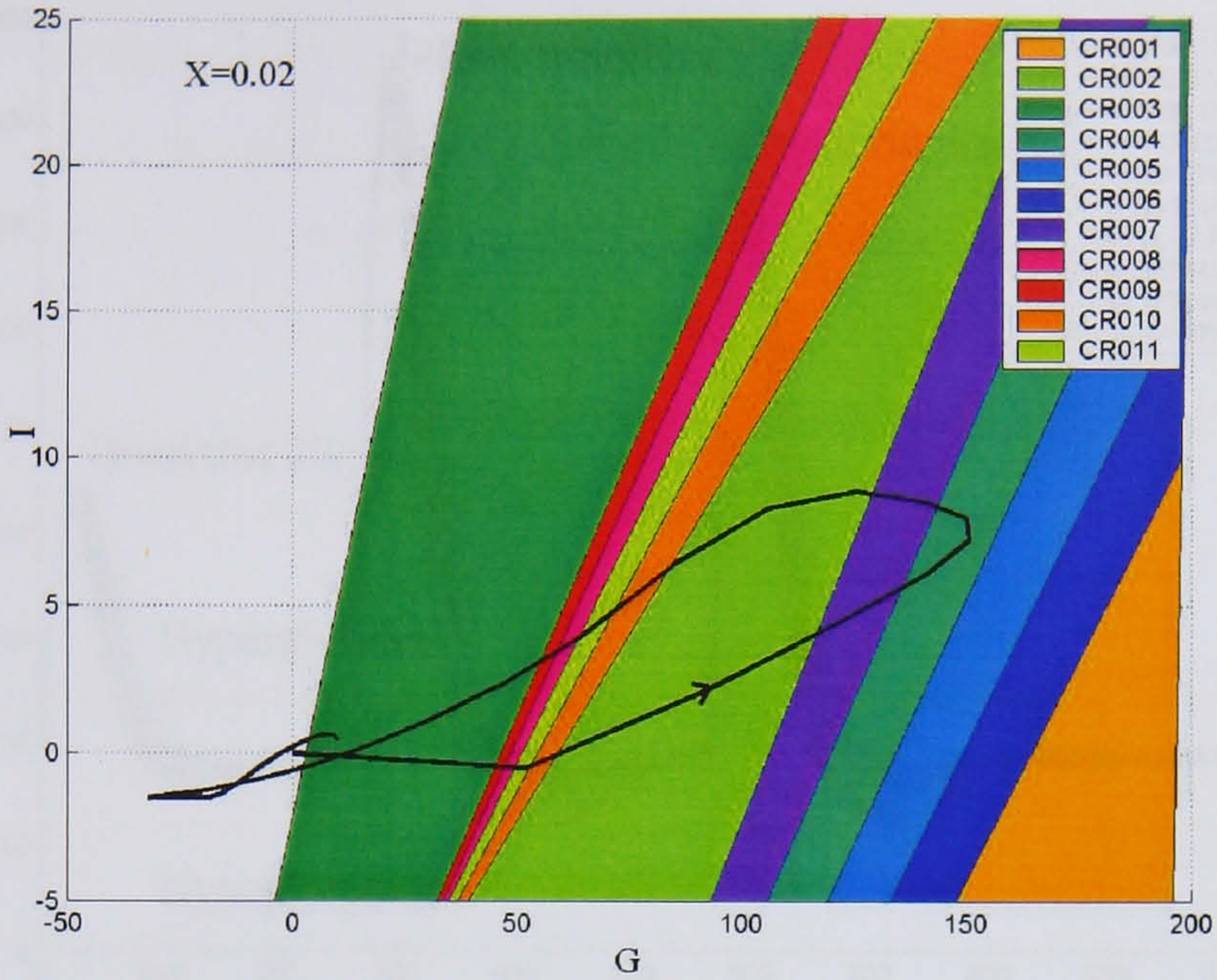


Figure 3.22 Critical regions for X = -0.02: nominal case. The trajectory depicts the values of G and I for a meal disturbance of 25 g and the insulin infusion rate corresponding to the nominal control law obtained for A and B given in (3.10) and for $54 \leq G+G_b \leq 270$

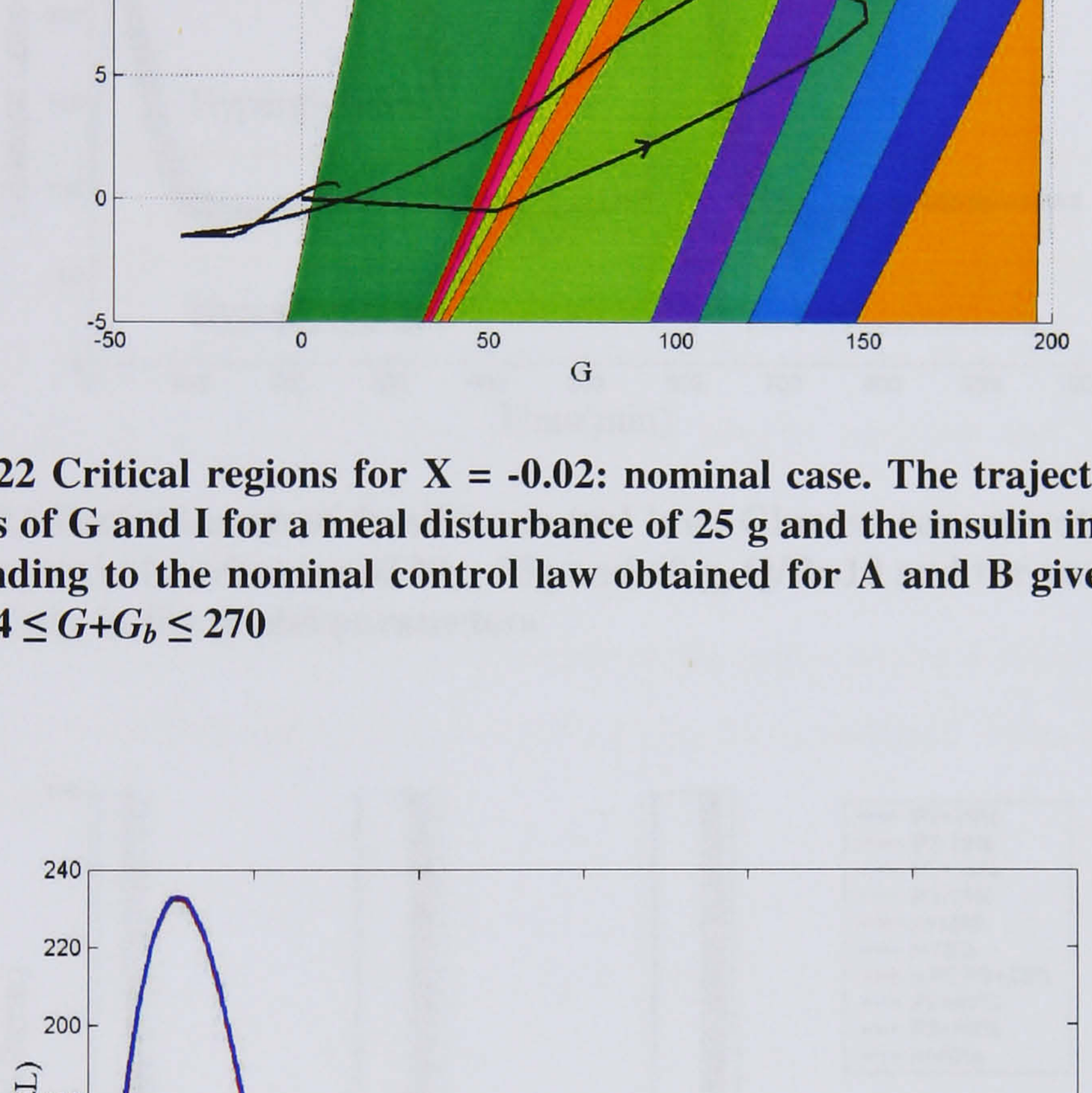


Figure 3.23 Comparison of the feasible and the nominal control law. Feasible control law (blue line) ensures that the constraint $54 \leq G+G_b$ is not violated whereas the state of hypoglycemia is reached for the nominal control law (red line)

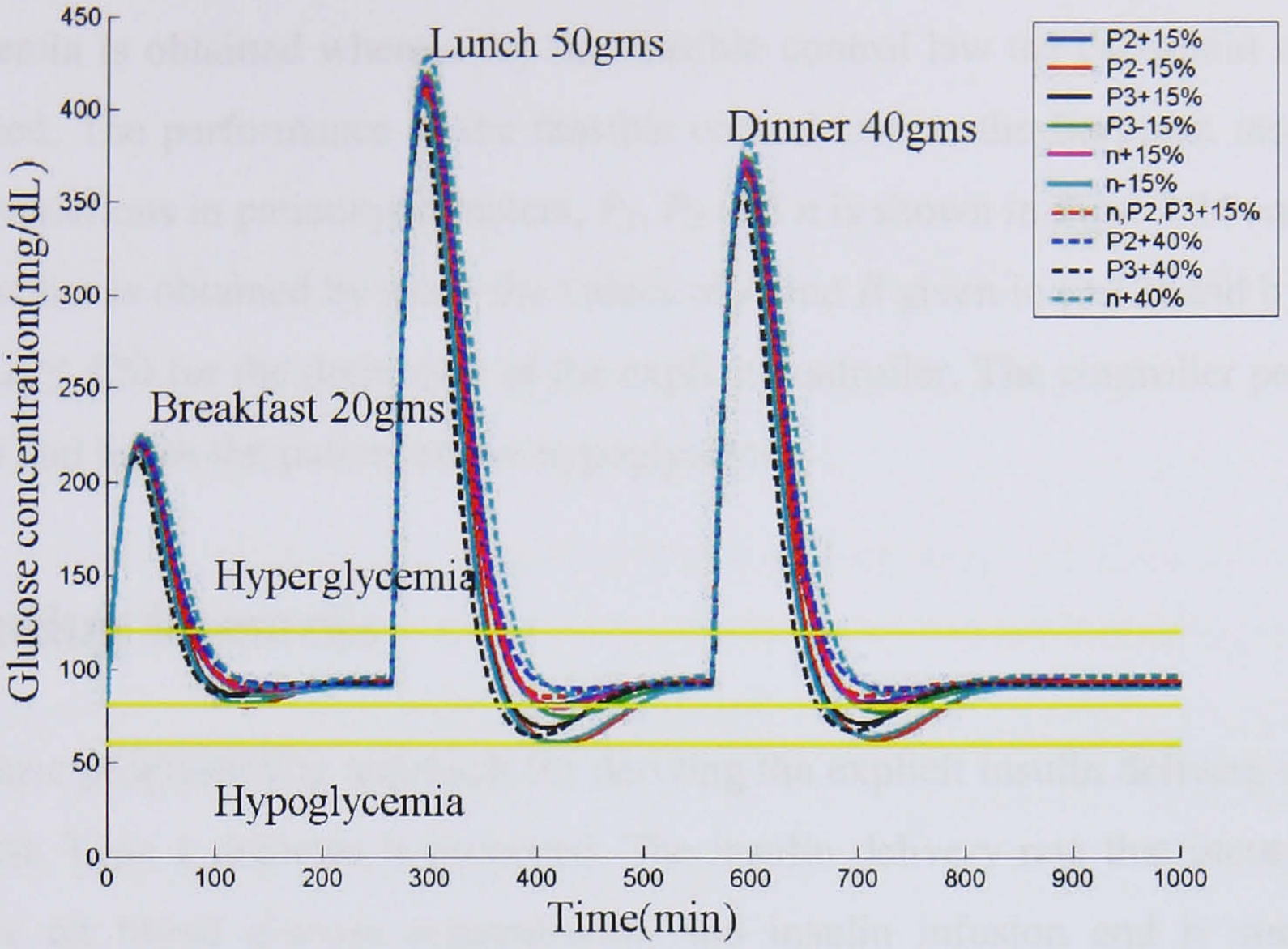


Figure 3.24 Performance of feasible control law: Glucose concentration profiles for Fisher meal disturbances of 20g, 50g and 40 g, Q/R=10 and for various values of uncertainty in the model parameters

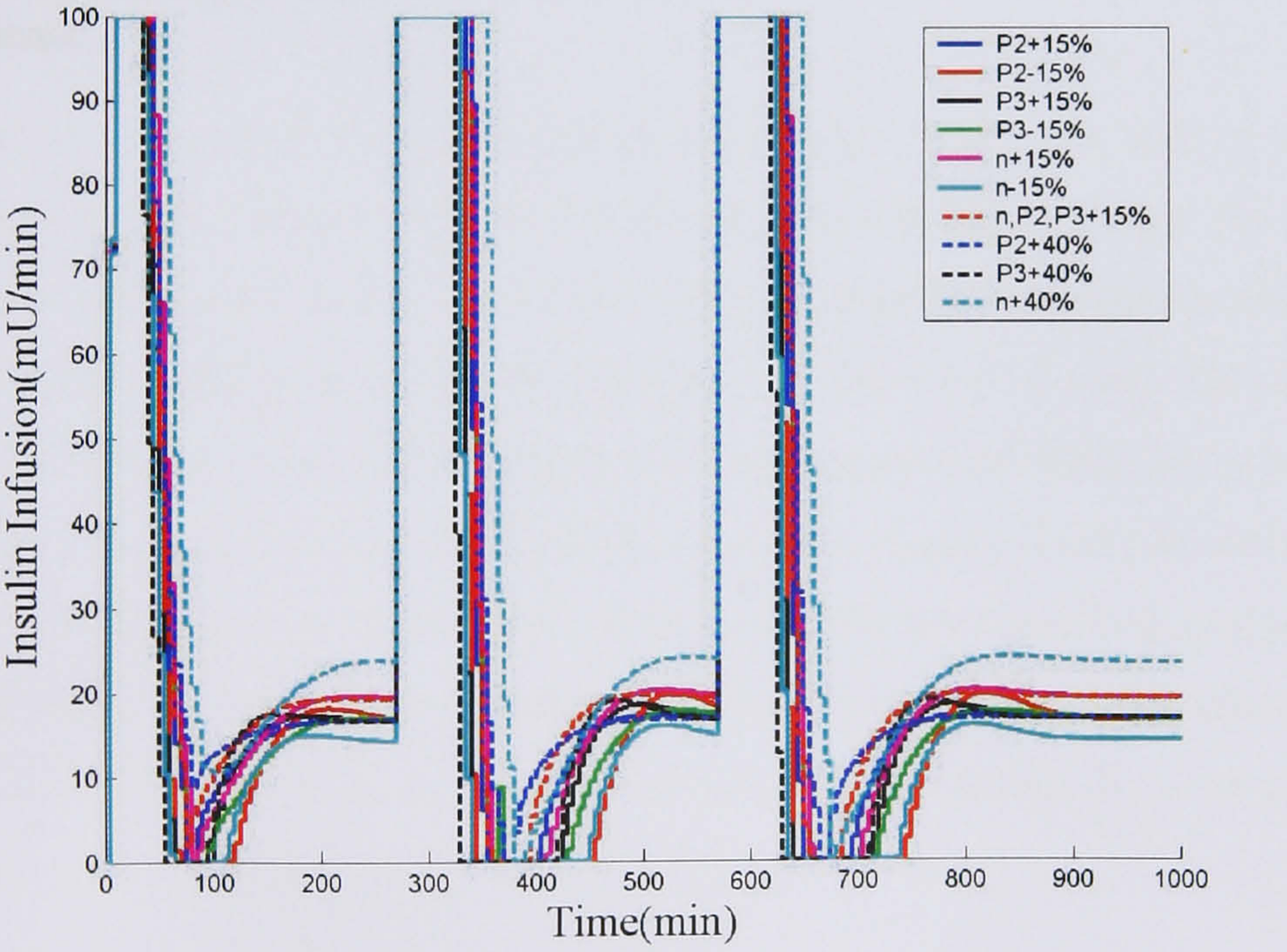


Figure 3.25 Performance of feasible control law: Insulin infusion rate profiles for Fisher meal disturbances of 20g, 50g and 40 g, Q/R=10 and for various values of uncertainty in the model parameters

The nominal controller violates the constraint $54 \leq G+G_b$ and the state of hypoglycemia is obtained whereas for the feasible control law the constraint on G is not violated. The performance of the feasible control law on the Bergman model for different variations in patient parameters, P_2, P_3 and n is shown in Figs. 3.24 and 3.25. This controller is obtained by using the values of A and B given in (3.12) and by using $60 \leq G+G_b \leq 120$ for the derivation of the explicit controller. The controller performs quite well and keeps the patient above hypoglycemia.

Concluding Remarks

A parametric programming approach for deriving the explicit insulin delivery rate for people with Type 1 diabetes is proposed. The insulin delivery rate that incorporates constraints on blood glucose concentration and insulin infusion and is simple to implement is obtained. A methodology that takes into account uncertainty in the patient model is also proposed. These developments are expected to enhance the automation of insulin delivery by implementing the controller on a microchip, take a step towards "providing personalized health care control strategies" and reduce patient inconvenience.

Chapter 4

Multi-objective Control for Type 1 Diabetes

The key motivation behind the work reported in this chapter is that in the medical literature, hypoglycemia is considered to be more harmful to an individual's health than hyperglycemia. A multi-objective controller that can take into account this asymmetry in the objective function and can be implemented with minimal computational effort, by using parametric programming techniques, is proposed. An alternative technique that gives higher priority to the satisfaction of constraints on hypoglycemia than on hyperglycemia is also presented. The performance of both controllers is analyzed under meal disturbances.

4.1 Introduction

As discussed in the previous chapter, people with type 1 diabetes rely on regular insulin injections for controlling the blood glucose concentration between the desired range of 60 to 120 mg/dL and at the target level of 81 mg/dL. The amounts and times of insulin intake usually depend on the amounts and the times of meal. This usually leads to significant deviations of the blood glucose concentration from the target level due to the manual and open loop nature of the control. A shortage in the insulin supply may lead to hyperglycemia, whereas an excessive supply may lead to hypoglycemia. Both these states are harmful to an individual's health but negative deviations from the target value of 81 mg/dL are considered to be more harmful than the positive deviations.

The motivation behind the current work is that traditional approaches to characterizing engineering "performance" are rarely equated to a physician's characterization of patient "performance". In particular, the asymmetry between the

previously described states of hypo- and hyper-glycemia is noteworthy. In this chapter, two multi-objective control techniques for addressing this issue are presented. The first technique addresses the issue by designing an asymmetric objective function in the model based control framework with more weighting given to the negative deviations from the setpoint, 81 mg/dL, than to the positive deviation. The problem is then reformulated as a multi-parametric quadratic program and solved to obtain the optimal insulin infusion rate as an explicit function of the state of the patient. The second technique is concerned with the prioritization of objectives (Tyler and Morari, 1999). The "objective" that the constraint corresponding to the hypoglycemic state is not violated has a higher priority than the constraint corresponding to the hyperglycemic state. Similarly, a number of such constraints are identified and prioritized. The constraint prioritization corresponding to various objectives are formulated by using boolean variables that results in a mixed integer program. This problem can then be recast as a multi-parametric mixed integer program by treating state variables as parameters and control and integer variables as optimization variables. The final solution is given by the insulin delivery rate as an explicit function of the state of patient. Since the on-line solution of a mixed integer program is computationally expensive, the parametric programming approach can be used for the incorporation of the prioritized objectives that can significantly improve the performance of blood glucose control.

The rest of the chapter is organized as follows. In the next section a parametric programming approach where asymmetry in the objective function is considered is presented to derive the optimal insulin infusion rate as an explicit function of the state of the patient. Section 4.3 considers the case where constraints on blood glucose concentration are prioritized and finally concluding remarks are presented.

4.2 Asymmetric Objective Function

Consider the model predictive control problem (3.3) of the following form:

$$\min_{U} J(U, x(t)) = x_{t+N_y|t}^T P x_{t+N_y|t} + \sum_{k=0}^{N_y-1} \left[x_{t+k|t}^T Q x_{t+k|t} + u_{t+k}^T R u_{t+k} \right]$$

$$s.t. \quad x_{\min} \le x_{t+k|t} \le x_{\max}, k = 1,....., N_c \tag{4.1}$$

$$u_{\min} \le u_{t+k} \le u_{\max}, \quad k = 1,....., N_c$$

$$x_{t+k+1|t} = A x_{t+k|t} + B u_{t+k}, k \ge 0$$

This formulation weighs equally the positive and negative deviations. It can be recast as follows:

$$\min_{U} J(U, x(t)) = \varepsilon_{t+N_y|t}^T P \varepsilon_{t+N_y|t} + \sum_{k=0}^{N_y-1} \left[\varepsilon_{t+k|t}^T Q \varepsilon_{t+k|t} + u_{t+k}^T R u_{t+k} \right] \tag{4.2}$$

$$s.t. \quad \varepsilon_{t+k|t} \ge -x_{t+k|t}, \quad k \ge 0 \tag{4.3}$$

$$\varepsilon_{t+k|t} \ge x_{t+k|t}, \quad k \ge 0 \tag{4.4}$$

$$x_{\min} \le x_{t+k|t} \le x_{\max}, \qquad k = 1,....., N_c \tag{4.5}$$

$$u_{\min} \le u_{t+k} \le u_{\max}, \qquad k = 1,....., N_c \tag{4.6}$$

$$x_{t+k+1|t} = A x_{t+k|t} + B u_{t+k}, \quad k \ge 0 \tag{4.7}$$

where $\varepsilon(t)$ is a vector representing the absolute values of $x(t)$. Equations (4.3) and (4.4) weigh positive and negative values of x equally. Asymmetric weights on positive and negative deviations can be enforced by modifying constraints (4.3) and (4.4) as follows (Parker *et al.* 2000b):

$$\tau_{-} \varepsilon_{t+k|t} \ge -x_{t+k|t}, \quad k \ge 0 \tag{4.8}$$

$$\tau_{+} \varepsilon_{t+k|t} \ge x_{t+k|t}, \quad k \ge 0 \tag{4.9}$$

where τ_{-} and τ_{+} are used for weighing the negative and positive deviations x, respectively.

The asymmetric MPC problem therefore becomes:

$$\min_{U} J(U, x(t)) = \varepsilon_{t+N_y|t}^T P \varepsilon_{t+N_y|t} + \sum_{k=0}^{N_y-1} \left[\varepsilon_{t+k|t}^T Q \varepsilon_{t+k|t} + u_{t+k}^T R u_{t+k} \right]$$

$$\text{s.t.} \quad \tau_{-} \varepsilon_{t+k|t} \geq -x_{t+k|t}, \quad k \geq 0$$

$$\tau_{+} \varepsilon_{t+k|t} \geq x_{t+k|t}, \quad k \geq 0 \qquad (4.10)$$

$$x_{\min} \leq x_{t+k|t} \leq x_{\max}, \quad k = 1, \ldots\ldots, N_c$$

$$u_{\min} \leq u_{t+k} \leq u_{\max}, \quad k = 1, \ldots\ldots, N_c$$

$$x_{t+k+1|t} = A x_{t+k|t} + B u_{t+k}, \quad k \geq 0$$

This formulation allows positive and negative values of x to have different effects in the objective function. Note that this problem has continuous objective function and constraints and can be solved by using gradient based optimization techniques. In this chapter we present an approach that provides the vector of control variables U as an explicit function of the state variables, $x(t)$; similar to that presented in Chapter 3. The key feature of this approach is that it is very general and can also be extended to have different weights for different intervals within $[x_{min}, x_{max}]$. For the case considered in this chapter where positive and negative values of x have different weights, two MPC problems can be formulated:

$$\min_{U} J(U, x(t)) = x_{t+N_y|t}^T P x_{t+N_y|t} + \sum_{k=0}^{N_y-1} \left[x_{t+k|t}^T Q^{-} x_{t+k|t} + u_{t+k}^T R u_{t+k} \right]$$

$$s.t. \quad x_{\min} \leq x_{t+k|t} \leq 0, \quad k = 1, \ldots\ldots, N_c \qquad (4.11)$$

$$u_{\min} \leq u_{t+k} \leq u_{\max}, \quad k = 1, \ldots\ldots, N_c$$

$$x_{t+k+1|t} = A x_{t+k|t} + B u_{t+k}, \quad k \geq 0$$

$$\min_{U} J(U, x(t)) = x_{t+N_y|t}^T P x_{t+N_y|t} + \sum_{k=0}^{N_y-1} \left[x_{t+k|t}^T Q^{+} x_{t+k|t} + u_{t+k}^T R u_{t+k} \right]$$

$$s.t. \quad 0 \leq x_{t+k|t} \leq x_{\max}, \quad k = 1, \ldots\ldots, N_c \qquad (4.12)$$

$$u_{\min} \leq u_{t+k} \leq u_{\max}, \quad k = 1, \ldots\ldots, N_c$$

$$x_{t+k+1|t} = A x_{t+k|t} + B u_{t+k}, \quad k \geq 0$$

Note that these two MPC problems are independent, i.e. have exclusive solution spaces. Each MPC problem is reformulated as an mp-QP and solved to obtain U as an explicit function of $x(t)$. The two solutions are then combined together to obtain solution for all the values of $x(t)$ in $[x_{min}, x_{max}]$.

These developments are used to derive the explicit insulin delivery rate for people with type 1 diabetes where hypo- and hyper-glycemia are weighted asymmetrically. This concept is demonstrated via the Bergman model (3.7 - 3.9) described in chapter 3.

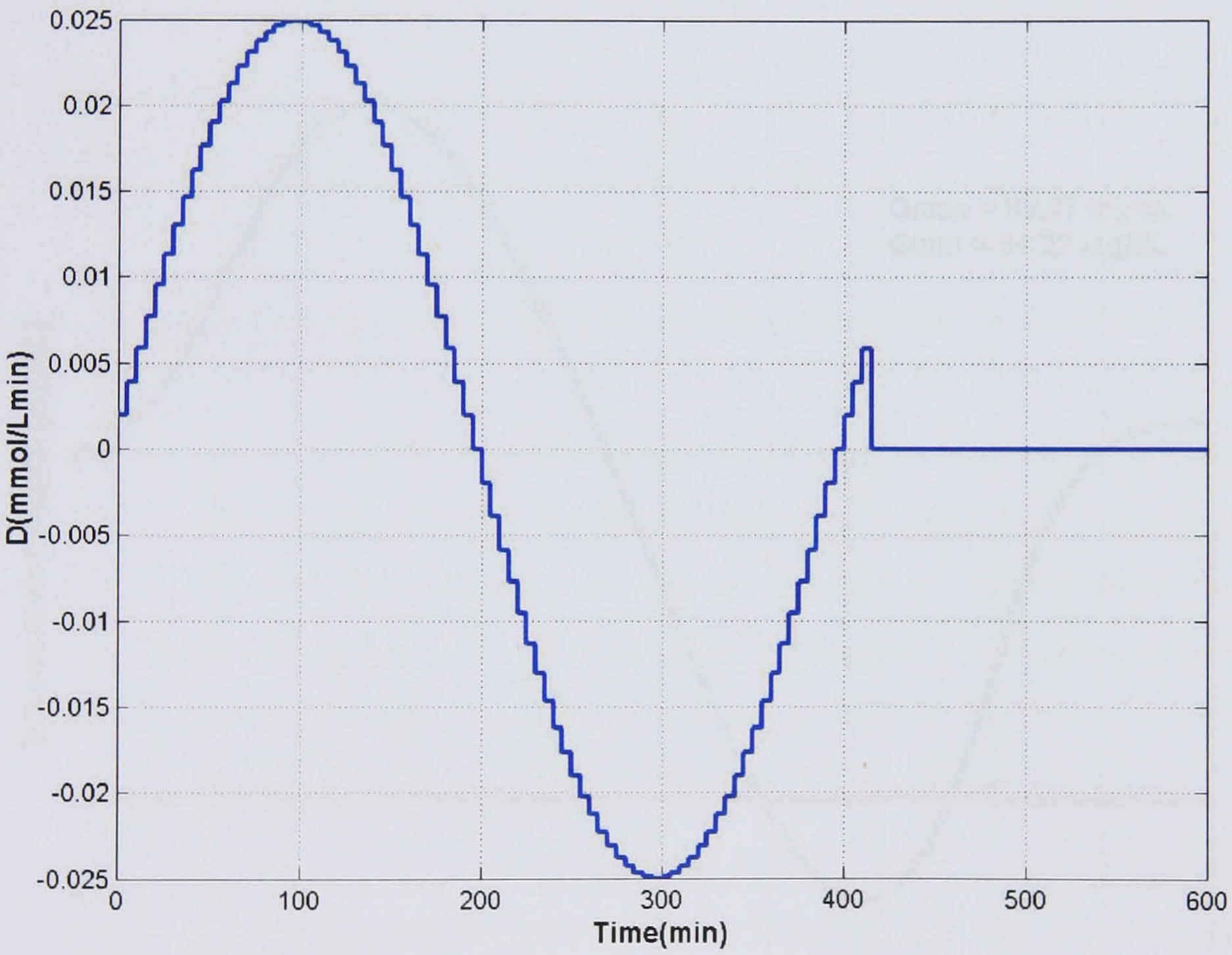


Figure 4.1 Sinusoidal Disturbance

To illustrate the concept of asymmetric objective function, first consider the symmetric case where hypo- and hyper-glycemia are equally weighted. To invoke the occurrence of hypoglycemia a sinusoidal disturbance of the form shown in Figure 4.1 is considered. The positive disturbance corresponds to an intake of meal whereas negative disturbance can be attributed to for example excessive bolus of insulin or

exercise. For the case when there are equal or symmetric weightings on hypo- and hyper-glycemia, there is violation of the constraint on hypoglycemia and the blood glucose concentration falls below 60 mg/dL – see Figure 4.2. This situation can be avoided by solving two parametric programs, one for $G \geq 81$ mg/dL and the other for $G \leq 81$ mg/dL. For the second parametric program, Q^-, the weighting on blood glucose deviation is taken to be 10 times higher than, Q^+, used for the first parametric program. Then the solution of both these programs is combined to provide the parametric controller for the whole range of blood glucose concentration. Figure 4.3 shows the variation of blood glucose concentration with time for the sinusoidal disturbance – a much smaller negative deviation from 81 mg/dL is obtained and hypoglycemia is avoided.

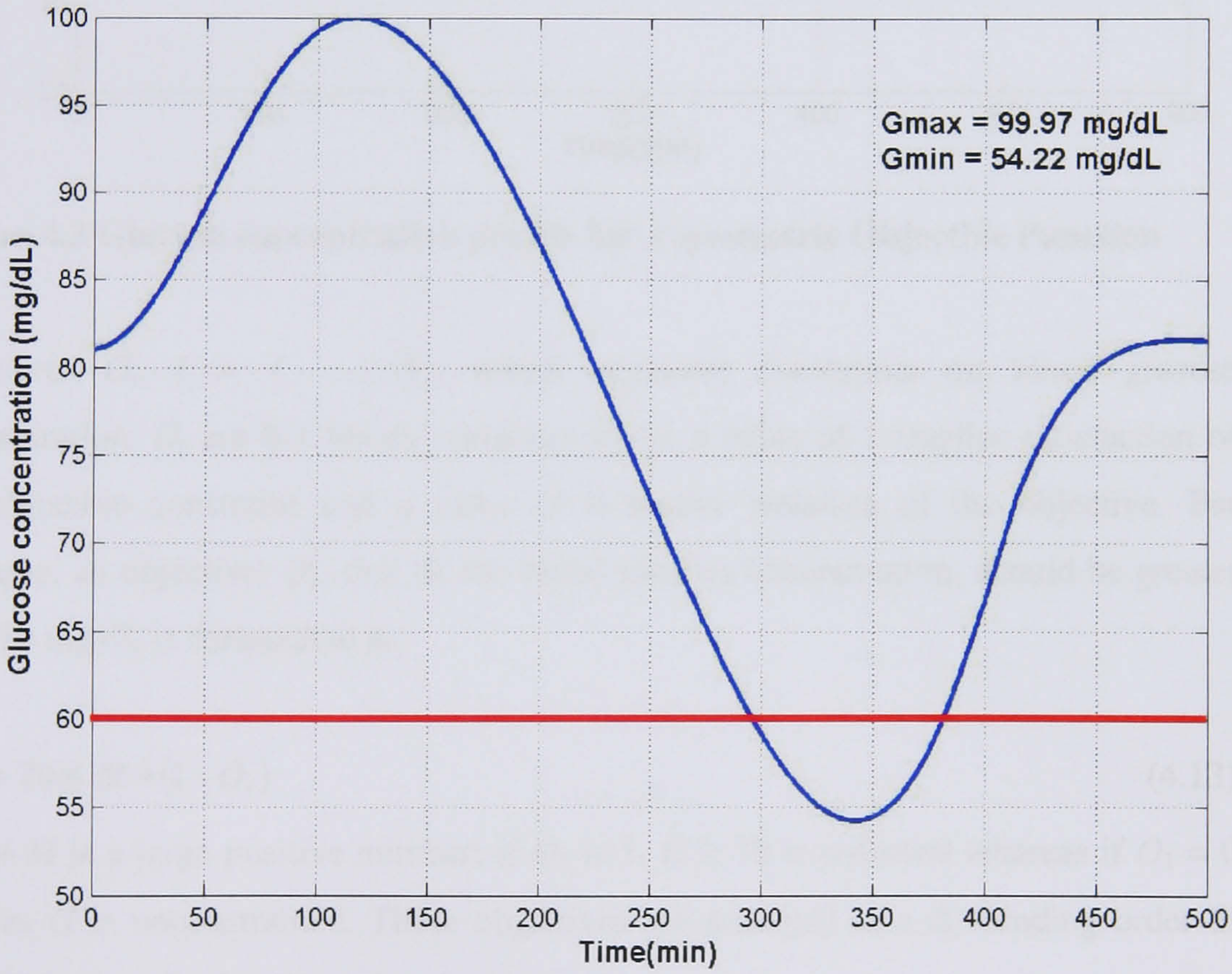


Figure 4.2 Glucose concentration profile for Symmetric Objective Function

4.3 Constraint Prioritization

As an alternative to the asymmetric objective function approach for reducing the hypoglycemic excursions, the problem can be formulated such that we have a set of

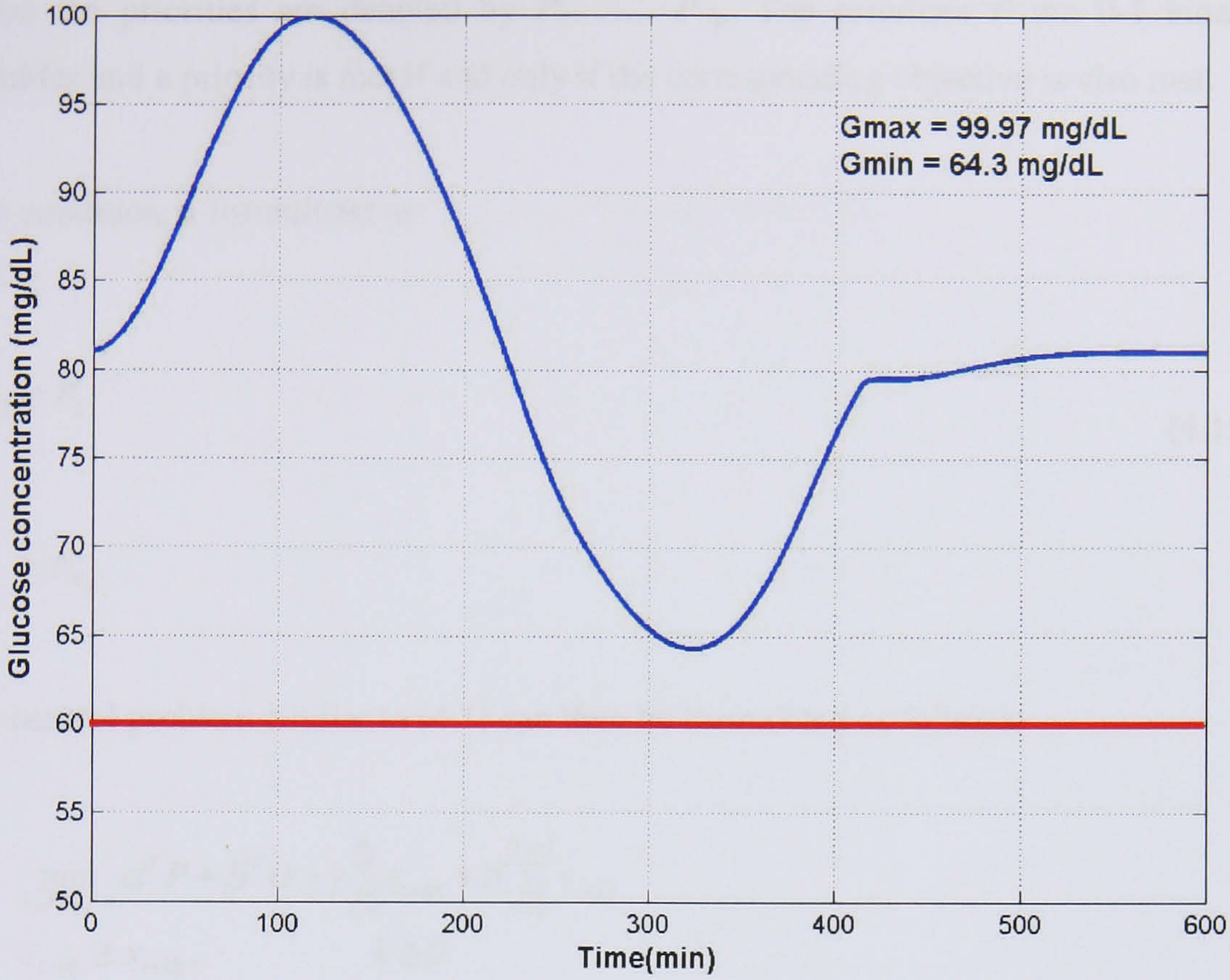


Figure 4.3 Glucose concentration profile for Asymmetric Objective Function

objectives O_i, $i = 1, \ldots, N_o$, which represent constraints on blood glucose concentration. O_i are 0-1 binary variables where a value of 1 implies satisfaction of the objective constraint and a value of 0 means violation of the objective. For example, an objective, O_1, that G, the blood glucose concentration, should be greater than 70 mg/dL is formulated as:

$$-G + 70 \leq M * (1 - O_1) \tag{4.13}$$

where M is a large positive number; if O_1 is 1, $G \geq 70$ is enforced whereas if $O_1 = 0$ implies G is unconstrained. These objectives are arranged in a descending order of priority by introducing the constraints:

$$\begin{aligned} P_1 &\geq P_2 \\ P_2 &\geq P_3 \\ &\vdots \\ &\vdots \\ P_{N_p-1} &\geq P_{N_p} \end{aligned} \tag{4.14}$$

where the priorities are denoted by P_1, ..., P_{Np}. The priorities P are 0-1 binary variables and a priority is met if and only if the corresponding objective is also met.

This condition is formulated as:

$$\begin{aligned} & O_1 \geq P_1 \\ & O_2 \geq P_2 \\ & \vdots \\ & \vdots \\ & O_{N_p} \geq P_{N_p}. \end{aligned} \tag{4.15}$$

The control problem similar to (4.1) can then be formulated as follows:

$$\begin{aligned} & \min_{U,P,O,\nu,\varepsilon} \alpha^T P + \beta^T O + \gamma \sum_{k=0}^{N_y} \varepsilon_{t+k|t} + \delta \sum_{k=0}^{N_y-1} \nu_{t+k|t} \\ s.t. \quad & \varepsilon_{t+k|t} \geq x_{t+k|t}, \qquad k \geq 0 \\ & \varepsilon_{t+k|t} \geq -x_{t+k|t}, \qquad k \geq 0 \\ & \nu_{t+k} \geq u_{t+k}, \qquad k \geq 0 \\ & \nu_{t+k} \geq -u_{t+k}, \qquad k \geq 0 \\ & u_{\min} \leq u_{t+k} \leq u_{\max}, \qquad k = 1, \cdots, N_c \\ & x_{t+k|t} = A x_{t+k|t} + B u_{t+k}, \quad k \geq 0 \\ & P_1 \geq P_2 \\ & P_2 \geq P_3 \\ & \vdots \\ & P_{N_p-1} \geq P_{N_p} \\ & O_1 \geq P_1 \\ & O_2 \geq P_2 \\ & \vdots \\ & O_{N_p} \geq P_{N_p} \\ & \psi\left(O_i, x_{t+k|t}\right) \leq 0, \qquad k \geq 0 \end{aligned} \tag{4.16}$$

where α and β are constant vectors, γ and δ are constant scalars, ε and ν are absolute values of x and u respectively and $\psi(O,x_{t+k|t}) \leq 0$ represents the vector of objective constraints, of the form (4.13). This is a mixed-integer linear program (MILP) that can be reformulated as a multi-parametric mixed integer linear program (mp-MILP) by treating the state variable as parameters and the control and integer variables as

optimization variables, similar to that discussed in chapter 3, and solved by using the mp-MILP algorithm described in Appendix E.

Table 4.1 Objectives and Priorities

Priorities	Objectives
1	$G(k+\theta) > 70,\ \theta = 2$
2	$G(k+\theta) > 70,\ \theta = 1$
3	$G(k+\theta) > 70,\ \theta = 0$
4	$G(k+\theta) > 75,\ \theta = 2$
5	$G(k+\theta) > 75,\ \theta = 1$
6	$G(k+\theta) > 75,\ \theta = 0$
7	$G(k+\theta) < 110,\ \theta = 2$
8	$G(k+\theta) < 110,\ \theta = 1$
9	$G(k+\theta) < 110,\ \theta = 0$

Consider the case when there are 9 objectives in the descending order of priority as shown in Table 4.1. $G(k+\theta)$ is the blood glucose concentration at the $k+\theta$ time interval where k is the current time interval and θ is the number of steps over which the objective is not enforced. Figure 4.4 shows the performance of the controller, which although is not as good as observed for the asymmetric case (Figure 4.3) but is much better than for the symmetric case (Figure 4.2) and hypo-glycemia is avoided. A profile of objectives and priority variables is also shown in Figures 4.5-4.8. From Figure 4.4, the objective constraint $G < 110$ is never violated and therefore O_7, O_8 and O_9 remain equal to 1 in Figure 4.6. The objective constraints $G > 75$ and $G > 70$ are violated at around 300-400 minutes and the corresponding objective variables, O1-O6, take a value of 0 in this time interval. Since $O_i \geq P_i$, P_1 to P_6 also take a value 0. Finally, since $P_i \geq P_{i+1}$, P_7 to P_9 also take a value of 0 in this time interval.

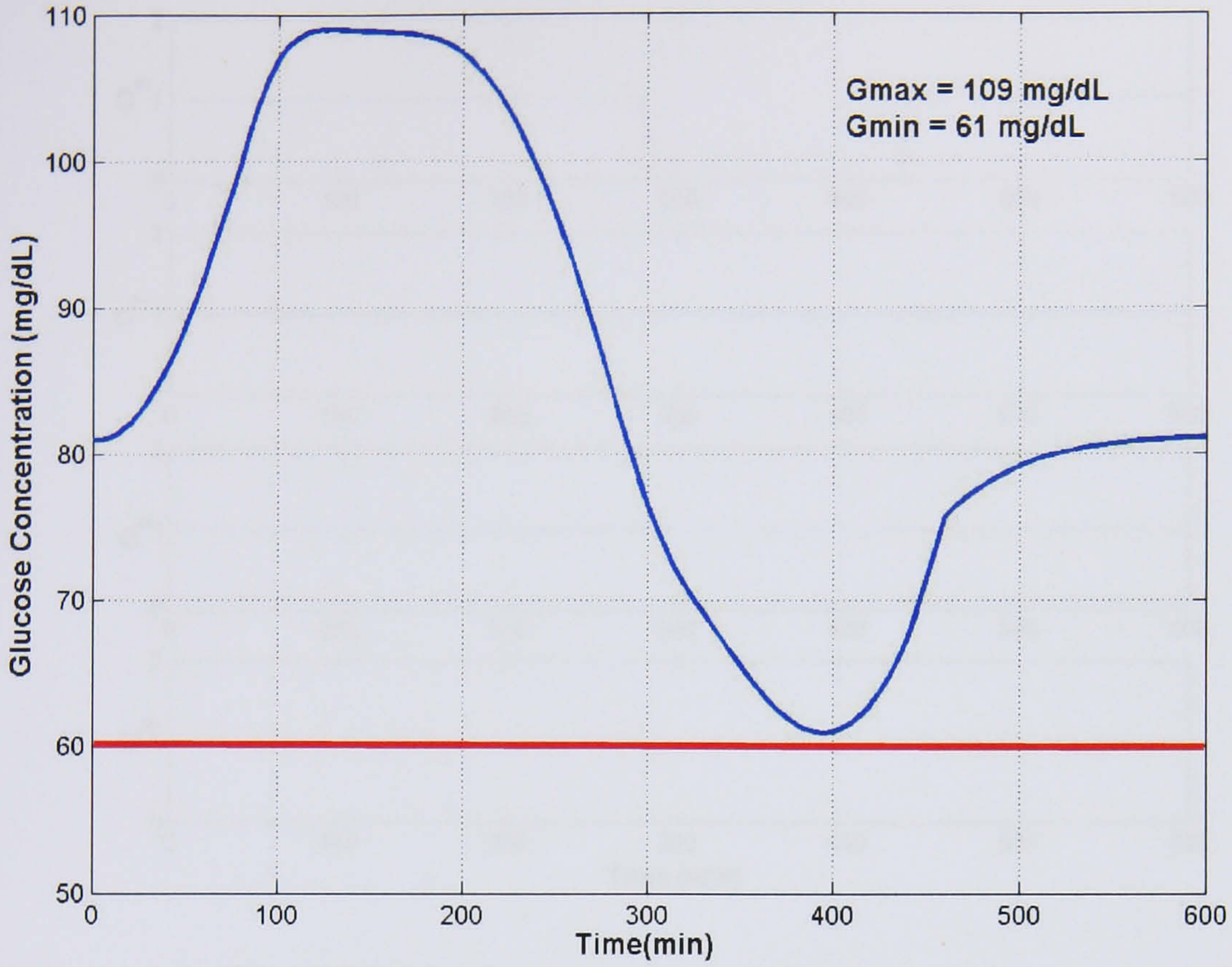


Figure 4.4 Glucose concentration profile for Prioritized Constraints

Figure 4.5 Profile of 0-1 Objective Variables, O_1 to O_5

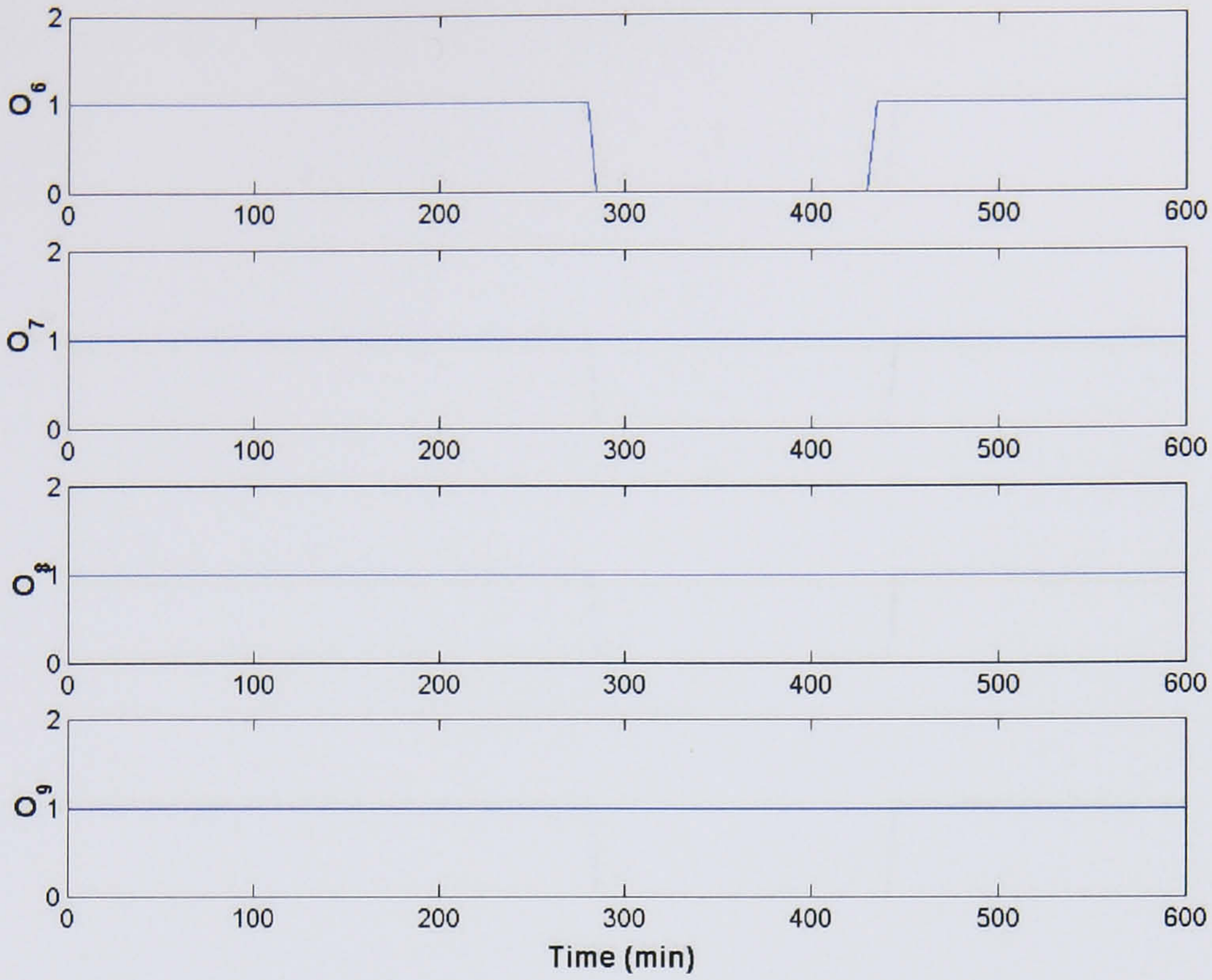


Figure 4.6 Profile of 0-1 Objective Variables, O_6 to O_9

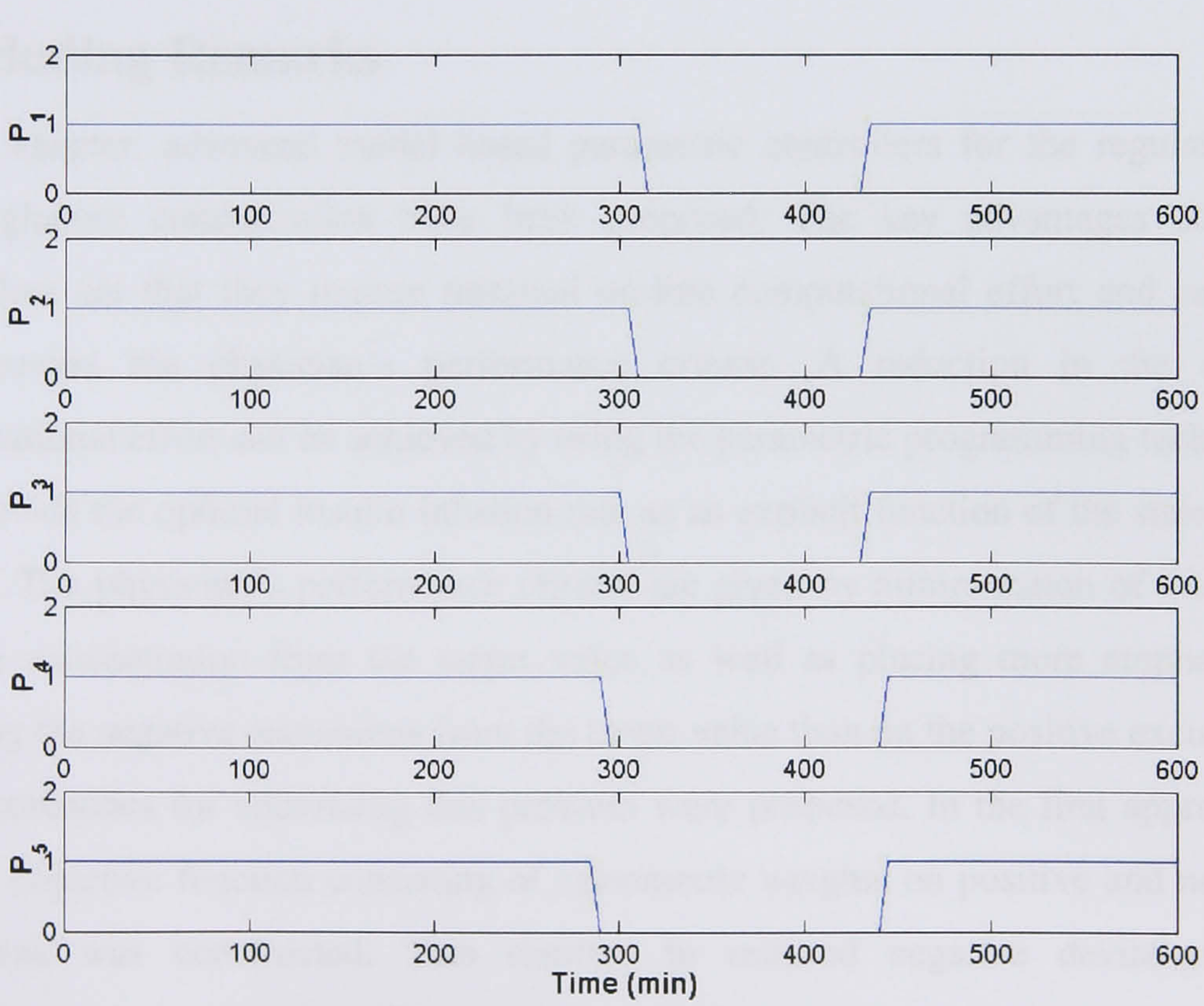


Figure 4.7 Profile of 0-1 Priority Variables P_1 to P_5

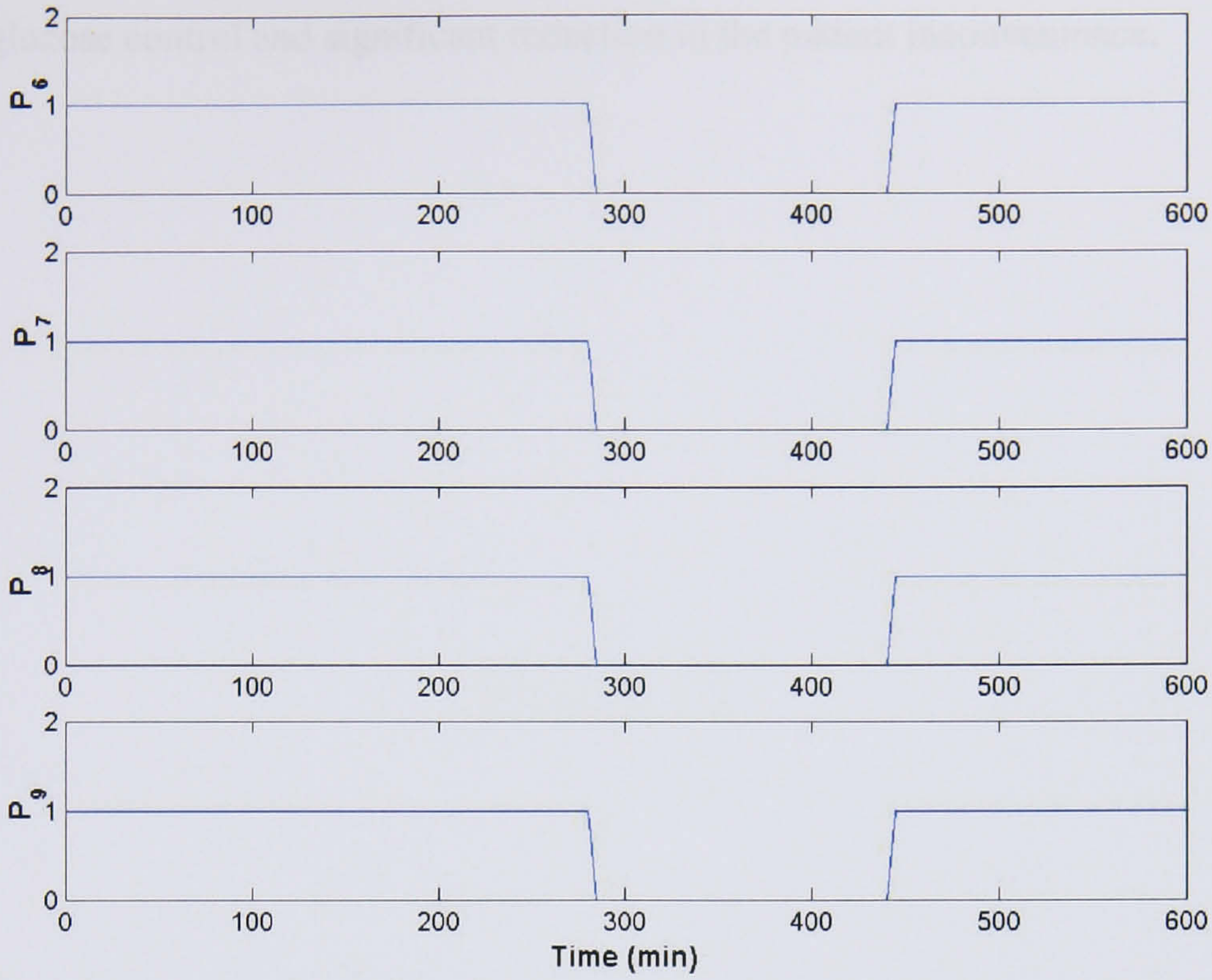


Figure 4.8 Profile of 0-1 Priority Variables, P_6 to P_9

Concluding Remarks

In this chapter, advanced model based parametric controllers for the regulation of blood glucose concentration have been proposed. The key advantages of these controllers are that they require minimal on-line computational effort and can take into account the physician's performance criteria. A reduction in the on-line computational effort can be achieved by using the parametric programming techniques that provide the optimal insulin infusion rate as an explicit function of the state of the patient. The physician's performance criteria are given by minimization of the blood glucose concentration from the target value as well as placing more emphasis on reducing the negative excursions from the target value than on the positive excursions. Two approaches for addressing this problem were proposed. In the first approach, a control objective function consisting of asymmetric weights on positive and negative deviations was constructed. This resulted in reduced negative deviations and hypoglycemia was avoided. The second approach relies on introducing 0-1 binary variables to enforce and prioritize constraints on blood glucose concentration. This approach also resulted in a reduction in negative deviations and avoided

hypoglycemia. These developments are expected to improve the automation of the blood glucose control and significant reduction in the patient inconvenience.

Part II

Delivery of Drugs for Surgery under Anesthesia and Optimal Control of Cancer

Chapter 5

Surgery under Anesthesia

In this work a compartmental model for the delivery of three drugs (isoflurane, dopamine and sodium nitroprusside) for anesthesia is presented. The key feature of this model is that mean arterial pressure, cardiac output and unconsciousness of the patient can be simultaneously regulated. A number of dynamic simulation experiments are carried out for the validation of the model. The model was then used for the design of model predictive and parametric controller and the performance of the controllers was analyzed.

5.1 Introduction

The word anesthesia, which originates from the Greek word *anaisthesis* meaning loss of sensation, was first used in 1846 by Oliver Wendell Holmes, a well-known doctor who taught anatomy and physiology at the Harvard Medical School. He demonstrated the use of ether for pain relief on a patient in a clinical setting (Figure 5.1) and since then many substances and drugs have been introduced for anesthesia leading to significant improvements in the surgery techniques. A modern operation theatre has a surgeon who is concerned mainly with the surgery of the patient while the anesthesiologist aims to guarantee not only pain relief but also that: hypnosis is achieved, the vital functions of the patient are maintained and muscle relaxation is provided. The surgeon and the anesthesiologist are separated by a curtain and the anesthesiologist has limited access to the patient. The anesthesiologist therefore has to mostly infer the state of the patient from the measurements available from the patient monitor (Figure 5.2) and accordingly manipulate the drug infusion rates. This task is further complicated in the presence of surgical disturbances, stress situations and in

case of complex surgeries. Automatic control of the state of the patient would greatly assist the anesthesiologist in carrying out some routine activities, allow for more time to be spent on critical issues and provide delivery of drugs in a much safer environment. A detailed introduction to anesthesia is provided in the next section and automation of anesthesia is discussed in section 5.1.2.



Figure 5.1 Demonstration of Pain Relief via Anesthetics in Ancient Times



Figure 5.2 Anesthesiologist in Modern Operation Theatre

5.1.1 An Introduction to Anesthesia

Signs and Stages of Anesthesia

Traditionally the observable effects of diethyl ether on the patient are usually correlated with the depth of anesthesia. These effects or signs refer to effects on the respiratory system, reflex activity and muscle tone and are divided into four main stages representing the level of depression of the central nervous system. These stages are:

1. Stage of Analgesia: An initial analgesia without amnesia is experienced.
2. Stage of Excitement: At this stage amnesia is attained and the patient appears to be delirious and excited, has irregular respiration and sometimes may become incontinent and even vomit. This stage ends with the restoration of the regular repiration.
3. Stage of Surgical Anesthesia: The stage begins with regular respiration and the depth of anesthesia can be assessed through changes in ocular movements, eye reflexes and pupil size.
4. Stage of Medullary Depression: This stage starts when spontaneous respiration stops and circulatory respiratory support is essential to prevent death. A characteristic of this stage is the severe depression of the vasomotor center in the medulla and the respiratory center.

In the modern anesthetic procedure, a single anesthetic drug is not used and instead a combination of drugs is used. These drugs have much faster onset time than diethyl ether and the signs of the four stages of anesthesia are vague; some new techniques being developed to characterize these stages are described in the next section.

Triad of Anesthesia

Adequate general anesthesia can be defined as a reversible pharmacological state where it is guaranteed that the triad of anesthesia (Figure 5.3) given by muscle relaxation, analgesia and hypnosis is achieved and the vital functions of the body are maintained. Muscle relaxation facilitates access to internal organs and depresses any movement responses to surgical stimulation. An estimate of the extent of relaxation

can be obtained by measuring the force of thumb adduction induced by stimulation of the Ulnar nerve or by single twitch force depression. Analgesia which is concerned with pain relief is difficult to quantify because there are no direct measurement techniques and also due to the fact that the muscle relaxants partially suppress the clinical signs such as tearing, pupil reactivity, eye movement and grimacing. Hypnosis which is used to describe the unconsciousness and the absence of postoperative recall of events that occur during surgery is concerned mainly with the effect of anesthetics on the brain. The level of hypnosis can be estimated by measuring the activity of the central nervous system by using electroencephalogram (EEG) to provide Bispectral Index (BIS). A BIS value of 100 represents an awake patient and a value between 40 and 65 is considered to be suitable for most surgeries. The relation between different BIS ranges and the corresponding clinical situations is given in Table 5.1.

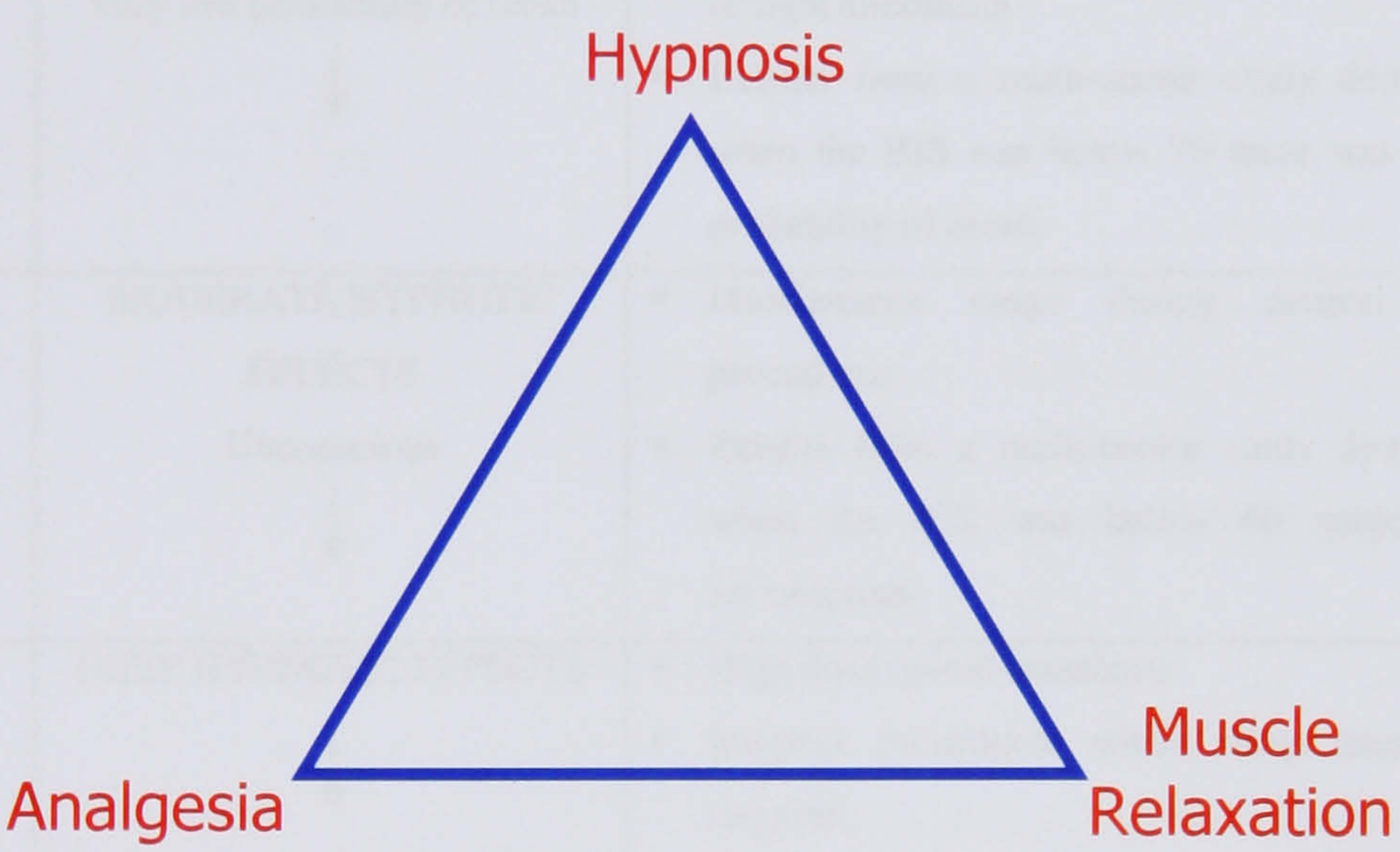


Figure 5.3 Triad of Anesthesia

The level of hypnosis can also be inferred by estimating depth of anesthesia by measuring Mid Latency Auditory Evoked Potentials (MLAEP). MLAEPS are the responses in the EEG to clicks applied in the ear and are measured by using scalp electrodes.

Anesthetic Agents

There are two main theories that describe the effect of the anesthetic agents on the cell membrane. Lipid theory postulates that the anesthetic agents dissolve in the membrane lipid and alter its membrane function. Protein theory hypothesizes that the anesthetic agents interact with the hydrophobic domains of the membrane protein and disrupt the normal ion permeability of the membrane.

Table 5.1 Relation between BIS and Clinical Endpoints

BIS	CLINICAL ENDPOINTS AND SEDATION RANGES	CLINICAL SITUATION
100	AWAKE Sedated ↓	▪ Awake or resting state ▪ Sedated for special procedures; conscious-sedation ▪ Response to vigorous stimulation during surgery ▪ Emergence from general anesthesia
70	LIGHT HYPNOTIC EFFECTS Very low probability of recall ↓	▪ Short surgical procedures requiring deep sedation or light anesthesia ▪ Results from a multi-center study demonstrated when the BIS was below 70 there was very low probability of recall
60	MODERATE HYPNOTIC EFFECTS Unconscious ↓	▪ Maintenance range during general surgical procedures ▪ Results from a multi-centre study demonstrated when the BIS was below 60 subjects were unconscious
40	DEEP HYPNOTIC EFFECTS ↓	▪ High dose opioid anesthesia ▪ Surgical procedures where deep anesthesia is required ▪ Barbiturate coma ▪ Profound hypothermia
0	EEG SUPRESSION	

Anesthetic agents are usually induced through inhalation or intravenously. A list of some of the common inhalation anesthetics is given in Table 5.2. The extent of the effect of the inhalation agents on the depth of anesthesia is determined by their concentration in the brain, which is determined by the following factors.

1. Solubility

The transfer of an anesthetic agent from lungs to blood is affected by its solubility which can be measured in terms of blood/gas partition coefficient. An anesthetic agent with high blood/gas partition coefficient is much more soluble in blood than it is in the gas and since the depth of anesthesia strongly depends upon the partial pressure of anesthetic, an agent with high partition coefficient will have longer induction time.

Table 5.2 Common Inhalation Anesthetics

Inhalation Anesthetic	Chemical Formula	Characteristics
Halothane	CF_3-CHClBr	▪ Widely used ▪ Hypotensive ▪ About 30% metabolized ▪ May cause dysryrhmias and liver damage if used repeatedly
Nitrous Oxide	N_2O	▪ Analgesic with rapid induction and recovery ▪ Usually combined with other agents due to low potency ▪ Prolonged administration may result in bone marrow depression
Enflurane	CHClF-CF_2-O-CHF_2	▪ Similar to halothane but less metabolized and therefore less risk of toxicity ▪ Faster induction and recovery than halothane ▪ Risk of epilepsy-like seizures
Isoflurane	CF_3CHCl-O-CHF_2	▪ Optical isomer of enflurane ▪ Hypotensive ▪ Simultaneously lowers blood pressure and increases depth of anesthesia ▪ Low metabolism and therefore suitable for patients with liver disease ▪ Best anesthetic agent for use in neurosurgical anesthesia

2. Anesthetic concentration in the inspired air

A high concentration of the anesthetic in the inspired air will increase the rate of transfer into the blood and rate of induction. This fact is used for agents with moderate blood solubility and slow onset.

3. Pulmonary ventilation

The effect of pulmonary ventilation on the partial pressure of the anesthetic depends upon the solubility of the anesthetic. An increase in pulmonary ventilation only slightly increases the partial pressure of an anesthetic with low blood/gas partition coefficient but significantly increases the partial pressure of an anesthetic with high partition coefficient.

4. Pulmonary blood flow

The transfer of the anesthetic agent to and from the lungs is affected by the changes in the rate of blood flow. For anesthetics with moderate to high blood solubility the rate of increase in partial pressure slows down with an increase in pulmonary blood flow or cardiac output. This phenomenon can be attributed to an increase in the amount of blood that is available to the anesthetic resulting in an increase in the blood capacity and therefore slow increase in partial pressure.

5. Arteriovenous concentration gradient

The concentration gradient between the arterial and venous blood depends upon the anesthetic uptake by the tissues. The larger this gradient is, the longer it takes to reach the equilibrium. The uptake of the anesthetics by the tissues is also affected by factors similar to those for transfer from lungs to blood: tissue/blood partition coefficient, rate of blood flow to the tissues and concentration gradients.

Intravenous anesthetics act in about 20 seconds which is much more rapid than the inhalation anesthetics. These are usually used for the induction of anesthesia and have very fast rates of recovery allowing them to be used in outpatient anesthesia. Also, unlike inhaled anesthetics no specialized and expensive equipment for their delivery and recovery are required. Some intravenous anesthetics are listed in Table 5.3.

Vital Functions

During the surgery a wide range of vital functions, such as mean arterial pressure (MAP), heart rate and cardiac output (CO), should be monitored and maintained within the desired ranges. Note that not all the vital functions can be measured directly and hence are inferred indirectly. These vital functions are maintained by the

anesthesiologist by regularly infusing various anesthetic drugs and/or intravenous fluids.

Table 5.3 Common Intravenous Anesthetics

Intravenous Anesthetic	Chemical Formula	Characteristics
Etomidate	$C_{14}H_{16}N_2O_2$	▪ Similar to thiopentone ▪ Faster metabolism that thiopentone and less risk of cardiovascular disease ▪ Sometimes causes involuntary movements during induction
Propofol	$C_{12}H_{18}O$	▪ Introduced recently ▪ Fast metabolism ▪ Rapid recovery and no cumulative effect
Ketamine	$C_{13}H_{16}ClNO$	▪ Different action from other agents ▪ Slow onset ▪ Causes dissociative anesthesia – though amnesia and insensitivity to pain are achieved the patient remains conscious ▪ Mainly used for minor procedures in children
Dopamine	$C_8H_{11}NO_2$	▪ More effective on peripheral blood vessels than on the heart itself ▪ Low dose causes selective renal vasodilatation and simultaneous increase in blood pressure ▪ High dose used for direct myocardial stimulant action increasing the force of contraction, cardiac output and blood pressure
Sodium Nitroprusside	$Na_2[Fe(CN)_5NO]2H_2O$	▪ Although dose dependent it produces extremely rapid fall in arterial blood pressure by peripheral vasodilatation ▪ Dilates arteries and vessels equally and therefore maintains blood flow to vital organs at low blood pressures ▪ Widely used for elective hypotension in neuro, cardiac and vascular surgery where fine and rapid control of blood pressure is essential ▪ Its action wears off within two minutes of discontinuation

It must be emphasized that a tight control of these vital functions has paramount consideration; otherwise it may lead to fatal situations (Simpson and Popat, 2002).

5.1.2 Automation in Anesthesia

Automation of anesthesia for monitoring of vital functions is desirable as it will provide more time and flexibility to the anesthesiologist to focus on critical issues, monitor the conditions that cannot be easily measured and overall improve patient's safety. Also, the cost of the drugs will be reduced and shorter time will be spent in the post-operative care unit.

The anesthesiologist seeks to achieve adequate anesthetic conditions, while maintaining the patient's vital functions within acceptable ranges to ensure the safety of the patient. This can be achieved by administering various drugs and intravenous fluids as shown in Figure 5.4. The control variables are given by infusion of intravenous anesthetics, volatile anesthetics, muscle relaxants, ventilation parameters and vasodilators and the measurable outputs are the EEG parameters, heart rate, blood pressure, CO_2 concentration and the inspired and expired concentrations. The non-measurable outputs given by hypnosis, analgesia and muscle relaxation cannot be estimated directly and must be inferred from the measurable outputs. The anesthesiologist has to act as a feedback controller by analyzing the measurable outputs, inferring the non-measurable outputs and optimally manipulating the control variables under disturbances arising from surgical stimulus and blood loss.

A significant amount of improvement can be achieved in the implementation of control of anesthesia by developing an automated system that can take into account the complex interactions between the control and output variables and disturbances. A number of benefits can be derived from such an implementation. A much tighter control can be obtained by having a continuous monitoring system and overdosing of drugs can be reduced by using precise and automatic infusion devices. The automatic control system can also take into account the interactions between the drugs and can be tuned for any variations in the operating procedure. Overall, this will result in reduced drug consumption by the patient, less effort by the anesthesiologist, less time

spent by the patient in postoperative care unit and a more economic and safe anesthetic procedure.

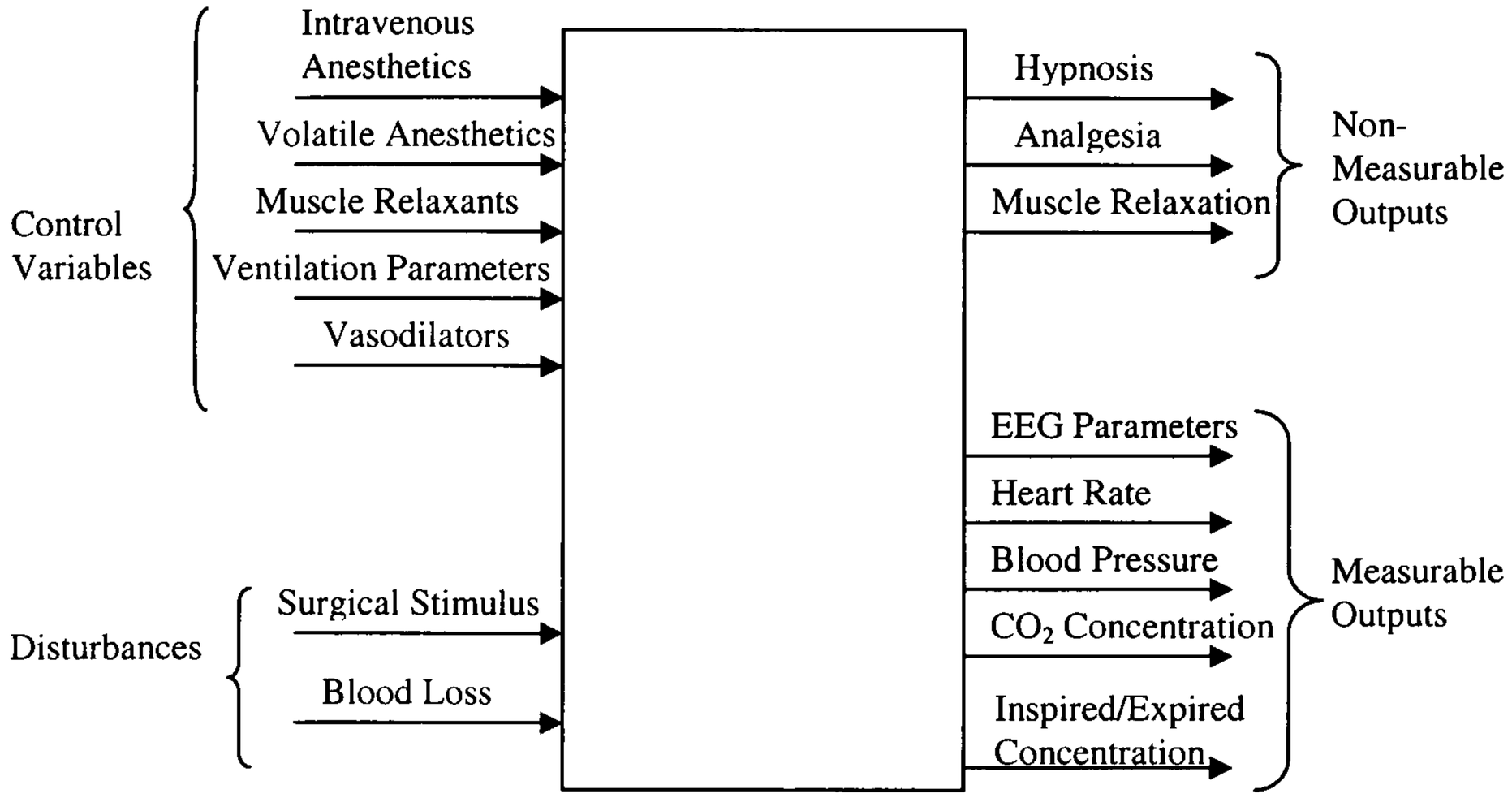


Figure 5.4 Anesthesia Control System (adapted from Gentilini *et al.* 2001)

A number of models and control strategies have been reported in the open literature for the automation of anesthesia (Derighetti *et al.*, 1997; Zwart *et al.*, 1972; Yasuda *et al.*, 1989-1991; Gopinath *et al.*, 1995; Rao *et al.*, 2001; Mahfouf *et al.*, 2003). Gentilini *et al.* (2001) proposed a model for the regulation of mean arterial pressure (MAP) and hypnosis with isoflurane. It was observed that controlling both MAP and hypnosis simultaneously with isoflurane was difficult. Yu *et al.* (1990) proposed a model for regulating MAP and cardiac output (CO) using dopamine (DP) and sodium nitroprusside (SNP), but the control of hypnosis was not considered.

In this chapter, a compartmental model is proposed, which allows the simultaneous regulation of the MAP, CO and the unconsciousness of the patients. Three major aspects characterize the model:

1) pharmacokinetics, which describes the uptake and distribution of the drugs
2) pharmacodynamics which is concerned with the effect of the drugs on the vital functions

3) baroreflex which accounts for the reaction of the central nervous system to changes in the blood pressure.

The model involves choice of three drugs, isoflurane, DP and SNP. This combination of the drugs allows simultaneous regulation of MAP, CO and hypnosis.

5.2 Modelling Anesthesia

The model is based on the distribution of isoflurane in the human body (Yasuda *et al.*, 1991) and on the works of Gentilini *et al.* (2001) and Yu *et al.* (1990). It consists of five compartments organized as shown in Figure 5.5. The compartments stand for:

1: Lungs
2: Vessel Rich organs (e.g. liver)
3: Muscles
4: Other organs and tissues
5: Fat tissues

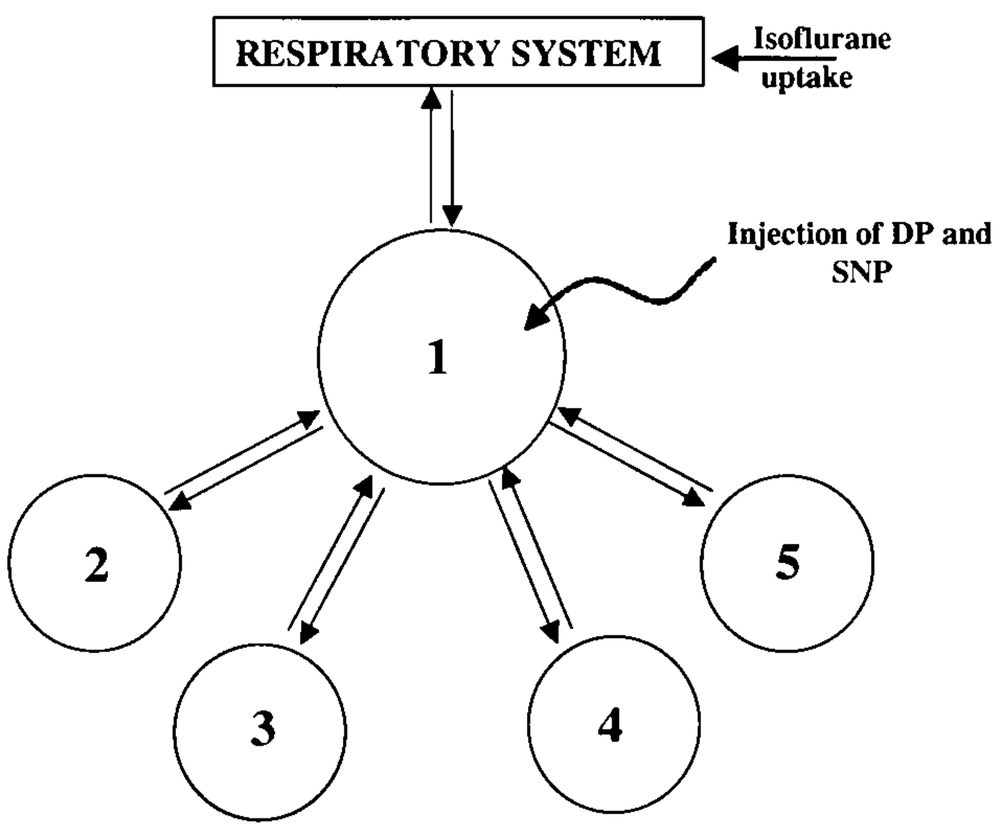


Figure 5.5 Compartmental Model

Isoflurane is a volatile drug that first enters the respiratory system and then the lungs. SNP and DP are intravenous drugs; SNP is a vasodilator that dilates the arteries and

effectively lowers MAP and DP is an inotropic agent that enhances the cardiac performance by improving the heart contractility. These drugs are distributed to the compartments via the circulatory system and therefore the heart can be taken as if belonging to the central compartment. The transfers from the central compartment to the peripheral compartments *i.e.* compartments 2-5 occur via the arteries and the transfers from the peripheral compartments to the central, via the veins. The introduction of drugs can be related to the first compartment as shown on Figure 5.5.

5.2.1 Pharmacokinetic Modelling

Assuming that all the compartments are well-stirred, the differential equations resulting from mass balances for a generic i^{th} compartment can be written as:

$$V_i \frac{dC_{i,j}}{dt} = Q_i \left(C_{a,j} - \frac{C_{i,j}}{R_i} \right) - k_{i,j} C_{i,j}$$

where

V_i is the volume of compartment i

$C_{i,j}$ is the drug concentration in the compartment

Q_i is the blood flow to the compartment i

$k_{i,j}$ is the relevant rate constant

$C_{a,j}$ is the drug concentration in the arterial pool and

R_i is the partition coefficient between blood and tissues in compartment i.

The partition coefficient R_i defines the ratio of blood, which will be kept by the living tissue constituting the ith compartment. Its role is not to modulate the concentration of drug, but the flow rate of blood according to the following relation:

$$Q_{i,out} = \frac{Q_{i,in}}{R_i}$$

where

$Q_{i,in}$ is the inlet flow rate of blood (i.e. Q_i) and

$Q_{i,out}$ is the outlet flow rate of blood.

Considering the organization of the compartment, the concentration of the drug in the arteries is equal to the concentration in the outlet flows from compartment 1, i.e. the concentration of drug within this well-stirred compartment. Thus equation becomes:

$$V_i \frac{dC_{i,j}}{dt} = Q_i\left(C_{1,j} - \frac{C_{i,j}}{R_i}\right) - k_{i,j}C_{i,j}$$

Respiratory System

The uptake of isoflurane in central compartment occurs via the respiratory system. Considering a well-stirred system, this is modelled as:

$$V\frac{dC_{insp}}{dt} = Q_{in}C_{in} - (Q_{in} - \Delta Q)C_{insp} - f_R(V_T - \Delta)(C_{insp} - C_{out})$$

where

C_{insp} is the concentration of isoflurane inspired by the patient (g/mL)

C_{in} is the concentration of isoflurane in the inlet stream (g/mL)

C_{out} is the concentration of isoflurane in the outlet stream (g/mL)

Q_{in} is the inlet flow rate (mL/min)

ΔQ are the losses (mL/min)

V is the volume of the respiratory system (L)

f_R is the respiratory frequency (1/min)

V_T is the tidal volume (L) and

Δ is the physiological dead space (mL).

Central Compartment

The distribution of isoflurane within the central compartment is governed by:

$$V_1\frac{dC_1}{dt} = \sum_{i=2}^{5}\left(Q_i\left(\frac{C_i}{R_i} - C_1\right)\right) + f_R(V_T - \Delta)(C_{insp} - C_1)$$

where

C_i is the concentration of the drug in compartment i (g/mL)

R_i is the partition coefficient between blood and tissues in compartment i

Q_i is the blood flow in compartment i (mL/min).

The infusion of intravenous drugs DP and SNP in the central compartment is modelled as follows:

$$V_1 \frac{dC_1}{dt} = \sum_{i=2}^{5}\left(Q_i\left(\frac{C_i}{R_i} - C_1\right)\right) + C_{\text{inf}} - \frac{1}{\tau_{1/2}} C_1 V_1$$

where

C_{inf} is the flowrate of the drug infused (g/min)

V_i is the volume of compartment i (mL) and

$\tau_{1/2}$ is the half life of the drug (min).

Peripheral Compartments

Elimination of isoflurane by exhalation and metabolism in liver, the 2nd compartment, is given by:

$$V_2 \frac{dC_2}{dt} = Q_2\left(C_1 - \frac{C_2}{R_2}\right) - k_{20} C_2 V_2$$

where

k_{20} is the rate of elimination of isoflurane in the 2nd compartment (min^{-1}).

The concentration of isoflurane in compartments 3 to 5 is given by

$$V_i \frac{dC_i}{dt} = Q_i\left(C_1 - \frac{C_i}{R_i}\right), \; i = 3,\ldots,5.$$

DP and SNP naturally decay in the body, hence the equations for compartments 2 to 5 are

$$V_i \frac{dC_i}{dt} = Q_i\left(C_1 - \frac{C_i}{R_i}\right) - \frac{1}{\tau_{1/2}} C_i V_i \ , i = 2,\ldots,5.$$

Blood flows

The average change in regional blood flows under the uptake of isoflurane can be computed from the literature (Derighetti, 1999). These flows depend on the concentration of this anesthetic agent.

$$Q_i = Q_{i0} \cdot \left(1 + \Delta_{flowi} \cdot C_{in}\right) , i = \{2, 3, 4, 5\}$$

$$Q_1 = \sum_{i=2}^{5} Q_i$$

where

Δ_{flowi} is the ratio of flow rate change in the ith compartment and

C_{in} is the concentration of isoflurane in the inlet flow of the respiratory system.

5.2.2 Pharmacodynamic Modelling

Effect of DP and SNP on MAP

DP and SNP indirectly affect MAP via two of the heart's characteristic parameters, Maximum Elastance (E_{max}) (the heart's contractility, maximum pressure/volume ratio in the left ventricle) and Systemic Resistance (R_{sys}) (resistance of tissues to blood flow), and Cardiac Output (CO) (blood volume injected by the heart on a minute basis, L/min). The equation dictating the relationship between blood pressure and cardiac output is:

$$MAP = R_{sys} \cdot CO \ .$$

These physiological variables MAP and CO, the so-called hemodynamic variables, are considered to be highly interconnected in many ways. SNP is a vasodilator drug, administered in order to control hypotension during anesthesia in surgery. It causes relaxation of arterial and venous smooth muscles, leading to a rapid and predictable decrease in blood pressure and providing a nearly bloodless surgical field. More specifically, it is known to act principally on R_{sys}, causing an important reduction in it, while it causes a mild reduction on CO, thus leading to an overall decrease in MAP.

DP is an inotropic agent, infused in order to cure "septic shock", i.e. hypotension, systemic vasodilation and low cardiac output. Consequently, DP increases CO and R_{sys}, indirectly leading to an overall increase in blood pressure.

The action of these two drugs on these parameters is given by:

$$\frac{dEff}{dt} = k_1 C^N \left(Eff_{\max} - Eff \right) - k_2 Eff$$

where

Eff is the measure of the effect of drug on the parameters of interest

k_1, k_2 are the rate constants

N is the non-linearity constant and

C refers to the concentration of either DP or SNP.

The affected parameters are related to different aspect of the distribution of drugs in the circulatory system: E_{max} is linked to the concentration of DP in the large arteries, whereas R_{sys} is linked to the concentration of DP and SNP in the small ones. However, considering the compartmental model and the fact that the compartments are considered well-stirred, those two concentrations are equal to the concentration of DP in the central compartment:

$$\frac{dEff}{dt} = k_1 C_1^N \left(Eff_{\max} - Eff \right) - k_2 Eff$$

E_{max} and R_{sys} are related to the previous equation as follows:

$$E_{\max} = E_{\max,0}\left(1 + Eff_{DP-E_{\max}}\right)$$
$$R_{sys} = R_{sys,0}\left(1 - Eff_{DP-R_{sys}} - Eff_{SNP-R_{sys}}\right)$$

where

R_{sys} is the systemic resistance (mmHg/(mL/min))

E_{max} is the maximum elastance (mmHg/mL)

$E_{max,0}$ is nominal maximum elastance

$R_{sys,0}$ is nominal systemic resistance

$Eff_{DP\text{-}Emax}$ is effect of DP on E_{max}

$Eff_{DP\text{-}Rsys}$ is effect of DP on R_{sys}

$Eff_{SNP\text{-}Rsys}$ is the effect of SNP on R_{sys} .

Relationship between E_{max}, R_{sys} and MAP

Applying Bernoulli's equation to the heart, a relation between CO and MAP can be obtained. As E_{max} is the maximum pressure/volume ratio in the left ventricle, it can be related to CO by Bernoulli's equation for two points on the same streamline:

$$P + \frac{1}{2}\rho u^2 = \text{constant}$$

where

P is the pressure,

ρ is the density and

u is the velocity.

It is assumed that gravity effects are negligible, blood density is constant and the flow is steady. The assumption is unlikely to hold for this system, but the equation should still provide a good approximation of the relationship between E_{max} and CO. Also, E_{max} applies to the systolic elastance of the heart, which is the pressure-volume ratio at the height of contraction. This will determine the pressure at which blood is expelled from the left ventricle and can therefore be used in this analysis.

If the first point on a streamline is in the left ventricle and the second point in the aorta, just after the heart, then for this system,

$$V_{LV}E_{\max} + \frac{1}{2}\rho\left(\frac{CO}{A_{LV}}\right)^2 = MAP + \frac{1}{2}\rho\left(\frac{CO}{A_{aorta}}\right)^2$$

where

MAP is the mean arterial pressure (mmHg)

A_{aorta} is the cross sectional area of the aorta (cm^2)

A_{LV} is the cross sectional area of the left ventricle (cm^2)

V_{LV} is the mean volume of the left ventricle (mL) (averaged on a complete cardiac cycle) and

ρ is the blood density (g/mL).

Rearranging the above equation,

$$CO = K\left(2V_{LV}E_{\max} - 2MAP\right)^{1/2}$$

where, $K = \dfrac{A_{aorta}A_{LV}}{\sqrt{\rho}\sqrt{A_{LV}^2 - A_{aorta}^2}}$.

Since, $MAP = R_{sys} \cdot CO$, MAP can be expressed as a function of E_{max} and R_{sys} as:

$$MAP^2\frac{1}{R_{sys}^2} + 2K^2MAP - 2K^2V_{LV}E_{\max} = 0.$$

Effect of Isoflurane on MAP

The equation describing the hemodynamic effect of isoflurane has been obtained from the modeling structure derived by Zwart *et al.*(1972) for halothane, where the Ohm's law is applied to the circulatory system (Figure 5.6).

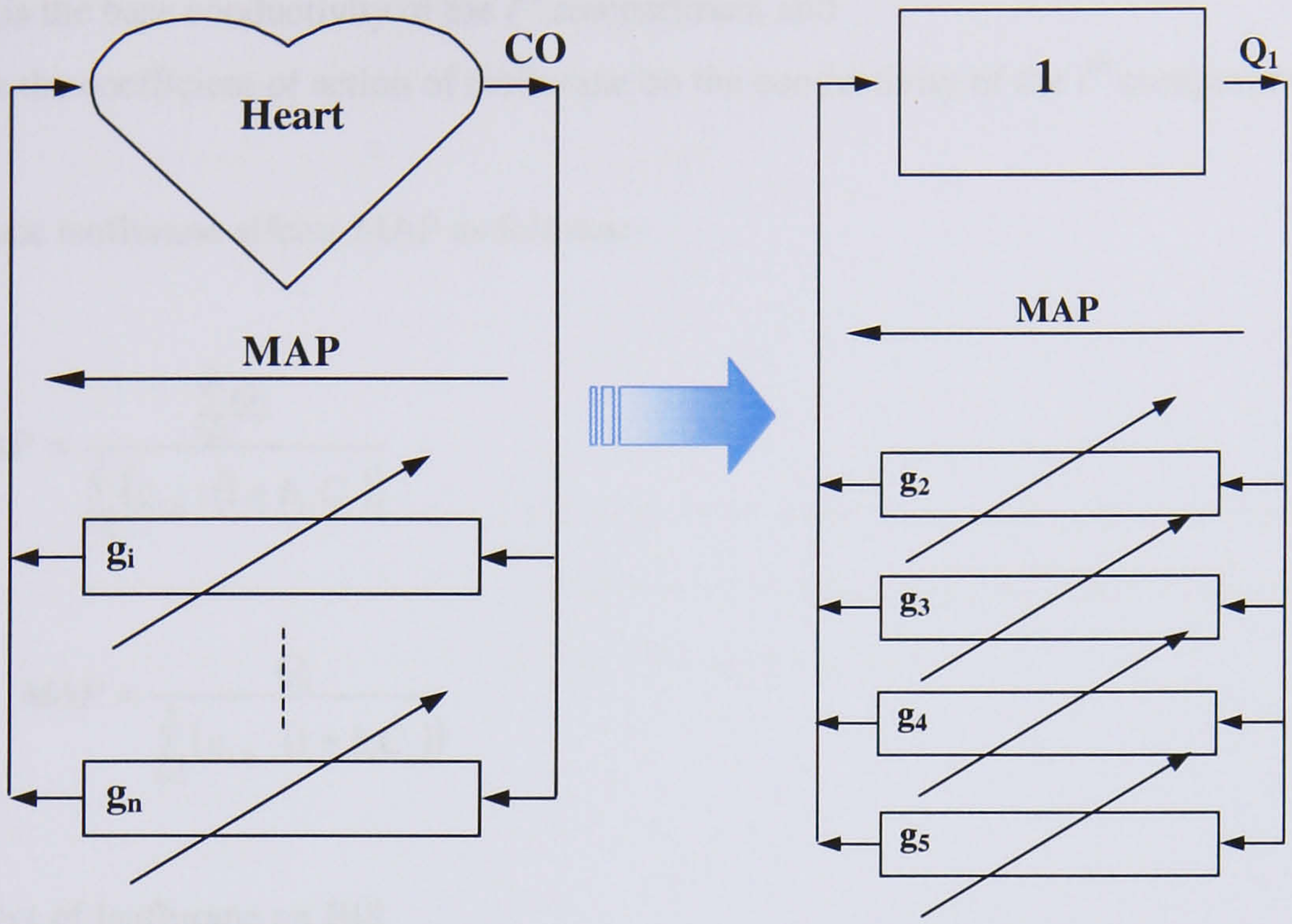


Figure 5.6 Electrical analogy of the circulatory system (Zwart, 1972) and its application in this study

Each compartment presents a certain conductance to blood flow, which can be related to *MAP* and *CO* as follows:

$$MAP = \frac{CO}{\sum_{i=1}^{n} g_i}$$

where

g_i is the conductance of the ith compartment and

n is the total number of compartments.

But,

$$CO = \sum_{i=1}^{n} Q_i \quad \text{and}$$

$$g_i = g_{i,0} \cdot (1 + b_i \cdot C_i)$$

where

$g_{i,0}$ is the base conductivity of the ith compartment and

b_i is the coefficient of action of isoflurane on the conductivity of the ith compartment.

Hence isoflurane affects MAP as follows:

$$MAP = \frac{\sum_{i=2}^{5} Q_i}{\sum_{i=2}^{5} \left(g_{i,0} \cdot (1 + b_i . C_i) \right)}$$

i.e. $$MAP = \frac{Q_1}{\sum_{i=2}^{5} \left(g_{i,0} \cdot (1 + b_i C_i) \right)} .$$

Effect of Isoflurane on BIS

There is experimental evidence that a transportation delay exists between the lungs and the site of effect of isoflurane. To model this, an effect compartment is linked to the central compartment. Assuming that this new compartment has negligible volume, the mass balances derived so far remain the same. The concentration of isoflurane within this compartment is related to the central compartment, which is given by:

$$\frac{dC_e}{dt} = k_{e0}(C_1 - C_e)$$

where

C_e is the concentration of isoflurane in the effect compartment (g/mL) and

k_{e0} is the equilibration constant (min^{-1}).

The action of isoflurane can be then expressed as follows:

$$\Delta BIS = \Delta BIS_{MAX} \frac{C_e^{\gamma}}{C_e^{\gamma} + EC_{50}^{\gamma}}$$

$$\Delta BIS = BIS - BIS_0$$

$$\Delta BIS_{MAX} = BIS_{MAX} - BIS_0$$

where

BIS_0 is the baseline value of BIS (assumed to be 100)

BIS_{MAX} represents the minimum value of BIS (assumed to be 0)

EC_{50} is the patient's sensitivity to the drug and

γ is the measure of the degree of non-linearity.

5.2.3 Baroreflex

Yu *et al.* (1990) described baroreflex as a set of transfer functions relating the mean arterial pressure to the maximum elastance, the systemic resistance, the heart rate and the unstressed ventricular volume by the following equation:

$$bfc = \frac{e^{c(MAP-MAP0)}}{1+e^{c(MAP-MAP0)}}$$

where c is the empirical constant (mmHg).

In this model, only maximum elastance and the systemic resistance are involved and hence the baroreflex is limited to its action on them. The regulatory mechanism of the baroreflex may vary with the depth of anesthesia and several other factors. However the parameters involved in the transfer functions are assumed constant. The values of the parameters used in this model are given in Table 5.4 and are taken from Gentilini *et al.* (2001), Yasuda *et al.* (1991), Gopinath *et al.* (1995) and Derighetti (1999).

5.3 Model Validation

A number of dynamic simulations were performed using gPROMS (2003) to validate the model. First, a simulation was carried out to see the effect of isoflurane on MAP and BIS. Figure 5.7 shows the profile of MAP when subjected to an uptake of 1% vol. of isoflurane. Figure 5.8 shows the drop in BIS when there is an uptake of 1% vol. of isoflurane and then an increase in BIS at 1000 minutes when there is no uptake of isoflurane. It is observed that BIS drops to 40 for an isoflurane uptake of 1% vol.

Table 5.4 Model Parameters

Model Parameters	Value	Units
A_{aorta}	4.15	cm^2
A_{lv}	12	cm^2
b_1	0	mL/g
b_2	435.2574	mL/g
b_3	4194.299	mL/g
b_4	3205.077	mL/g
b_5	-1345.34	mL/g
BIS_0	100	
BIS_{MAX}	0	
c	0.06263	mmHg
EC_{50}	6.15E-5	g/mL
Eff_{max} (DP on E_{max})	1.3	
Eff_{max} (DP on R_{sys})	0.5	
Eff_{max} (SNP on R_{sys})	0.635	
$E_{max,0}$	2.12	mmHg/mL
f_R	14.5	1/min
$g_{1,0}$	0	mL/(min.mmHg)
$g_{2,0}$	24.456	mL/(min.mmHg)
$g_{3,0}$	8.412	mL/(min.mmHg)
$g_{4,0}$	4.667	mL/(min.mmHg)
$g_{5,0}$	1.247	mL/(min.mmHg)
k_{20}	0.0093	min^{-1}
k_{e0}	0.948	min^{-1}
K	4.316	$cm^{7/2}.g^{-1/2}$
MAP0	90	mmHg
R_1	1.59	
R_2	1.4	
R_3	2.92	
R_4	44.9	
R_5	44.9	
$R_{sys,0}$	0.0258	mmHg/(mL/min)
V	5	L
V_1	2310	mL
V_2	7100	mL
V_3	11300	mL
V_4	3000	mL
V_5	5100	mL
V_{lv}	85	mL
V_T	0.5	L
Δ	150	mL
ΔQ	300	mL/min
γ	1.6	
ρ	1.05	g/mL
$\tau_{1/2}$ (DP)	2	min
$\tau_{1/2}$ (SNP)	0.25	min

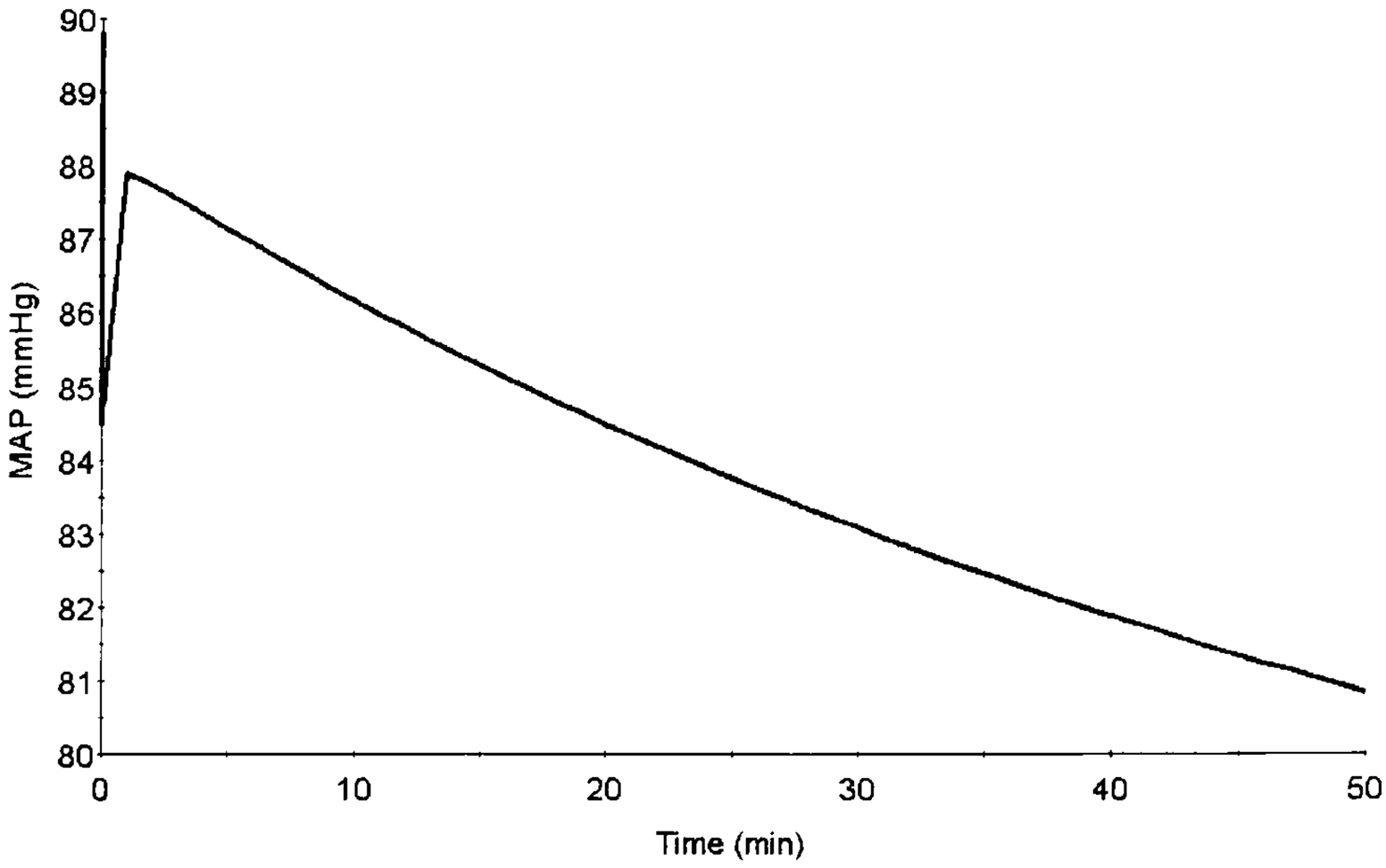


Figure 5.7 MAP response to an uptake of 1% vol. of isoflurane

Another simulation was performed to see the effect on BIS when subjected to an uptake of 0.5% vol. of isoflurane. Figure 5.9 shows the performance where it is observed that BIS reaches a value of 65. General anesthesia corresponds to BIS value between 40 and 65. Hence, this range can be maintained by an uptake of isoflurane between 0.5% and 1% vol.

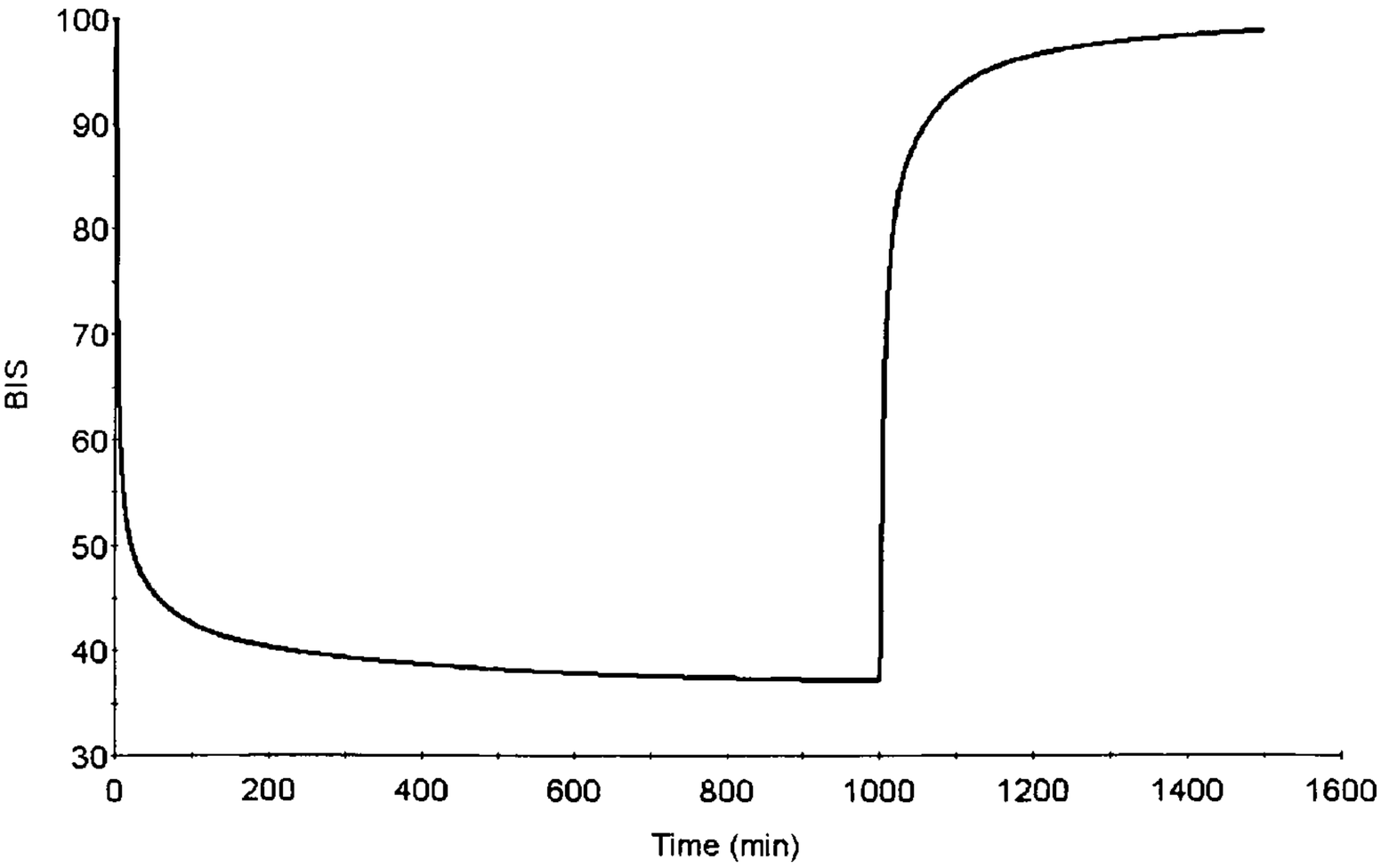


Figure 5.8 BIS response to an uptake of 1% vol. of isoflurane

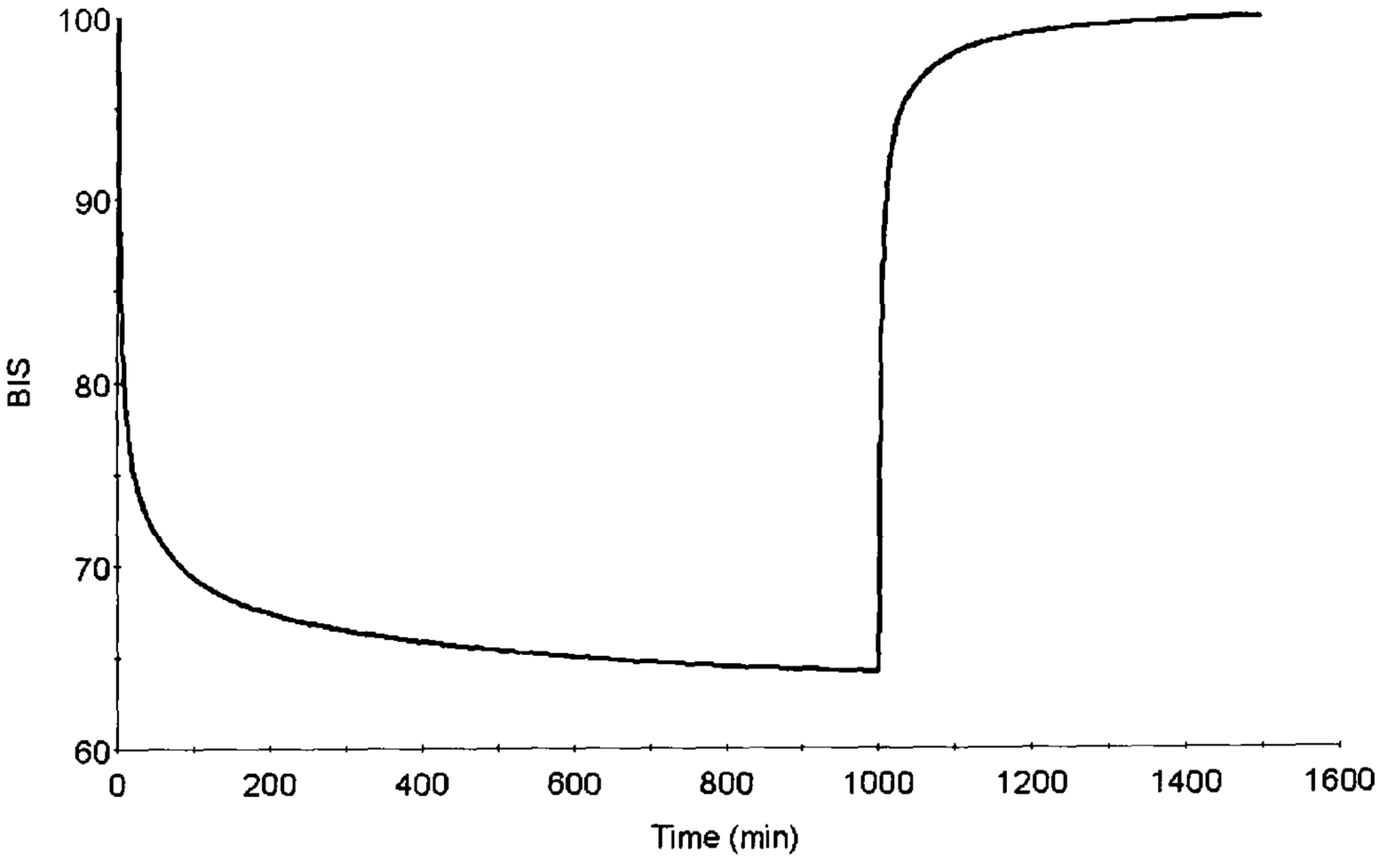


Figure 5.9 BIS response to an uptake of 0.5% vol. of isoflurane

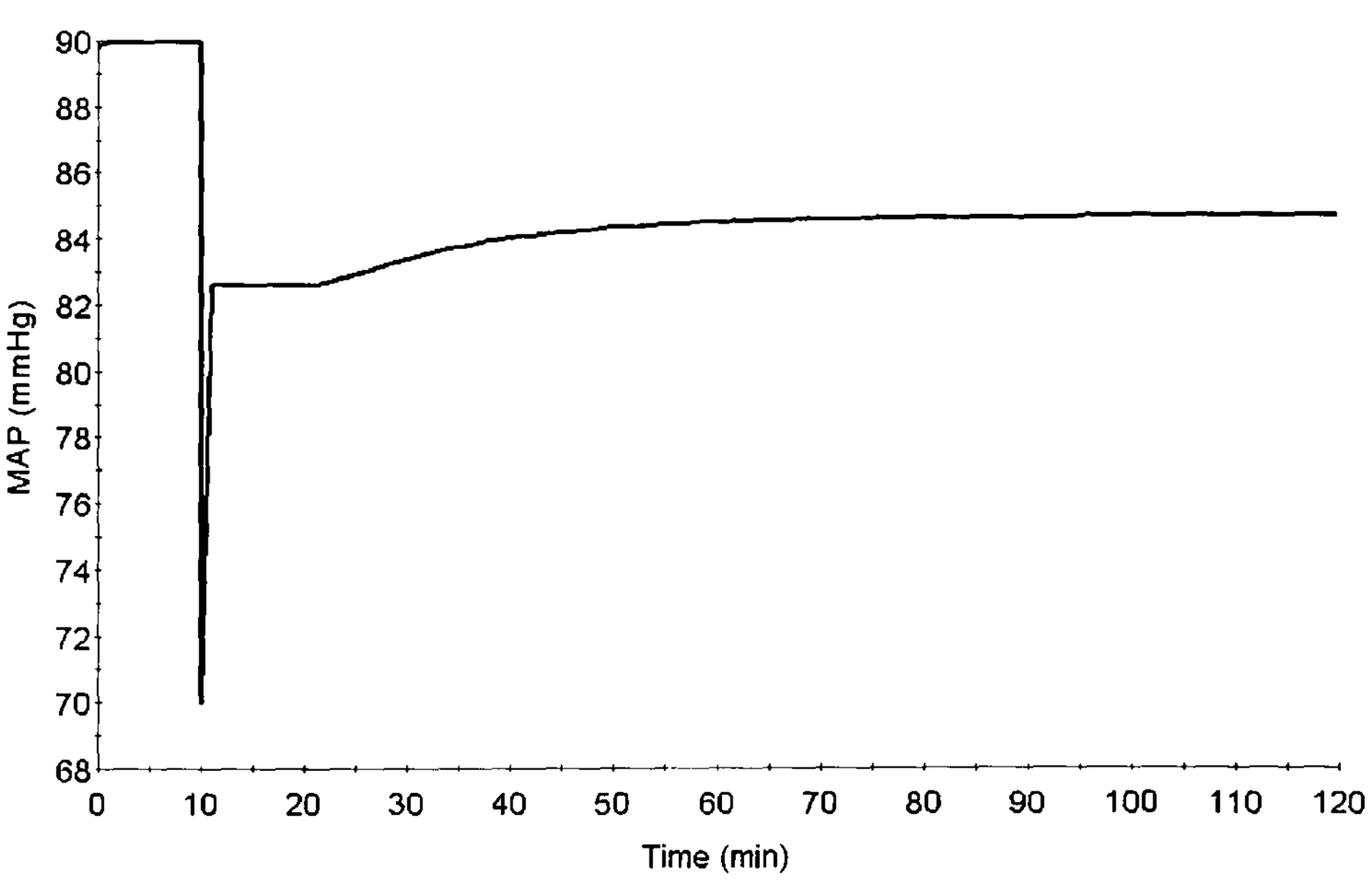


Figure 5.10 DP infusion in response to a drop in MAP

To see the effect of dopamine on MAP, a simulation was performed, where the model was run at steady state for the first 10 minutes, then a drop of 20 mmHg in MAP was induced and finally 10 minutes after the drop, 5 μg/kg/min of dopamine was infused. Figure 5.10 shows that MAP decreases to 70 mmHg after the drop and then increases

to approximately 82 mmHg due to the baroreflex and then finally reaches the steady state after the infusion of dopamine.

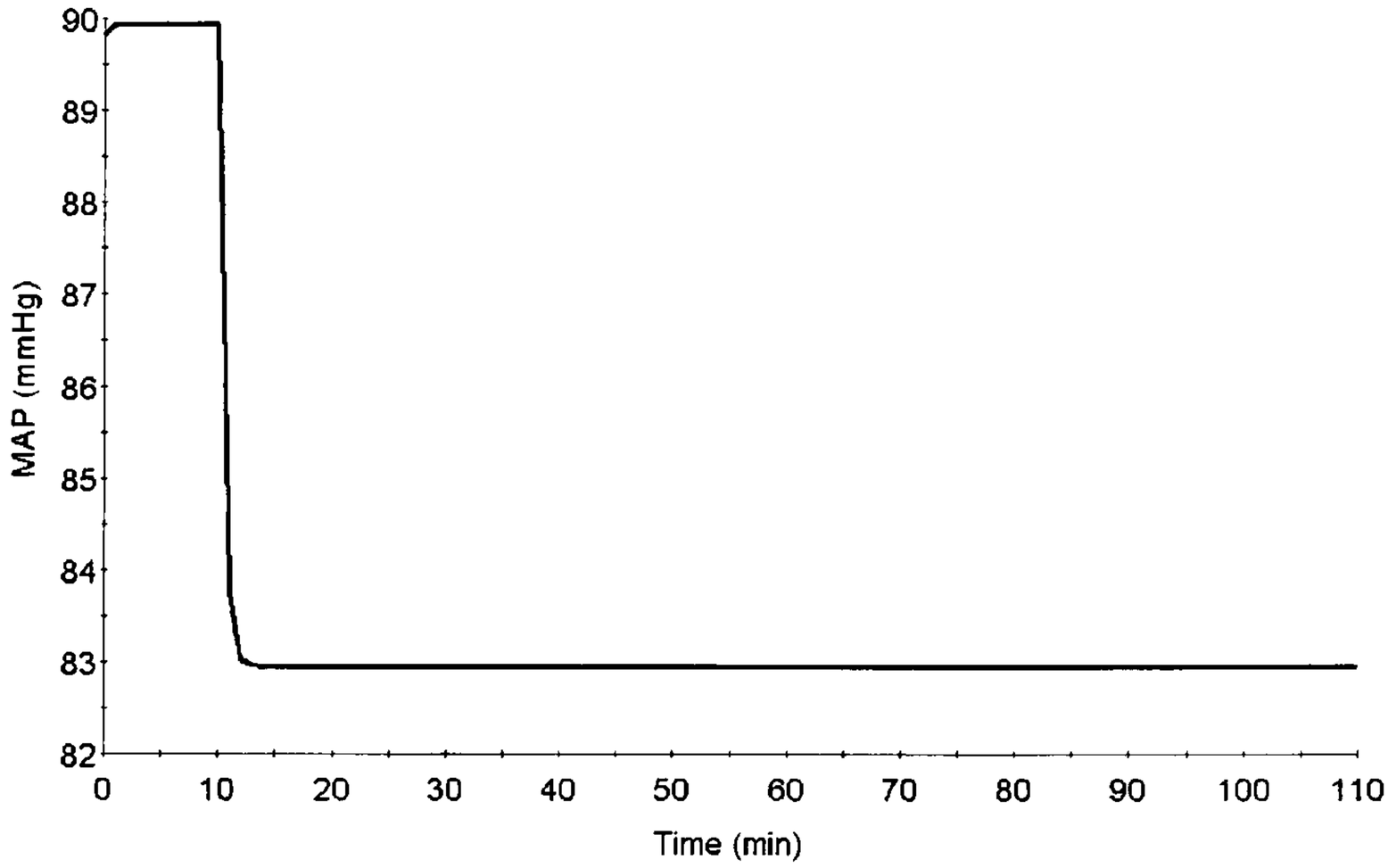


Figure 5.11 MAP response to a continuous injection of 1 μg/kg/min of SNP after 10 minutes

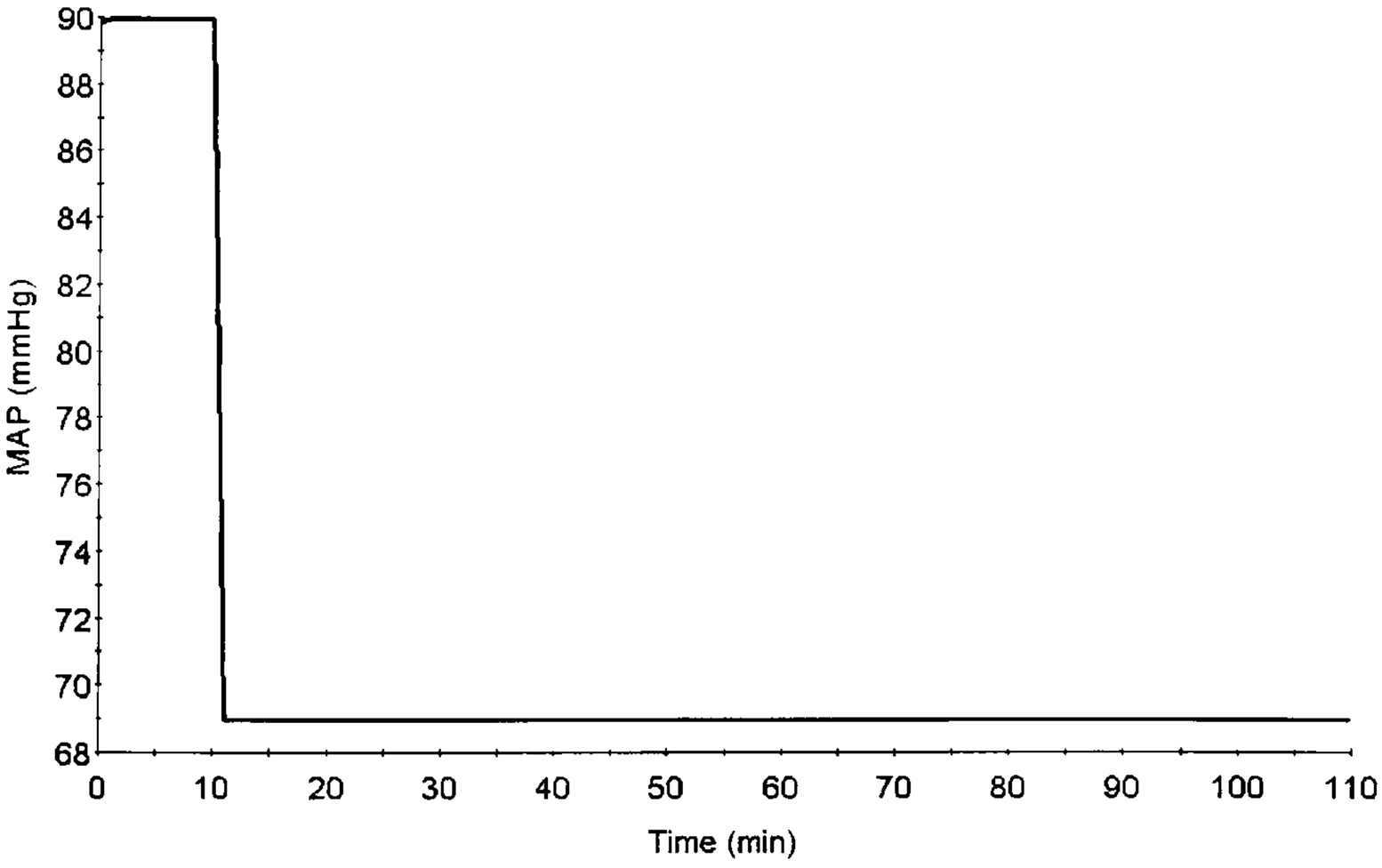


Figure 5.12 MAP response to a continuous injection of 10 μg/kg/min of SNP after 10 minutes

Similarly, simulations were performed to see the effect of SNP on MAP. It was observed that 1 μg/kg/min of SNP results in a drop in MAP from 90 mmHg to 83 mmHg (Figure 5.11) and 10 μg/kg/min of SNP decreases MAP to approximately 69 mmHg (Figure 5.12).

To validate the model's general behaviour, an anesthetic procedure has been simulated, which consists of five parts. For the first 10 minutes, it is assumed that the patient is awake. Then 0.8% vol. of isoflurane is infused alongwith 0.7 μg/kg/min of SNP to attain the anesthetic state and lower the blood pressure to 60 mmHg. After 800 minutes, when the steady state is reached, a drop of 20 mmHg in MAP is induced. It was assumed for the sake of simulation that the anesthesiologist would react only after 5 minutes of the drop by giving an infusion of 4.5 μg/kg/min of DP to counteract the drop. Then after 60 minutes, MAP does not drop and hence DP infusion was stopped. After another 40 minutes, the uptake of isoflurane and SNP was stopped and it was observed that the patient smoothly wakes up. Figures 5.13 and 5.14 shows the results of this simulation.

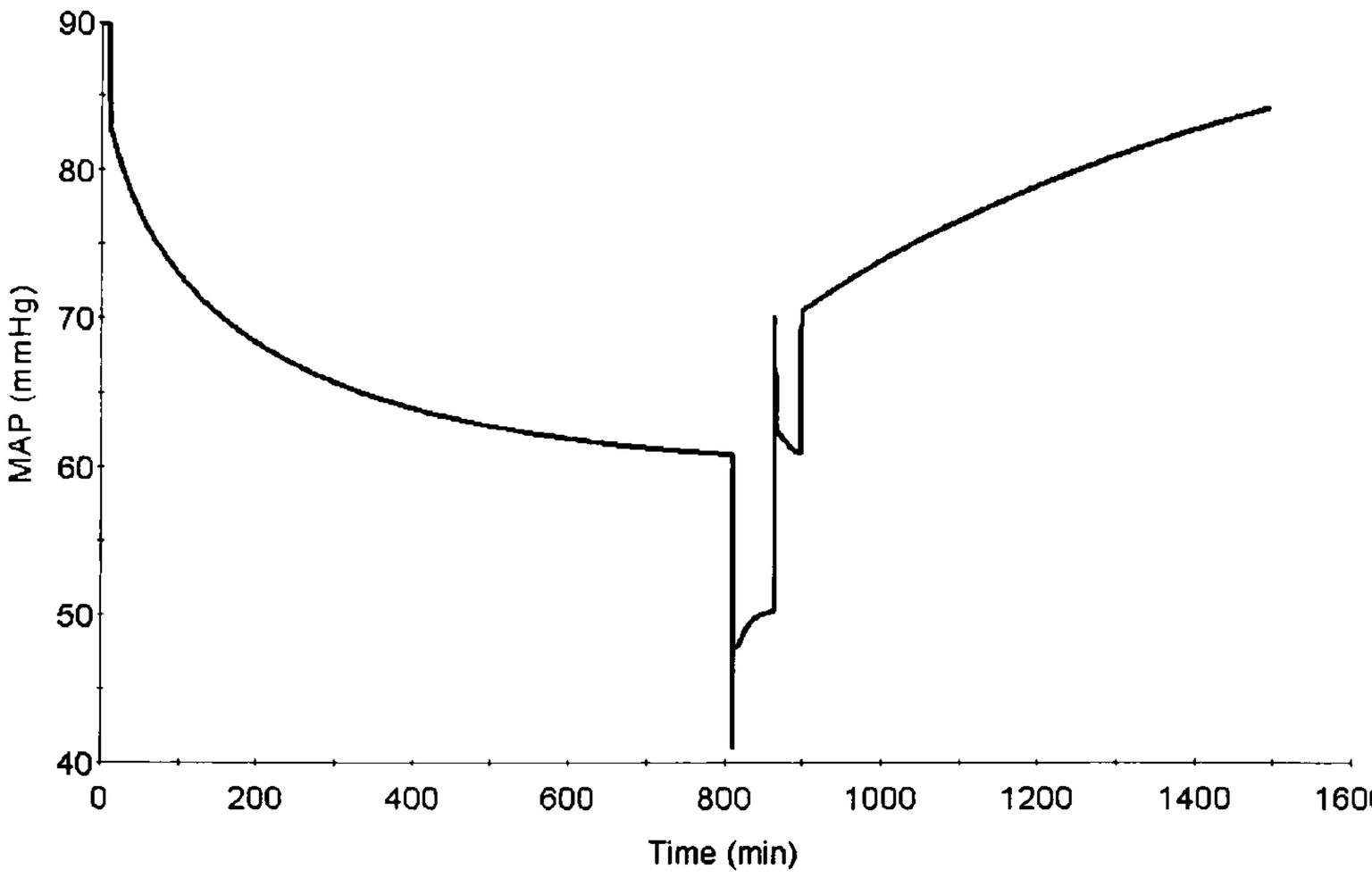


Figure 5.13 Simulation of the regulation of MAP during anesthesia

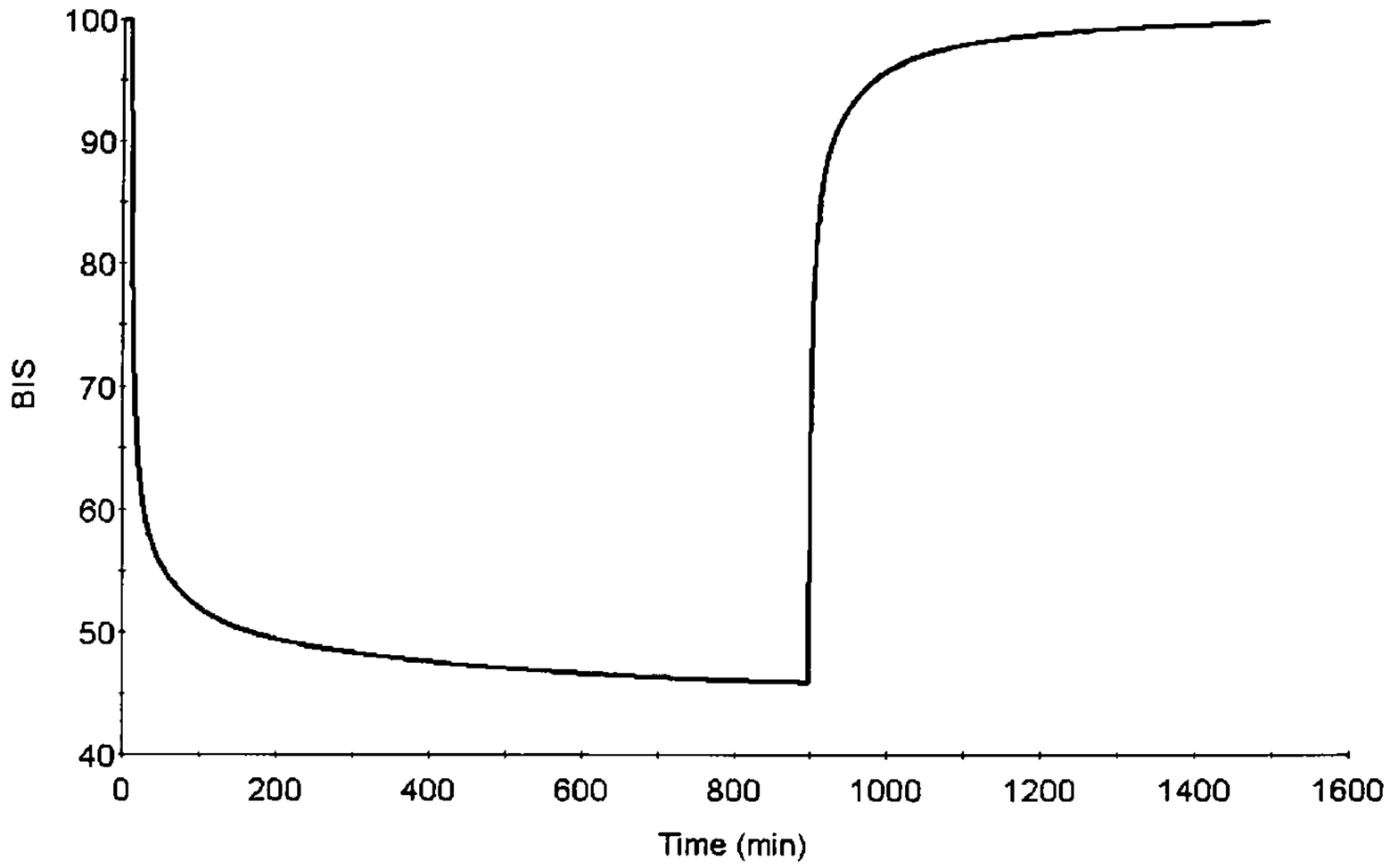


Figure 5.14 Simulation of the regulation of BIS during anesthesia

It must be stressed that this procedure is oversimplified. First, the anesthesiologist would give high dosages of drugs at the beginning of the procedure to induce quick response from the patient and then gradually adjust the infusions to keep BIS, MAP and infusion rates within safe ranges. Also, the patient would be subject to greater number of disturbances starting with the intubation at the beginning of procedure, which was not considered in this simulation. Despite these simplifications, it was observed that the accuracy of the model is not altered by multiple drug infusions.

In this work, a number of dynamic simulation studies have been reported to validate the applicability of the model to simultaneously regulate MAP, CO and hypnosis. The quantitative and qualitative trends of the plots presented in this section are similar to those observed in clinical trials (Gentilini, 2001; Rao *et al.*, 2001) – for example, the value of BIS can be maintained between 40 and 65 by manipulating the concentration of isoflurane between 0.5% to 1% vol., which is similar to that observed by Gentilini (2001). Clinical trials can now be carried out to further fine tune the model and model parameters presented in this section.

5.4 Control of Anesthesia

For designing controllers, the model in the previous section was linearized at the nominal values of inputs: 0.6% vol. of isoflurane, 2 μg/kg/min of DP and 4 μg/kg/min of SNP to obtain a state-space model of the following form:

$$x_{t+1} = Ax_t + Bu_t$$
$$y_t = Cx_t + Du_t \tag{5.1}$$

subject to the following constraints:

$$x_{\min} \le x_t \le x_{\max}$$
$$y_{\min} \le y_t \le y_{\max} \tag{5.2}$$
$$u_{\min} \le u_t \le u_{\max}$$

where $x_t \in R^n, y_t \in R^l, u_t \in R^m$, are the state, output and input vectors respectively and the subscripts *min* and *max* denote lower and upper bounds respectively; the corresponding values of outputs at the linearization point are: 57.38 mmHg of MAP, 61.1 BIS and 1.21 L/min of CO. Model predictive control (MPC) problem can then be posed as the following optimization problem:

$$\begin{aligned}
&\min_U J(U, x(t)) = x_{t+N_y|t}^T P x_{t+N_y|t} + \sum_{k=0}^{N_y-1} \left[x_{t+k|t}^T Q x_{t+k|t} + u_{t+k}^T R u_{t+k} \right] \\
&s.t. \quad x_{\min} \le x_{t+k|t} \le x_{\max}, k = 1,....., N_c \\
&\quad y_{\min} \le y_{t+k|t} \le y_{\max}, k = 1,....., N_c \\
&\quad u_{\min} \le u_{t+k} \le u_{\max}, \quad k = 1,....., N_c \\
&\quad x_{t+k+1|t} = Ax_{t+k|t} + Bu_{t+k}, k \ge 0 \\
&\quad y_{t+k|t} = Cx_{t+k} + Du_{t+k}, k \ge 0 \\
&\quad u_{t+k} = Kx_{t+k|t}, N_u \le k \le N_y
\end{aligned} \tag{5.3}$$

where $U = \left[u_t^T, ..., u_{t+N_u-1}^T \right]^T$, Q and R are constant, symmetric and positive definite

matrices, P is given by the solution of the Riccati or Lyapunov equation, N_y, N_u and N_c are the prediction, control and constraint horizons respectively and the superscript T denotes transpose of the vector. Problem (5.3) is solved at the current time t for the current state x_t to obtain the vector of predicted state variables, $x_{t+1|t},\ldots..,x_{t+Ny|t}$ and the control actions $u_t,\ldots.,u_{t+Ny-1}$ are obtained.

5.5 Results

The model consists of 23 states, 3 outputs and 3 inputs. Figures 5.15 and 5.16 depict a comparison between the behaviour of two outputs (MAP and BIS) with respect to time in two different cases: when simulating the nonlinear model and the linearized one.

It is apparent that there is a different behaviour between the two models, especially during the first period of simulation (0-50 minutes). It seems that the linearized model "overestimates" the Bispectral Index. However, the two models have the same steady behaviour and their trends overlap after the first period of simulation. Similarly, in the case of MAP, there is some deviation initially but the same trend is observed after a while.

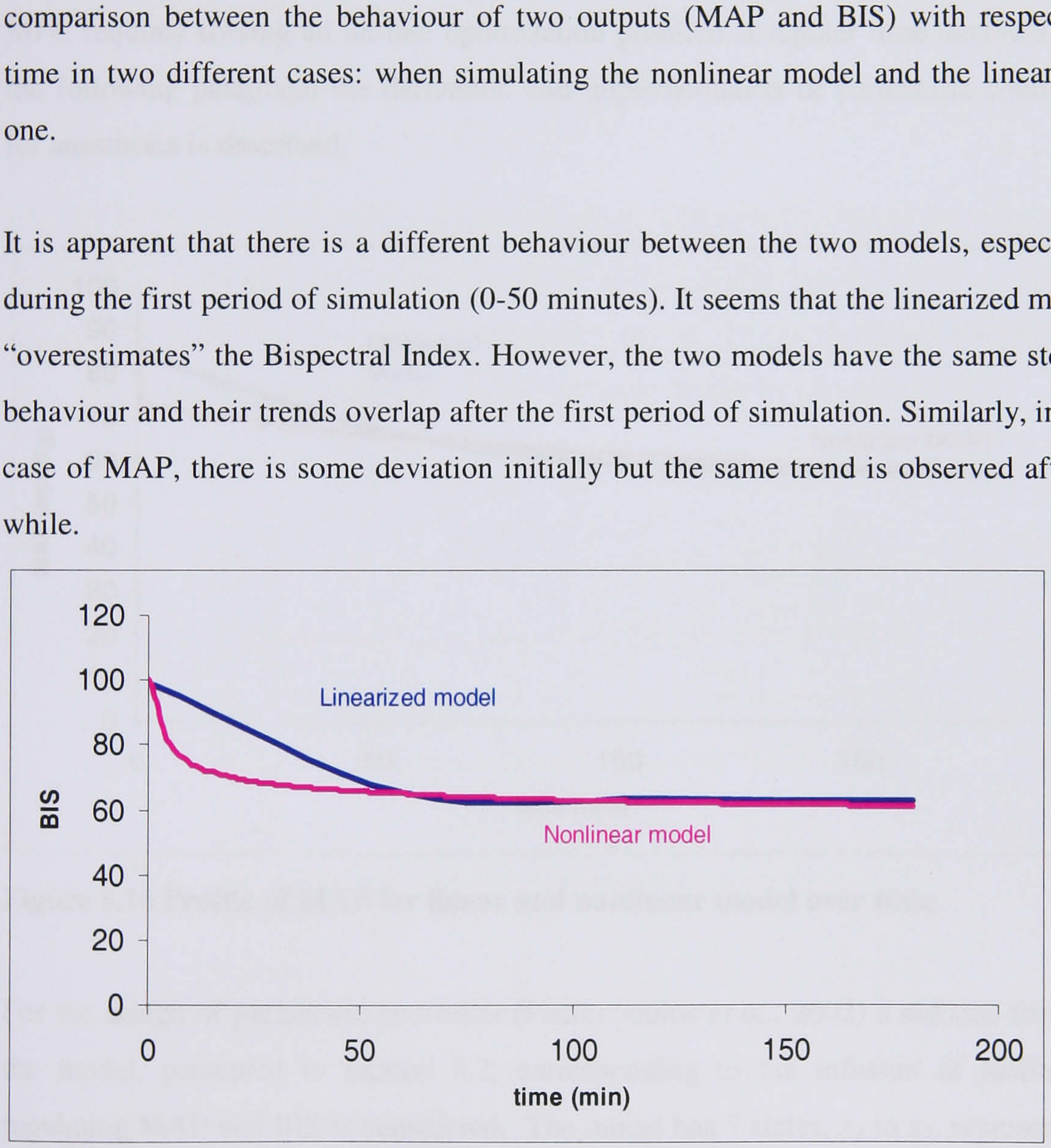


Figure 5.15 Profile of BIS for linear and nonlinear models over time

This linearized state-space form of the model is then adapted for designing model

predictive controller by using the MATLAB (1998). For designing the MPC controller, the following input: $0 \leq DP \leq 7$ *μg/kg.min*, $0 \leq SNP \leq 10$ *μg/kg.min*, $0 \leq$ *Isoflurane* $\leq 5\%$ *vol.*, and output constraints: $40 \leq MAP \leq 150$ *mmHg*, $40 \leq BIS \leq 65$, $1 \leq CO \leq 6.5$ *L/min* are used. A prediction horizon of 5, control horizon of 3 and sampling time of 0.5 minutes are considered. A set point of $[20\ -10\ 1]^T$ deviation from the nominal point of the output variables is given and the performance of the controller is shown in Figure 5.17. It is observed that the MPC tracks the set point quite well. From the above it can be inferred that the model based control technology provides a promising platform for the automation of anesthesia. As discussed earlier, MPC requires solving an on-line optimization problem at regular time intervals – in the following paragraph the derivation and implementation of parametric controller for anesthesia is described.

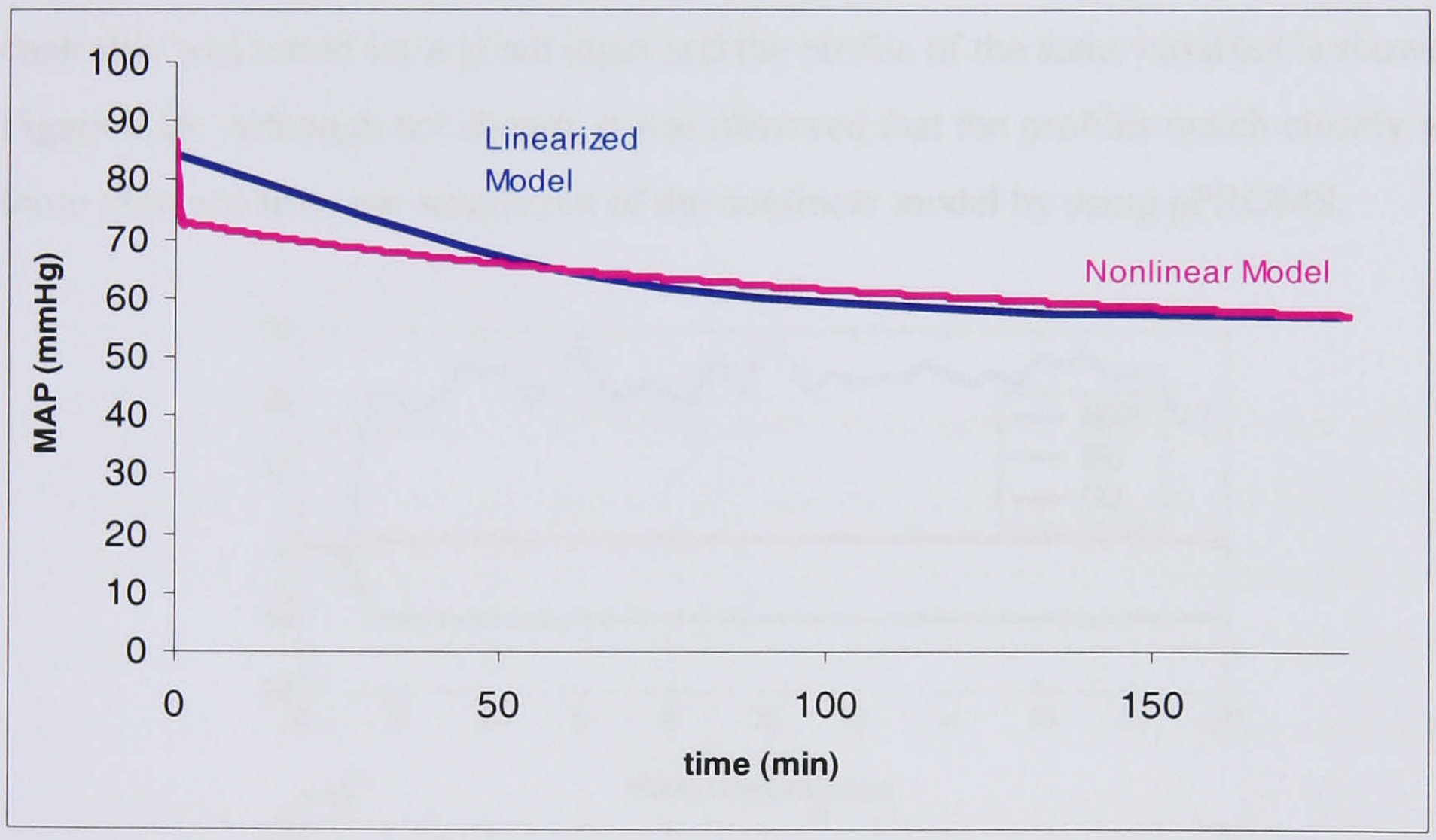


Figure 5.16 Profile of MAP for linear and nonlinear model over time

For the design of parametric controller (Pistikopoulos *et al.,* 2002) a reduced form of the model, presented in section 5.2, corresponding to the infusion of isoflurane regulating MAP and BIS is considered. The model has 7 states, x_1 to x_7, representing the concentration of isoflurane in the 5 compartments and its effect on E_{max} and R_{sys} and the input variable is given by the inlet concentration of isoflurane. Prediction and control horizons of 3 and equal weightings on state and control variables are used

resulting in 48 regions in the space of the state variables. The profile of the parametric controller in one of the regions is given by:

u = [-359.64 –717.4 -166.32 -57.109 -15.711 -5.5925 0.77529] x + 0.077971

and the corresponding region by:

$$\begin{bmatrix} -0.501 & -1 & -0.231 & -0.079 & -0.021 & -0.007 & 0.001 \\ 0.501 & 1 & 0.231 & 0.079 & 0.021 & 0.007 & -0.001 \\ 0.1853 & -1 & 0.085 & 0.210 & 0.100 & 0.027 & -0.002 \\ -0.057 & -1 & -0.026 & 0.238 & 0.335 & 0.130 & -0.014 \end{bmatrix} x \leq \begin{bmatrix} 0.0000639 \\ 0.0000059 \\ -0.0000215 \\ -0.0003263 \end{bmatrix}$$

$$x_4, x_5 \geq 0$$

where x is the vector of deviation state variables. The performance of the parametric controller was tested for a given input and the profile of the state variables is shown in Figure 5.18. Although not shown, it was observed that the profiles match closely with those obtained from the simulation of the nonlinear model by using gPROMS.

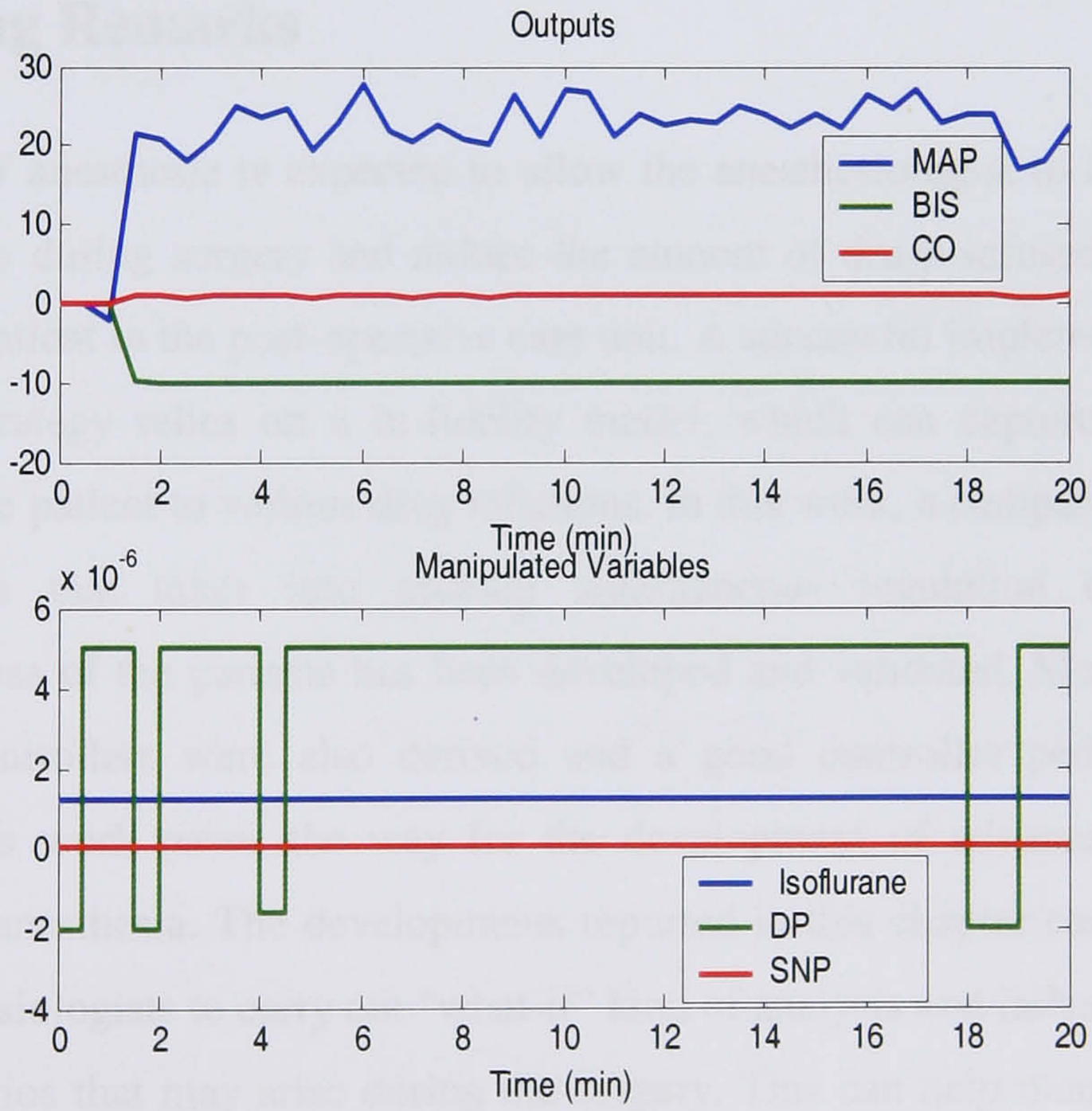


Figure 5.17 MPC performance for anesthesia for a set point of [20 -10 1]^T deviation from the nominal point

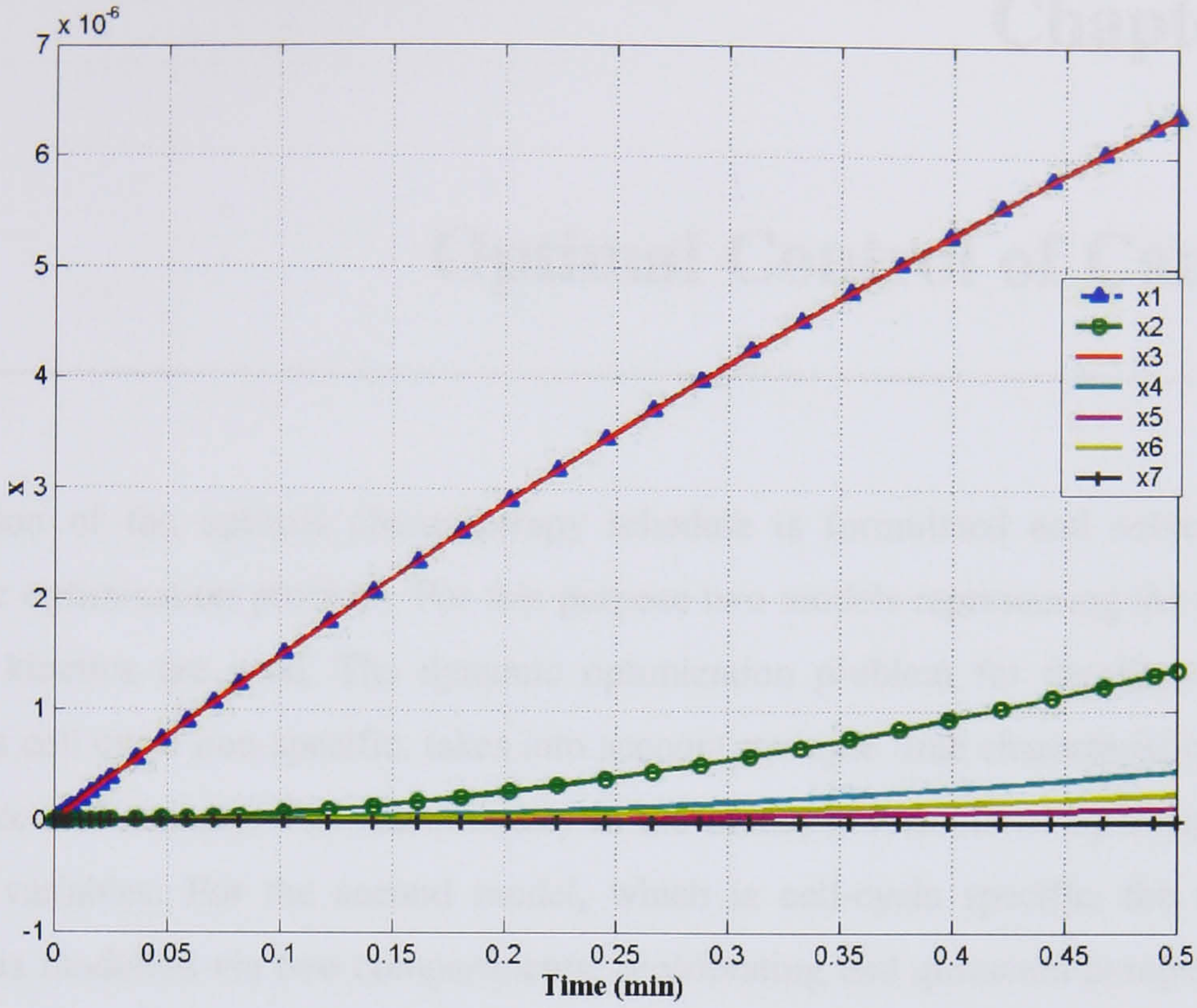


Figure 5.18 Parametric Controller: State Profiles

Concluding Remarks

Automation of anesthesia is expected to allow the anesthesiologist to focus more on critical aspects during surgery and reduce the amount of drugs infused and the time spent by the patient in the post-operative care unit. A successful implementation of the automation strategy relies on a hi-fidelity model, which can capture the dynamic response of the patient to various drug infusions. In this work, a compartmental model for anesthesia that takes into account simultaneous regulation of MAP and unconsciousness of the patients has been developed and validated. Model based and parametric controllers were also derived and a good controller performance was observed. This work paves the way for the development of advanced automation strategies for anesthesia. The developments reported in this chapter can also be used by the anesthesiologists to carry out "what-if" kind of analysis and failsafe analysis for various scenarios that may arise during the surgery. This can help them in executing optimal drug infusion strategies and also reduce the risks involved in surgery under anesthesia.

Chapter 6

Optimal Control of Cancer

Derivation of the optimal chemotherapy schedule is formulated and solved as a dynamic optimization problem. For this purpose two models representing the tumour growth kinetics are used. The dynamic optimization problem for the first model, which is cell cycle non-specific, takes into account multiple time characteristics, drug resistance and toxicity. The discontinuity in the model is formulated by introducing integer variables. For the second model, which is cell-cycle specific, the tumour growth is modelled via two compartments: proliferating and quiescent compartment. The optimal chemotherapy schedule obtained from the two models differ is some ways and also share some common features.

6.1 Introduction

Cancer is a collective term that describes a group of diseases characterized by uncontrolled and unregulated growth of cells leading to invasion of surrounding tissues and spreading to the parts of the body that are distant from the site of origin. There are around 200 types of cancer and the cancer of lungs, breast, bowel and prostrate are the most common ones. There are three main stages in the process of carcinogenesis: initiation, promotion and progression. As shown in Figure 6.1, the normal cell changes to an initiated cell and then to cancer differentiated cell and finally invades and spreads to the surrounding cells.

The growth and death of cells in normal tissues is regulated by the genes whereas in the malignant tissues the genes are mutated and therefore the proliferation of the cells in uncontrolled. The specific genes that get mutated are known as oncogenes and are responsible for the lack of regulation of the growth and function of the cells. The

genes of normal cell, known as proto-oncogenes may transform to oncogenes by exposure to environmental or chemical carcinogens, viruses or radiations.

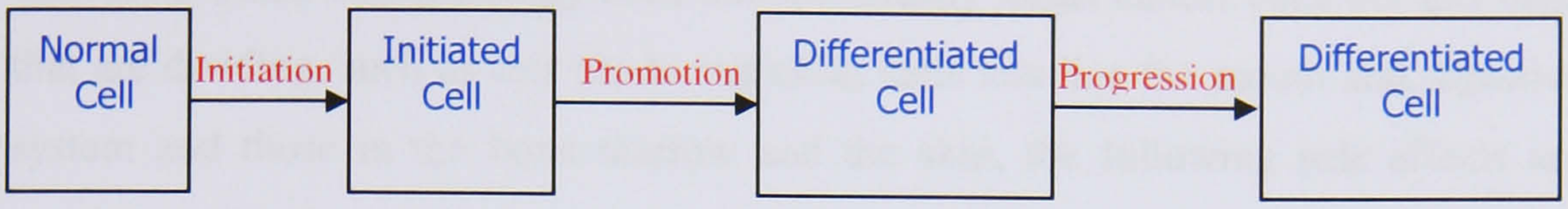


Figure 6.1: Stages of carcinogenesis

A number of environmental and genetic factors that contribute to the development of cancer have been identified by analytic epidemiological studies. Tobacco has been associated with lung, larynx, pharynx, pancreas, oesophagus, bladder, kidney, and cervix cancer. The effect of tobacco when combined with smoking seems to exceed their separate additive effects. Alcohol, hormonal and reproductive factors, dietary factors, occupational exposure and other environmental exposures have also been shown to be responsible for carcinogenesis.

6.1.1 Chemotherapy for the treatment of Cancer

Surgery, chemotherapy, radiotherapy, hormone therapy and immunotherapy are the most commonly used treatments for cancer. In this chapter the focus is on chemotherapy which can be used with a combination of any of these other treatments. The word chemotherapy derives from the words chemical and therapy. It uses anticancer or cytotoxic drugs to destroy or kill cancer cells. Currently there are about 60 anticancer drugs that are available and new agents are being developed. The suitability of chemotherapy and the choice of drugs depend on many factors including the type of cancer, the location of the origin of the cancer in the body, how mature the cancer cells are and whether the cancer cells have spread to the other parts of the body.

Cancer cells divide much more often than most of the normal cells. A cell is more likely to be damaged when it is dividing and therefore the damage caused by chemotherapy to cancer cells is more than that caused to the healthy cells. The damage

to the cancer cells can be caused at different stages in the process of cell division: at the point of splitting or while they are making copies of their genes before splitting. By using more than one type of drug the chances of killing more cells can be increased. Since chemotherapy does not specifically target cancer cells but any cells that are dividing, such as hair producing cells, cells that line the mouth and digestive system and those in the bone marrow and the skin, the following side effects are usually observed:

- Hair loss
- Sore mouth, mouth ulcers and changes in the sense of taste
- Nausea and vomiting
- Diarrhoea or constipation
- Tiredness.

While most chemotherapy drugs are given directly into the bloodstream, the other drug delivery methods include:

- Tablets
- Injections into muscle
- Injections into the area around the spinal cord
- Injections into the cavity such as the bladder
- Injections under the skin and
- Creams for skin cancer.

Infusion pumps can be used to deliver controlled amount of drug directly in the bloodstream. These are portable pumps about the size of the personal stereo and are often used for over weeks or months. Some chemotherapy drugs are given as oral tablets and others are not because they cannot be absorbed properly from the digestive system, get destroyed or damaged by the acid in the stomach or cannot be given in large enough doses as a tablet. Injections into the muscles of thighs and buttocks allow the drugs to be absorbed into the blood more slowly than in intravenous chemotherapy. This means that the effects of intramuscular chemotherapy last longer than having injections into the vein. The common sites for subcutaneous

chemotherapy are the skin in the abdomen, thigh and upper arm. Intra arterial chemotherapy relies on having a tube put into the artery, under local anesthesia, which is feeding the cancer. Liver cancer is usually treated in this way where the drugs are directly given into the hepatic artery. Chemotherapy treatments into the area around the spinal cord and a body cavity are used for the treatment of leukemia and ovarian cancer respectively.

Chemotherapy involves the course, and not just a single treatment, which may last for about six months. A course would probably have six cycles of treatment. A cycle would have treatments on certain fixed days, say 1st, 2nd and 3rd day, over a period of time, say 4 weeks, that would be repeated over the periods of the time. A reason for having chemotherapy as a course of treatment is that some of the cells that are resting during the first treatment will be killed during the second treatment when they are dividing. Also the gap between the treatments allows the body to recover from the side effects.

The factors influencing the success of chemotherapy include the general status of the patient, timing of the therapy and interaction of the drugs. The actions of the chemotherapeutic agents are based upon an understanding of the cell mechanisms. The cell cycle is a sequence of phases that both normal and malignant cells enter from their birth to cell death. This is a continuous process during which the cells replicate.

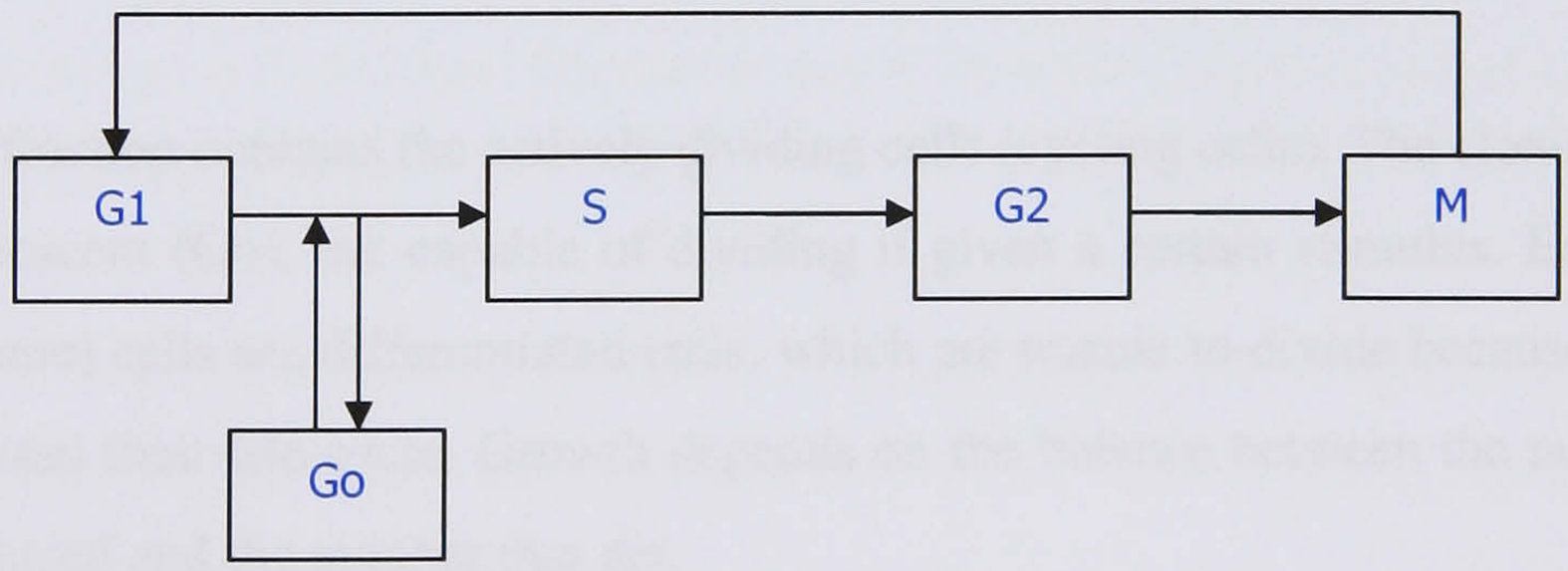


Figure 6.2 The cell cycle

The cycle comprises of four stages (Figure 6.2):

G1: Post mitotic gap. The cell prepares for DNA synthesis

S: DNA synthesis takes place in preparation for cell division (many anticancer drugs act by interfering with DNA at this stage, causing cell death)

G2: Pre-mitotic gap. Specialized proteins and RNA are synthesized in preparation for cell division

M: Mitotic phase. Cell division takes place to produce two identical daughter cells

Go: Resting phase. Cell is quiescent; viable but unable to divide.

A basic knowledge of tumour growth is also helpful in understanding the way chemotherapy works. Growth in all tissues involves three different cell populations: the growth fraction, the clonogenic fraction and the end (non-clonogenic cells) (Figure 6.3).

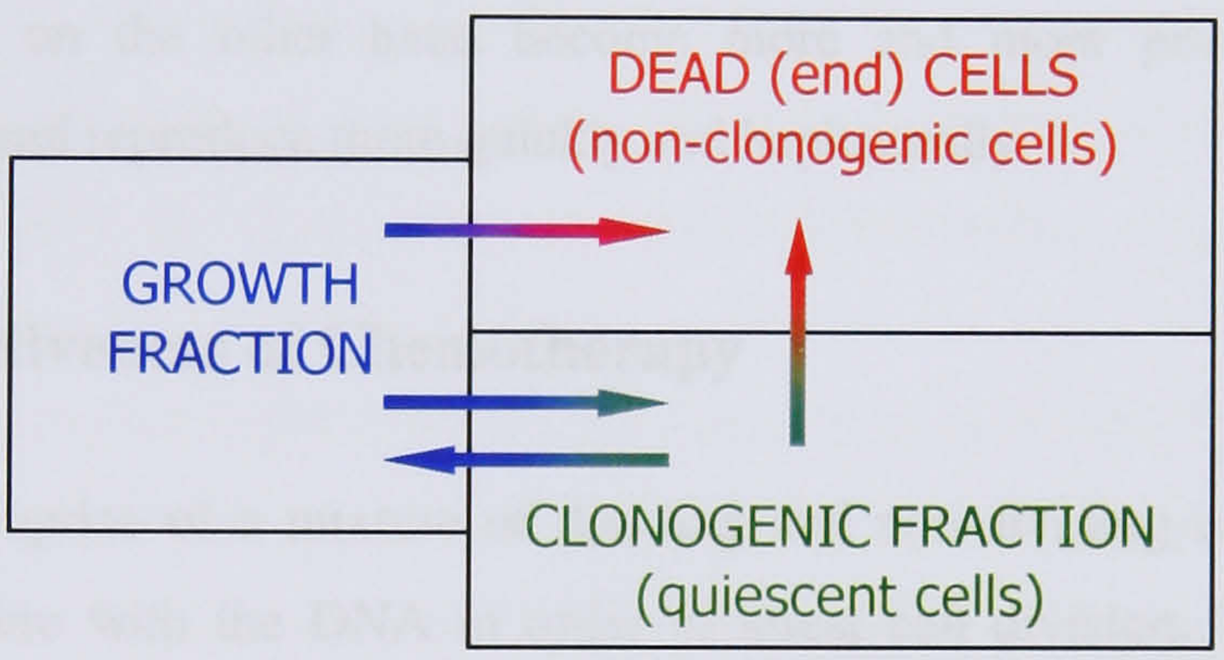


Figure 6.3 Functional compartments within tumours

The growth fraction contains the actively dividing cells (cycling cells). The clonogenic cells are quiescent (Go), but capable of dividing if given a certain stimulus. End (or non-clonogenic) cells are differentiated cells, which are unable to divide because they have completed their life cycle. Growth depends on the balance between the number of cells produced and the number that die.

Another issue that is important to understand is the difference between normal and cancer cells. A number of important characteristics of normal cells are:

- They reproduce exactly
- The reproduction stops at the right time
- They stick together in the right place
- If they are damaged they destroy themselves
- They become specialized or mature.

On the other hand, cancer cells carry on reproducing even after they have doubled 50 or 60 times. They may also become more resistant to self destruction than normal cells. The genes that normally regulate the reproduction of the cell get lost or damaged, so the cancer cell keeps on doubling irrespective of the damage caused to the surrounding part of the body. The normal cells have certain molecules that keep them together; cancer cells lose these molecules, get detached from their neighbours and can spread to other parts of the body. Most of the normal cells become mature, specialized for their particular job in the body and lose their ability to reproduce, cancer cells on the other hand become more and more primitive, lose genetic information and reproduce more quickly and haphazardly.

6.1.2 Effectiveness of Chemotherapy

Tumours comprise of a mixture of dividing and non-dividing cells. All anti-cancer agents interfere with the DNA in order to arrest cell division. Thus they are more effective when the cells are preparing for or actively involved in cell division. Tumours with a high growth fraction are more sensitive to chemotherapy than the ones with small growth fraction. Chemotherapy is therefore more effective against small, rapidly growing tumours.

The choice of anti-cancer agents depends on the characteristics of the tumour growth. An initial tumour growth can occur without new blood vessels (angiogenesis) but additional growth requires the production of angiogenic. For a drug to be effective the supply of blood and a certain concentration of the drug are essential at the tumour site. Solid tumours are responsible for the majority of cancer deaths. The effectiveness of chemotherapy is also influenced by the growth phase of the tumour. Cycle-specific drugs are more effective when the tumour is growing rapidly whereas cycle non-

specific drugs perform better on tumours in which the growth fraction is small. Cell cycle-specific drugs kill only a fraction of the cells in the tumour because they destroy proliferating cells only in a specific phase of the cell cycle. The action of cell cycle non-specific drugs, on the other hand, is not limited to a particular phase which is advantageous in the case of resting cells (Go). The cancer cells may develop mechanisms making them resistant to the drugs and reducing the effectiveness of the therapy. This can be attributed to factors such as poor vascularisation and gene mutations that result in drug resistant cells.

6.1.3 Chemotherapeutic Drugs

Cancer chemotherapy was first successfully practiced in the 1950s when nitrogen mustard, which was used as a war gas, was found to be effective in inhibiting tumour growth. Since then, many anti cancer drugs have been developed and used for clinical purposes. Anti cancer drugs can be classified in four categories, based on their biochemical activities or their origin: Alkylating agents, Antimetabolites, Natural Products and their derivatives and a group of miscellaneous drugs.

Alkylating agents are highly reactive and function by interacting with DNA, RNA and proteins in order to prevent replication. As a group they are considered cycle non-specific agents. They also are active against resting cells. Common alkylating agents include: Nitrogen Mustard, Melphalan, Nitrosoureas.

Antimetabolites (Methotrexate, Cytosine Arabinoside, Gemcitabine) are structural analogues of normal metabolites, so they are used to disrupt cellular metabolism. They are more active against fast growing tumours. They are cell cycle specific agents.

Anthracyclines (Doxorubicin, Mitoxantrone), Vinca Alkaloids (Vinblastine, Vincristine) and Taxanes (Paclitaxel, Docetaxel) are natural products or synthesised chemicals. Anthracyclines are cycle non specific, whereas Vinca Alkaloids and Taxanes are cycle specific.

Anticancer drugs can also be classified as killing agents or blocking agents, depending on whether they destroy cancer cells or inhibit some of their functions. Killing agents include Vincristine, Vinblastine, Bleomycin, Taxol (Paclitaxel) and many others. Blocking agents are the antibiotics Adriamycin (Doxorubicin) and Daunomycin.

6.1.4 Problems Related to Chemotherapy

Although anti cancer agents are used in cancer treatment, their effects are not limited only to cancer cells, but the normal tissues are also damaged. Fortunately, normal cells have the ability to better repair the damage caused by chemotherapy, than cancer cells. However, certain types of cells (bone marrow) have low tolerance to these agents. Toxicity to normal cells is the main limit for determining the dose of a chemotherapeutic drug. Hypersensitivity (exaggerated response to a foreign agent, e.g. protein or drug) effects may also occur during chemotherapy administration.

6.2 General Approaches to Modelling Cancer Chemotherapy

To model cancer chemotherapy, one has to consider several different factors: tumour growth kinetics, pharmacodynamics and pharmacokinetics of the anti-cancer agents, side effects of toxicity and drug resistance. A brief description of the ways that each one of the above factors can be modelled is presented below.

6.2.1 Tumour Growth

Modelling tumour growth involves several processes and mechanisms. Three scales that are considered when modelling tumour evolution are: the microscopic, mesoscopic and macroscopic scale. The microscopic scale refers to those phenomena that occur at the subcellular level and therefore to activities that take place within the cell at the cell membrane, such as, DNA synthesis and degradation, gene expression and transduction of chemical signals between cells that regulate cellular activities. The mesoscopic scale refers to the cellular level and therefore to the main activities of the cell populations, such as, statistical description of the progression and activation state and interactions among tumour cells and the other types of cells present in the body.

The macroscopic scale refers to the tissue level and therefore to those phenomena which are typical of continuous systems, such as, cell migration, convection and diffusion of nutrients and chemical factors. It is apparent that all three scales must be taken into consideration to completely describe tumour growth. On the other hand, extremely detailed models lack simplicity and become difficult to use for engineering purposes. In this chapter the focus is on mathematical models in which the tumour details and spatial structure are neglected and the focus is on the overall volume of the tumour or the total number of cells present within the tumour.

These models describe the growth of solid and homogeneous tumours and consist of a system of differential equations that predict how the numbers of proliferating, quiescent and dead cells contained within a tumour change over time. A differential equation can be used to model the growth of a tumour provided that an initial tumour cell population *No* is specified together with some general assumptions about the way in which the tumour is growing. These assumptions are used to formulate the *growth function*: a positive-valued, continuous, monotonically increasing function that describes the increase per unit time in the tumour cell population. There are several specific models that fit clinical data: the exponential equation, the Gompertz equation, the logistic equation and others.

Tumour growth is assumed to be exponential when the doubling time of the tumour, τ, is constant and is modelled with the following equation:

$$\dot{N}(t) = \lambda_E N(t)$$

$$N(0) = No \tag{6.1}$$

and its analytical solution is given by:

$$N(t) = No\exp(\lambda_E t) \tag{6.2}$$

where

λ_E is the proportional increase in the tumour cell population per unit time.

The relationship between the doubling time and the parameter λ_E is given by:

$$\lambda_E = \ln(2)/\tau \tag{6.3}$$

Although the exponential model has a good fit at the early stages of cancer, it can not reproduce the reduction of the growth fraction at the late stages of the disease, for example, a five-fold increase in mean tumour doubling times between early and late breast cancer. For this purpose, two sigmoidal functions are used: the logistic and the Gompertz equations. As time increases the tumour mass approaches a stable level θ called the plateau population or the carrying capacity of the tumour. For human and animal tumours the plateau population is above the level that is lethal to the host.

The logistic growth function is given by:

$$\dot{N}(t) = \lambda_L N(t)(1 - N(t)/\theta) \tag{6.4}$$

The parameter λ_L can be calculated from the tumour doubling time:

$$\lambda_L = \frac{1}{\tau}\ln\left[\frac{\theta - No}{\theta/2 - No}\right] \tag{6.5}$$

The Gompertz growth function is given by:

$$\dot{N}(t) = \lambda_G N \ln(\theta / N(t)) \tag{6.6}$$

and the growth rate constant λ_G is calculated as a function of the doubling time:

$$\lambda_G = \frac{1}{\tau}\ln\left[\frac{\ln(\theta/No)}{\ln(\theta/2No)}\right] \tag{6.7}$$

Figure 6.4 depicts the growth of the tumour as described by the three different functions, exponential, logistic and Gompertz.

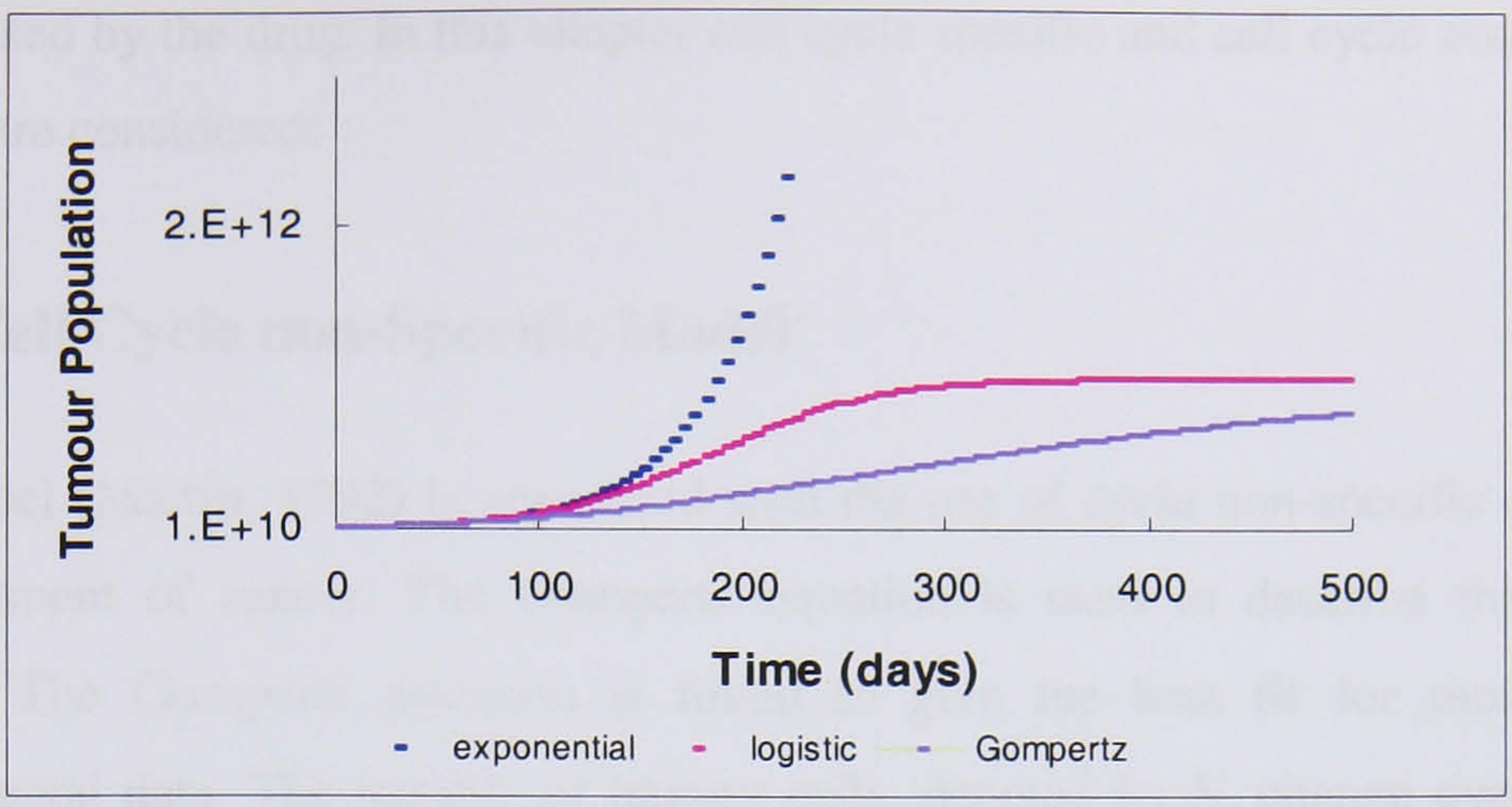


Figure 6.4 Tumour growth equations

6.2.2 Drug Distribution and Effect

Many pharmacokinetic models have been reported in the literature, which are based upon the specific drug that is used, or which are more general and fit statistical data. The pharmacodynamic effects of the drug on the tumour are generally modelled by first order kinetics. The toxic effects of the drugs are modeled so as to have a lower bound on the number of normal cells or alternatively put bounds on the drug schedule based on the clinical data. Some models can also incorporate constraints on the White Blood Cells, (protection from leucopoenia). Constraints for drug resistance can also be incorporated and the case when the tumour includes both drug resistant and drug non-resistant cells can be addressed via compartmental modeling.

6.3 Model Formulation

The simplest mathematical model describes the entire cell cycle as a uniform entity, where all the cells contained in a tumour are of the same type. The cell cycle non-specific models consist of one compartment so that the effect of the anticancer agents is same on all the cells. However these models fail to describe the action of cycle specific drugs due to their over-simplified nature. The more detailed multi-compartment models (cell cycle specific models) are introduced for this purpose. Here the cell cycle is divided into compartments depending on the types of cells that

are affected by the drug. In this chapter cell cycle specific and cell cycle non-specific models are considered.

6.3.1 Cell Cycle non-Specific Model

The model (Martin, 1992) is concerned with the use of cycle non-specific drugs for the treatment of cancer. The Gompertz equation is used to describe the tumour growth. The Gompertz equation is found to give the best fit for most of the experimental data. The number of tumour cells, denoted by N, change over time in accordance to the differential equation:

$$\dot{N}(t) = \lambda N(t) \ln\left(\theta / N(t)\right), \qquad (6.8)$$

$$N(0) = No = 10^{10}$$

where

λ is a growth parameter and

θ is the carrying capacity.

The value of θ is considered to be 10^{12} cells in this chapter.

The drug concentration at the tumour site is described by following equations:

$$\dot{\upsilon}(t) = u(t) - \gamma \upsilon(t) \qquad (6.9)$$

$$\upsilon(0) = \upsilon o = 0$$

where

υ is the concentration of the drug at the tumour site

u is the rate of delivery of the drug and

γ is a parameter that is related to the decay of the drug (γ =0.27days).

The function $u(t)$ is assumed to be piecewise continuous in time. The half life of the

drug concentration is $ln(2)/\gamma$. The following three assumptions are made concerning the delivery of the drug: (i) the drug is delivered by infusion, (ii) there is an instantaneous mixing of the drug with the plasma and (iii) there is an immediate delivery of the drug to the cancer site. These assumptions emanate from the fact that the amount of time needed for the drug to reach the cancer site right after the infusion, is negligible compared to the duration of the therapy.

The relation between the tumour growth and the effect of the anticancer drug is described as:

$$\dot{N}(t) = \lambda N(t) \ln(\theta / N(t)) - L(N(t), \upsilon(t)) \tag{6.10}$$

where the first term represents the increase in cells due to proliferation and L is a function used to describe the decrease in cells due to the drug. L is linear in N, due to the fact that most anti-cancer agents have been shown to kill cells by first order kinetics, i.e. the fraction of tumour cells killed by a drug of fixed concentration is not dependent upon the size of the tumour. For the cell cycle non-specific agents considered here, the difference in tumour growth is even less important. The cell-loss term is an affine function of drug concentration and has the form:

$$L(N(t), \upsilon(t)) = k(\upsilon(t) - \upsilon_{th}) H(\upsilon(t) - \upsilon_{th}) N(t) \tag{6.11}$$

where

H is the Heaviside function:

$$\begin{cases} \text{if } \upsilon(t) - \upsilon_{th} < 0 \text{ , then } H = 0 \\ \text{if } \upsilon(t) - \upsilon_{th} \geq 0 \text{ , then } H = 1 \end{cases} \tag{6.12}$$

υ_{th} is the therapeutic threshold level and

k is the kill rate of the drug (tumour cells killed per unit time per unit drug concentration).

Toxicity to normal tissue is modelled with the use of two constraints. The first constraint is an inequality that limits the drug concentration between a lower and an upper bound:

$$0 \leq \upsilon(t) \leq \upsilon_{\max}, \qquad \forall\, t \in [0,T] \tag{6.13}$$

where υ_{max} is a positive constant.

The second inequality places an upper bound on the total cumulative toxicity at the end of the treatment period:

$$\int_0^T \upsilon(s)\, ds \leq \upsilon_{cum} \tag{6.14}$$

where υ_{cum} is a positive constant.

Drug resistance is also modelled with the form of a multiple characteristic time (MCT) constraint:

$$N(\tau_{i+1}) \leq \varepsilon N(\tau_i), \qquad i = 0,1,....,M\text{-}1 \tag{6.15}$$

This constraint forces the tumour to decrease at, or faster than, a given rate. The treatment period T is divided into $M+1$ sub periods with the use of $M+1$ strictly increasing characteristic times $0 = \tau_o < \tau_1 <.....< \tau_M \leq T$. A minimum fractional reduction, ε, is imposed on the tumour size where the parameter ε is a positive constant. The data used in this model are listed in Table 6.1.

The treatment was assumed to last for 12 weeks (T=84 days). The multiple characteristic time constraints were set to three ($M=3$), with characteristic times $\tau_i = iT/4$, for $i = 0,1,2,3$. The minimum fraction reduction in tumour size over each three-weekly period was fixed to be 50%, i.e. $\varepsilon = ½$.

Table 6.1 Parameter values for the cell cycle non-specific model

Parameter	Value
λ	$9.9 * 10^{-4}$ days^{-1}
θ	10^{12} cells
γ	0.27 days^{-1}
No	10^{10} cells
v_{th}	10 [D]*
v_{max}	50[D]*
k	$8.4*10^{-3}$ days^{-1}[D]$^{-1}$
v_{cum}	$2.1*10^{3}$ [D] days

*[D] is the unit of drug concentration.

According to the above equation 6.15 becomes:

$$N(21) \leq 0.5\times10^{10}$$
$$N(42) \leq 0.25\times10^{10} \qquad (6.16)$$
$$N(63) \leq 0.125\times10^{10}.$$

6.3.2 Cell Cycle Specific Model

This model (Panetta and Adam, 1995) describes the administration of the anticancer drug in the case of cell cycle specific chemotherapy. The model is based on five basic assumptions:

(i) The tumour growth model is linear (first-order kinetics). This limits the model to either exponential growth or decay without any intermediate equilibrium. This is a satisfactory approach since chemotherapy will prevent the tumour from growing near its carrying capacity, so there is no need to use the Gompertz or the logistic equation.

(ii) All the parameters used in this model are constant.

(iii) Any spatial or age effects are not taken into account in the model. The drugs are assumed to reach all cells equally and cells of all ages are affected uniformly.

(iv) Although the cell cycle is divided into four sub-compartments (the gap period [G1], the synthetic period [S], the second gap period [G2] and mitosis [M]) (Figure 6.2), in this case the four sub-compartments are combined into one compartment. The overall result is a two compartment model that describes the effects of the drug for both cycling and non cycling cells.

(v) The final assumption is concerned with the resting cells. Generally, the faster proliferating cells are affected more by the drugs. This model assumes that the resting cells [Go] are not affected by the anticancer agents.

The two-compartment model is described in Figure 6.5.

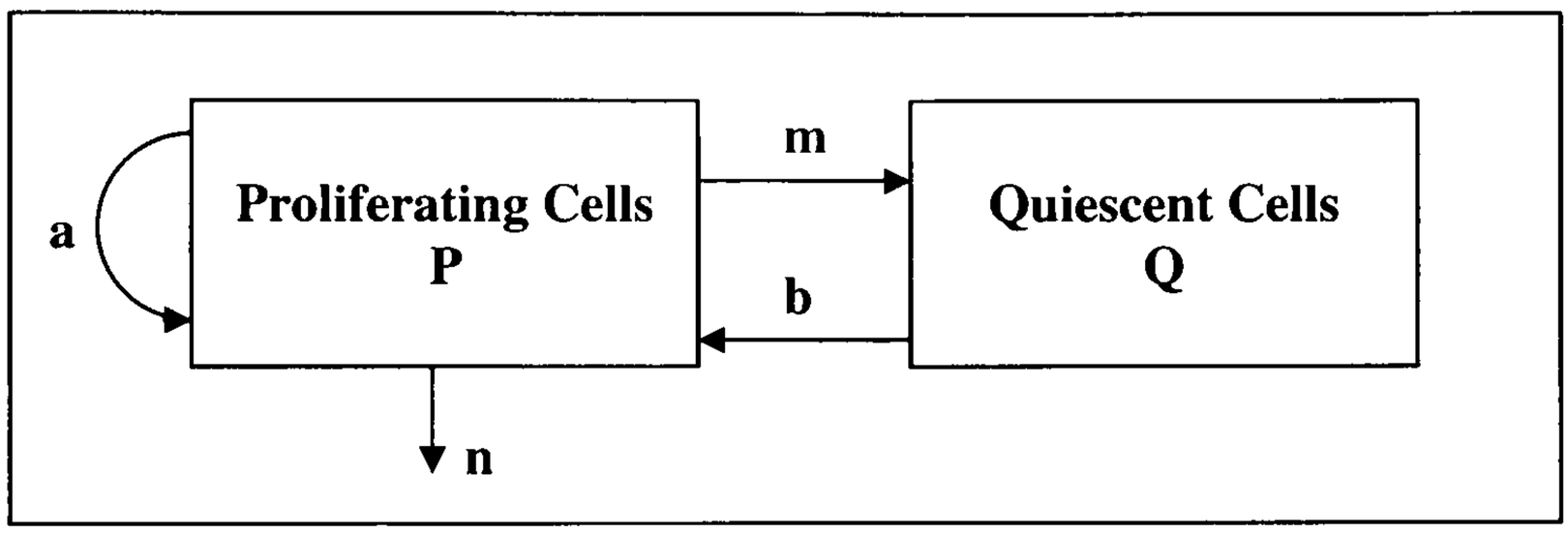


Figure 6.5 Two compartment model

The mathematical model is given by:

$$\dot{P}(t) = (a - m - n)P(t) + bQ(t) - g(t)P(t), \quad P(0) = P_0 \tag{6.17}$$

$$\dot{Q}(t) = mP(t) - bQ(t), \qquad Q(0) = Q_0 \tag{6.18}$$

The parameters are defined as follows:

a is the cycling cells growth rate

m is the rate at which cycling cells become noncycling

n is the natural decay of cycling cells

b is the rate at which noncycling cells become cycling.

All the parameters are constant and positive. The parameter values are taken from breast cancer data (Panetta and Adam, 1995). P and Q represent the cycling and noncycling tumour cell mass, respectively. It is assumed that there is positive net growth rate ($a > n$), so that the tumour will grow without bound in the absence of chemotherapy. It is also assumed that a large number of proliferating cells become resting cells ($a - m - n < 0$). Natural decay of non cycling cells is taken to be zero.

The chemotherapeutic effects are described with the use of the exponential decay function:

$$g(t) = he^{-\gamma(t-n\tau)}, \qquad n\tau \leq t < (n+1)\tau, \tag{6.19}$$

where

h is the cell kill parameter and

γ is the decay of the drug.

The function $g(t)$ is a piecewise continuous function describing the chemotherapeutic effects on the tumour. Since this model describes cycle-specific chemotherapy, the drugs will only affect the cycling cells, P.

It is well known that chemotherapy affects not only cancer cells but also the normal tissues. To control toxicity to normal tissue it is assumed that the normal cells have limited growth during treatment. The logistic equation is used to describe the growth of normal tissue:

$$\dot{y}(t) = \delta y(t)(1 - \frac{y(t)}{K}) - g(t)\,y(t), \qquad n\tau \leq t < (n+1)\tau \tag{6.20}$$

$$y(0) = y_0$$

where

y is the number of normal cells

δ is the growth rate and

K is the carrying capacity of normal tissue.

The parameter values are listed in Table 6.2. It was assumed that the period of chemotherapy treatment, T, is 40 days. The initial value of normal cells, y_0, is taken to be equal to the number of bone marrow cells. Bone marrow is very sensitive and can be extremely damaged by the toxic effects of the drugs.

Table 6.2 Parameter values for the cell cycle specific model (Breast cancer data)

Parameter	Value
a	0.5 $days^{-1}$
m	0.218 $days^{-1}$
n	0.477 $days^{-1}$
b	0.05 $days^{-1}$
h	0.8 $days^{-1}$
γ	0.1 $days^{-1}$
δ	0.1 $days^{-1}$
K	10^9 cells
P_0	$0.2*10^{12}$ cells
Q_0	$0.8*10^{12}$ cells
y_0	10^9 cells

6.4 Simulation Results

Both models were validated by using gPROMS to examine and compare their performance. The most important results and conclusions derived from the simulations are presented.

6.4.1 Cell Cycle non-Specific Model

Several simulations were carried out to find the maximum rate of delivery of the drug that can be applied once to the patient,

without causing any harm due to toxicity effects, for the given highest allowable value of concentration, v_{max}, 50[D]. The maximum dose, u, was obtained to be around 51[D] day^{-1}. Note that the total cumulative toxicity, v_{cum}, reached the value of 309 [D] days. This is a high value considering that one maximum dose of the drug reaches almost 15% of its upper limit (2100 [D]days). This indicates that toxicity effects limit the maximum value of many drug doses during chemotherapy. After the maximum injected dose has been defined, two cases were examined. First, the maximum dose was applied at the beginning of the therapy and then, the same amount of drug was applied towards the end of the therapy.

Figures 6.6 and 6.7 show how the number of cancer cells change with time in both cases. It is obvious that the final tumour population is the same, about 6.78×10^9 cells. This indicates why, although in clinical practice the anti-cancer agents are applied at the beginning of the therapy, the optimal control results show that the drug should be injected towards the end of the chemotherapy period. Finally, there may exist different chemotherapy schedules resulting in the same value of final tumour cells.

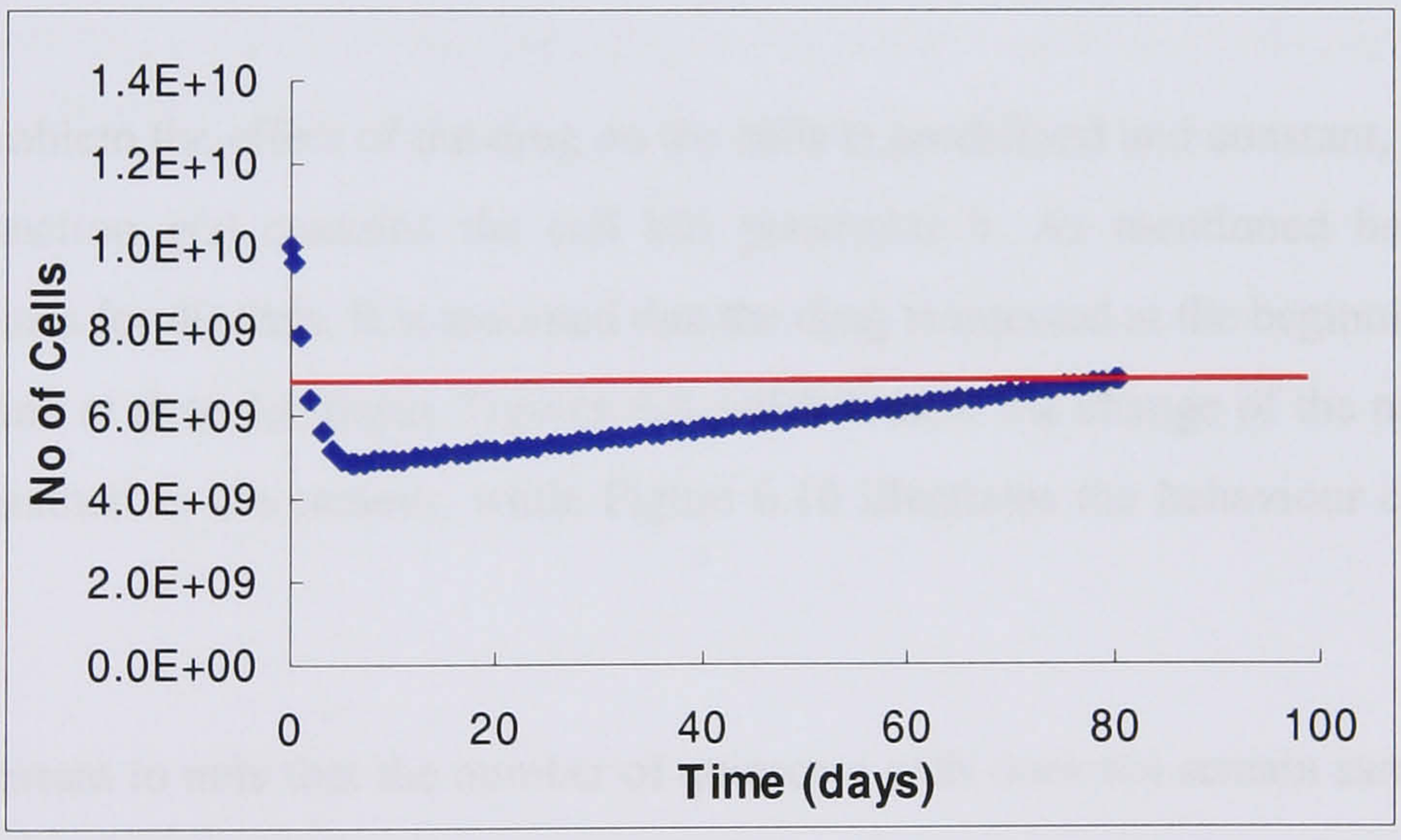


Figure 6.6 The evolution with time of tumour cell population, when the maximum dose of the drug is administered at the beginning of the therapy

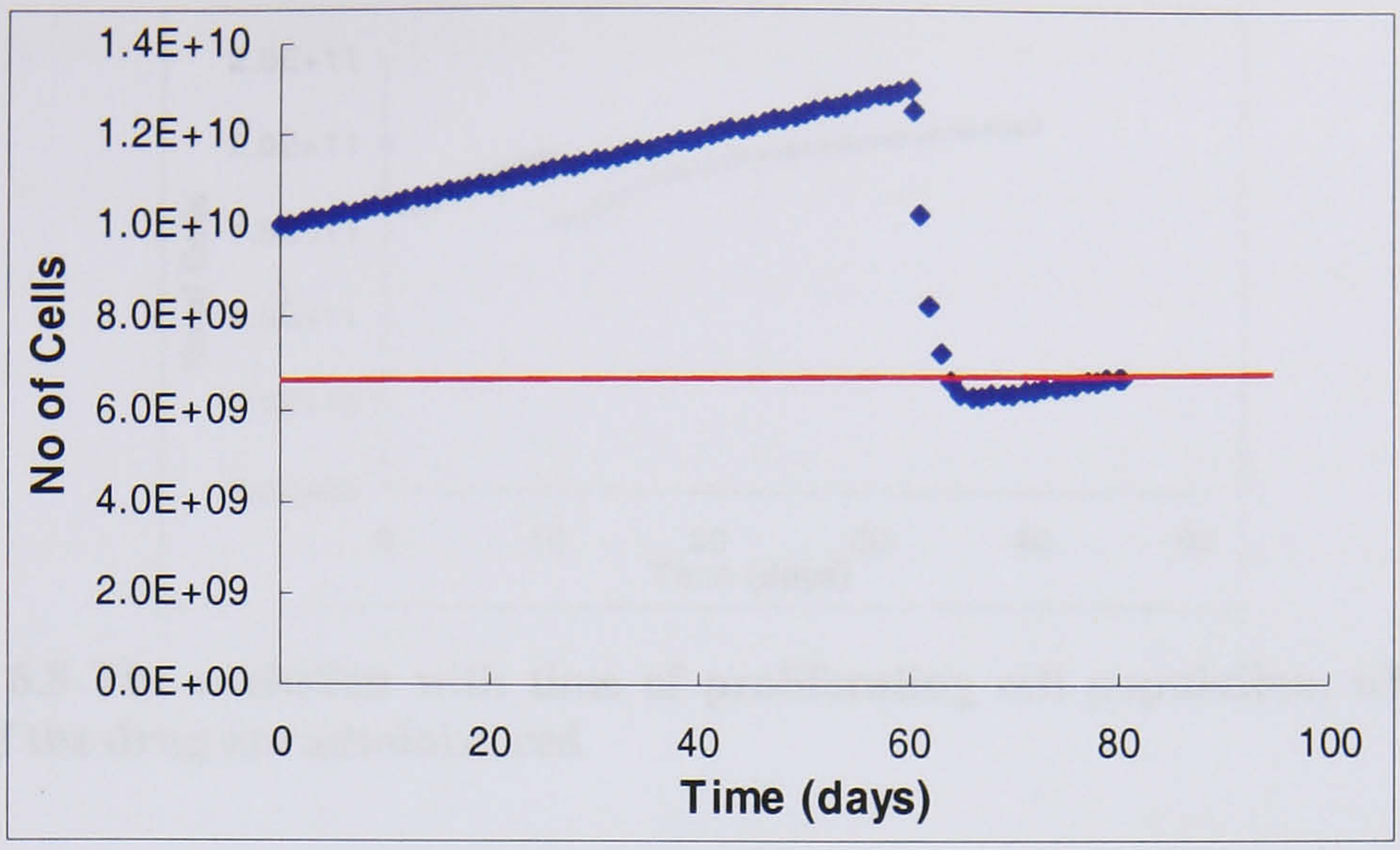


Figure 6.7 The evolution with time of tumour cell population, when the maximum dose of the drug is administered towards the end of the therapy

6.4.2 Cell Cycle Specific Model

The tumour population is assumed to be 10^{12} and the number of normal cells to be 10^{9}, based on clinical data from several sources. It has been observed that 80% of the tumour consists of the resting cells, while the remaining 20% consists of the cycling cells.

In this problem the effect of the drug on the cells is predefined and constant, since the decay function $g(t)$ contains the cell kill parameter h. As mentioned before, the therapy lasts for 40 days. It is assumed that the drug is injected at the beginning of the therapy and at time 10 (days). Figures 6.8 and 6.9 show the change of the number of cells contained in the tumour, while Figure 6.10 illustrates the behaviour of normal cells.

It is important to note that the number of quiescent cells does not remain same during the therapy. The resting cells are not directly affected by the drug, but the total number changes because of the interaction between the compartments.

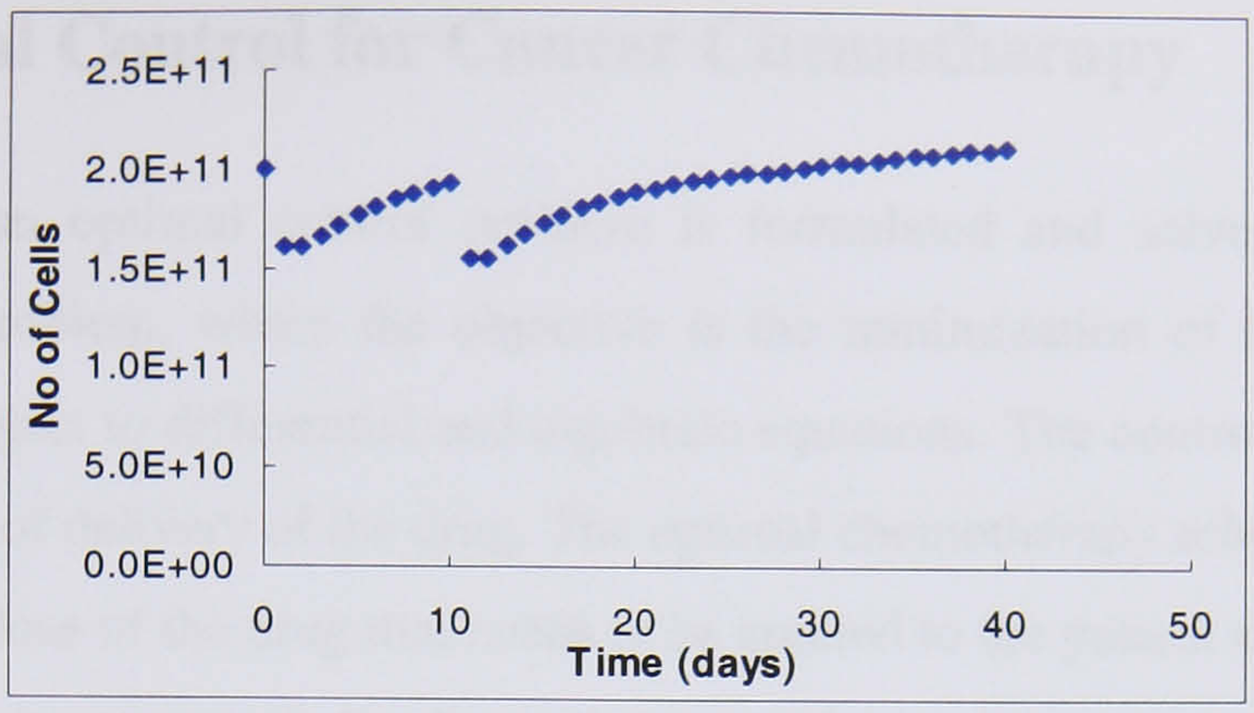


Figure 6.8 The evolution with time of proliferating cell population, when two doses of the drug are administered

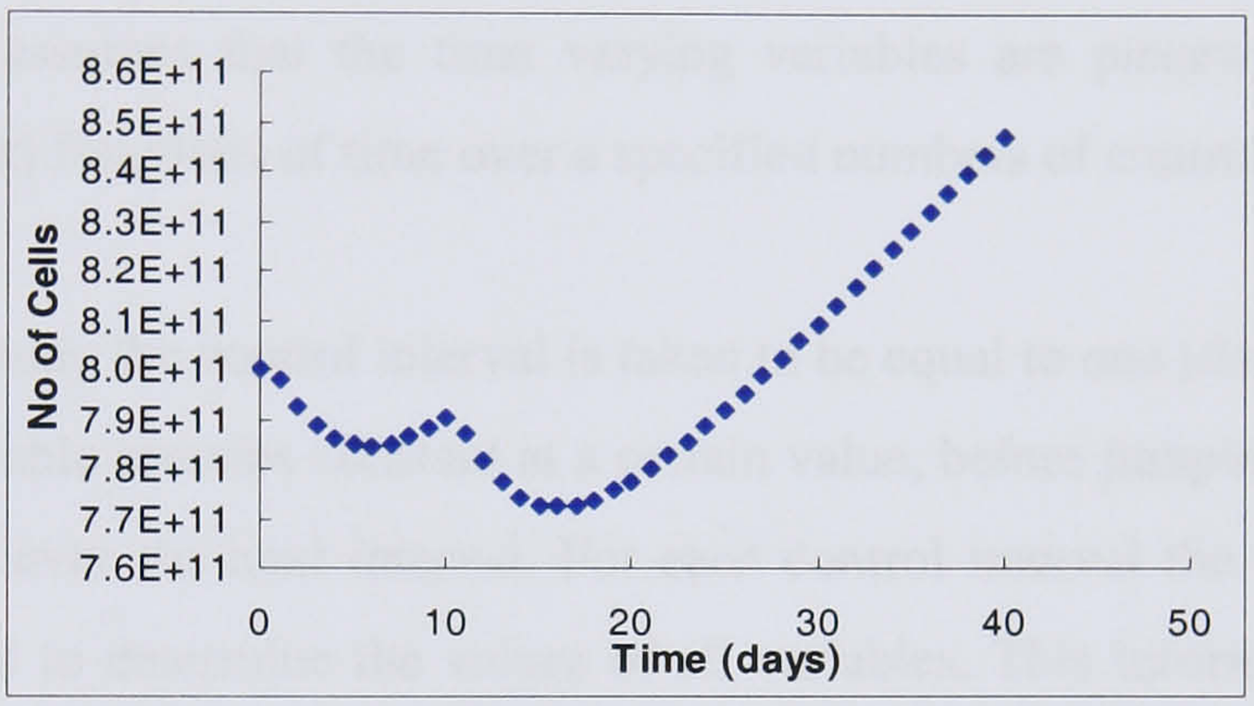


Figure 6.9 The evolution with time of resting cell population, when two doses of the drug are administered

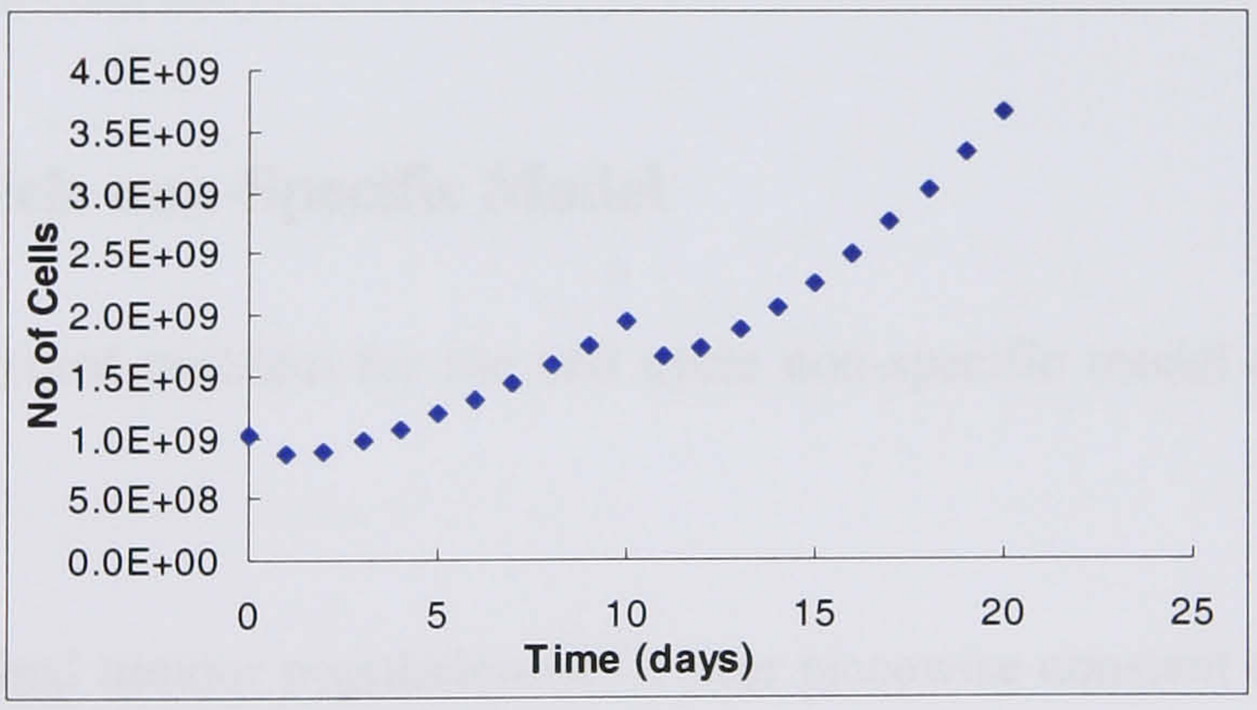


Figure 6.10 The evolution with time of normal cell population, when two doses of the drug are administered

6.5 Optimal Control for Cancer Chemotherapy

In this study an optimal control problem is formulated and solved as a dynamic optimization problem, where the objective is the minimization of the final tumour population, subject to differential and algebraic equations. The control variable in this case is the rate of delivery of the drug. The optimal chemotherapy schedule which will determine the dose of the drug that needs to be applied to the patient each day, so as to achieve the minimum tumour burden at the end of the treatment period is obtained.

The optimization models are solved using gPROMS. The dynamic optimization algorithms in gPROMS are based on a control vector parameterisation (CVP) approach that assumes that the time varying variables are piecewise constant (or piecewise linear) functions of time over a specified numbers of control intervals.

In the current study the control interval is taken to be equal to one (day), during which the control variable remains constant at a certain value, before jumping discretely to a different value over the next interval. For each control interval the dynamic system model is solved to determine the values of all variables. This information is used to evaluate the objective function and the constraints, and the procedure is repeated until the objective function is optimized and all constraints are satisfied. The next section presents the formulation of the mathematical models for both cell cycle non-specific and cell cycle specific cases.

6.5.1 Cell Cycle non-Specific Model

The optimal control problem for the cell cycle non-specific model can be stated as follows:

Minimize the final tumour population $N(T)$, over piecewise constant control variables $u = (u_1,\ldots,u_n)^T$, subject to the differential equations (6.9)-(6.11) and the constraints (6.13), (6.14) and (6.16).

Mathematically, this can be formulated as follows:

$$\min_{u(t)} J_1(u) = N(T) \tag{6.21}$$

where $u = [u_1,...,u_n]^T \in \Re^n$, subject to the differential equation of the tumour evolution:

$$\dot{N}(t) = \lambda N(t)\ln(\theta / N(t)) - k(\upsilon(t) - \upsilon_{th})H(\upsilon(t) - \upsilon_{th})N(t) \tag{6.22}$$

the differential equation for the drug concentration:

$$\begin{aligned} &\dot{\upsilon}(t) = u(t) - \gamma\upsilon(t) \\ &\upsilon(0) = \upsilon o = 0 \end{aligned} \tag{6.23}$$

the constraint on the maximum drug concentration:

$$0 \le \upsilon(t) \le \upsilon_{\max}, \qquad \text{for all } t \in [0,T] \tag{6.24}$$

the cumulative toxicity constraint:

$$\int_0^T \upsilon(s)\,ds \le \upsilon_{cum} \tag{6.25}$$

and the constraints on the tumour burden:

$$\begin{aligned} &N(21) \le 0.5\times10^{10} \\ &N(42) \le 0.25\times10^{10} \\ &N(63) \le 0.125\times10^{10} \end{aligned} \tag{6.26}$$

The following transformation:

$z=ln(\theta/N)$

is introduced to make the model tractable and tumour size dimensionless.

Equations (6.22) and (6.26) are transformed as follows:

$$\dot{z}(t) = -\lambda z(t) + k(\upsilon(t) - \upsilon_{th}) H(\upsilon(t) - \upsilon_{th}), \tag{6.27}$$

$$z(0) = \ln(\theta / No)$$

$$\begin{aligned} z(21) &\geq \ln(200) \\ z(42) &\geq \ln(400) \\ z(63) &\geq \ln(800) \end{aligned} \tag{6.28}$$

The discontinuity in the model:

$$\begin{cases} \text{if } \upsilon(t) - \upsilon_{th} < 0 \text{ , then } H = 0 \\ \text{if } \upsilon(t) - \upsilon_{th} \geq 0 \text{ , then } H = 1 \end{cases} \tag{6.29}$$

is incorporated by introducing binary variable y. Equation (6.27) becomes:

$$\dot{z}(t) = -\lambda z(t) + k(\upsilon(t) - \upsilon_{th}) y, \tag{6.30}$$

$$z(0) = \ln(\theta / No)$$

and equation (6.29) is reformulated as:

$$\upsilon(t) \geq y\upsilon_{th}, \qquad \forall t \in [0,T] \tag{6.31}$$

$$\upsilon(t) - \upsilon_{th} \leq yM, \qquad \forall t \in [0,T], \tag{6.32}$$

where M is a very large number (10^{30}).

These constraints force the binary variable y to take the value 0, if $0 \le v(t) \le v_{th}$, or the value 1, if $v(t) \ge v_{th}$.

The optimal control problem is thus formulated as:

$$\min_{u,y} J(u) = -z(T),$$

$$\begin{aligned}
\text{s.t.} \quad & \dot{z}(t) = -\lambda z(t) + k(v(t) - v_{th})\, y \\
& z(0) = \ln(\theta / No) \\
& \dot{v}(t) = u(t) - \gamma v(t) \\
& v(0) = vo = 0 \\
& 0 \le v(t) \le v_{\max}, \qquad \text{for all } t \in [0,T] \\
& \int_0^T v(s)\, ds \le v_{cum} \\
& z(21) \ge \ln(200) \\
& z(42) \ge \ln(400) \\
& z(63) \ge \ln(800) \\
& v(t) \ge y v_{th}, \qquad \text{for all } t \in [0,T] \\
& v(t) - v_{th} \le yM, \qquad \text{for all } t \in [0,T]
\end{aligned}$$

The data used for the solution of this problem are listed in Table 6.1. This is a Mixed Integer Dynamic Optimization (MIDO) problem that can be solved by using the algorithms presented by Bansal *et al.* (2003).

6.5.2 Cell Cycle Specific Model

The cell cycle specific model, as stated in section 6.3.2, does not allow for the use of the optimization strategy that was previously discussed. This is due to the formulation of function $g(t)$ (equation 6.19) that describes the chemotherapeutic effects of the drug to the cells. The function includes the cell kill rate parameter h, which is a constant number, so the effect of the drug ($g(t)$) depends only on the duration of the injection and not on the amount of the drug that is injected.

For this reason, equation (6.19) is replaced by equations (6.33) and (6.34), which relate the effect of the drug with the rate of delivery of the drug (amount of drug per unit time):

$$g(t) = k_1 v_1(t) \tag{6.33}$$

$$\dot{v}_1(t) = u(t) - \gamma v_1(t), \qquad v(0) = v_0 \ , \tag{6.34}$$

where

g is the effect of the drug to the cells

v_1 is the concentration of the drug in the body

u is the rate of delivery of the drug

k_1 is the parameter for the kill rate and

γ is the parameter for the decay of the drug.

Equation (6.34) is similar to equation (6.23), used in the case of cell cycle non-specific chemotherapy. The objective of the optimal control problem for the cell cycle specific case is therefore to minimize the final tumour population $P(t)+Q(t)$, over all piecewise constant controls $u = (u_1,\ldots,u_n)^T$.

An additional restriction is placed on the number of normal cells to ensure that the toxic effects will not affect the patient. The number of normal cells is bounded between a lower acceptable level (y_{min}) and the carrying capacity of normal cell population (K), by using the following constraint:

$$y_{\min} \le y(t) \le K, \qquad \text{for all } t \in [0,T] \tag{6.35}$$

Based upon the above discussion the optimal control problem is given by:

$$\min_{u(t)} J(u) = P(T) + Q(T)$$

$$
\begin{aligned}
s.t.\quad & \dot{P}(t) = (a-m-n)P(t) + bQ(t) - g(t)P(t), && P(0) = P_0 \\
& \dot{Q}(t) = mP(t) - bQ(t), && Q(0) = Q_0 \\
& \dot{y}(t) = \delta y(t)\left(1 - \frac{y(t)}{K}\right) - g(t)y(t), && y(0) = y_0 \\
& \dot{v}_1(t) = u(t) - \gamma v_1(t), && v_1(0) = v_0 \\
& g(t) = k_1 v_1(t) \\
& y_{\min} \le y(t) \le K, && \text{for all } t \in [0,T]
\end{aligned}
$$

It is important to note that this model does not include any constraints on the concentration or the cumulative toxicity, whereas toxicity is controlled directly by placing a lower bound to the number of normal cells. Drug resistance is ignored in this case, but this is an acceptable approach since the treatment period is small. The parameter values used for the solution of this problem are shown in Table 6.3.

6.6 Optimization Results

6.6.1 Cell Cycle non-specific Model

The model described in section 6.5.1 was solved by using gPROMS starting from a random choice of initial guesses for each one of the control variables. The solution of this type of problems is very sensitive to the initial guess of the control variable. After extensive investigation a good set of initial values was determined and the optimal solution was obtained.

The dynamic optimization results suggest that the optimal chemotherapy profile is of the form shown in Figure 6.11. It is apparent that most of the drug is delivered at the end of the treatment, which is in accordance to other optimal control results from the literature. Initially no drug is delivered until the time approaches the first interval of the MCT constraint. This can be attributed to the fact that an initial high dose may not necessarily result in an overall decrease in the tumour size at the end of the time period as compared to the minimum tumour size obtained by the optimal chemotherapy protocol, while the constraints on toxicity and drug resistance are

satisfied. Moreover, drugs are given in large doses intermittently rather than in small doses continuously.

Table 6.3 Parameter values for the cell cycle specific model

Parameter	Value
a	0.5 $days^{-1}$
m	0.218 $days^{-1}$
n	0.477 $days^{-1}$
b	0.05 $days^{-1}$
h	0.8 $days^{-1}$
γ	0.1 $days^{-1}$
δ	0.1 $days^{-1}$
K	10^9 cells
k_1**	$8.4*10^{-3}$ $days^{-1}$ [D]*
y_{min}	10^8 cells
P_0	$0.2*10^{12}$ cells
Q_0	$0.8*10^{12}$ cells
y_0	10^9 cells

* [D] is the unit of drug concentration

** k_1 is taken to be equal to the parameter k listed in Table 6.1 used in the cell cycle non specific model

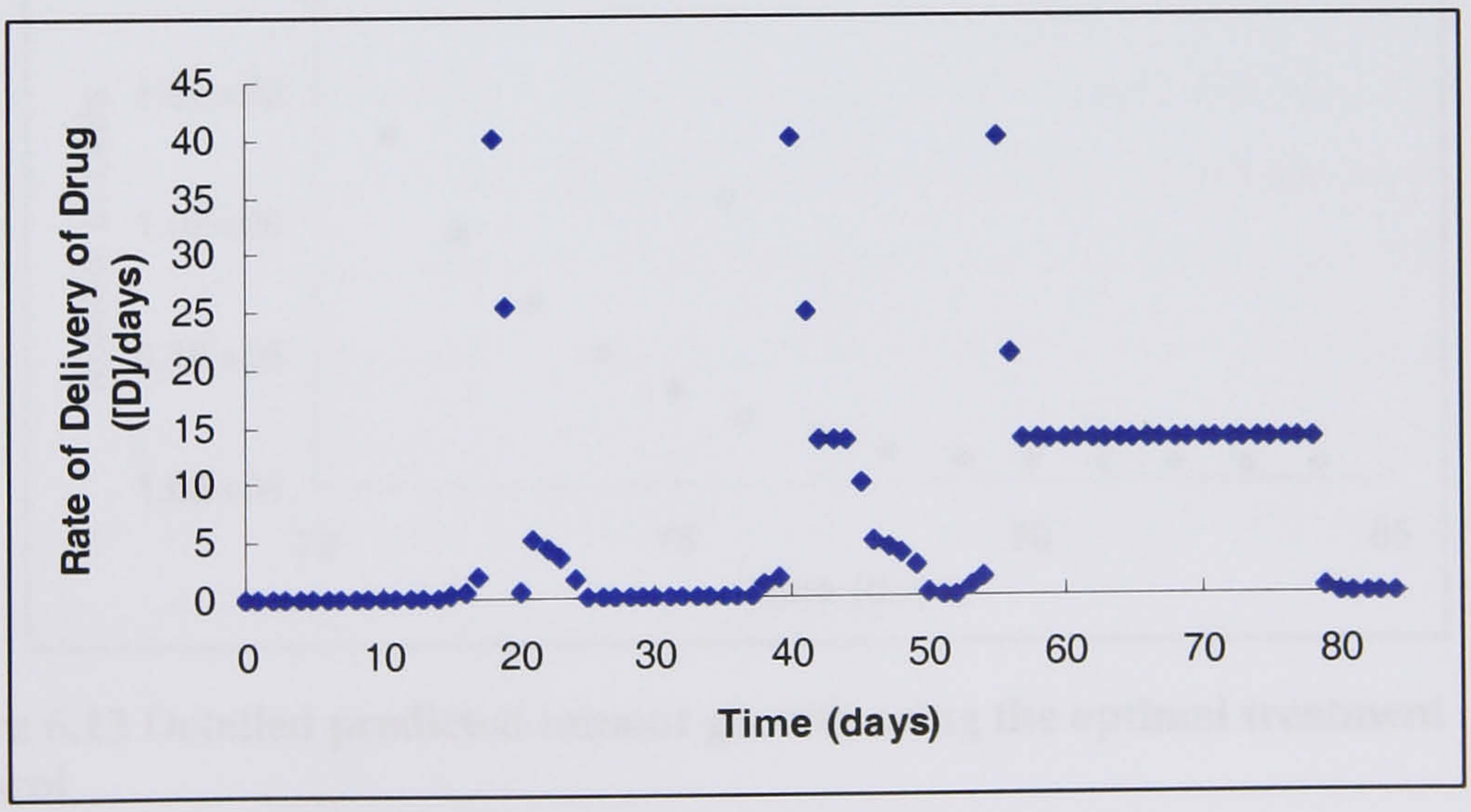


Figure 6.11 Optimal chemotherapy protocol for the cell cycle non specific case

The effect of the drug on tumour growth is shown in Figure 6.12. The tumour follows the Gompertz growth until the first injection of the drug that results in a reduction of 70% of the initial tumour size. High intensity chemotherapy, from time 40 (days) till the end of the therapy, results in an increase in the rate of tumour reduction. The value of the objective function at the end of the treatment is given by 7.5×10^4 cancer cells.

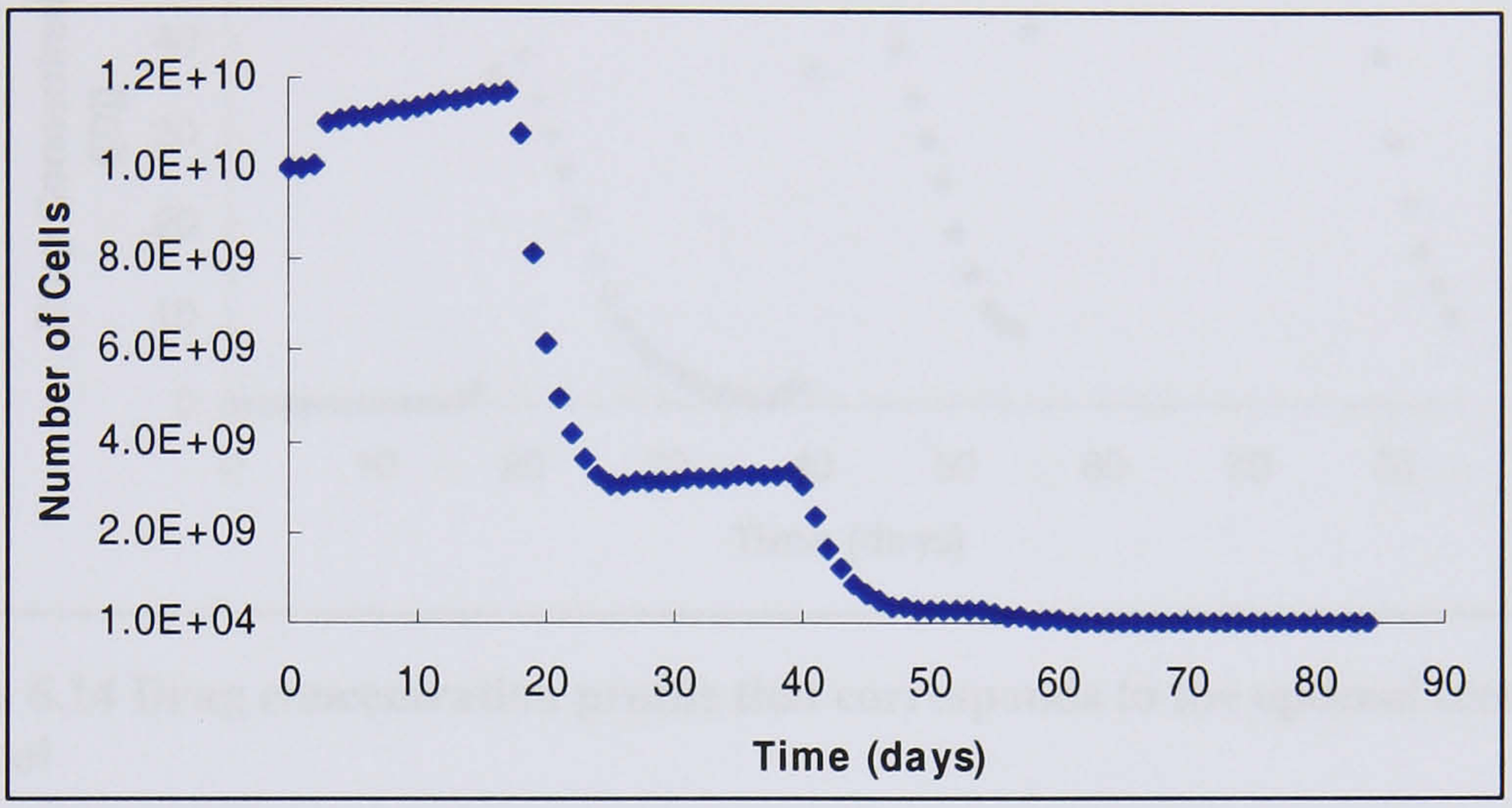


Figure 6.12 Predicted tumour growth using the optimal treatment protocol

The increase in the rate of tumour reduction can be better observed in Figure 6.13, which illustrates the behaviour of the tumour during the last 14 days of treatment.

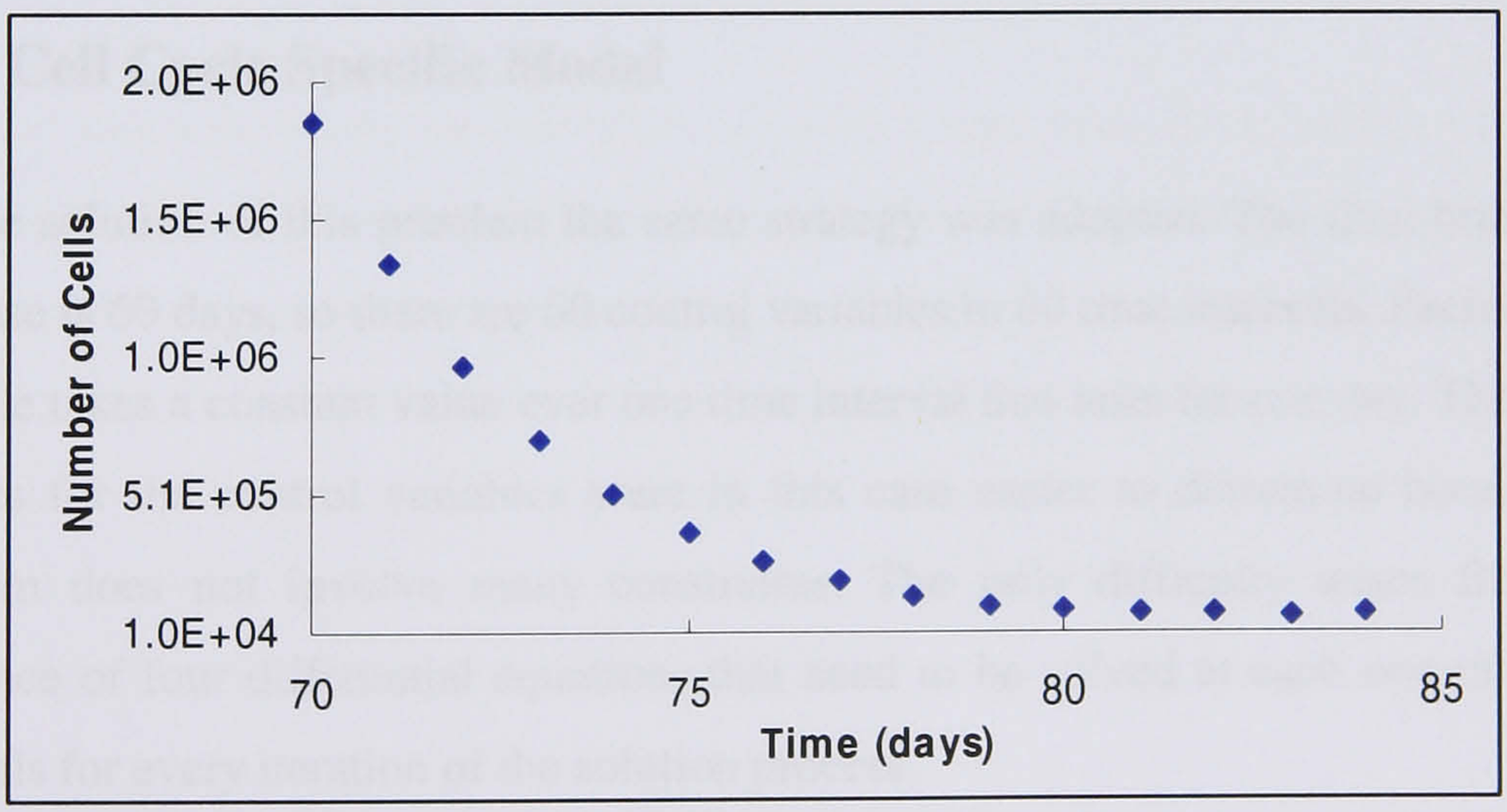


Figure 6.13 Detailed predicted tumour growth using the optimal treatment protocol

Figure 6.14 displays the drug concentration profile. The concentration reached the maximum value near the characteristic times and remained at this value for the time period 56 to 78 days.

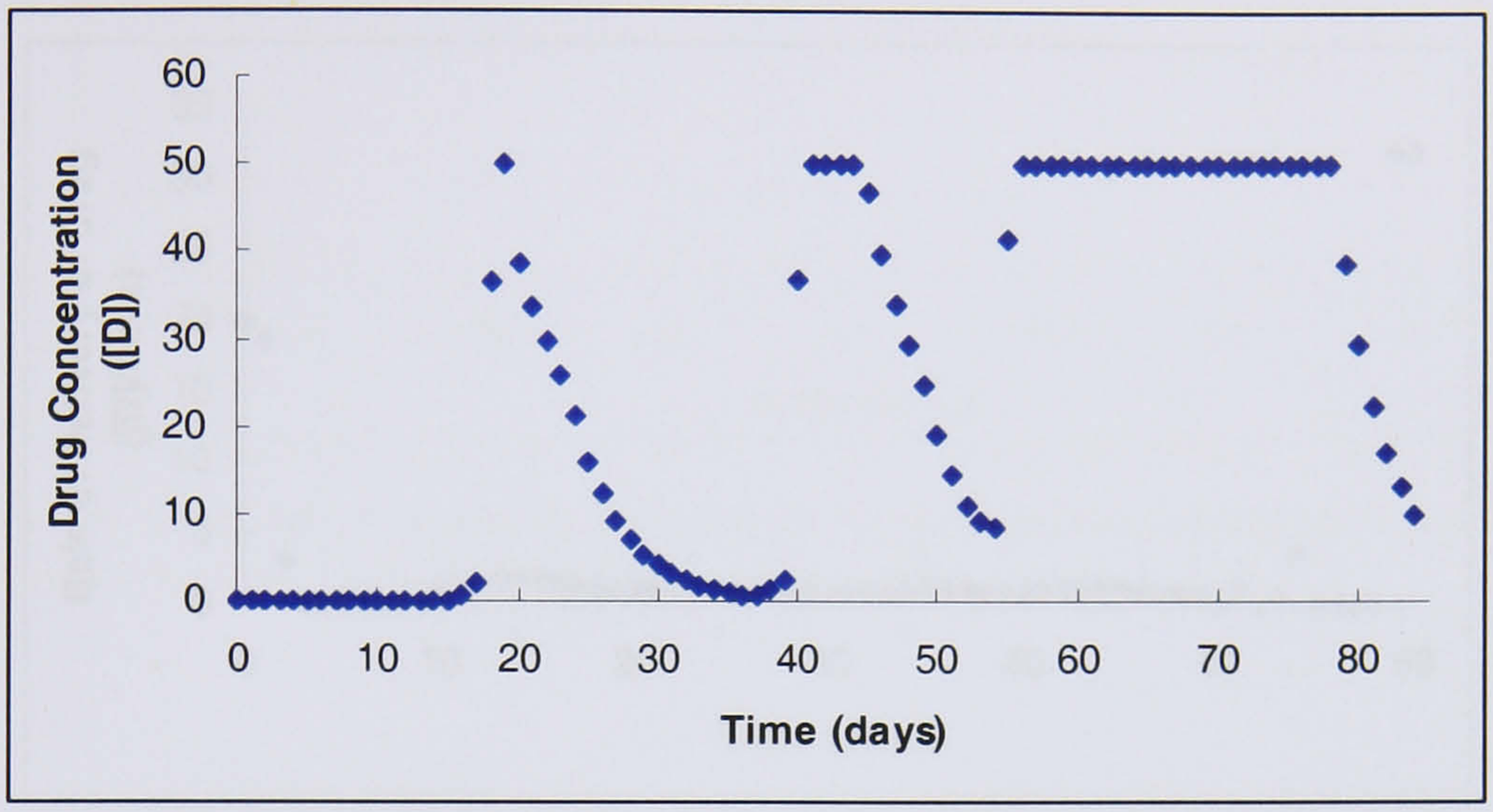


Figure 6.14 Drug concentration profile that corresponds to the optimal treatment protocol

As a conclusion, the optimal way to reduce the tumour size was to apply high intensity therapy towards the end of the chemotherapy period. The optimal chemotherapy protocol displayed in Figure 6.11 produces a 99.9% reduction of the initial tumour size.

6.6.2 Cell Cycle Specific Model

For the solution of this problem the same strategy was adopted. The time horizon in this case is 60 days, so there are 60 control variables in 60 time intervals. Each control variable takes a constant value over one time interval that lasts for one day. The initial guesses for the control variables were in this case easier to determine because the problem does not involve many constraints. The only difficulty arises from the existence of four differential equations that need to be solved at each one of the 60 intervals for every iteration of the solution process.

The optimal chemotherapy schedule derived is shown in Figure 6.15. Initially, the drug is delivered at a high dose, followed by a low intensity therapy for almost the rest of the treatment period. Finally, a large amount of drug is applied in the last two days.

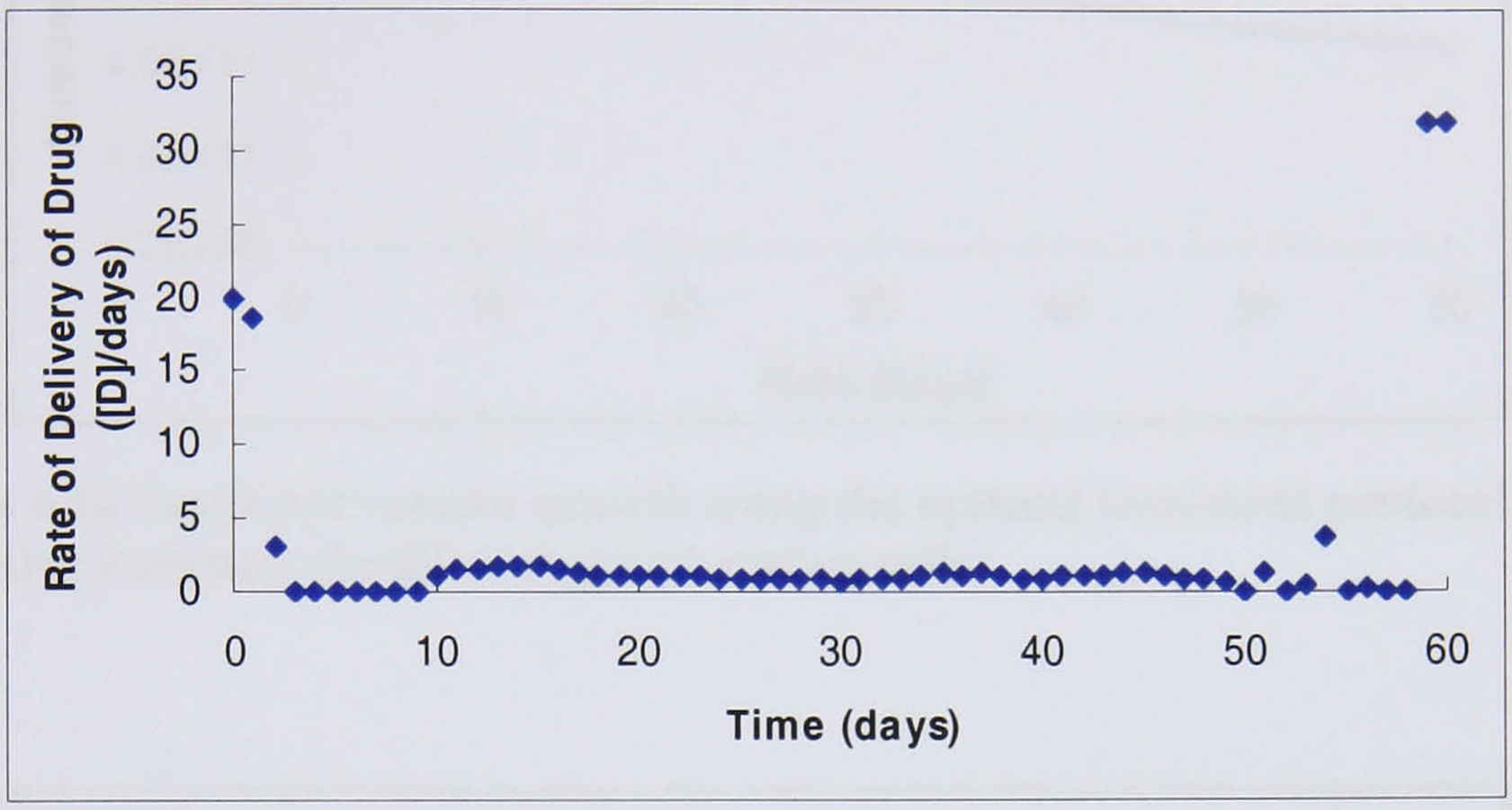


Figure 6.15 Optimal chemotherapy protocol for the cell cycle specific case

The objective function represents the size of the tumour, including both the proliferating and resting compartments. The evolution of the number of cancer cells during the therapy period is illustrated in Figure 6.16. After the optimal drug protocol is applied to the patient, the predicted number of cancer cells drops from 10^{12} cells to 4×10^{11} cells, which corresponds to 60% reduction of the initial tumour size.

The final reduction in the number of cancer cells is less when compared to the results obtained for the cell cycle non specific case. Nevertheless, the cell cycle specific model includes the constraint that places strict limits to the acceptable number of normal cells. As shown in Figure 6.17, for almost the entire treatment period, the level of normal cells is near to its lower bound. It is obvious that the first high dose of the drug had an enormous effect on normal cells, which did not allow further applications of high doses, apart from that in the last two days.

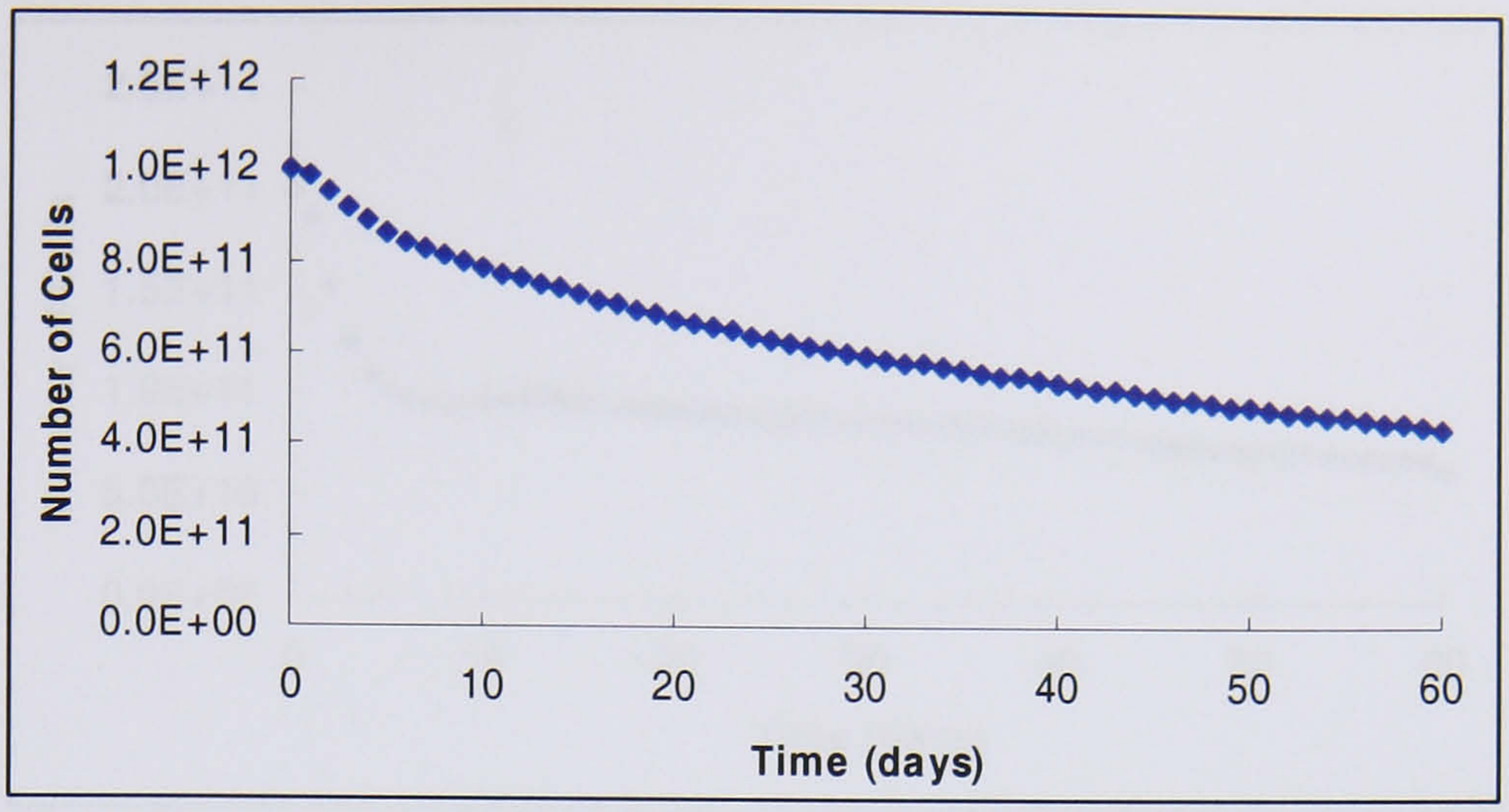


Figure 6.16 Predicted tumour growth using the optimal treatment protocol – Objective Function (proliferating and resting cells)

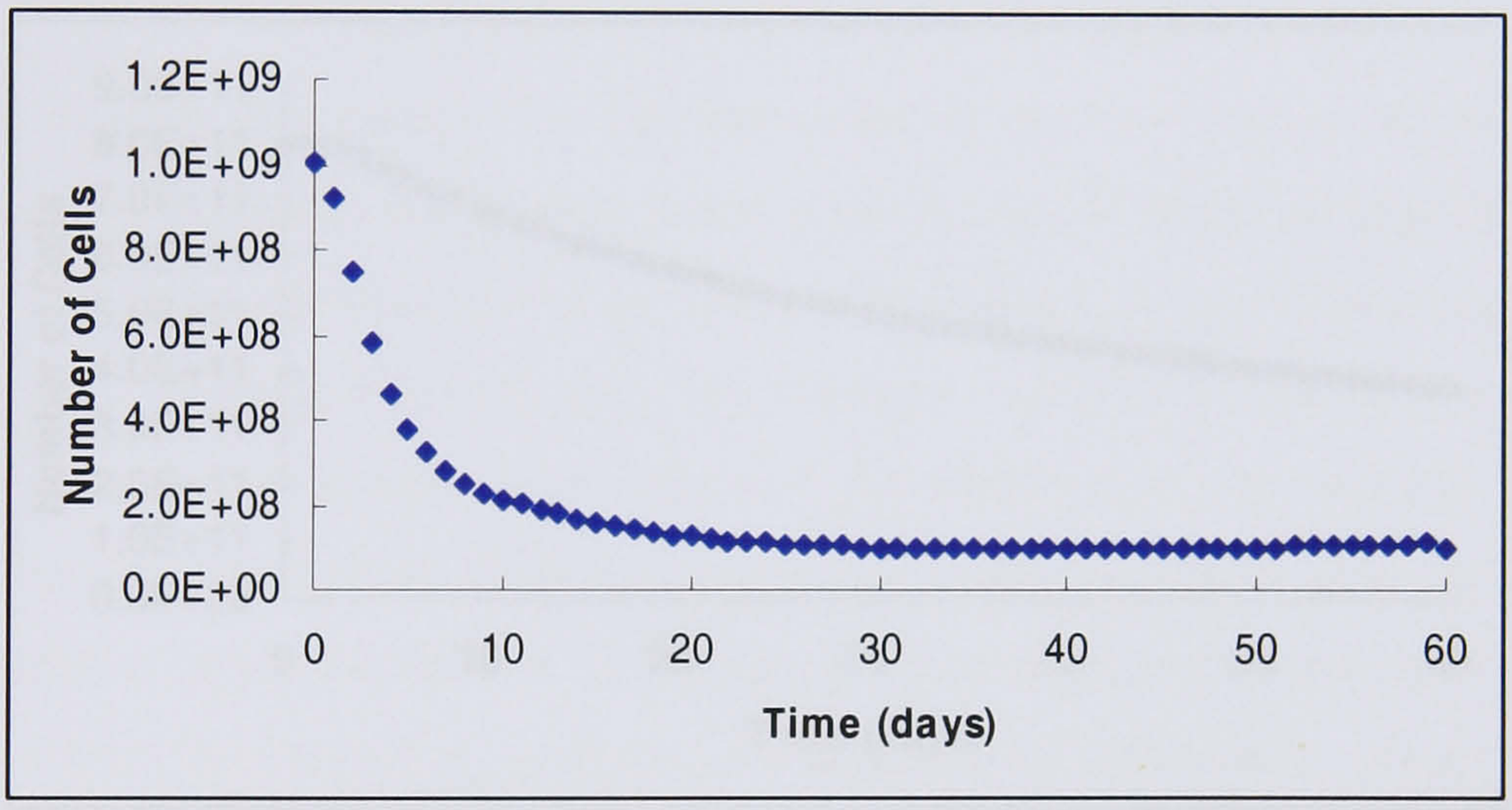


Figure 6.17 Predicted growth of the normal cell population using the optimal treatment protocol

Figures 6.18 and 6.19 illustrate the predicted growth for the proliferating and quiescent compartment respectively. The reduction in the number of resting cells is 50%, while proliferating cells are affected more by the drugs, resulting in a reduction of 70% of the initial size.

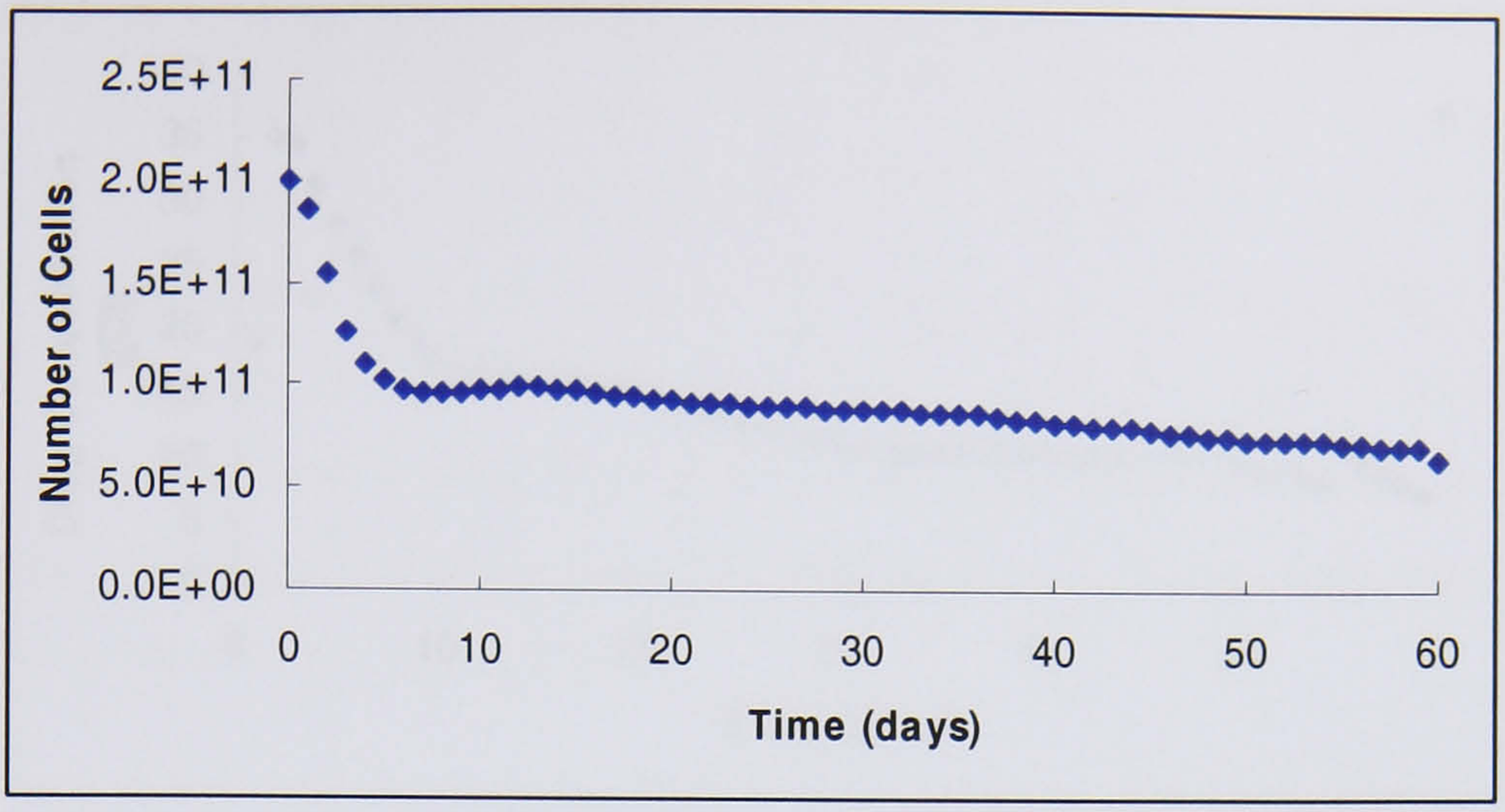


Figure 6.18 Predicted growth of the proliferating compartment using the optimal treatment protocol

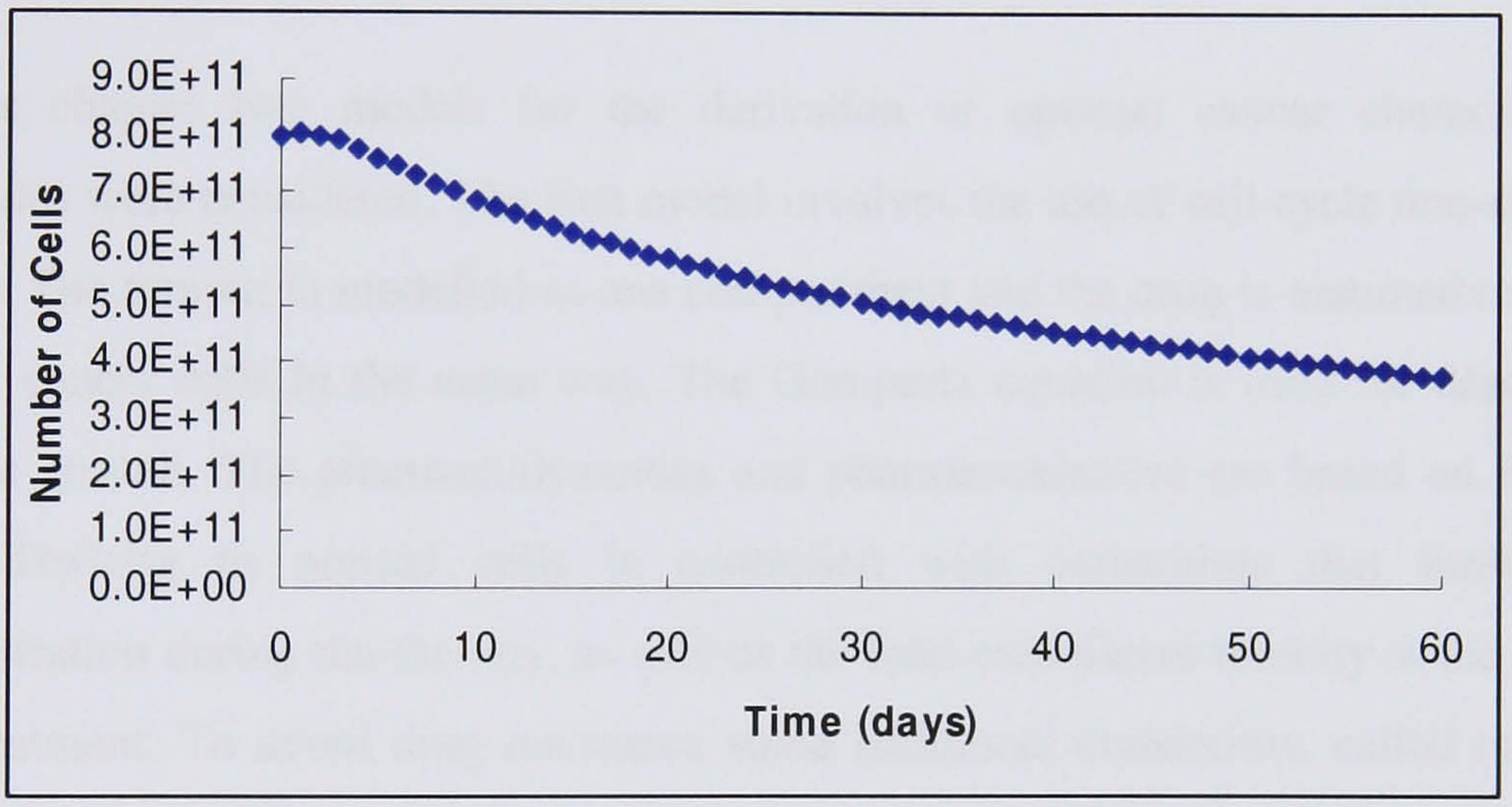


Figure 6.19 Predicted growth of the resting compartment using the optimal treatment protocol

The profile of drug concentration in the body after the optimal drug regimen has been applied is shown in Figure 6.20. As expected, the highest drug concentrations occurred near the applications of the highest doses, that is at the beginning and at the end of chemotherapy.

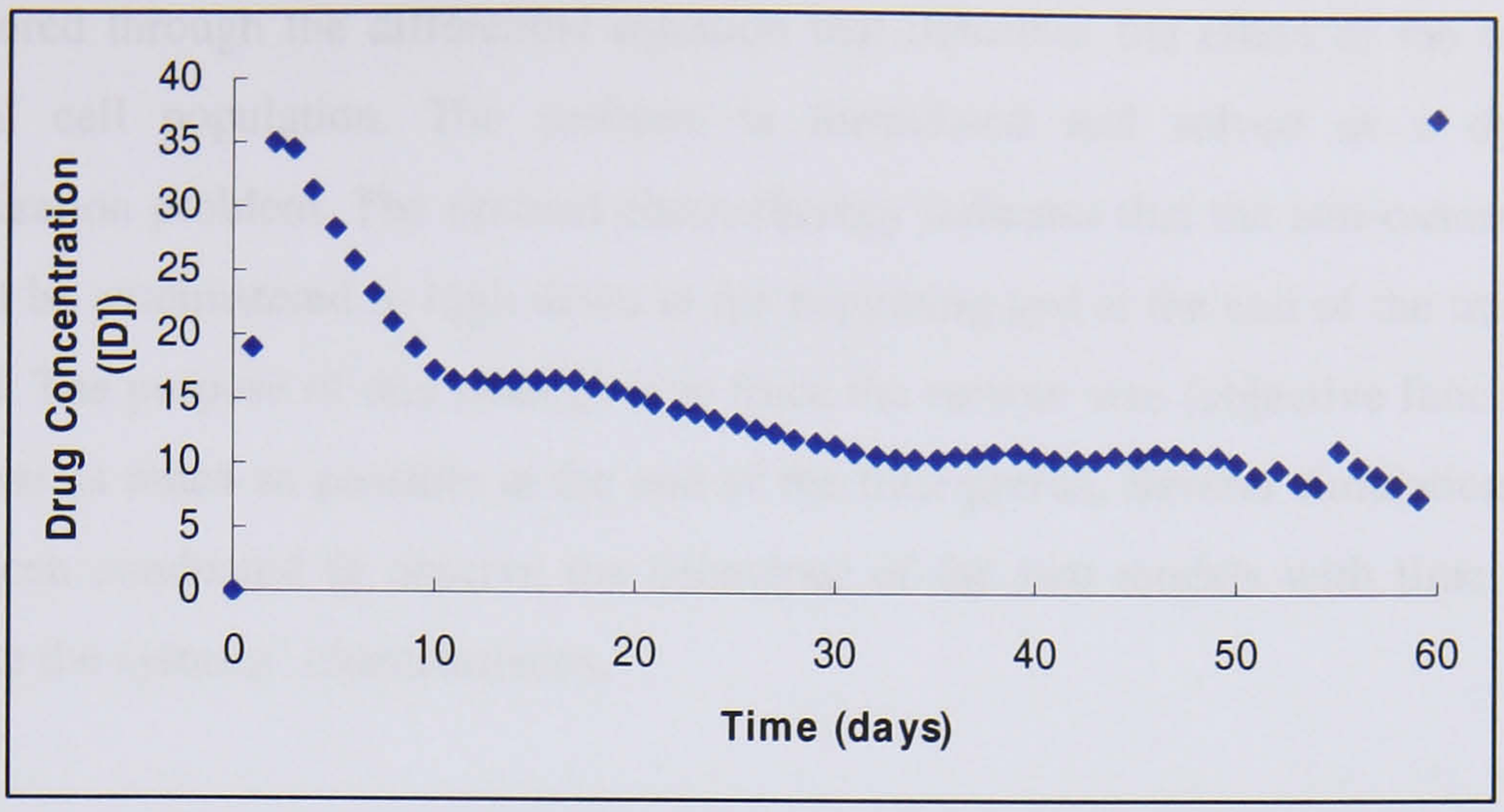


Figure 6.20 Drug concentration profile that corresponds to the optimal treatment protocol

Concluding Remarks

In this chapter two models for the derivation of optimal cancer chemotherapy schedules were considered. The first model involves the use of cell cycle non-specific agents. The tumour is modelled as one compartment and the drug is assumed to affect all the cancer cells in the same way. The Gompertz equation is used for describing tumour growth. The pharmacodynamics and pharmacokinetics are based on clinical data. Toxicity to normal cells is controlled with constraints that limit drug concentration during the therapy, as well as the total cumulative toxicity at the end of the treatment. To avoid drug resistance some additional constraints, called multiple characteristic time constraints, are used that force the tumour to decrease at, or faster than, a given rate. The problem if formulated and solved as a mixed integer dynamic optimization problem. The optimal chemotherapy protocol derived in this case kept the initial administration of the drug at a low level, while most of the drug was delivered towards the end of the therapy.

The second model describes the effects of cell cycle specific drugs. The tumour is divided into two compartments; the proliferating and the quiescent compartment. Tumour growth is modelled with the exponential equation in the case of cancer cells. The logistic function is used to describe the growth of normal tissue. The pharmacodynamics and pharmacokinetics are based on clinical data. Toxicity is

monitored through the differential equation that describes the effect of the drug on normal cell population. The problem is formulated and solved as a dynamic optimization problem. The optimal chemotherapy indicates that the anti-cancer agent should be administered in high doses at the beginning and at the end of the treatment period. The purpose of this strategy is to force the tumour size (objective function) to decrease as much as possible at the end of the time period. Several simulations have also been conducted to observe the behaviour of the two models with time and to analyze the systems' characteristics.

Chapter 7

Conclusions and Future Directions

This thesis presents models and model based control strategies for drug delivery systems. Models incorporating pharmacokinetic and pharmacodynamic aspects of drugs are developed and used for designing model based controllers. Physician's performance criteria, patient compliance, safety in the presence of disturbances and constraints on input and output variables are taken into account. Three drug delivery systems, insulin delivery for type 1 diabetes, surgery under anesthesia and delivery of chemotherapeutic agents in cancer are investigated in detail.

7.1 Summary of Key Contributions

7.1.1 Blood Glucose Control for Type 1 Diabetes

A portable and automatic insulin delivery device can significantly improve the living standard of people with type 1 diabetes. For the first time, an advanced model based parametric controller that can take into account the model of the patient and constraints, on insulin delivery rate and state of the patient, and yet can be implemented on a microchip, has been derived. This microchip can be embedded within a portable device system comprising of an insulin infusion pump and glucose sensor. Some preliminary simulation experiments have been carried out on the microchip. The blood glucose sensor measurement was changed arbitrarily by varying the voltage. An extensive testing of the controller has also been carried out on a pilot plant reactor.

The parametric controller has been derived for a given patient model comprising of three states. A detailed physiology based model with nineteen states has also been analyzed for its dynamic response. This model also provides glucose and insulin

concentrations in various organ compartments of the body. The models describing the glucose-insulin dynamics for people with type 1 diabetes involve a number of parameters that may vary within as well as amongst the patients. A parametric controller has been derived that incorporates inter- and intra-patient variability and keeps the controller feasible for a given meal disturbance while maintaining bounds on insulin infusion rates.

Many important aspects, from a physician's point of view, have also been addressed. In medical practice, hypoglycemia is considered to be more harmful to an individual's health than hyperglycemia. A physician's controller performance criterion therefore places more emphasis on preventing negative deviations from the target glucose concentration value than it does on positive deviations. This issue was addressed in a multi-objective optimization framework by using asymmetric objective function and also by incorporating prioritization of the constraints. The asymmetric objective function approach imposes uneven weights on positive and negative deviations and results in reduced hypoglycemic excursions. The constraint prioritization approach puts higher priority on the satisfaction of constraints on negative deviations than on positive deviation. This results in a mixed integer program where 0-1 binary variables are introduced for modelling the priorities and objectives. This approach does not perform as good as the asymmetric objective function approach but still manages to avoid the dangerous hypoglycemic conditions.

7.1.2 Surgery under Anesthesia

Automation of anesthesia can provide an optimal and safe platform for the delivery of anesthetics for patients being operated under surgery. Model based control strategies are expected to provide significant advances in this field. These controllers rely on a model that can accurately describe the response of the patient to various drug infusion rates.

For the first time in open literature, a new model, which allows for the simultaneous control of the mean arterial pressure (MAP), cardiac output (CO) and the unconsciousness of the patient, has been proposed. It describes the dynamic response of the patient to three drugs, isoflurane, dopamine (DP) and sodium nitroprusside

(SNP). This combination of drugs was chosen for its ability to handle any situation that can occur during surgery. The model consists of three parts, describing the distribution of the drugs, their effect on the outputs and the central nervous system reaction.

A number of simulations were carried out to check the reliability and the accuracy of the model. These simulations validate the pharmacokinetic aspect of the model and the pharmacodynamic aspect was partially validated due to a lack of experimental data on the effect of DP and SNP on MAP. However, the effect of isoflurane on MAP and BIS was validated. The action of DP and SNP was also validated qualitatively. The baroreflex model describes accurately the central nervous system response to changes in MAP.

An objective of this work was to use model based control strategies to derive a control scheme capable of simultaneously regulating the patient's mean arterial pressure, cardiac output and depth of anesthesia (through Bispectral Index) by manipulating the infusion rates of two intravenous agents (Sodium Nitroprusside and Dopamine) and the inlet concentration of an anesthetic agent (Isoflurane) in the breathing mixture. The model was linearized by using gPROMS and the controller was designed by using MATLAB MPC Toolbox. Simultaneous control of all three physiological variables was successfully implemented, where all input and output constraints were satisfied. A simpler, 7 state model that ignores SNP and DP administration was linearized and the parametric controller was derived. The patient state profile for a given input was obtained and compared with that obtained from simulation in gPROMS.

7.1.3 Delivery of Chemotherapeutic Agents in Cancer

An approach for deriving the optimal chemotherapy schedule was developed in chapter 6. The objective is to find a sequence of doses of the drug that will be delivered to the patient and lead to the minimum number of cancer cells at the end of the therapy. Two models from literature are used to simulate the effects of cancer chemotherapy. The choice of the models is primarily based on their use for control purposes. Some simplifying assumptions are made to keep the mathematical

formulation simple and tractable. However, it is important to note that making the system more complex does not necessarily make it more useful. Even with these assumptions the models provide significant information about the behaviour of the system.

The first model involves the use of a cell cycle non-specific drug, while the second one considers the application of a cell cycle specific agent. The two models consider different ways of modelling tumour growth kinetics and toxicity to normal tissue. Both the models are then used for the formulation of optimal control problems and solved using dynamic optimization in gPROMS. The solution of the optimization problem is given by the optimal chemotherapy schedule. The most important results obtained in each of the two cases are listed below.

Cell Cycle non-Specific Model: The optimal chemotherapy protocol derived in this case kept the initial administration of the drug at low level, while most of the drug was delivered towards the end of the therapy.

Cell Cycle Specific Model: The optimal chemotherapy schedule indicates that the anti-cancer agent should be administered in huge doses at the beginning and at the end of the treatment period.

It is important to mention that both models are nonlinear and that the solution is very sensitive to the initial guess of the control variables, which make the problems difficult to solve. Additionally, the cell cycle non-specific optimization model is in fact a mixed integer dynamic optimization problem, due to the presence of binary variables that are treated as control variables.

There are some differences between the two chemotherapy protocols, due to the different use of constraints in each model. For instance, drug resistance is modelled in the first case, by using multiple characteristic time constraints. On the other hand both protocols indicate the application of high intensity therapy towards the end of the treatment, which is consistent with the chemotherapy schedules, reported in the optimal control literature.

7.2 Key Contributions

The contributions of the work presented in this thesis can be summarized as follows:

- An advanced model based parametric controller that can take into account the model of the patient and constraints on insulin delivery rate and state of the patient and yet can be implemented on a microchip has been developed. This is for the first time that an advanced model based parametric controller that can compute the optimal amount of insulin and can be implemented on a microchip has been proposed. This will play an important part in the development of closed loop glucose control system that can be embedded with the glucose sensor and insulin pump.

- A parametric controller has been derived that can incorporate the inter- and intra-patient variability that usually results from factors such as gender, age, weight, change in hormones, stress, illness and activity levels. This issue is addressed by deriving the controller for a population of patients by considering a variation in the model parameters from certain nominal values. The controller remains feasible for the considered patient population and meal disturbance.

- A multi-objective controller that can take into account physician's performance criteria is designed. The key issue here is that negative deviations from a target blood glucose level are more harmful to a patient's health than the positive deviations. This issue is addressed by formulating an asymmetric control objective function and also by incorporating prioritization of constraints in a multi-objective control framework.

- For the first time in open literature, a new model, which allows for the simultaneous control of the mean arterial pressure, cardiac output and the unconsciousness of the patient, has been proposed. The model is based upon the pharmacokinetic and pharmacodynamic aspects of three drugs, sodium nitroprusside, dopamine and isoflurane. A number of dynamic simulations

for various drug infusion rates were carried out for the validation of the model.

- This model for surgery under anesthesia was then used for the derivation of the model based and parametric controllers that can take into account the constraints on the output variables and drug infusion rates.

- Optimal drug delivery schedules have been derived for delivery of chemotherapeutic agents for cancer patients. Two models, cell cycle specific and cell cycle non-specific, are considered and the corresponding dynamic optimization problems are solved. The objective is to minimize the tumour size at the end of the therapy subject to constraints on toxicity and drug resistance. Some very interesting results, suggesting the infusion of large doses of the drugs at the beginning and end of the therapy, are obtained.

- For the first time parametric controllers have been tested on an experimental pilot plant scale reactor set-up. This successful implementation of the parametric controllers via a microchip provides encouragement for the development of portable drug delivery systems and application of parametric controllers to other biological and process systems.

7.3 Recommendations for Future Research Developments

7.3.1 Blood Glucose Control for Diabetes

- Most of the current modelling techniques consider a lumped representation of glucose and insulin transport and dynamics in the body. Development of models from a systems biology perspective at various levels, ranging from cellular, tissue, organ to the whole body, and taking into account various phenomena such as, absorption, transport and binding of insulin, can provide a greater insight into the blood glucose control problem and provide significant improvements in the development of effective therapy. This issue is particularly important for the treatment of type 2 diabetes where although

the body secrets insulin but the cells of the body cannot use it for the absorption of glucose. Development of such detailed, large and complex mathematical models is expected to enhance the understanding of the underlying phenomena, but will result in increased computational complexity, rendering the model based control impractical. For such a case development of model based parametric controllers that although may provide sub-optimal solutions, but give adequate controller performance can be investigated.

- The models should also be able to realistically quantify the effects of disturbances due to exercise and meal. Exercise results in a dynamic state which results in an increasing need of glucose, its production and transport to the muscle tissues of the body. A reduction in plasma insulin and increased glucagon production aim to maintain the blood glucose concentration within the desired levels. Variations in uptake of oxygen, blood flow rate and resistance to transport of insulin and glucose are also usually associated with exercise. These aspects are seldom incorporated within an integrated model for people with diabetes, despite their significant importance in achieving efficient blood glucose control. The models that can accurately address the effects of meal intakes are also lacking and the development of such models is expected to provide a realistic estimate of glucose absorption rate via the gut and hence improve the control of blood glucose concentration via exogenous insulin infusion. Uncontrolled fatty acid catabolism results in a state known as diabetic ketoacidosis. Modelling of metabolism of fatty acids and ketone body is expected to further improve the accuracy and predictability capabilities of the model.

- For the further development of a portable blood glucose control system, a number of future directions can be investigated. Estimation of the states of the patient based upon the current blood glucose concentration can further enhance the controller performance. The parametric controller framework can also be extended to incorporate the time delays in sensor measurement and insulin delivery from the pump.

- Controllers that can also take into account other routes of insulin delivery, such as subcutaneous and pulmonary, can also be developed. Model based control methodologies that can also take into account various insulin preparations, such as short acting or long acting, and a combination of various preparations can significantly improve controller performance.

- Development of blood glucose sensor is an area, which is actively being researched. The key issues here are the noninvasiveness and biocompatibility of the sensor. Here new biomaterials can be designed to increase the life cycle of the sensor.

- The parametric controllers developed in this thesis can be validated and tuned by carrying out extensive clinical trials. The data collected in the clinical trials can also be used for developing detailed models and further understand the variations in the inter- and intra-patient model parameters.

- Design of polymer matrices that release appropriate amounts of insulin, can greatly simplify the process of insulin delivery. Such systems would be sensitive to the surrounding environment and have the capability of estimating the surrounding blood glucose concentration. This estimate would then trigger the polymer matrix to release adequate amount of insulin into the body. Such systems are expected to provide insulin delivery via oral administration and would degrade naturally in the body. Design and development of such systems would require developing new polymeric materials that can release insulin in a precise manner without endangering the life of the patient.

7.3.2 Surgery Under Anesthesia

- A model that allows the simultaneous regulation of MAP, CO and hypnosis during anesthesia has been proposed for the first time in open literature. Some future directions that will further enhance the automation strategies are as follows. The modelled effects of DP and SNP on MAP should be

checked in a clinical setting in order to guarantee the total reliability of the new model. The data collected from extensive clinical trials can then also be used to tune the parameters in the model.

- The control strategies presented in this work should also be tested in a clinical setting for further tuning of the controller parameters and updating the model parameters. This will also provide platform for developing controllers that can take into account variations in the inter- and intra-patient model parameters, similar to that discussed in chapter 3 for delivery of insulin for people with type 1 diabetes. This is particularly important in this case because safety of the patient can be at a greater risk. Multi-objective control described in chapter 4 can also be used for incorporating multiple-objectives and prioritization of constraints for surgery under anesthesia.

- Infusion of multiple drugs provides a more desirable anesthetic state but introduces a significant amount of complexity in the model due to the interaction of drugs. Future work should focus on carrying out clinical trials to elicit information about the detailed drug interactions and their incorporation in the models. These developments can also be used for the design of new anesthetic drugs.

- The models for delivery of anesthesia are quite complex and nonlinear. Design of model based nonlinear controllers for this purpose can be investigated and its performance can be compared with linear controllers.

- Another major challenge for the automation of anesthesia is the development of sensors that can adequately measure the activity of brain. Here the key issues are the location and the non-invasiveness of the sensors.

- During anesthesia, a patient goes through a number of stages. An advisory system for the anesthesiologist that provides them with the expected state trajectory of the patient and effects of various drug dosages at different times can be extremely beneficial. Such a system can significantly simplify the task of the anesthesiologist and improve the safety of the patients. Such

a system should be user friendly and should also have a graphical user interface. This system can also be used for the training purposes of new anesthesiologists.

7.3.3 Delivery of Chemotherapeutic Agents in Cancer

- A number of future directions can be explored for developing better chemotherapy schedules. The solution procedure used in this work is not based upon global optimization; instead it can be regarded to provide one of the possible local optimum solutions. Future work can explore using global optimization techniques for the derivation of the chemotherapy schedule.

- An effort should also be devoted to developing models that consider the used of multiple drugs, especially killing and blocking agents. An important issue that should be addressed is the case where the parameters in the model can vary with time, especially at high levels of the drug dosage. Models that are built specifically for particular types of cancer, i.e. breast, blood etc., and also take into account the cause of the cancer, such as smoking, can provide a much more detailed understanding of the system and aid in developing better cures for the disease.

- Instead of optimizing drug delivery for a fixed period of treatment, the case of optimizing the period of treatment can also be investigated. A model predictive control approach for cancer chemotherapy scheduling can also be used to update the schedule after each treatment, based upon the updated state of the patient.

7.3.4 Other Drug Delivery Systems

- The developments reported in this thesis can also be applied to other drug delivery and biomedical systems such as dialysis. While advanced modelling and control techniques are essential for automation, such systems should be validated and tested on human and animal subjects. This is quite

expensive and may involve situations which may endanger the life of the subjects. A systems approach for the design of experiments can reduce the cost and help elicit maximum information with minimum number of clinical trials.

Publications from this Thesis

Journal Publications

1. P. Dua and E. N. Pistikopoulos, Modelling and Control of Drug Delivery Systems, *Computers and Chemical Engineering, in press (available online: 14th July)*, 2005.
2. P. Dua, F. J. Doyle III and E. N. Pistikopoulos, Model Based Blood Glucose Control for Type 1 Diabetics via Parametric Programming, *submitted to IEEE Transactions on Biomedical Engineering*.
3. P. Dua, F. J. Doyle III and E. N. Pistikopoulos, Multi-objective Blood Glucose Control for Type 1 Diabetes, *submitted to Journal of Process Control.*
4. P. Dua, V. Dua and E. N. Pistikopoulos, Model Based and Parametric Control of Drug Delivery Systems, *in preparation.*
5. P. Dua, V. Dua and E. N. Pistikopoulos, Model Based and Parametric Control for Anesthesia, *in preparation.*
6. P. Dua, V. Sakizlis, L. S. Kershenbaum and E. N. Pistikopoulos, Parametric Controller for the Operation of a Partially Simulated Exothermic Reactor, *in preparation.*

Conference Papers

1. P. Dua, V. Sakizlis, V. Dua, F. J. Doyle III and E. N. Pistikopoulos, Model Based Control for Insulin Delivery for Type 1 Diabetics via Parametric Programming, *Proceedings of the European Symposium on Computer Aided Process Engineering, Lisbon,* 2004, 1045-1050.
2. P. Dua, V. Sakizlis, L. S. Kershenbaum and E. N. Pistikopoulos, Model Based Parametric Controller for the Operation of an Exothermic Reactor, *Proceedings of the European Symposium on Computer Aided Process Engineering, Lisbon,* 2004, 637-642.
3. P. Dua, V. Dua and E. N. Pistikopoulos, Model Based Control for Drug Delivery Systems, *Proceedings of the IASTED International Conference Biomedical Engineering, Innsbruck*, 2005, 691-696.

4. P. Dua and E.N. Pistikopoulos, Modelling and Control of Drug Delivery Systems, *Proceedings of Symposium on Modelling of Complex Processes, Texas,* 2005.
5. P. Dua, V. Dua and E. N. Pistikopoulos, Model Based Parametric Control in Anesthesia, *Proceedings of the European Symposium on Computer Aided Process Engineering, Barcelona*, 2005, 1015-1020.
6. P. Dua, V. Dua and E. N. Pistikopoulos, Model Based Drug Delivery for Anesthesia, *Proceedings of the 16th IFAC World Congress, Prague*, 2005.
7. P. Dua, V. Dua and E. N. Pistikopoulos, Modelling and Parametric Control of Drug Delivery Systems, *Proceedings of the 7th World Congress of Chemical Engineering, Glasgow,* 2005.
8. P. Dua, V. Dua and E. N. Pistikopoulos, Modelling Of Surgery Under Anesthesia, *Proceedings of the Foundations of Systems Biology in Engineering, Santa Barbara,* 2005, 169-172.
9. E. N. Pistikopoulos and P. Dua, Parametric Programming and Control, *Proceedings of the PSE ASIA 2005: The 3rd International Symposium on Design, Operation and Control of Chemical Processes,* 2005, 3-22.
10. P. Dua, F. J. Doyle III and E. N. Pistikopoulos, Multi-Objective Parametric Control of Blood Glucose Concentration for Type 1 Diabetes, accepted for publication in the *Proceedings of the 44th IEEE Conference on Decision and Control and European Control Conference ECC 2005, Seville.*

List of Abstracts

1. P. Dua, V. Dua and E. N. Pistikopoulos, Optimal Control of Cancer by Delivery of Chemotherapeutic Agents, to be presented at the *AIChE Annual Meeting, Cincinnati,* 2005.
2. P. Dua, V. Dua and E. N. Pistikopoulos, Model Based Automation in Anesthesia, *Advanced Modelling and Control in Anesthesia, Monte Verita, 2005.*
3. P. Dua, V. Dua and E. N. Pistikopoulos, Advanced Model Based Control Technology for Better Healthcare, *Set for Britain, House of Commons, London, 2005.*

4. P. Dua, V. Dua and E. N. Pistikopoulos, Applications of Parametric Model Based Control, *Indian Chemical Engineering Congress CHEMCON 2004, Mumbai.*
5. P. Dua, F. J. Doyle III and E. N. Pistikopoulos, Multi-objective Model Based Parametric Control of Blood Glucose Concentration in Type 1 Diabetics, *AIChE Annual Meeting, Austin,* 2004.
6. P. Dua, F. J. Doyle III and E. N. Pistikopoulos, Multi-objective Parametric Control of Blood Glucose Concentration in Type 1 Diabetics, *Diabetes Technology and Therapeutics, 7,* 374, 2005.
7. P. Dua and E. N. Pistikopoulos, Automation of Drug Delivery Systems, *Set for Britain, House of Commons, London*, 2004.
8. P. Dua, V. Sakizlis, V. Dua, F. J. Doyle III and E. N. Pistikopoulos, Robust Model Based Control of Blood Glucose in Type 1 Diabetic Patients under Meal Disturbances, *AIChE Annual Meeting, San Francisco*, 2003.
9. P. Dua, V. Sakizlis, V. Dua, F. J. Doyle III and E. N. Pistikopoulos, Explicit Robust Model Based Glucose Control under Meal Disturbances for Type 1 Diabetic Patients, *Diabetes Technology and Therapeutics, 6,* 239, 2004.
10. P. Dua, V. Sakizlis, V. Dua, F. J. Doyle III and E. N. Pistikopoulos, Explicit Model Based Control of Blood Glucose in Type I Diabetic Patients via Parametric Programming, *AIChE Annual Meeting, Indianapolis*, 2002.
11. P. Dua, V. Sakizlis, V. Dua, F. J. Doyle III and E. N. Pistikopoulos, Control and Automation for the Regulation of Blood Glucose in Type I Diabetic Patients via Parametric Programming, *Diabetes Technology and Therapeutics, 5,* 266, 2003.

Other Publications

1. P. Panjwani, M. Schenk, M. C. Georgiadis and E. N. Pistikopoulos, Optimal design and control of a reactive distillation system, *Engineering Optimization, in press.*
2. P. Panjwani, M. Schenk, M. C. Georgiadis and E. N. Pistikopoulos, Process design and control of a reactive distillation system, *Proceedings of Dynamics and Control of Process Systems, Cambridge,* 2004.

References

Abbod, M. F., and Linkens, D. A. (1998). Anesthesia simulator: intelligent monitoring and control of depth of anesthesia. *IEE Colloquium on Simulation in Medicine*, 4/1-4/5.

Acevedo, J., and Pistikopoulos, E. N. (1996). A parametric MINLP algorithm for process synthesis problems under uncertainty. *Industrial and Engineering Chemistry Research*, *35*, 147-158.

Acevedo, J., and Pistikopoulos, E. N. (1997). A multiparametric programming approach for linear process engineering problems under uncertainty. *Industrial and Engineering Chemistry Research*, *36*, 717-728.

Acevedo, J., and Salgueiro, M. (2003). An efficient algorithm for convex multiparametric nonlinear programming problems. *Industrial and Engineering Chemistry Research*, *42*, 5883-5890.

Ackerman, E. Gatewood, L. C., Rosevear, J. W., and Molnar, G. D. (1965). Model studies of blood glucose regulation. *Bulletin of Mathematical Biophysics*, *27 (Suppl.)*, 21-37.

Bajzer, Z., Marusic, M., and Vuk-Pavlovic, S. (1996). Conceptual frameworks for mathematical modelling of tumour growth dynamics. *Mathematical and Computer Modelling*, *23*, 31-46.

Banerjee, I., and Ierapetritou, M. G. (2003). Parametric process synthesis for general nonlinear models. *Computers and Chemical Engineering*, *27*, 1499-1512.

Bansal, V., Perkins, J. D., and Pistikopoulos, E. N. (2000). Flexibility analysis and design of linear systems by parametric programming. *AIChE Journal*, *46*, 335-354.

Bansal, V., Sakizlis, V., Ross, R., Perkins, J. D., and Pistikopoulos, E. N. (2003). New algorithms for mixed integer dynamic optimization. *Computers and Chemical Engineering*, *27*, 647-668.

Barbolosi, D., and Iliadis, A. (2001). Optimizing drug regimens in cancer chemotherapy. *Computers in Biology and Medicine*, *31*, 157-172.

Behbehani, K., and Cross, R. R. (1991). A controller for regulation for mean arterial pressure using sodium optimum nitroprusside infusion rate. *IEEE Transactions on Biomedical Engineering*, *38*, 513-521.

Bellazi, R., Nucci, G., and Cobelli, C. (2001). The subcutaneous route to insulin-dependent diabetes therapy. *IEEE Engineering in Medicine and Biology*, *20*, 54-64.

Bemporad, A., Morari, M., Dua, V., and Pistikopoulos, E. N. (2002). The explicit linear quadratic regulator for constrained systems. *Automatica*, *38*, 3-20.

Benson, H. P. (1982). Algorithms for parametric nonconvex programs. *Journal of Optimization Theory and Applications*, *38*, 319-334.

Bergman, R. N., Philips, L. S., and Cobelli, C. (1981). Physiologic evaluation of factors controlling glucose tolerance in man: Measurement of insulin sensitivity and β-cell glucose sensitivity from the response to intravenous glucose. *The Journal of Clinical Investigation*, *68*, 1456-1467.

Bolie, V. W. (1961). Coefficients of normal blood glucose regulation. *Journal of Applied Physiology*, *16*, 783-788.

Boroujerdi, M. A., Umpleby, A. M., Jones, R. H., and Sonksen, P. H. (1995). A simulation model for glucose kinetics and estimates of glucose utilization rate in type 1 diabetic patients. *American Journal of Physiology*, *268*, E766-E774.

Chrysafi, S. (2004). Model-based and parametric control of anesthesia. *MSc Thesis, Imperial College London.*

Clemens, A. H. (1979). Feedback control dynamics for glucose controlled insulin infusion system. *Medical Progress through Technology*, *6*, 91-98.

Cobelli, C., Federspil, G., Pacini, G., Salvan, A., and Scandellari, C. (1982). An integrated mathematical model of the dynamics of blood glucose and its hormonal control. *Mathematical Biosciences*, *58*, 27-60.

Cobelli, C., Toffolo, G., and Ferrannini, E. (1984). A model of glucose kinetics and their control by insulin: compartmental and noncompartmental approaches. *Mathematical Biosciences*, *72*, 291-315.

Costa, M. I. S., Boldrini, J. L., and Bassanezi, R. C. (1994). Optimal chemotherapy: a case study with drug resistance, saturation effect and toxicity. *IMA Journal of Mathematics in Applied Medicine*, *11*, 45-59.

Costa, M. I. S., Boldrini, J. L., and Bassanezi, R. C. (1995). Drug kinetics and drug resistance in optimal chemotherapy. *Mathematical Biosciences*, *125*, 191-209.

Dalla Man, C., Caumo, A., Basu, R., Rizza, R., Toffolo, G., and Cobelli, C. (2004). Minimal model estimation of glucose absorption and insulin sensitivity from oral test: validation with a tracer method. *American Journal of Physiology*, *287*, E637-E643.

Damming D., and Patel, J. H. (2004). A novel parametric closed loop glucose control system. *Final Year Undergraduate Project Report, Department of Chemical Engineering, Imperial College London.*

DCCT- The Diabetes Control and Complications Trial Research Group (1993). The effect of intensive treatment of diabetes on the development and progression of long-term complications in insulin-dependent diabetes mellitus. *The New England Journal of Medicine*, *329*, 977-986.

Derighetti, M. P. (1999). Feedback control in anaesthesia. *PhD Thesis, Swiss Federal Institute of Technology (ETH), Zurich, Switzerland.*

Derighetti, M., Frei, C. W., Buob, M., Zbinden, A. M., and Schnider, T. W. (1997). Modelling the effect of surgical stimulation on mean arterial blood pressure. *Proceedings of the 19th International Conference IEEE/EMBS*, 2172-2175.

Doyle III, F. J., Dorski, C., Harting, J. E., and Peppas, N. A. (1995). Control and modeling of drug delivery devices for the treatment of diabetes. *Proceedings of the American Control Conference, Seattle*, 776-780.

Dua, V., and Pistikopoulos, E. N. (1998). Optimization techniques for process synthesis and material design under uncertainty. *Transactions of Institute of Chemical Engineers*, *76*, 408-416.

Dua, V., and Pistikopoulos, E. N. (1999). Algorithms for the solution of multiparametric mixed-integer nonlinear optimization problems. *Industrial and Engineering Chemistry Research*, *38*, 3976-3987.

Dua, V., and Pistikopoulos, E. N. (2000). An algorithm for the solution of multiparametric mixed integer linear programming problems. *Annals of Operations Research*, *99*, 123-129.

Dua, V., Bozinis, N. A., and Pistikopoulos, E. N. (2002). A multiparametric programming approach for mixed-integer quadratic engineering problems. *Computers and Chemical Engineering*, *26*, 715-733.

Dua, V., Papalexandri, K. A., and Pistikopoulos, E. N. (2004). Global optimization issues in multiparametric continuous and mixed-integer optimization problems. *Journal of Global Optimization*, *30*, 59-89.

Fiacco, A. V. (1983). *Introduction to sensitivity and stability analysis in non-linear programming*. Academic Press, New York.

Fisher, M. E. (1991). A semiclosed loop algorithm for the control of blood glucose levels in diabetics. *IEEE Transactions on Biomedical Engineering*, *38*, 57-61.

Fisher, M. E., and Teo, K. L. (1989). Optimal insulin infusion resulting from a mathematical model of blood glucose dynamics. *IEEE Transactions on Biomedical Engineering*, *36*, 479-486.

Frei, C. W., Derighetti, M., and Zbinden, A. M. (1997). Modelling for control of mean arterial blood pressure (MAP) during anesthesia. *Proceedings of the 2nd International Symposium on Mathematical Modelling (MATHMOD), Vienna*, 395-400.

Frei, C. W., Gentilini, A., Derighetti, M., Glattfelder, A. H., Morari, M., Schnider, T. W., and Zbinden, A. M. (1999). Automation in anesthesia. *Proceedings of the American Control Conference, San Diego*, 1258-1263.

Frei, C. W. (2000). Fault tolerant control concepts applied to anesthesia. *PhD Thesis, Swiss Federal Institute of Technology (ETH), Zurich, Switzerland.*

Furler, S. M., Kraegen, E. W., Smallwood, R. H., and Chisholm, D. J. (1985). Blood glucose control by intermittent loop closure in the basal model: computer simulation studies with a diabetic model. *Diabetes Care*, *8*, 553-561.

Gal, T. (1995). *Postoptimal Analyses, Parametric Programming and Related Topics.* 2nd Edition, Walter de Gruyter, New York.

Garcia, C. E., Prett, D. M., and Morari, M. (1989). Model predictive control: theory and practice – a survey. *Automatica*, *25*, 335-348.

Gentilini, A. (2001). Feedback control of hypnosis and analgesia in humans. *PhD Thesis, Swiss Federal Institute of Technology (ETH), Zurich, Switzerland.*

Gentilini, A., Frei, C. W., Glattfelder, A. H., Morari, M., Sieber, T. J., Wymann, R., Schnider, T. W., and Zbinden, A. M. (2001). Multiasked closed-loop control in anesthesia. *IEEE Engineering in Medicine and Biology*, *20*, 39-53.

Gentilini, A., Schaniel, C., Morari, M. Bieniok, C., Wymann, R., and Schnider, T. (2002). A new paradigm for the closed-loop intraoperative administration of analgesics in humans. *IEEE Transactions on Biomedical Engineering*, *49*, 289-299.

Gopinath, R., Bequette, B. W., Roy, R. J., and Kaufman, H. (1995). Issues in the design of a multirate model-based controller for a nonlinear drug infusion system. *Biotechnology Progress*, *11*, 318-332.

gPROMS (2003). Introductory user's guide, Release 2.2. *Process Systems Enterprise Limited, London, UK.*

Grossmann, I. E., and Floudas, C. A. (1987). Active constraint strategy for flexibility analysis in chemical processes. *Computers and Chemical Engineering*, *11*, 675-693.

Guyton, J. R., Foster, R. O., Soeldner, J. S., Tan, M. H., Kahn, C. B., Koncz, L., and Gleason, R. E. (1978). A model of glucose-insulin homeostasis in man that incorporates the heterogeneous fast pool theory of pancreatic insulin release. *Diabetes*, *27*, 1027-1042.

Held, C. M., and Roy, R. J. (1995). Multiple drug hemodynamic control by means of a supervisory-fuzzy rule-based adaptive control system: validation on a model. *IEEE Transactions on Biomedical Engineering*, *42*, 371-385.

Heller, A. (2005). Integrated medical feedback systems for drug delivery. *AIChE Journal*, *51*, 1054-1066.

Hernjak. N. (2004). Control-relevant process nonlinearity characterization. *PhD Thesis, University of Delaware, Delaware, USA.*

Hernjak, N., and Doyle III, F. J. (2005). Glucose control design using nonlinearity assessment techniques. *AIChE Journal*, *51*, 544-554.

Holford, N. H. G., and Benet, L. Z. (1998). *Pharmacokinetics & Pharmacodynamics: Dose Selection & the Time Course of Drug Action*. In Basic & Clinical Pharmacology, 7th Edition, Editor: B. G. Katzung, Appleton and Lange, Stamford, Connecticut.

Hovorka, R., Canonico, V., Chassin, L. J., Haueter, U., Massi-Benedetti, M., Federici, M., Pieber, T. R., Schaller, H. C., Schaupp, L., Vering, T., and Wilinska, M. E. (2004). Nonlinear model predictive control of glucose concentration in subjects with type 1 diabetes. *Physiological Measurement*, *25*, 905-920.

Hussain, M. A., and Kershenbaum, L. S. (2000). Implementation of an inverse model-based control strategy using neural networks on a partially simulated exothermic reactor. *Transactions of Institution of Chemical Engineers*, *78*, 299-311.

Iliadis, A., and Barbolosi, D. (2000). Optimizing drug regimens in cancer chemotherapy by an efficacy-toxicity mathematical model. *Computers and Biomedical Research*, *33*, 211-226.

Isaka, S., and Sebald, A.V. (1993). Control strategies for arterial blood pressure regulation. *IEEE Transactions on Biomedical Engineering*, *40*, 353-363.

Jaremko, J., and Rorstad, O. (1998). Advances towards the implantable artificial pancreas for treatment of diabetes. *Diabetes Care*, *21*, 444-450.

Jetha, A., and Lawal, J. (2003). Compartmental modelling for type 1 diabetes. *Final Year Undergraduate Project Report, Department of Chemical Engineering, Imperial College London.*

Kennedy, F. P. (1991). Recent developments in insulin delivery techniques: current status and future potential. *Drugs*, *42*, 213-227.

Kershenbaum, L. S. (2000). Experimental testing of advanced algorithms for process control: when it is worth the effort? *Transactions of Institution of Chemical Engineers*, *78*, 509-521.

Kienitz, K. H., and Yoneyama, T. (1993). A robust controller for insulin pumps based on H-infinity theory. *IEEE Transactions on Biomedical Engineering*, *40*, 1133-1137.

Kimmel, M., and Swierniak, A. (2003). Using control theory to make cancer chemotherapy beneficial from phase dependence and resistant to drug resistance.

Kittisupakorn, P. (1995). The use of nonlinear model predictive control techniques for the control of a reactor with exothermic reactions. *PhD Thesis, Imperial College London, London, UK.*

Kozusko, F., Chen, P. H., Grant, S. G., Day, B. W., and Panetta, J. C. (2001). A mathematical model of in vitro cell growth and treatment with the antimitotic agent Curacin A. *Mathematical Biosciences*, *170*, 1-16.

Ledzewicz, U., and Schattler, H. (2000). Optimal control for a mathematical model of cancer chemotherapy. *Proceedings of the IASTED International Conference: Control and Applications, Cancun, Mexico,* 8-14.

Lehmann, E. D., and Deutsch, T. (1992). A physiological model of glucose-insulin interaction in type 1 diabetes mellitus. *Journal of Biomedical Engineering*, *14*, 235-242.

Linkens, D. A., and Mahfouf, M. (1994). Generalized predictive control (GPC) with prespecified set-points in clinical anesthesia. *Proceedings of the 3rd IEEE conference on control applications,* 3, 1669-1674.

Lynch, S. M., and Bequette, B. W. (2001). Estimation-based model predictive control of blood glucose in type I diabetics: a simulation study. *Proceedings of the IEEE 27th Annual Northeast Bioengineering Conference,* 79-80.

Lynch, S. M., and Bequette, B. W. (2002). Model predictive control of blood glucose in type I diabetic patients. *Proceedings of the American Control Conference, Anchorage*, *5*, 4039-4043.

Mahfouf, M., Asbury, A. J., and Linkens, D. A. (2003). Unconstrained and constrained generalized predictive control of depth of anaesthesia during surgery. *Control Engineering Practice*, *11*, 1501-1515.

Mansour, N. E., and Linkens, D. A. (1989). Pole-assignment self-tuning control in postoperative patients: a simulation study. *IEE Proceedings: Control Theory and Applications*, *136*, 1-11.

Martin, R. B. (1992). Optimal control drug scheduling of cancer chemotherapy. *Automatica*, *28*, 1113-1123.

Martin, R. B., and Teo, K. L. (1992). A worst case optimal parameter selection model of cancer chemotherapy. *IEEE Transactions on Biomedical Engineerring*, *39*, 1081-1085.

MATLAB (1998). Model Predictive Control Toolbox, User's Guide.

Mortier, E., Struys, M., De Smet, T., Versichelen, L., and Rolly, G. (1998). Closed-loop controlled administration of propofol using bispectral analysis. *Anaesthesia*, *53*, 749-754.

Muller, A. P. (2003). Model-based drug delivery system for the regulation of anaesthesia. *MSc Thesis, Imperial College London.*

Nalecz, M., Wojciki, J., and Zawicki, I. (1987). Control in Artificial Pancreas. *IFAC Control Aspects of Biomedical Engineering*, 123-127.

Nucci, G., and Cobelli, C. (2000). Models of subcutaneous insulin kinetics: A critical review. *Computer Methods and Programs in Biomedicine*, *62*, 249-257.

Ohtake, Y., and Nishida, N. (1985). A branch and bound algorithm for 0-1 parametric mixed integer programming. *Operations Research Letters*, *4*, 41-45.

Ollerton, R. L. (1989). Application of optimal control theory to diabetes mellitus. *International Journal of Control*, *50*, 2503-2522.

Pacini, G., and Cobelli, C. (1990). Estimation of β-cell secretion and insulin hepatic extraction by the minimal modelling technique. *Computer Methods and Programs in Biomedicine*, *32*, 241-248.

Panetta, J. C. (1997). A mathematical model of breast and ovarian cancer treated with paclitaxel. *Mathematical Biosciences*, *146*, 89-113.

Panetta, J. C., and Adam, J. (1995). A mathematical model of cycle-specific chemotherapy. *Mathematical and Computer Modelling*, *22*, 67-82.

Papageorgiou, A. (2004). Model-based control of cancer chemotherapy. *MSc Thesis, Imperial College London.*

Papalexandri, K. A., and Dimkou, T. (1998). A parametric mixed integer optimization algorithm for multi-objective engineering problems involving discrete decisions. *Industrial and Engineering Chemistry Research*, *37*, 1866-1882.

Parker, R. S. (1999). Model-based analysis and control for biosystems. *PhD Thesis, University of Delaware, Delaware, USA.*

Parker, R. S., and Doyle III, F. J. (1999). A model-based algorithm for blood glucose control in type I diabetic patients. *IEEE Transactions on Biomedical Engineering*, *46*, 148-157.

Parker, R. S., Doyle III, F. J., Ward, J. H., and Peppas, N. A. (2000). Robust H_∞ glucose control in diabetes using a physiological model. *AIChE Journal*, *46*, 2537-2549.

Parker, R. S., Gatzke, E. P., and Doyle III, F. J. (2000b). Advanced model predictive control (MPC) for type I diabetic patient blood glucose control. *Proceedings of the American Control Conference, Chicago,5,* 3483-3487.

Parker, R. S., Doyle III, F. J., and Peppas, N. A. (2001a). The intravenous rotue to blood glucose control. *IEEE Engineering in Medicine and Biology*, *20*, 65-73.

Parker, R. S., and Doyle III, F. J. (2001b). Control-relevant modeling in drug delivery. *Advanced Drug Delivery Reviews*, *48*, 211-228.

Pereira, F. L., Pedreira, C. E., Pinho, M. R., Fernandes, M. H., and Sousa, J. B. (1990). An optimal control algorithm for multidrug cancer chemotherapy design. *Proceedings of the 12th Annual International Conference of the IEEE Engineering in Medicine and Biology Society*, *12*, 1021-1022.

Pertsinidis, A. (1992). On the parametric optimization of mathematical programs with binary variables and its application in the chemical engineering process synthesis. *PhD Thesis, Carnegie Mellon University, Pittsburgh, USA.*

Pickup, J., McCartney, L., Rolinski, O., and Birch, D. (1999). In-vivo glucose sensing for diabetes management: progress towards non-invasive monitoring. *British Medical Journal*, *319*, 1-4.

Pillai, O., and Panchagnula, R. (2001). Insulin therapies – past, present and future. *Drug Discovery Today*, *6*, 1056-1061.

Pinheiro, C. I. C., and Kershenbaum, L. S. (1999). Model predictive control of reactor temperature in a CSTR pilot plant operating at an unstable steady-state. *Computers and Chemical Engineering*, S859-S862.

Pistikopoulos, E. N., and Dua, V. (1998). Planning under uncertainty: a parametric optimization approach. *Proceedings of 3rd International Conference on Foundations of Computer-Aided Process Operations,* Editors: J. F. Pekny and G. E. Blau, 164-169.

Pistikopoulos, E. N., Dua, V., Bozinis, N. A., Bemporad, A., and Morari, M. (2002). On-line optimization via off-line parametric optimization tools. *Computers and Chemical Engineering*, *26*, 175-185.

Puckett, W. R., and Lightfoot, E. N. (1995). A model for multiple subcutaneous insulin injections developed from individual diabetic patient data. *American Journal of Physiology*, *269*, E1115-E1124.

Rao, R., Palerm, C., Aufderheide, B., and Bequette, B. W. (2001). Automated regulation of hemodynamic variables. *IEEE Engineering in Medicine and Biology*, *20*, 24-38.

Rao, R., Aufderheide, B., and Bequette, B. W. (2003). Experimental studies on multiple-model predictive control for automated regulation of hemodynamic variables. *IEEE Transactions on Biomedical Engineering*, *50*, 277-288.

Sakizlis, V. (2003). Design of model based controllers via parametric programming. *PhD Thesis, Imperial College London, London, UK.*

Sakizlis, V., Kakalis, N. M. P., Dua, V., Perkins, J. D. and Pistikopoulos, E. N. (2004). Design of robust model-based controllers via parametric programming. *Automatica, 40,* 189-201.

Saltzman, W. M. (2001). *Drug Delivery: Engineering Principles for Drug Therapy.* Oxford University Press

Salzsieder, E., Albrecht, G., Fischer, U., Rutscher, A. and Thierebach, U. (1990). Computer-aided systems in the management of type I diabetes: the application of a model-based strategy. *Computer Methods and Programs in Biomedicine, 32,* 215-224.

Selam, J. L., and Charles, M. A. (1990). Devices for insulin administration. *Diabetes Care, 13,* 955-979.

Simpson, P. J., and Popat, M. (2002). *Understanding Anaesthesia,* 4th Edition, Butterworth-Heinemann, Oxford.

Slate, J. B., Sheppard, L. C., Rideout, V. C., and Blackstone, E. H. (1979). A model for design of a blood pressure controller for hypertensive patients. *Proceedings of the IEEE Engineering in Medicine and Biology Conference, Denver,* 867-872.

Sorensen, J. T. (1985). A physiologic model of glucose metabolism in man and its use to design and assess improved insulin therapies for diabetes. *PhD Thesis, Massachusetts Institute of Technology (MIT), Cambridge, USA.*

Stadler, K. S. (2003). Modelling and control in anaesthesia – from design to validation. *PhD Thesis, Swiss Federal Institute of Technology (ETH), Zurich, Switzerland.*

Swan, G. W. (1982). An optimal control model of diabetes mellitus. *Bulletin of Mathematical Biology*, *44*, 793-808.

Swan, G. W. (1987). Tumour growth models and cancer chemotherapy. In: *Cancer Modelling. Eds: J. Thompson and B. Brown*, *83*, 91-179.

Swierniak, A., Ledzewicz, U., and Schattler, U. (2003). Optimal control for a class of compartmental models in cancer chemotherapy. *Applied Mathematics and Computer Science*, *13*, 357-368.

Thomaseth, K. (2003). Multidisciplinary modelling of biomedical systems. *Computer Methods and Programs in Biomedicine*, *71*, 189-201.

Tiran, J., Avruch, L. I., and Albisser, A. M. (1979). A circulation and organs model for insulin dynamics. *American Journal of Physiology*, *237*, E331-E339.

Trajanoski, Z., Regittnig, W., and Wach, P. (1998). Simulation studies on neural predictive control of glucose using the subcutaneous route. *Computer Methods and Programs in Biomedicine*, *56*, 133-139.

Tucker, G. T. (1990). Pharmacokinetic and pharmacodynamic models. *Advances in Pain Research and Therapy*, *14*, 181-201.

Tyler, M. L., and Morari, M. (1999). Propositional logic in control and monitoring problems. *Automatica*, *35*, 565-582.

Wada, D. R., and Ward, D. S. (1995). Open loop control of multiple drug effects in anesthesia. *IEEE Transactions on Biomedical Engineering*, *42*, 666-677.

Yasuda, N., Targ, A.G., and Eger, E.I. (1989). Solubility of I-653, Sevoflurane, isoflurane and halothane in human tissues. *Anesthesia and analgesia*, *69*, 370-373.

Yasuda, N., Lockhart, S.H., Eger, E.I., Weiskopf, R.B., Laster, M., Taheri, S., and Peterson, N.A. (1991a). Comparison of kinetics of sevoflurane and isoflurane in humans. *Anesthesia and analgesia*, *72*, 316-324.

Yasuda, N., Lockhart, S.H., Eger, E. I., Weiskopf, R.B., Johnson, B.H., Freire, B.A., and Fassoulaki, A. (1991b). Kinetics of desflurane, isoflurane and halothane in humans. *Anesthesiology*, *74*, 489-498.

Yu, C., Roy, R. J., and Kaufman, H. (1990). A circulatory model for combined nitroprusside-dopamine therapy in acute heart failure. *Medical Progress through Technology*, *16*, 77-88.

Yu, C., Roy, R. J., Kaufman, H., and Bequette, B. W. (1992). Multiple-model adaptive predictive control of mean arterial pressure and cardiac output. *IEEE Transactions on Biomedical Engineering*, *39*, 765-778.

Zhang, X. S., Roy, R., and Huang, J. W. (1998). Closed-loop system for total intravenous anesthesia by simultaneously administering two anesthetic drugs. *Proceedings of the 20th conference of the IEEE Engineering in Medicine and Biology Society*, *20*,

Zwart, A., Smith, N. T., and Beneken, J. E. W. (1972). Multiple model approach to uptake and distribution of halothane: the use of an analog computer. *Computers and Biomedical Research*, *5*, 228-238.

Appendix A

Closed Loop Blood Glucose Control

A closed-loop glucose control system based on the parametric controller derived in Chapter 3 was developed. The parametric control algorithm was transferred onto a chip and the controller performance was tested with a simulation experiment. This work provides a step towards carrying out the clinical trials for testing the parametric controller for the regulation of the blood glucose concentration.

A.1 Introduction

For people with type 1 diabetes, the aim of a closed loop parametric glucose control system is to maintain the blood glucose concentration within the desired range by continuously taking blood glucose measurements and regularly infusing the optimal amount of insulin. This appendix presents a step towards the implementation of such a controller. A vision of the closed loop system is given in Figure A.1: a sensor continuously measures the blood glucose concentration that is transmitted to the chip which computes the optimal infusion rate and drives the mechanical pump to infuse insulin. The rest of this appendix is organized as follows: Section A.2 presents a review of the currently available insulin pumps and the developments in the field of glucose sensors are given in section A.3. The details of the implementation of the parametric controller are provided in section A.4 and section A.5 reports the performance of the controller.

A.2 Insulin Pumps

An insulin pump is a device shaped and sized like a pager, which incorporates an insulin reservoir (or cartridge). The pump is connected via a long, thin tube to a

subcutaneous infusion set which consists of either a small needle or a cannula which is inserted under the skin and taped down to prevent dislodgement.

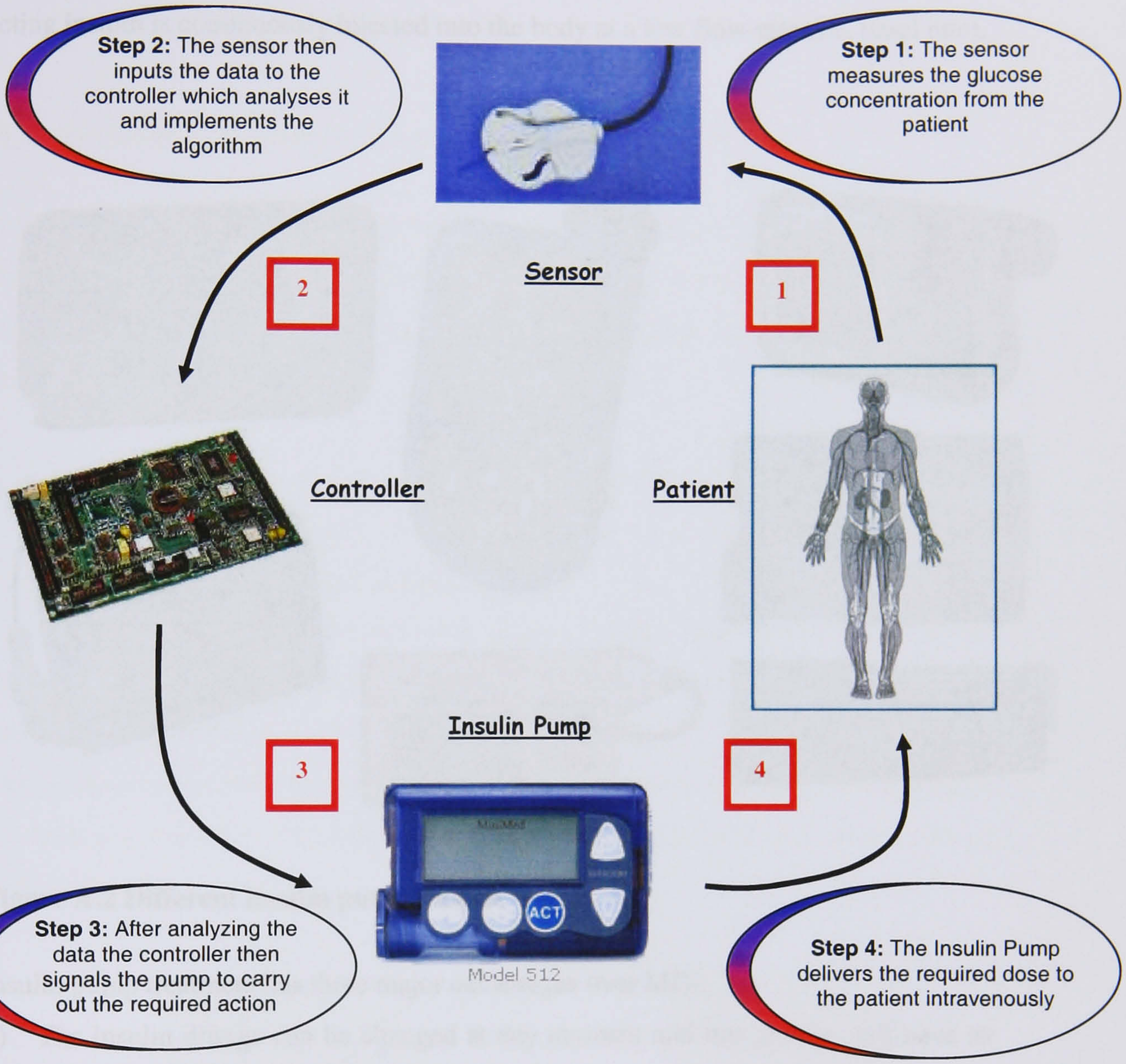


Figure A.1 Closed loop control system

There is a wide range of insulin pumps available on the market today with similar features. Figure A.2 displays a selection of the most popular models. In clockwise order, starting from the top left, the models shown in the figure are: Medtronic MiniMed 508, Deltec Cozmo, Animas IR1200, Medtronic MiniMed Paradigm 515, Roche Disetronic D-tron Plus, Dana DiabeCare II and finally the Nipro Amigo.

Insulin pumps use fast-acting insulin such as Regular or Lispro insulin, whereas in Multiple Daily Injection (MDI) treatment patients often use long-acting insulin (e.g. before going to sleep), such insulin is not used in the insulin pump treatment. The use of a single type of insulin greatly simplifies the treatment for the patient. The fast acting insulin is continuously injected into the body at a low flow-rate (i.e. basal rate).



Figure A.2 Different insulin pump models

Insulin pump treatment has three major advantages over MDI:

1) The insulin dosage can be changed at any moment and this change will have an almost immediate effect.
2) Fast-acting insulin is absorbed more efficiently by the body than the long-acting type and the action of insulin is more predictable.
3) The constant flow of insulin into the body provides a much more constant and effective treatment than for example two daily injections of long-lasting insulin.

When using an insulin pump, it is necessary to program the basal and bolus doses. The basal insulin is the constant flow of insulin and a bolus is an extra insulin boost used

during meals. A bolus can be administered in a variety of ways, be it in a single boost, over a period of time or perhaps a number of boosts following one another. Insulin pump therapy gives people with diabetes more flexibility than MDI. However, as with MDI, insulin pump therapy is still much less effective than the continuous control provided by a healthy individual's pancreas.

A.3 Sensors for Blood Glucose Measurement

A significant amount of research is being carried out in the area of developing sensors for continuous blood glucose monitoring. The four companies that are doing pioneering work in this field are Medtronic MiniMed, Cygnus, Animas and Pendragon.

A.3.1 Medtronic MiniMed

Continuous Glucose Monitoring System (CGMS)

MiniMed have developed a continuous glucose sensor which has been used for diagnosis in hospitals for many years now. The sensor is inserted under the skin of the patient's abdomen using a special inserter, and is then taped into place (Figure A.3). The sensor continuously measures the blood glucose level in the interstitial fluid in the layer of fat between the patient's skin and muscle. Each sensor can be worn for up to three days.



Figures A.3 CGMS Sensor

The CGMS sensor works on the principle of enzymatic electrode. The sensor's tip is made of a special membrane that is selectively permeable to glucose. Upon passing through the membrane, the glucose is oxidized to gluconic acid by the glucose oxidase

enzyme present in the sensor (steps 1 and 2 in Figure A.4). This redox reaction leaves reduced glucose oxidase, which is then oxidized by molecular oxygen, forming hydrogen peroxide as a by-product (step 3). At the electrode surface, this hydrogen peroxide oxidizes to form water: this reaction produces a small current (in the order of nano-amperes) which can be measured and correlated to the glucose concentration in the interstitial fluid (step 4). The sensor is connected to the CGMS monitor (Figure A.5). The current produced by the sensor is transmitted to the monitor, which analyzes the signal and records an average blood glucose concentration every five minutes. The data stored in the monitor over the diagnosis period (i.e. anything up to three days) can be downloaded onto a computer using the monitor's docking station.

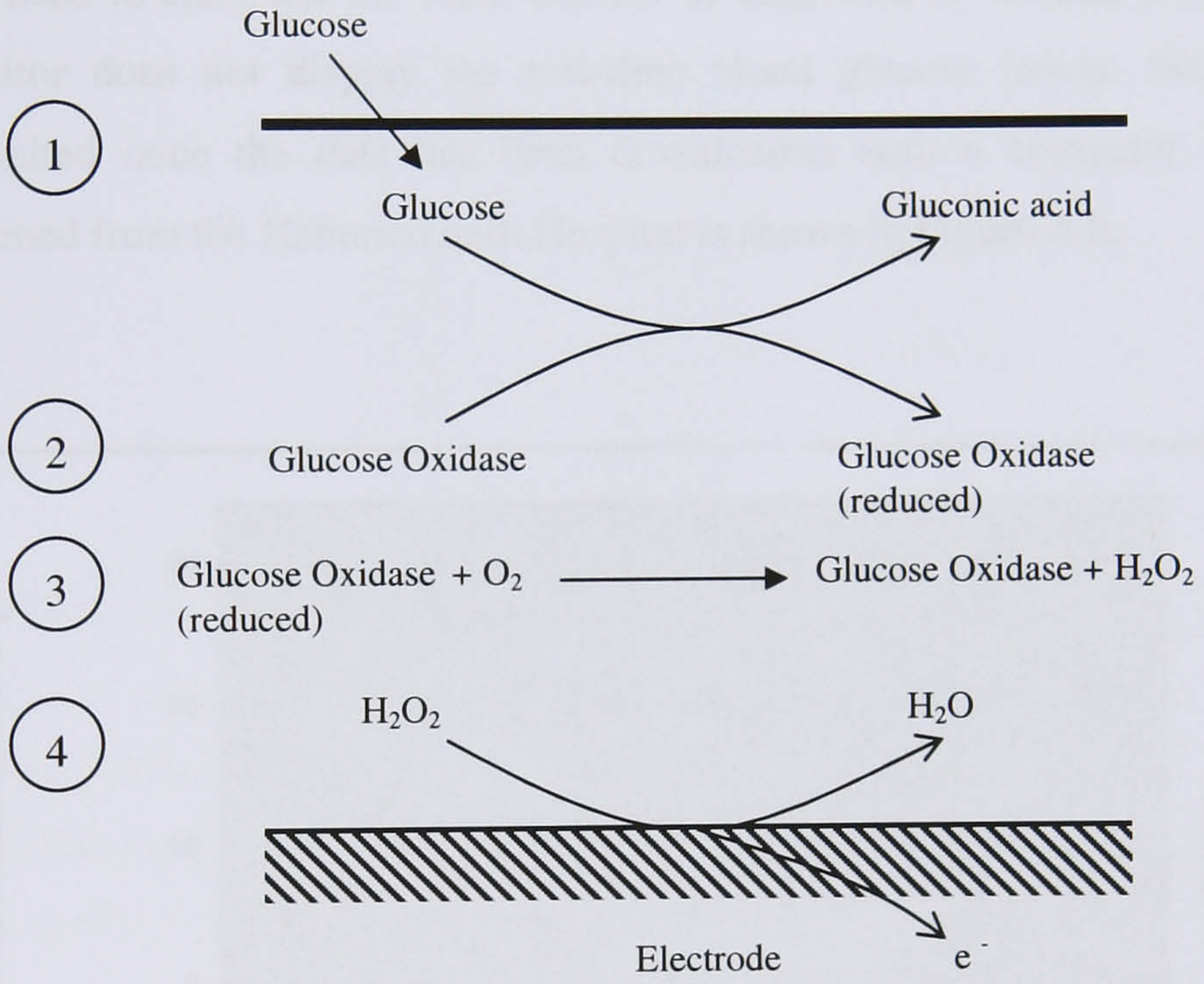
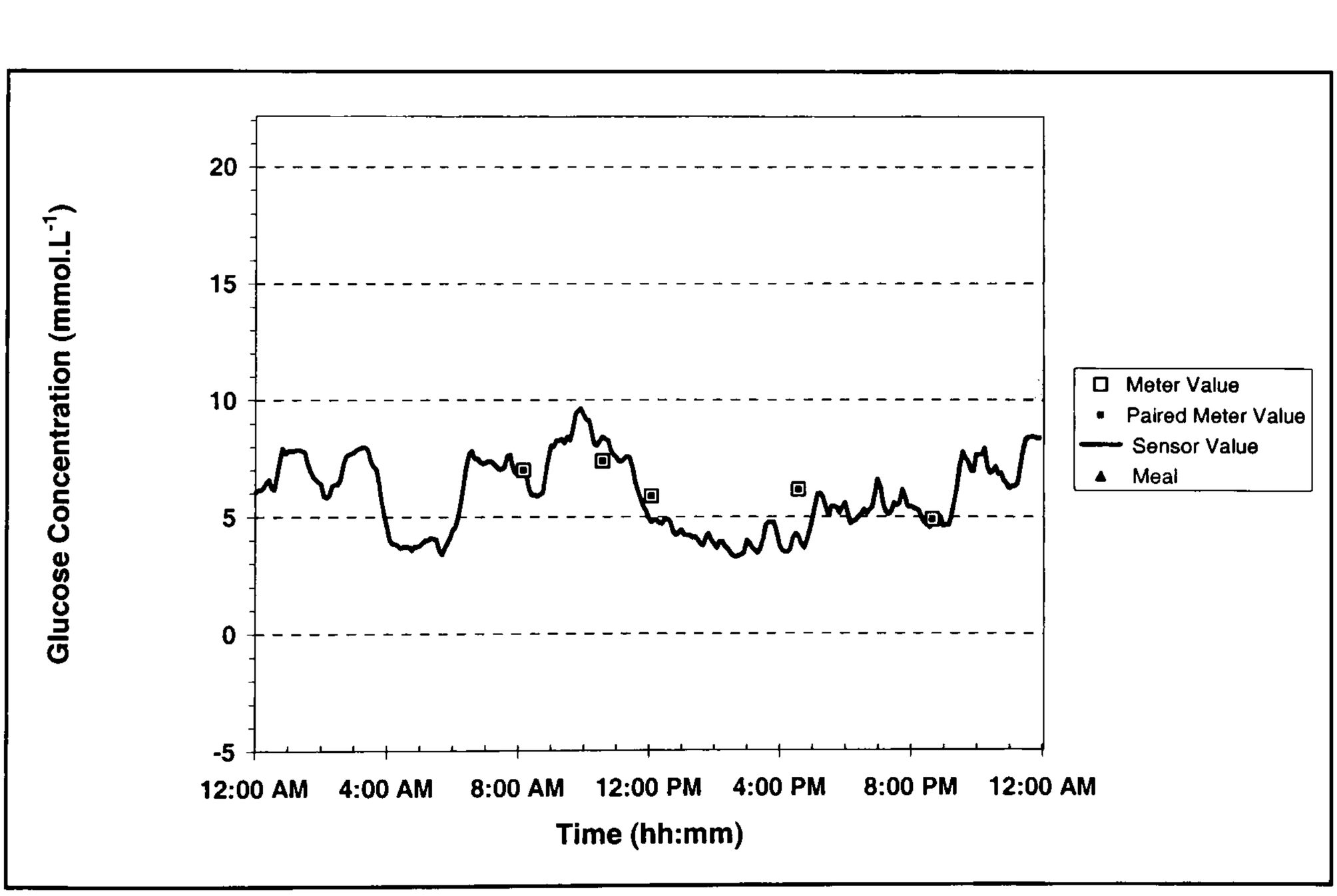


Figure A.4 Mechanism of the CGMS



Figure A.5 CGMS Monitor

The CGMS has some shortcomings: the first problem derives from the fact that glucose concentration is measured from the interstitial fluid which is not always the same as the blood glucose concentration. Another problem experienced with the CGMS sensor is the phenomenon known as "membrane biofouling". This term describes the clogging of the sensor's selective membrane by molecules present in the blood stream of interstitial area, most often manifested as the growth of tissue covering the membrane and therefore hampering the access of glucose to the sensor. For this reason the sensor needs to be constantly re-calibrated and can only be used for three days. From a practical point of view, the fact that a sensor can only be used for three days greatly limits the product's scope. Furthermore the required minimum of three finger-prick glucose tests per day in order to calibrate the sensor means patients still need to carry out the same number of tests with or without a CGMS. Also, the monitor does not display the real-time blood glucose levels: these can only be consulted once the data has been downloaded onto a computer. A sample data obtained from the Hammersmith Hospital is shown in Figure A.6.



A.6 Blood Glucose Concentration obtained by CGMS

Guardian System

The Guardian system (Figure A.7), which is in it final testing phase, is fundamentally a CGMS with some added features:

- The sensor and the monitor communicate wirelessly via radio waves.
- The monitor displays real-time blood glucose levels.
- The monitor sounds an alarm when blood glucose levels approach undesired levels.

The guardian system uses the same sensor technology as the CGMS and therefore can only be used for three days and needs calibration every 12 hours.

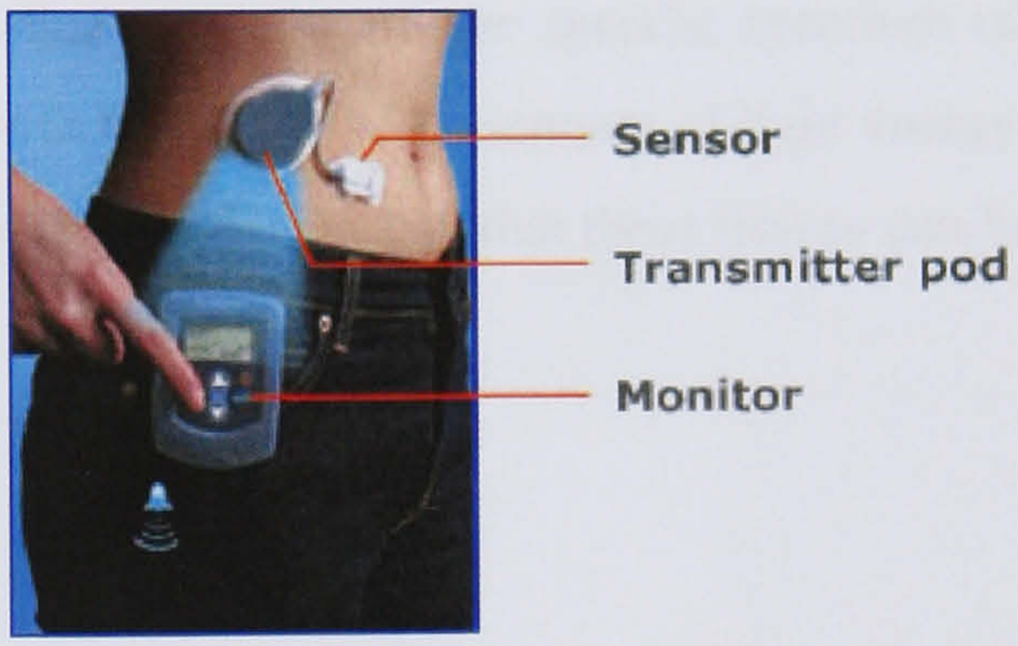


Figure A.7 Guardian System

Sensor Augmented Systems

MiniMed is currently working on what they define as "The World's First Sensor-Augmented Systems". Similarly to what Animas Corporation are developing, this project combines the CGMS/Guardian technology with MiniMed's pump technology - Figure A.8 depicts their vision.



Figure A.8 Sensor Augmented System

Long Term Sensor System (LTSS)

MiniMed is also developing the LTSS, a system meant to operate like an artificial pancreas, constituting of an implantable insulin pump and a long term implantable continuous glucose sensor.

A.3.2 Animas Corporation

Animas Corporation is currently developing an optical sensor based blood glucose concentration measurement technology. The continuous glucose sensor will work on the principles of spectroscopy. The problems faced in the development of this sensor are the fact that the low concentration of glucose in blood makes it more difficult to identify and that the various components, such as proteins, hemoglobin and water, in the blood have spectra that overlap with the specific spectrum of glucose. Another problem is concerned with the loss of large amount of light energy in the intervening tissue (e.g. bone and skin) and also the fact that these tissues can have similar spectra to that of glucose.

A.3.3 Pendragon

Pendragon has developed the PENDRA (see Figure A.9) continuous non-invasive glucose monitor that can be worn as a watch and it records blood glucose levels every minute, but is not yet commercially available. It has an alarm system that alerts the patient when the blood glucose levels approach hypo- or hyperglycemic levels. The data can be downloaded onto a computer and the real-time blood glucose concentration is displayed at all times. PENDRA's technology is completely non-invasive and is based on the principle of impedance spectroscopy. The technology works on the basis that fluctuations in the blood glucose levels and the transfer of glucose through cell membranes in the patient's body lead to a variation in the electrolyte concentration. This in turn causes a change in the interfacial polarisation of the cell membrane, resulting in variations in the cell membrane's conductivity and permittivity. These changes in the cell membrane's characteristics lead to alterations of the electromagnetic properties of the patient's skin and subcutaneous tissue,

which is measured by the device, and correlated with the blood glucose concentration (see Figure A.10).

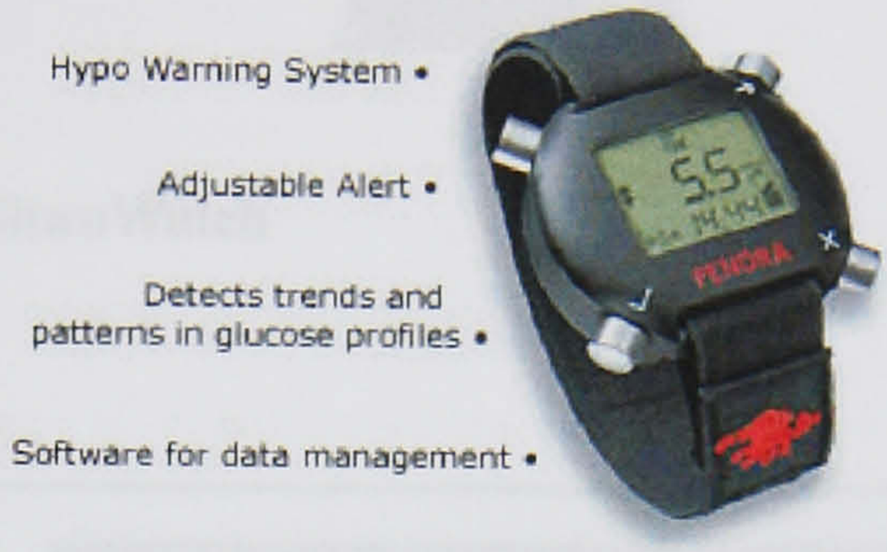


Figure A.9 Pendra Sensor

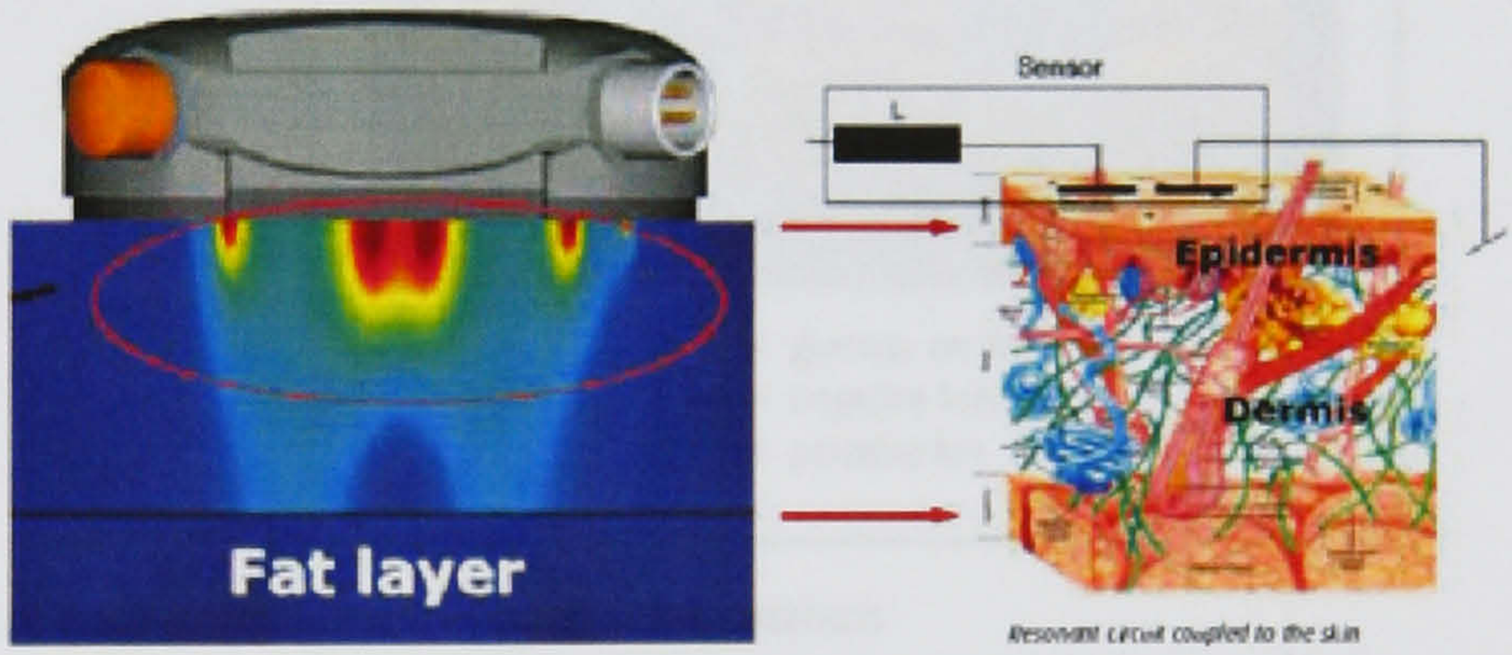


Figure A.10 Impedance Spectroscopy principle of the PENDRA sensor

A.3.4 Cygnus

Cygnus has developed GlucoWatch G2 Biographer (see Figure A.11) sensor which is based on the principle of reverse iontophoresis and is worn like a wrist-watch, similar to the Pendragon PENDRA. The sensor works by applying a small current to the patient's skin which leads to a movement of ions, ultimately causing glucose molecules to be pulled out of the patient through the skin (see Figure A.12).



Figure A.11 Cygnus GlucoWatch

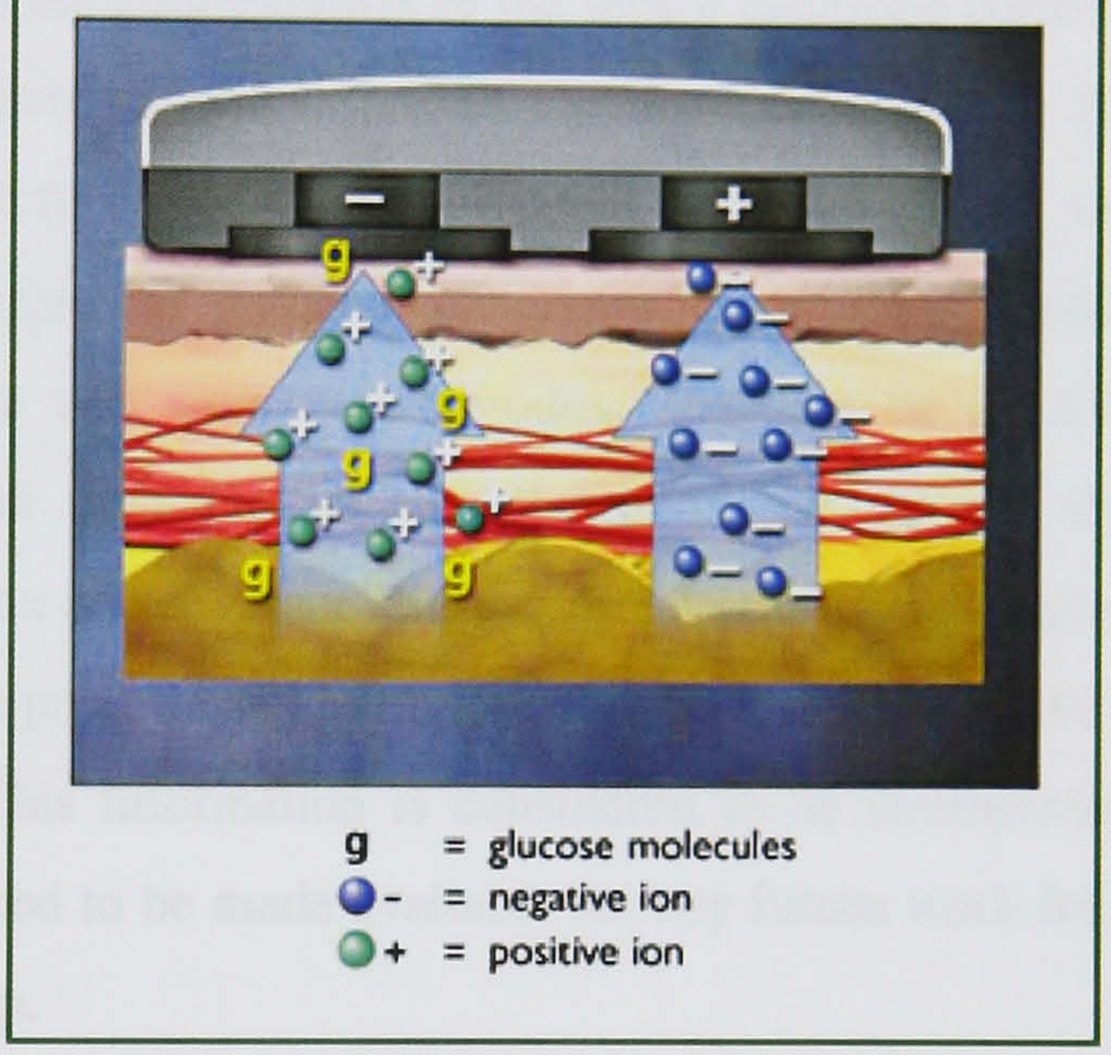


Figure A.12 Cygnus GlucoWatch Mechanism

The glucose is stored in two gel collection disks, where it is oxidized by reaction with the glucose oxidase enzyme (similar to the Medtronic sensor). The current generated by the redox reaction is proportional to the collected glucose level, therefore the GlucoWatch measures the resulting current to evaluate the blood glucose level, every 10 minutes. Although it is a non-invasive continuous glucose sensor, a number of patients have complained about severe irritation and bruising of the skin and the presence of sweat on the skin can severely impair the sensor's accuracy.

A.4 Implementation of the Parametric Controller

This section presents a prototype implementation of the parametric controller for blood glucose control. As discussed in section A.1 this would require developing a

closed loop system comprising of the sensor connected to the microchip that would drive the mechanical pump. The sensors and pumps that are currently available in the market do not allow for a direct connection with the microchip and therefore a laptop acts as a virtual patient and blood glucose measurements are provided via a D.C. voltage calibrator as discussed next.

The CGMS only allows for a continuous recording of the data that cannot be continuously transferred to the microchip where the controller is stored. This limitation comes from the configuration of the sensor electrode consisting of: counter electrode, working electrode and reference electrode as shown in Figure A.13. To power the sensor and force the required current to flow between the working and counter electrode, a constant potential difference of 535 mV needs to be applied between the reference and working electrodes. This can be achieved by using a potentiostat which can maintain the electrical potential between the working and reference electrodes at a preset value. This can then allow the connection of the sensor to the microchip via a potentiostat, but requires information about the material of the reference electrode. This information is considered to be confidential by MiniMed Medtronic and will need to be made available for any future work for connecting the sensor to the microchip.

Counter	*Working*	*Reference*

Figure A.13 Sensor Electrode Configuration

The connection of the insulin pumps to the microchip also faces some problems related to the programmability. The pumps work on the principle of delivering a continuous, preset basal rate of insulin and when required can deliver an additional preset bolus. This limits the continuous delivery of insulin at varying rates. It is envisaged that this limitation can be overcome in the future by having custom built pumps.

A.4.1 FM400 Chip

The Flash memory of FM400 chip can be programmed using a single 5 Volt supply and it has analogue inputs and outputs allowing for the connectivity to the sensor and pump. In the current study, FM400 (Figure A.14) is used and can be downsized to a much smaller chip for future applications.

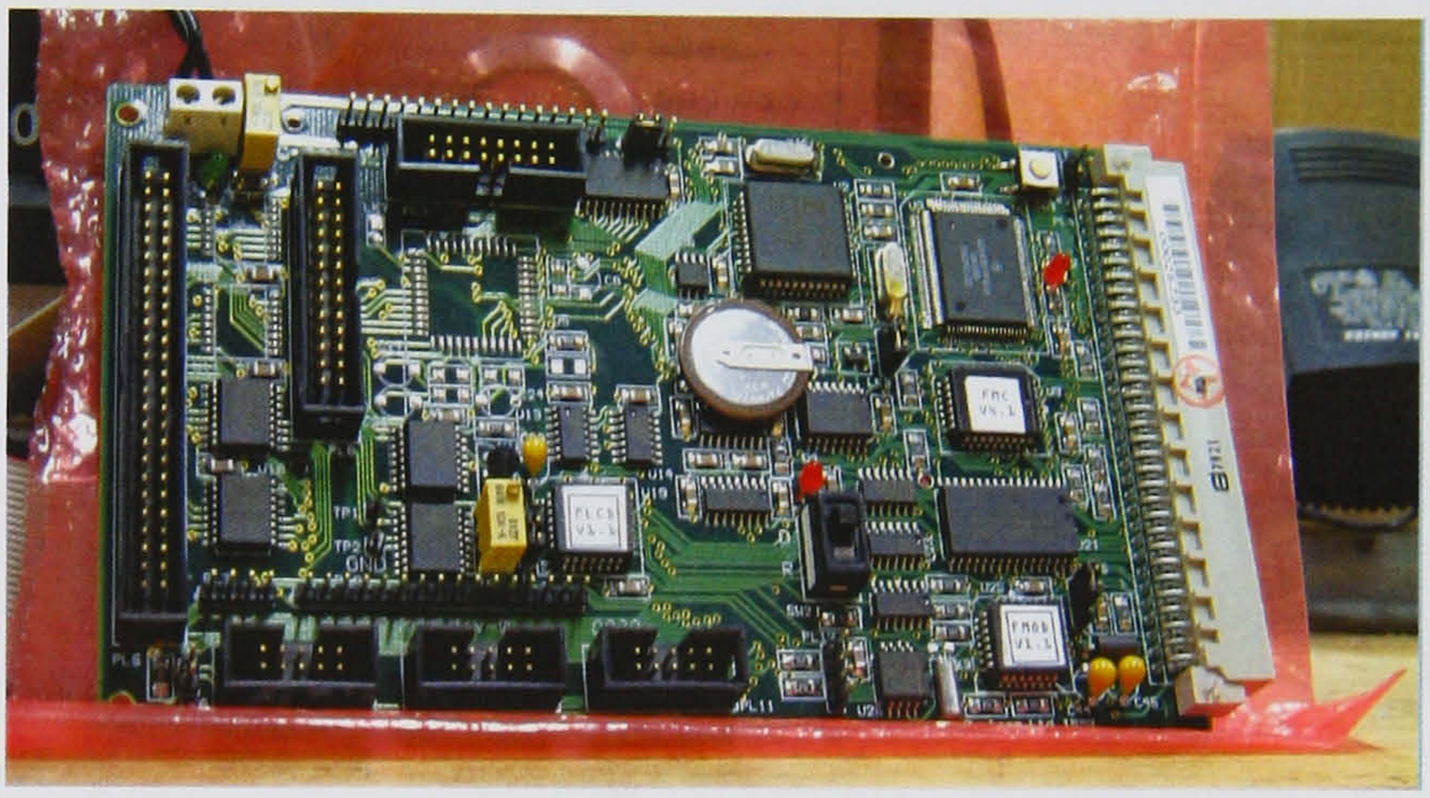


Figure A.14 FM400 chip

The parametric controller was stored on FM400 by using FM400's 'C-Builder' software. The blood glucose deviation (-10 to 25 mmol/L) from the nominal value and the insulin infusion range (0 to 100 mU/min) were calibrated with input voltage range of 0.5 to 2.5 V on FM400. The calibration curve for blood glucose deviation is shown in Figure A.15.

A.4.2 Experimental Set-up

Since no actual glucose sensor was used, an alternative experiment was devised in order to test the controller's performance. The voltage of the signal sent from the sensor to the controller is proportional to the measured blood glucose concentration and therefore this signal could be simulated by using a variable voltage supply i.e. voltage calibrator. Thus connecting a voltage calibrator to the controller would allow a

number of tests to be carried out, simulating various blood glucose trends based on real data. The experimental set-up used for testing the performance of the controller is shown in Figure A.16. The blood glucose concentration, G, is changed by the voltage calibrator and the laptop is used to estimate I and X, for the Bergman model, which is an input to the chip. For a given value of G, I and X, the insulin infusion rate is computed by the chip and all the data is continuously recorded on the laptop.

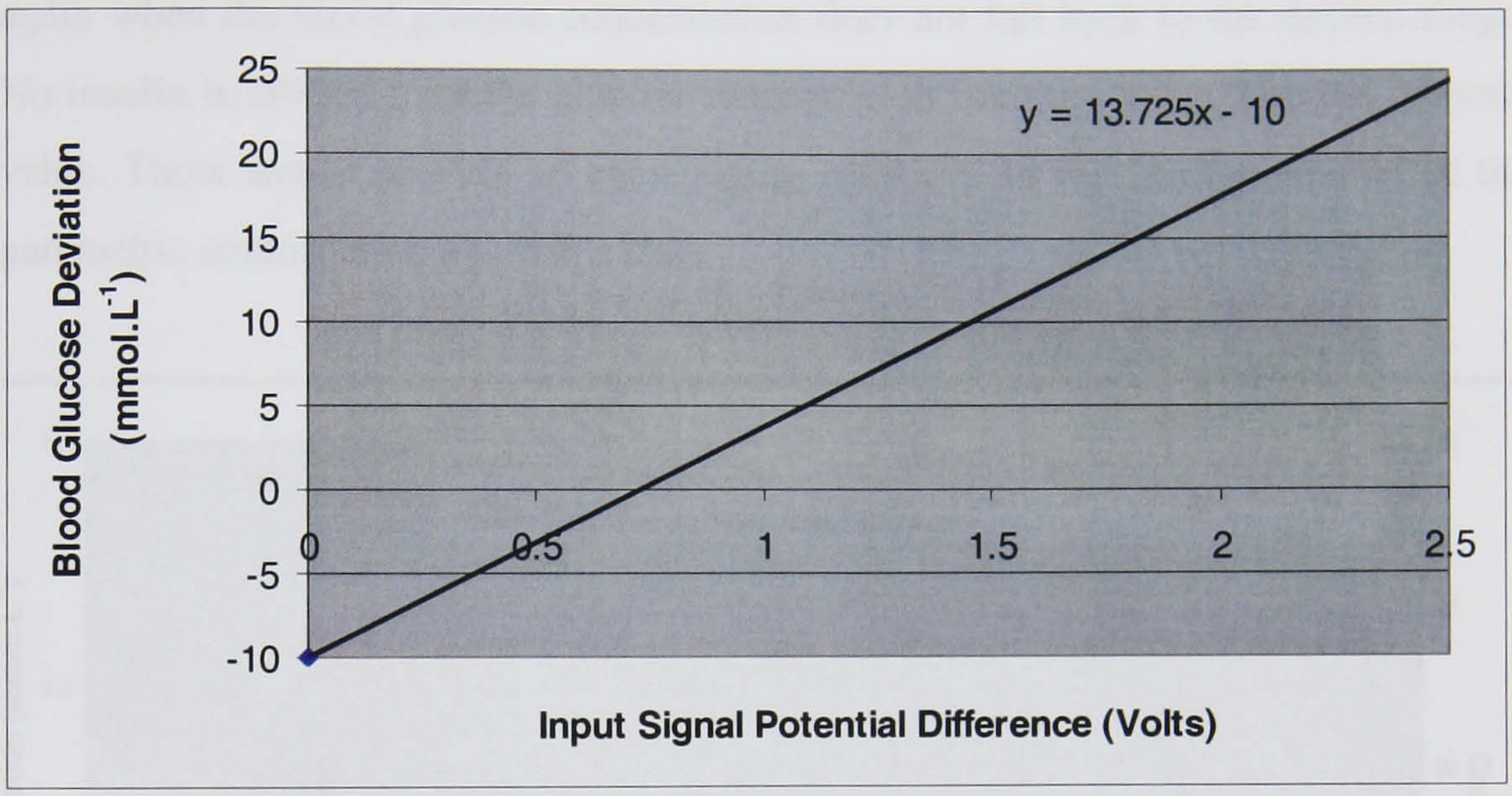


Figure A.15 Calibration Curve for Blood Glucose Deviation

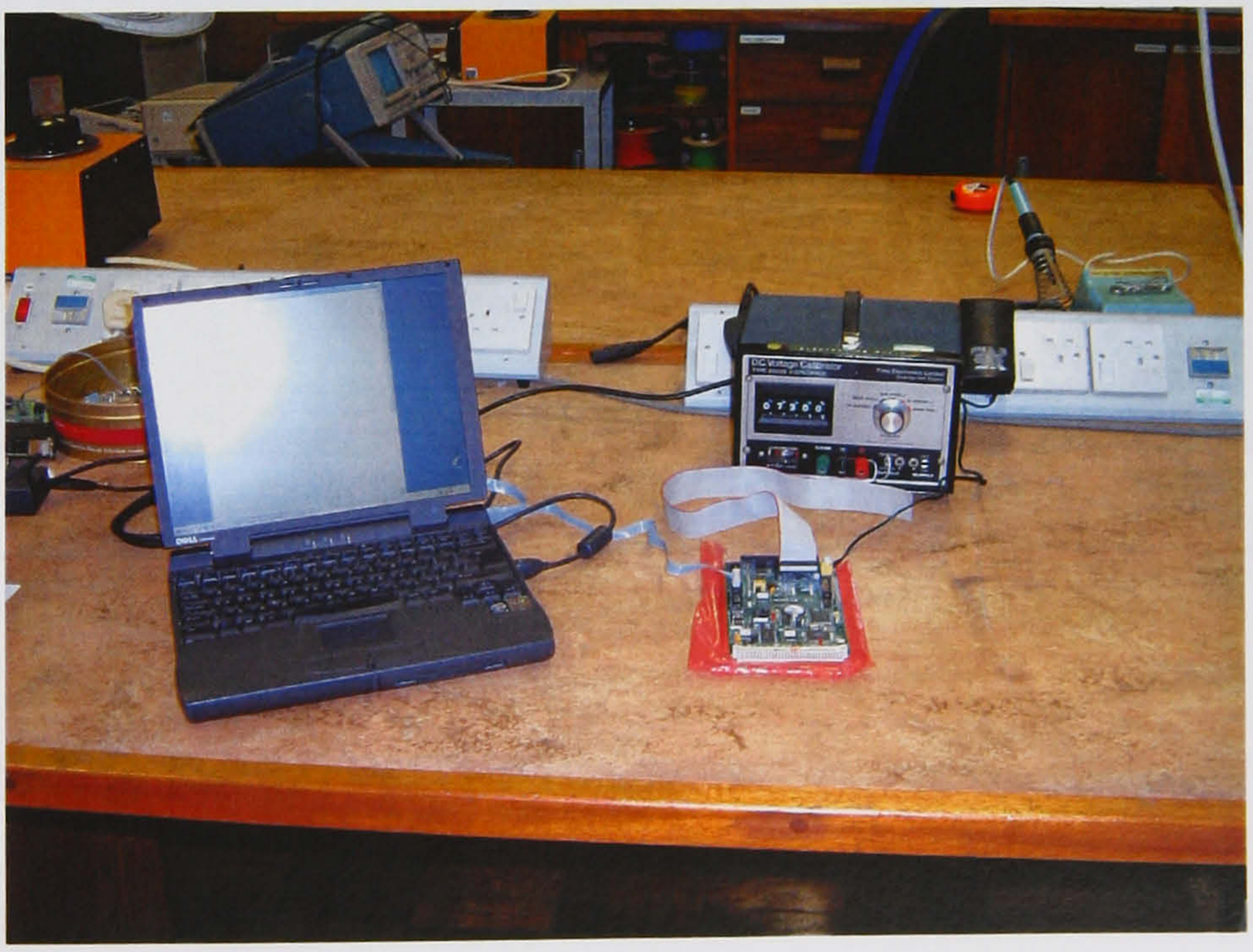


Figure A.16 Experimental Set-up

A.5 Performance of the Controller

A number of experiments were carried out by changing the blood glucose concentrations through the voltage calibrator – one such controller performance is shown in Figure A.17. As the controller senses the rise in blood glucose measurement due to meal disturbance, insulin at the rate of approximately 20 mU/min is infused. At the next time step this rate is reduced to avoid a large undershoot and then increased again when the blood glucose concentration does not fall back to the desired range. No insulin is infused once the glucose concentration becomes lower than the nominal value. These trends provide an encouraging platform for the implementation of the parametric controller on a portable chip.

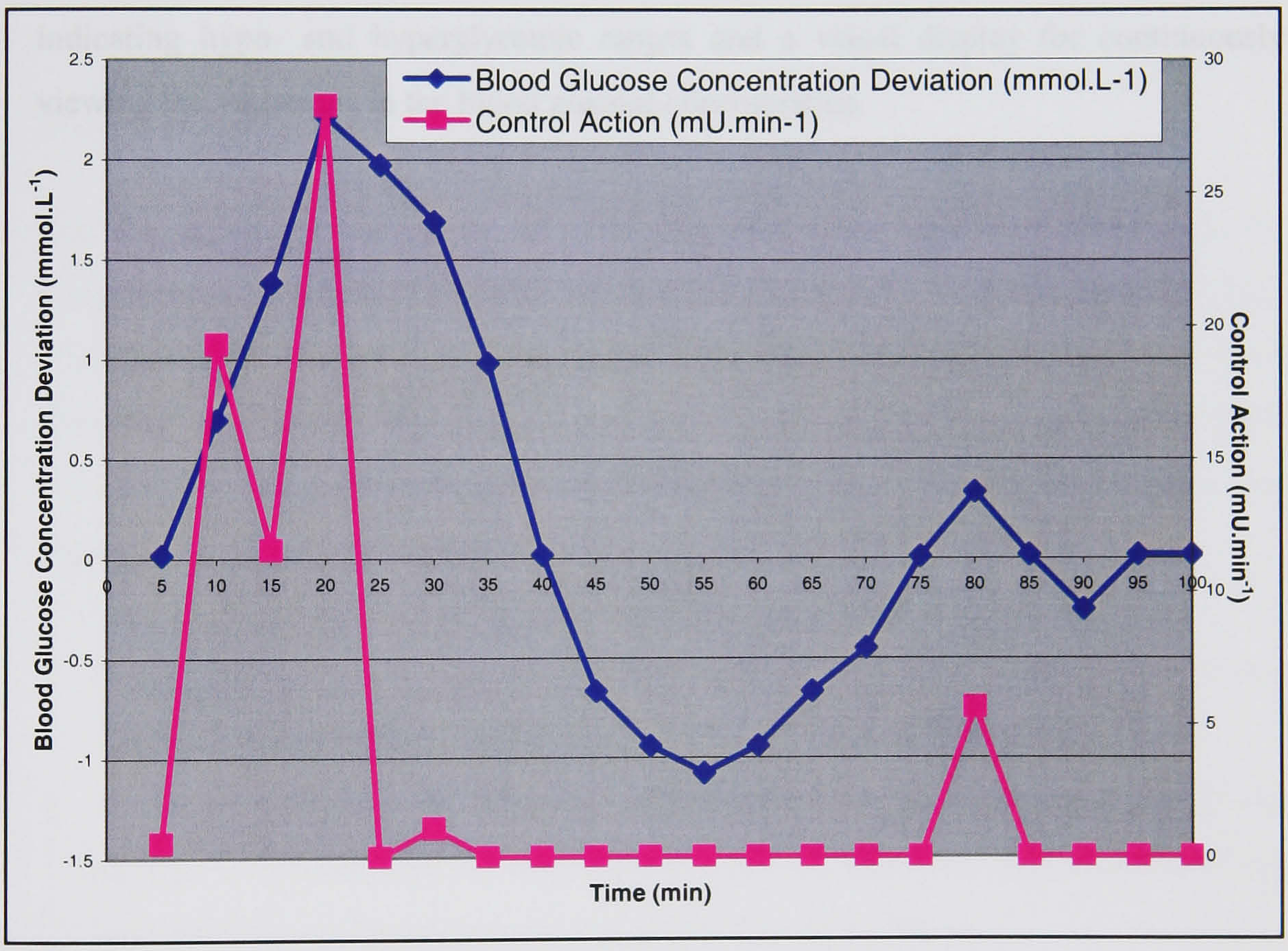


Figure A.17 Controller Performance

Concluding Remarks

The parametric controller for the regulation of the blood glucose concentration for people with type 1 diabetes was implemented and tested on a chip. This paves the way

for the development of a portable device that can take into account bounds on insulin infusion rate and blood glucose concentration. The future work requires working on some issues. The parametric controller can be implemented via a microchip which is much smaller than FM400 used in this study. Connection of the microchip to the CGMS would require information about the material of the reference electrode. The sensor companies are actively working on overcoming the limitations of the sensor regarding their usage for a maximum of three days and its calibration via finger prick method. Lack of the programmability features of the insulin pumps and subcutaneous route of delivery seem to be a minor limitation that can be overcome with little effort. Once programmable pumps are available the parametric controller can be modified to take into account the subcutaneous infusion of insulin. Some additional features that can be incorporated in the portable insulin delivery device are an alarm system for indicating hypo- and hyperglycemic ranges and a visual display for continuously viewing the variations in the blood glucose concentration.

Appendix B

Analysis of the Detailed Model for Diabetes

An analysis of the detailed model for people with type 1 diabetes is presented. The model is characterized by the distribution of the insulin and glucose to the six compartments, brain, heart and lungs, liver, gut, kidney and periphery, via circulation of the blood. A number of dynamic simulations were carried out for varying insulin infusion rates and meal disturbances and the dynamics of the blood glucose concentration were analyzed.

B.1 Introduction

The detailed model for type 1 diabetes studied in this appendix is based upon the compartmental model of insulin and glucose dynamics, developed by Sorensen (1985), which was modified by Parker (1999) to incorporate generalized meal disturbances. The model considers the body to be divided into six physiological compartments that represent the capillary beds of various organs and tissues (see Figure B.1). These compartments are:

1. Brain: This compartment represents the central nervous system consisting of two segments representing the capillary space and the brain tissue space.
2. Heart and Lungs: These represent the vascular volumes of the heart, lungs and arteries. This compartment closes the circulatory loop and represents the blood volume of the cardiopulmonary system and the major arteries.
3. Periphery: This includes skeletal muscles and adipose tissues.
4. Gut: The stomach and intestine are lumped into the gut.
5. Liver: This is a complex compartment that takes into account the hepatic artery and portal vein inputs.

6. Kidney: This compartment accounts for the rate of glucose excretion from the system.

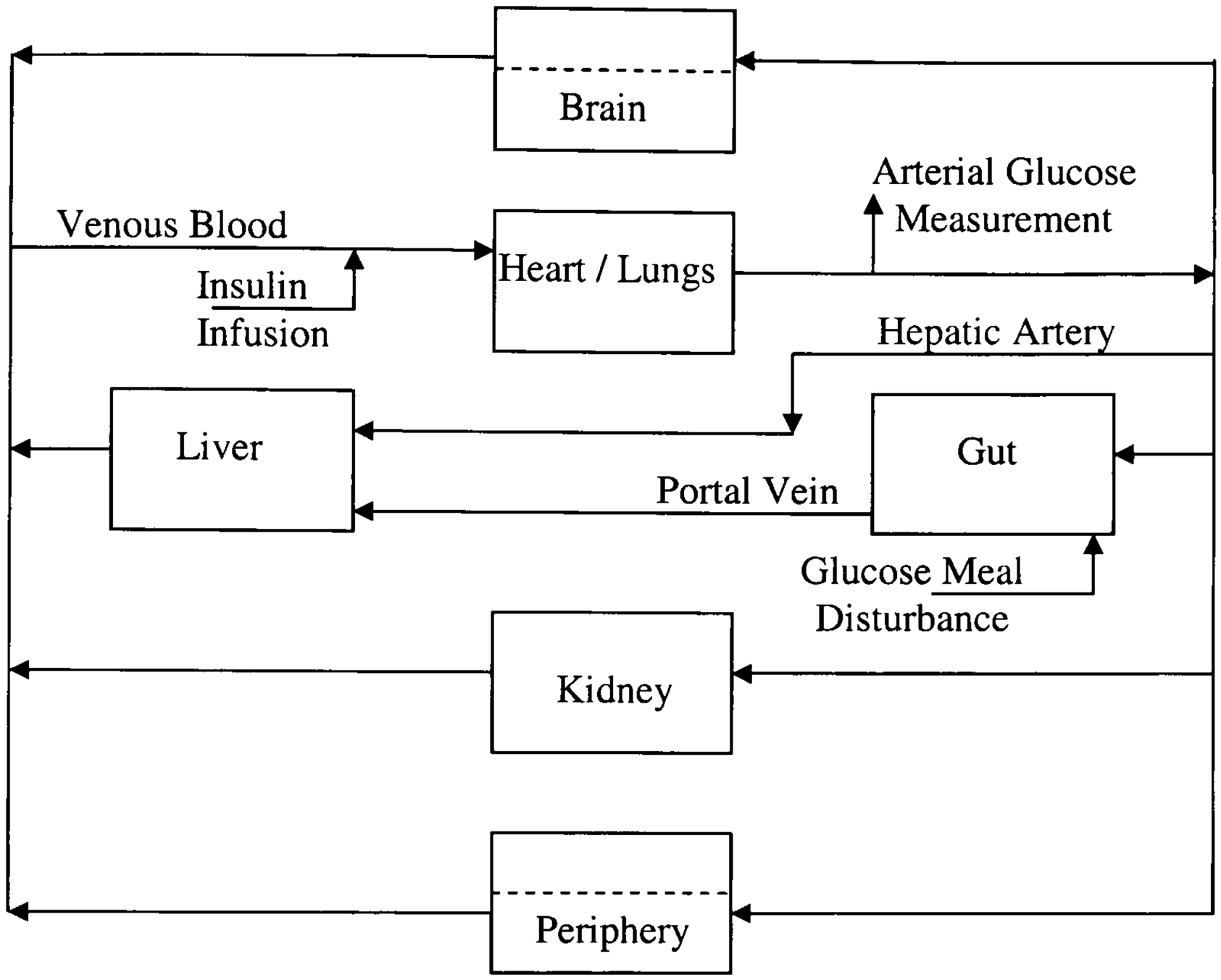


Figure B.1 Detailed compartmental model for people with type 1 diabetes

The mathematical formulation of the model is described in the next section and detailed model analysis and simulation results are presented in section B.3.

B.2 Mathematical Modelling

The model consists of two submodels, glucose submodel and insulin submodel. Also it was assumed that glucose or insulin transported by the blood leaving the compartment was in equilibrium with the glucose or insulin in the compartment. The transport of glucose or insulin to the tissues within a compartment occurs via diffusion. For compartments where this diffusion occurs it is assumed they are comprised of two subcompartments given by the tissue subcompartment and the blood subcompartment. The nomenclature used for the equations presented in the following sections is given in Table B.1.

B.2.1 Glucose submodel

This is given by a set of eight simultaneous nonlinear ordinary differential equations which are linked to the insulin submodel through the metabolic rate equations.

Brain Compartment:

$$\frac{dG_B^C}{dt} = \left(G_H^C - G_B^C\right)\frac{q_B}{v_B^C} - \left(G_B^C - G_B^T\right)\frac{v_B^T}{T_B v_B^C}$$

$$\frac{dG_B^T}{dt} = \left(G_B^C - G_B^T\right)\frac{1}{T_B} - \frac{\Gamma_{BU}}{v_B^T}$$

Heart & Lungs Compartment:

$$\frac{dG_H^C}{dt} = \left(G_B^C q_B + G_L^C q_L + G_K^C q_K + G_P^C q_P - G_H^C q_H - \Gamma_{RBCU}\right)\frac{1}{v_H^C}$$

Gut Compartment:

$$\frac{dG_S^C}{dt} = \left(G_H^C - G_S^C\right)\frac{q_S}{v_S^C} + \frac{\Gamma_{MEAL}}{v_S^C} - \frac{\Gamma_{SU}}{v_S^C}$$

Liver Compartment:

$$\frac{dG_L^C}{dt} = \left(G_H^C q_A + G_S^C q_S - G_L^C q_L\right)\frac{1}{v_L^C} + \frac{\Gamma_{HGP}}{v_L^C} - \frac{\Gamma_{HGU}}{v_L^C}$$

Kidney Compartment:

$$\frac{dG_K^C}{dt} = \left(G_H^C - G_K^C\right)\frac{q_K}{v_K^C} - \frac{\Gamma_{KE}}{v_K^C}$$

Periphery Compartment:

$$\frac{dG_P^C}{dt} = \left(G_H^C - G_P^C\right)\frac{q_P}{v_P^C} + \left(G_P^T - G_P^C\right)\frac{v_P^T}{T_P^G v_P^C}$$

$$\frac{dG_P^T}{dt} = \left(G_P^C - G_P^T\right)\frac{1}{T_P^G} - \frac{\Gamma_{PGU}}{v_P^T}$$

It was assumed that the glucose utilization of the brain, the red blood cells and the gut is insensitive to changes in glucose and insulin levels and hence take constant values. These metabolic sources and sink term values (Γ_i [=] mg/min) and a set of auxiliary equation states are defined as follows:

Brain Glucose Uptake Rate:

$\Gamma_{BU} = 70$ mg/min

Red Blood Cell Glucose Uptake Rate:

$\Gamma_{RBCU} = 10$ mg/min

Gut Compartment Glucose Uptake Rate:

$\Gamma_{SU} = 20$ mg/min

Glucose Hepatic Production Rate:

$$\Gamma_{HGP} = 155A_{IHGP}\left[2.7\tanh\left(0.388N\right) - A_{NHGP}\right]\times\left[1.425 - 1.406\tanh\left\{0.6199\left(\frac{G_L^C}{101} - 0.4969\right)\right\}\right]$$

Insulin Effect on the Hepatic Glucose Production:

$$\frac{dA_{IHGP}}{dt} = \frac{1}{25}\left[1.2088 - 1.138\tanh\left(1.669\frac{I_L^C}{21.43} - 0.8885\right) - A_{IHGP}\right]$$

Glucagon Effect on the Hepatic Glucose Production:

$$\frac{dA_{NHGP}}{dt} = \frac{1}{65}\left[\frac{2.7\tanh(0.388N) - 1}{2} - A_{NHGP}\right]$$

Rate of Hepatic Glucose Uptake:

$$\Gamma_{HGU} = 20A_{IHGU}\left[5.6648 + 5.6589\tanh\left\{2.4375\left(\frac{G_C^L}{101} - 1.48\right)\right\}\right]$$

Insulin Effect on the Glucose Uptake:

$$\frac{dA_{IHGU}}{dt} = \frac{1}{25}\left[2\tanh\left(0.549\frac{I_L^C}{21.43}\right) - A_{IHGU}\right]$$

Rate of Kidney Excretion:

$$\Gamma_{KE} = \begin{cases} 71 + 71\tanh\left[0.011\left(G_K^C - 460\right)\right] & \text{for } G_K^C < 460 \\ 0.872G_K^C - 300 & \text{for } G_K^C \geq 460 \end{cases}$$

Rate of Peripheral Glucose Uptake:

$$\Gamma_{PGU} = \frac{35G_P^T}{86.81}\left[7.035 + 6.51623\tanh\left\{0.33827\left(\frac{I_P^T}{5.304} - 5.82113\right)\right\}\right]$$

B.2.2 Insulin Submodel

For the insulin submodel, the brain interstitial fluid space has been omitted since it is impermeable to insulin. Similarly, the liver intracellular fluid volume has been omitted. The red blood cell membrane is also impermeable to insulin; thus, unlike glucose, insulin is only distributed throughout the plasma volume of whole blood. Therefore, it was assumed that insulin is uniformly distributed in the plasma volume of whole blood. Since the average red blood cell content of whole blood is about 40 volume percent, the blood volumes and flow rates as estimated for a 70kg man were reduced by 40 percent for insulin modelling.

Brain Compartment:

$$\frac{dI_B^C}{dt} = \left(I_H^C - I_B^C\right)\frac{X_B}{W_B^C}$$

Heart & lungs Compartment:

$$\frac{dI_H^C}{dt} = \left(I_B^C X_B + I_L^C X_L + I_K^C X_K + I_P^C X_P - I_H^C X_H + \Gamma_{IVI}\right)\frac{1}{W_H^C}$$

Gut Compartment:

$$\frac{dI_S^C}{dt} = \left(I_H^C - I_S^C\right)\frac{X_S}{W_S^C}$$

Liver Compartment:

$$\frac{dI_L^C}{dt} = \left(I_H^C X_A + I_S^C X_S - I_L^C X_L\right)\frac{1}{W_L^C} + \frac{\Gamma_{PIR} - \Gamma_{LC}}{W_L^C}$$

Considering no pancreatic insulin release for type 1 diabetes,

$$\Gamma_{PIR} = 0$$

Kidney Compartment:

$$\frac{dI_K^C}{dt} = \left(I_H^C - I_K^C\right)\frac{X_K}{W_K^C} - \frac{\Gamma_{KC}}{W_K^C}$$

Periphery Compartment:

$$\frac{dI_P^C}{dt} = \left(I_H^C - I_P^C\right)\frac{X_P}{W_P^C} - \left(I_P^C - I_P^T\right)\frac{W_P^T}{T_P^I W_P^C}$$

$$\frac{dI_P^T}{dt} = \left(I_P^C - I_P^T\right)\frac{1}{T_P^I} + \frac{\left(\Gamma_{SIA} - \Gamma_{PC}\right)}{W_P^T}$$

Insulin degrades in liver, kidney and peripheral tissues, at the target tissue plasma membrane via a degrative enzyme complex. The corresponding metabolic sinks (Γ_i [=] mU/min) are given as follows:

The Liver Clearance Rate:

$$\Gamma_{LC} = F_{LC}\left(I_H^C X_A + I_S^C X_S + \Gamma_{PIR}\right)$$

It was assumed that the fractional clearance of insulin by the liver Γ_{LC} is equal to 0.4 and is independent of the plasma insulin levels.

The Kidney Clearance Rate:

$$\Gamma_{KC} = F_{KC} I_K^C X_K$$

The kidney was assumed to clear 30 percent of the insulin presented to it independent of the arterial insulin level; the fractional clearance of insulin by the kidney Γ_{KC} equals 0.3.

The Peripheral Clearance Rate:

$$\Gamma_{PC} = \frac{I_P^T}{\frac{1-F_{PC}}{F_{PC}}\frac{1}{X_P} - \frac{1}{T_P^I W_P^T}}$$

The fractional clearance of insulin by peripheral tissues Γ_{PC} was assumed to be equal to 0.15.

The release and distribution of glucagon in the body was modeled by considering a single blood pool compartment as follows:

$$\frac{dN}{dt} = (\Gamma_{PNR} - N)\frac{F_{PNC}}{W_N}$$

where glucagon release from the α-cells of the pancreas is given by:

$$\Gamma_{PNR} = \left[1.3102 - 0.61016\tanh\left\{1.0571\left(\frac{I_C^H}{15.15} - 0.46981\right)\right\}\right]\times \left[2.9285 - 2.095\tanh\left\{4.18\left(\frac{G_C^H}{91.89} - 0.6191\right)\right\}\right]$$

B.3 Model Simulation and Analysis

The model presented in the previous section was simulated using gPROMS (gPROMS, 2003) and the model parameters are taken from Sorensen (1985) and Parker (1999). Figure B.2 shows the increase in glucose concentration in the various compartments when no exogenous insulin is infused. It can be observed that the liver

compartment has the highest glucose concentration followed by the kidney compartment. The liver glucose concentration variation for a set of insulin infusion rates is shown in Figure B.3.

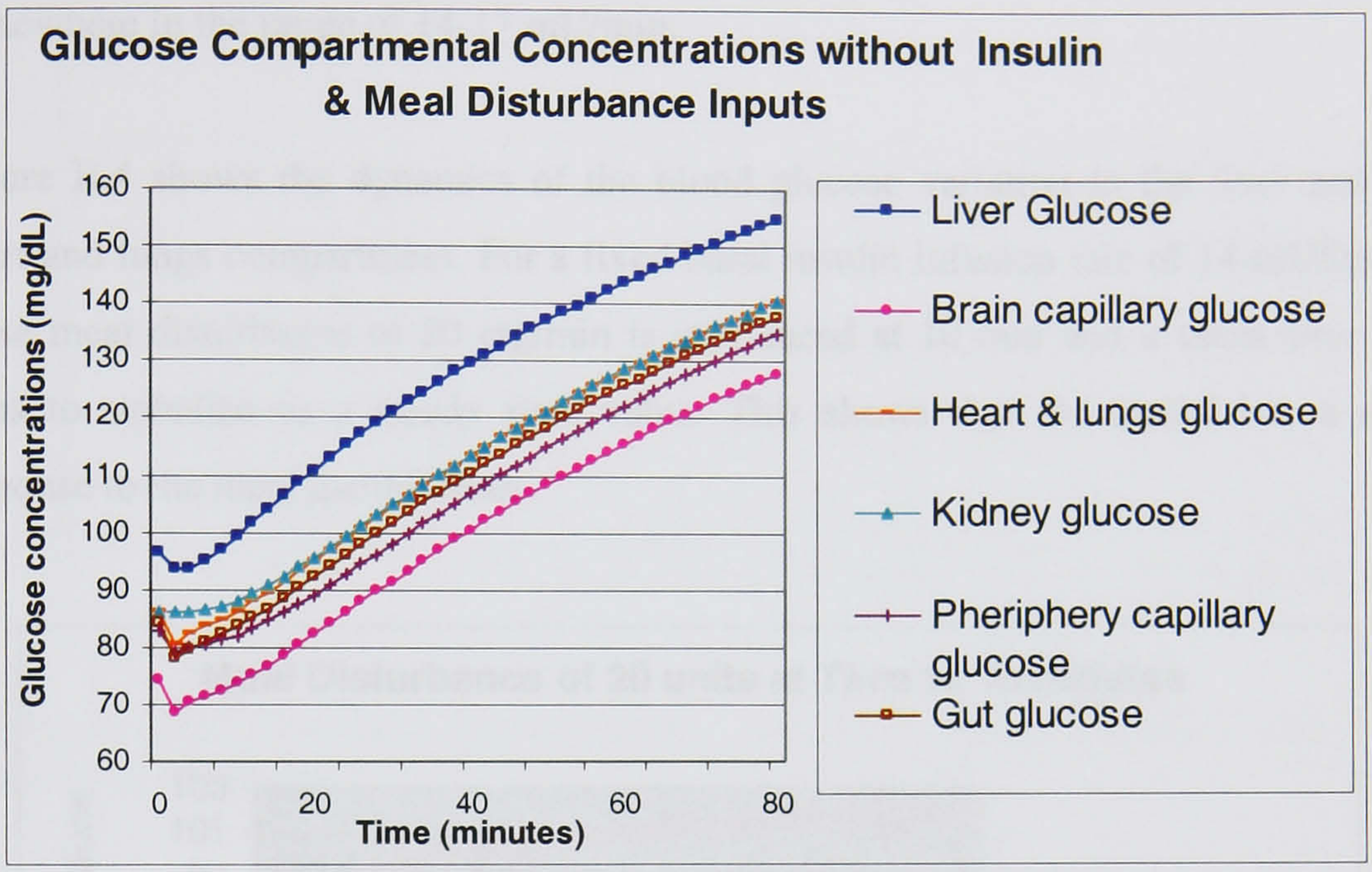


Figure B.2 Glucose compartmental concentration without insulin and meal disturbance inputs

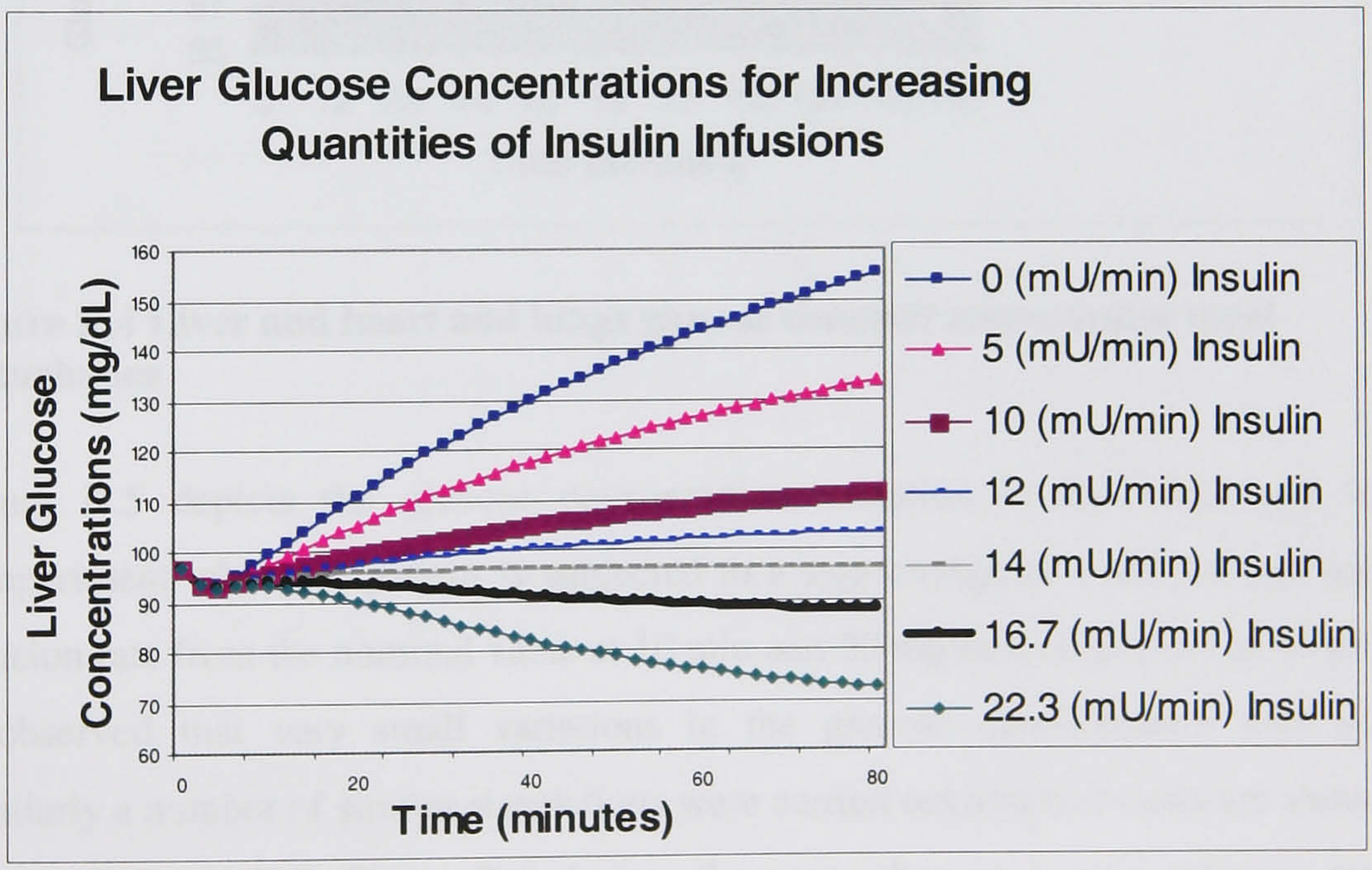


Figure B.3 Liver glucose concentration for different insulin infusion rates

Although as the insulin infusion rate is increased from 0 to 22.3 mU/min, the liver blood glucose concentration decreases, but it does not tend to stabilize to a nominal value for low (5 mU/min) or high (22.3 mU/min) insulin flowrates. Thus it can be concluded from Figure B.3 that a nominal or basal insulin infusion rate would lie somewhere in the range of 14-17 mU/min.

Figure B.4 shows the dynamics of the blood glucose variation in the liver and the heart and lungs compartment. For a fixed basal insulin infusion rate of 14 mU/min, a pulse meal disturbance of 20 mg/min is introduced at 10 min and it takes over 100 mins to stabalize to a steady state value. This shows that the model has a slow response to the meal disturbances.

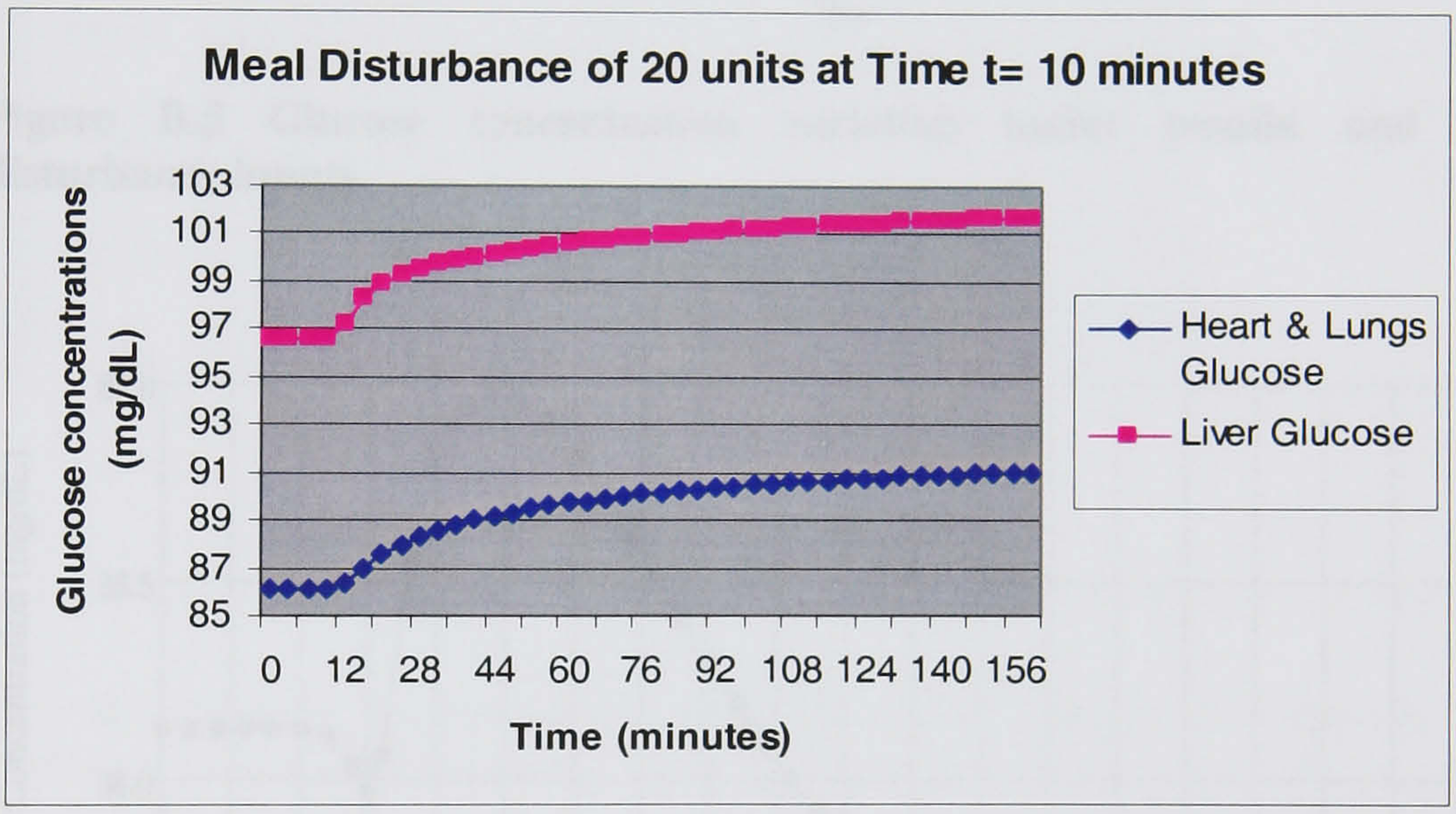


Figure B.4 Liver and heart and lungs glucose concentrations under meal disturbance

Figure B.5 depicts the glucose concentration variation in the heart and lungs compartment when the patient is subjected to a step change of 1 mU/min of insulin infusion rate from the nominal value at 10 min and 20 mg/min of glucose at 40 min. It is observed that very small variations in the glucose concentration take place. Similarly a number of similar simulations were carried out and two cases are shown in Figures B.6 and B.7. Figure B.6 depicts the case when an insulin infusion rate is increased by a step of 1.3 mU/min at 10 min and a glucose step change of 40 mg/min is induced at 30 min.

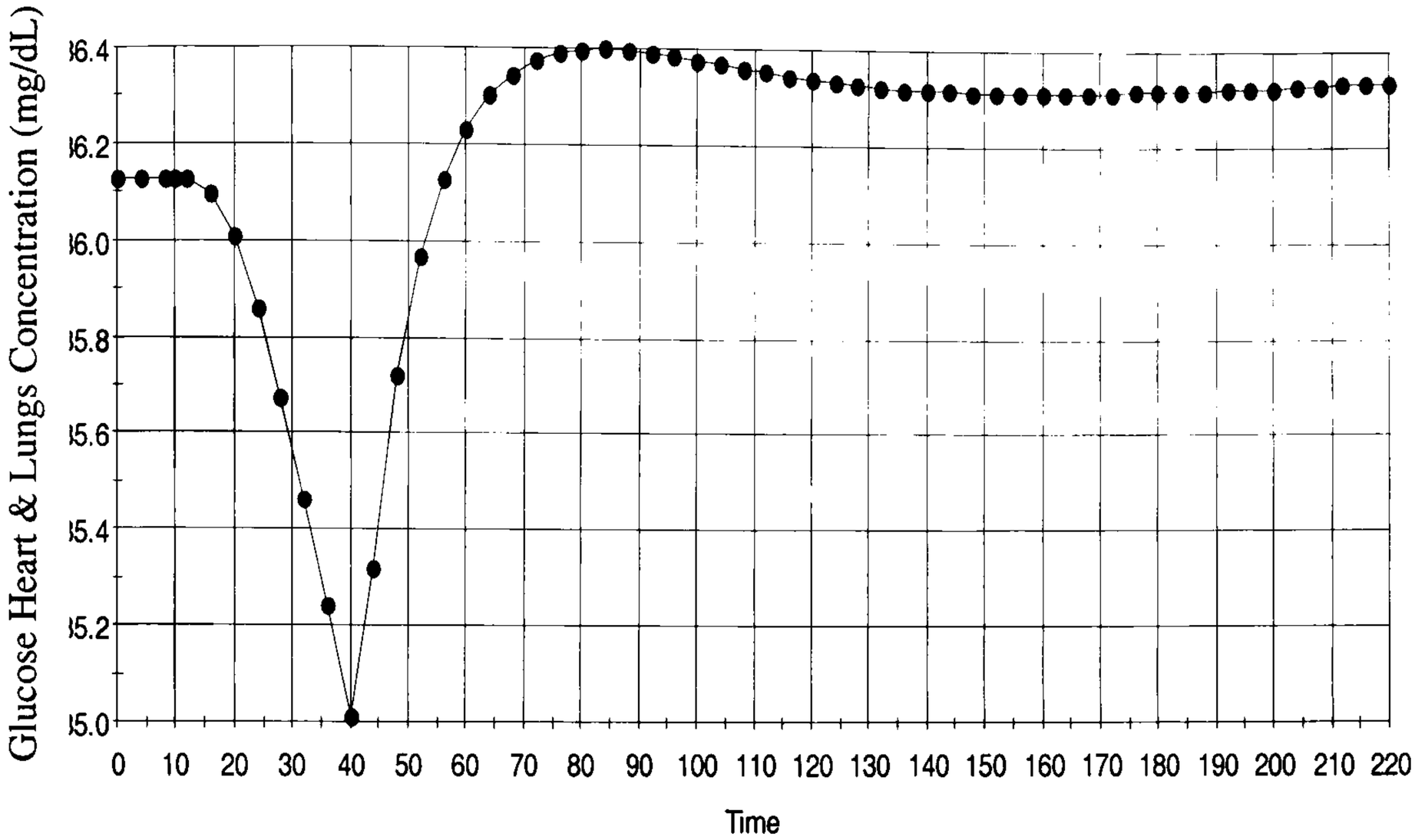


Figure B.5 Glucose concentration variation under insulin and meal disturbance inputs

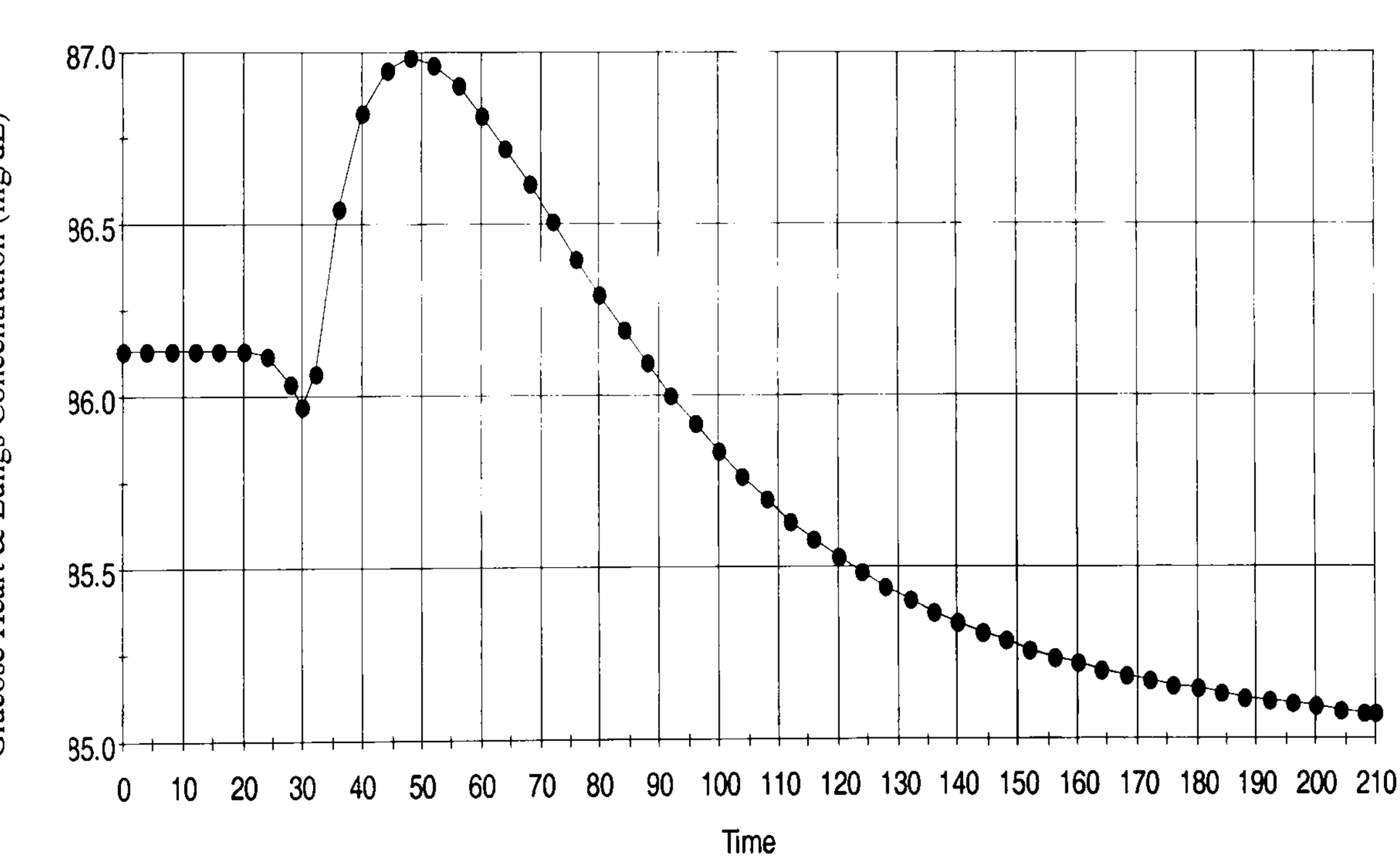


Figure B.6 Glucose concentration variation for insulin unit step change after 10 minutes and 20 units glucose step change after 40 minutes

An analysis for various time gaps between insulin and the glucose step changes is shown in Figure B.7. For a time gap of 6 minutes, the glucose concentration has the highest peak of approximately 87.6 mg/dL at time around 50 min. In comparison, a longer time gap of 14 minutes gives has the smallest peak of approximately 87.1 mg/dL at around 50 min.

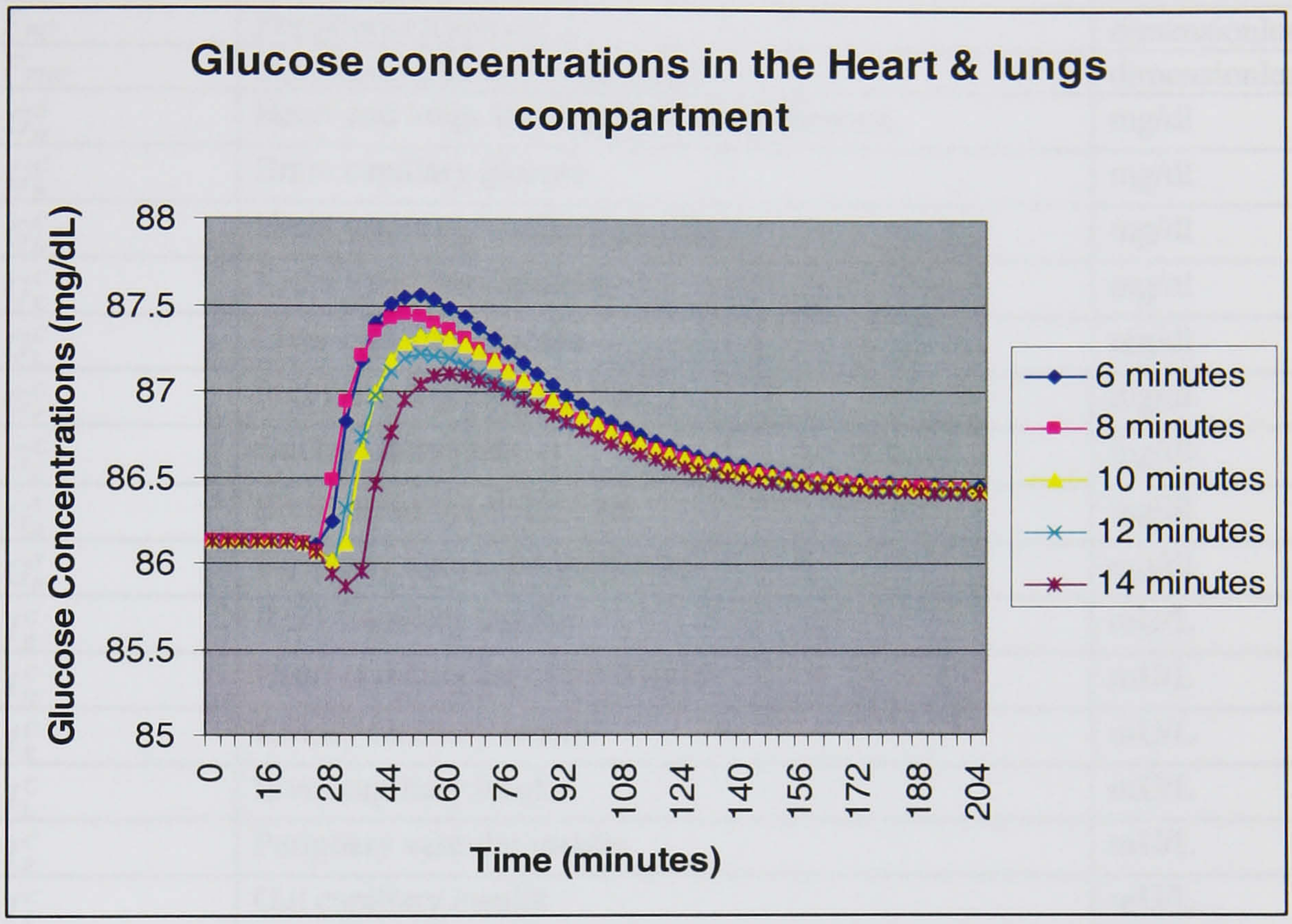


Figure B.7 Glucose concentration variation under insulin and glucose step disturbance at varying time gaps

Concluding Remarks

A detailed analysis of the physiological based compartmental model for people with type 1 diabetes was presented. The model consists of an insulin and glucose submodel where insulin and glucose are assumed to be transported by the blood leaving the compartment and the transport within the compartment, to the tissues, occurs via diffusion. Glucose concentration in the various organ compartments of the body, under meal and insulin inputs, was analyzed and found to be consistent with the physiology of the body. The dynamics of this model were however observed to be slower than the Bergman model discussed in chapter 3.

Table B.1 Nomenclature

Variable	Description	Units
A_{IHGP}	Insulin effect on hepatic glucose production	dimensionless
A_{IHGU}	Insulin effect on HGU	dimensionless
A_{NHGP}	Glucagon effect on hepatic glucose production	dimensionless
F_{LC}	Liver clearance	dimensionless
F_{KC}	Kidney clearance	dimensionless
F_{PC}	Periphery clearance	dimensionless
F_{PNC}	Pancreatic glucagons clearance	dimensionless
G_H^B	Heart and lungs Basal glucose concentration	mg/dl
G_B^C	Brain capillary glucose	mg/dl
G_H^C	Heart and lung capillary glucose	mg/dl
G_K^C	Kidney capillary glucose	mg/dl
G_L^C	Liver capillary glucose	mg/dl
G_P^C	Periphery capillary glucose	mg/dl
G_S^C	Gut capillary glucose	mg/dl
G_B^T	Brain tissue space glucose	mg/dl
G_P^T	Periphery tissue space glucose	mg/dl
I_B^C	Brain capillary insulin	mU/L
I_H^C	Heart and lung capillary insulin	mU/L
I_K^C	Kidney capillary insulin	mU/L
I_L^C	Liver capillary insulin	mU/L
I_P^C	Periphery vascular insulin	mU/L
I_S^C	Gut capillary insulin	mU/L
I_P^T	Periphery tissue space insulin	mU/L
N	Glucagon Concentration	dimensionless
q_A	Hepatic artery vascular blood flowrate	dL/min
q_B	Brain vascular blood flowrate	dL/min
q_H	Heart and lung capillary vascular blood flowrate	dL/min
q_K	Kidney vascular blood flowrate	dL/min
q_L	Liver vascular blood flowrate	dL/min
q_P	Periphery vascular blood flowrate	dL/min
q_S	Gut vascular blood flowrate	dL/min
T_B	Brain transcapillary diffusion time constant	min
T_P^G	Periphery glucose transcapillary diffusion time constant	min
T_P^I	Periphery insulin transcapillary diffusion time constant	min
v_B^C	Brain tissue space volume	dL
v_H^C	Heart and lung capillary volume	dL
v_K^C	Kidney capillary volume	dL
v_L^C	Liver capillary volume	dL
v_P^C	Periphery capillary volume	dL

v_S^C	Gut capillary volume	dL
v_B^T	Brain tissue space volume	dL
v_P^T	Periphery tissue space volume	dL
W_B^C	Brain capillary volume	L
W_H^C	Heart capillary volume	L
W_S^C	Gut capillary volume	L
W_L^C	Liver capillary volume	L
W_K^C	Kidney capillary volume	L
W_P^C	Periphery capillary volume	L
W_P^T	Periphery tissue space volume	L
W_N	Glucagon volume	L
X_A	Hepatic artery vascular plasma flowrate	L/min
X_B	Brain vascular plasma flowrate	L/min
X_H	Heart and lungs capillary insulin	L/min
X_K	Kidney vascular plasma flowrate	L/min
X_L	Liver vascular plasma flowrate	L/min
X_P	Periphery vascular plasma flowrate	L/min
X_S	Gut vascular plasma flowrate	L/min
Γ_{BU}	Brain uptake	mg/min
Γ_{HGP}	Hepatic glucose production	mg/min
Γ_{HGU}	Hepatic glucose uptake	mg/min
Γ_i	Metabolic source and sink terms of component	mg/min
Γ_{IVI}	Intravenous insulin infusion	mU/min
Γ_{KC}	Kidney Clearance	mU/min
Γ_{KE}	Kidney excretion	mg/min
Γ_{LC}	Liver clearance	mU/min
Γ_{MEAL}	Meal uptake	mg/min
Γ_{PC}	Peripheral Clearance	mU/min
Γ_{PGU}	Periphery glucose uptake	mg/min
Γ_{PIR}	Pancreatic insulin release	mU/min
Γ_{PIR}^B	Basal Pancreatic insulin release rate	mU/min
Γ_{PNR}	Pancreatic glucagons release	μg/min
Γ_{RBCU}	Red blood cell uptake	mg/min
Γ_{SIA}	Insulin absorption into blood stream from subcutaneous depot	mU/min
Γ_{SU}	Gut uptake	mg/min

Appendix C

Pilot Plant PARSEX Reactor

The aim of the work reported in this appendix is to demonstrate on a pilot-plant-scale partially simulated exothermic reactor the implementation and performance of the recently developed parametric controllers. A first-principles model of the process is used and then the parametric controller for the plant model is derived. The controller is given by a set of piecewise affine functions of the manipulating variables, the reactor input flow and cooling jacket temperature, in terms of the controlled variables, the temperature and concentration of the reactor. These affine functions are stored on a microchip and also on a computer, which is interfaced to the plant using PARAGON, 5.3. The on-line model-based control therefore reduces to simple affine function evaluations.

C.1 Introduction

Most of the real process systems are nonlinear and require sophisticated control techniques to ensure their safety and derive adequate economic performance. Continuously Stirred Tank Reactor (CSTR) is one such example that is not only nonlinear but may also have multiple steady states in the presence of exothermic reactions.

A pilot plant, PARSEX (PARtially Simulated Exothermic) reactor (Figure C.1) at Imperial College London, has been devised for testing the performances of control algorithms (Kittisupakorn, 1995; Pinheiro and Kershenbaum, 1999). A schematic diagram of this plant is shown in Figure C.2.

This plant consists of two main units: (i) a continuous well-stirred tank reactor of approximate volume 0.1 m^3 and (ii) a cooler with approximately 0.7 m^2 of heat transfer area. The reactor is charged with water and fed continuously with additional water; this represents the process stream in this PARSEX system. Fresh feed to the reactor is pumped from the feed tank via pump M12 at a measured and controlled flowrate through the valve V1. Heat from the process stream is exchanged with the cooling medium by recirculating the reactor contents through the external cooler via pump M6. The cooler is provided with efficient recirculation of cooling water by the pump M10 and fresh make-up water can be added. The temperature of the reactor, T14, is regulated by adjusting the cooling water temperature, T12.

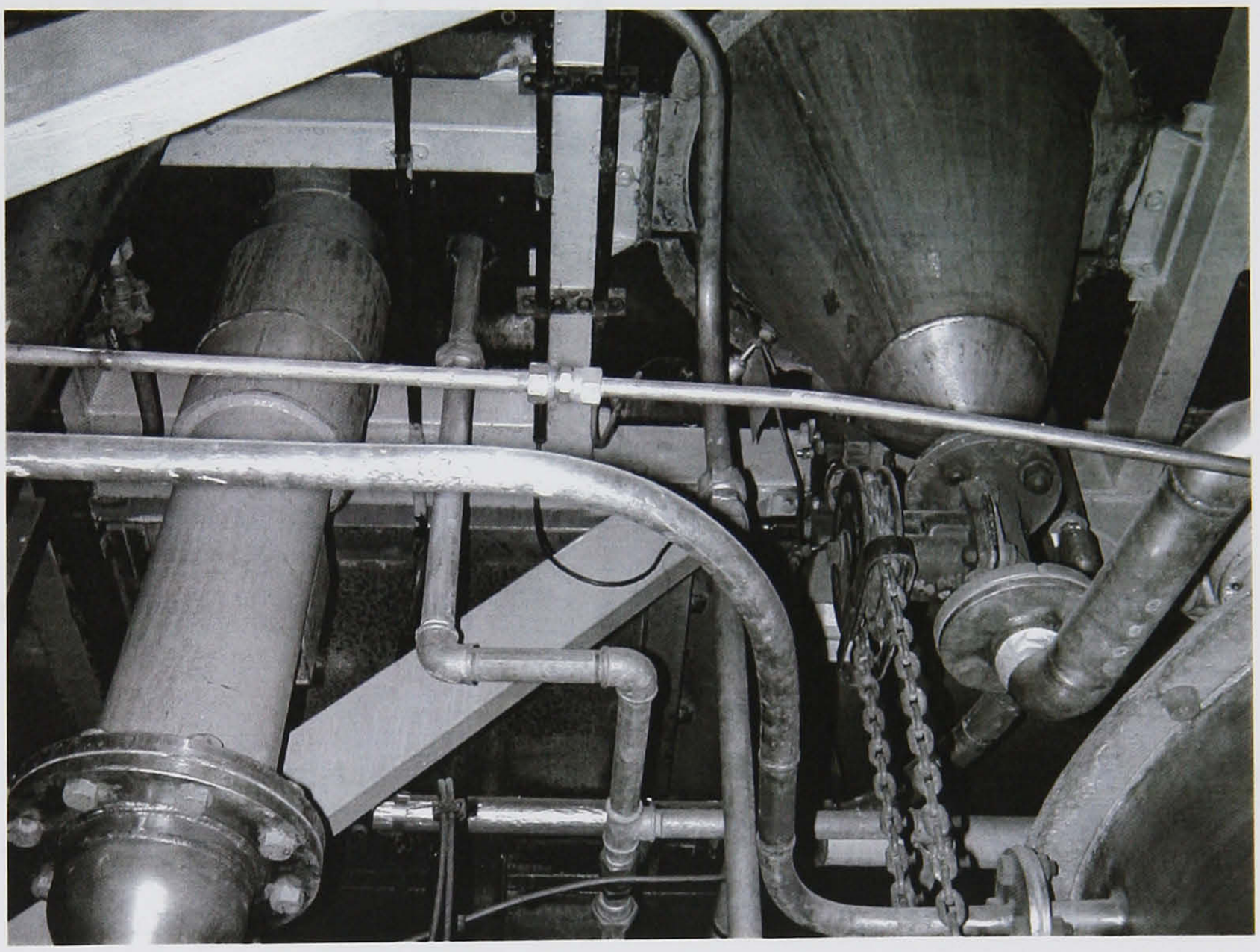


Figure C.1 Pilot Plant PARSEX Reactor

This cooling water temperature is controlled by the addition of fresh make-up cooling water through the control valve V5. No real reaction takes place in the system. The rate of heat evolution by chemical reaction is *simulated* by sparging live steam into the reactor, which is controlled by valve V3. Highly exothermic reactions can be experimentally simulated quite realistically in this setup by sparging the steam

equivalent to the heat generated by reaction, Q_r. The startup and shutdown procedure for the PARSEX reactor are given in Table C.1.

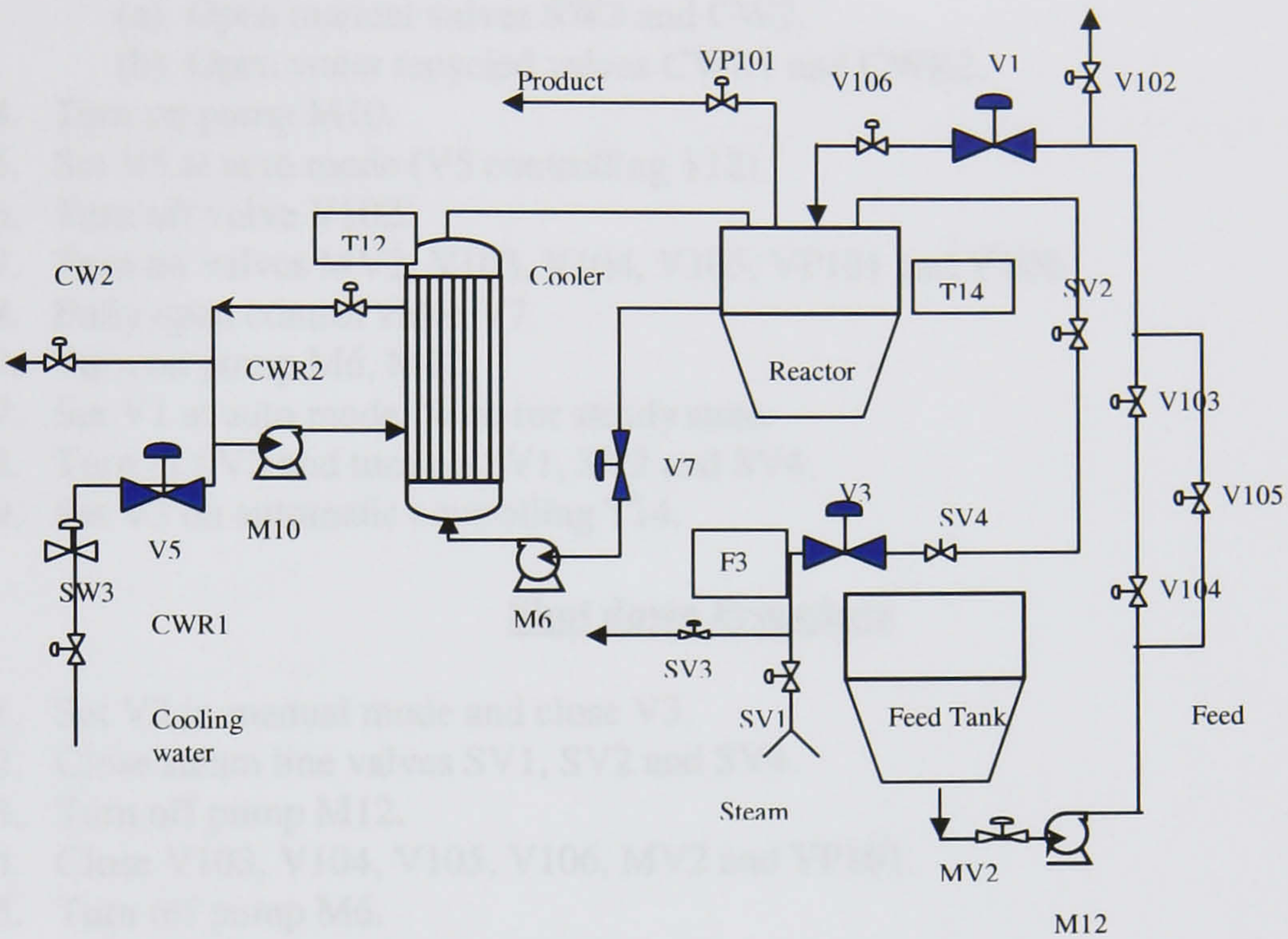


Figure C.2 Schematic diagram of the PARSEX reactor

The mathematical model of the PARSEX reactor, derived based on the first principles, is given below (Kittisupakorn, 1995):

$$\frac{dC_a}{dt} = -R_1 + \frac{F}{V_r}\left(C_{a0} - C_a\right) \tag{C.1}$$

$$\frac{dT_r}{dt} = \frac{Q_r}{\rho_r C_{pr} V_r} + \frac{F}{V_r}\left(T_f - T_r\right) + \frac{U_r A_r \left(T_j - T_r\right)}{\rho_r C_{pr} V_r} \tag{C.2}$$

$$\frac{dT_j}{dt} = \frac{F_j}{V_j}\left(T_{cw} - T_j\right) - \frac{U_r A_r \left(T_j - T_r\right)}{\rho_j C_{pj} V_j} \tag{C.3}$$

Table C.1 Startup and Shutdown Procedure

Start up Procedure

1. Fill water in the feed tank.
2. Close control valves V3 and V5.
3. Open cooling water loop.
   (a) Open manual valves SW3 and CW2.
   (b) Open water recycled valves CWR1 and CWR2.
4. Turn on pump M10.
5. Set V5 at auto mode (V5 controlling T12).
6. Turn off valve V102.
7. Turn on valves MV2, V103, V104, V105, VP101 and V106.
8. Fully open control valve V7.
9. Turn on pump M6, M12.
7. Set V1 at auto mode. Wait for steady state.
8. Turn of SV3 and turn on SV1, SV2 and SV4.
9. Set V3 on automatic controlling T14.

Shut down Procedure

1. Set V3 in manual mode and close V3.
2. Close steam line valves SV1, SV2 and SV4.
3. Turn off pump M12.
4. Close V103, V104, V105, V106, MV2 and VP101.
5. Turn off pump M6.
6. Close V7.
7. Set V5 in manual mode.
8. Turn off M10 and close V5.
9. Close SW3, CW2, CWR1 and CWR2.

---

where,

$$R_1 = k_0 \exp\left(\frac{-E}{RT_r}\right) C_a$$

$$Q_r = (-\Delta H) R_1 V_r$$

C_a is the concentration of the reactant, kmol/m^3

C_{a0} is the nominal feed concentration, kmol/m^3

T_r is the reactor temperature, K,

T_j is the jacket temperature, K,

T_{cw} is the cooling water temperature, K,

T_f is the feed temperature, K,

F is the feed flowrate, m^3/min,

F_j is the jacket flowrate, m^3/min.

The states in this model are: C_a and Tr. The jacket dynamics are fast enough to assume steady state behaviour in the jacket heat exchanger, i.e.

$$\frac{dT_j}{dt} = 0$$

The manipulating variable is T_j and the disturbance is F. For the current experimental setup, the model parameters considered are:

$U_r = 68.0$ kcal/(min.m^2 °C)

$A_r = 0.7$ m^2

$C_{pr} = C_{pj} = 1.0$ kcal /kg°C

$\rho_r = \rho_j = 1000$ kg/m^3

$k_0 = 3.43568\times10^6$ min^{-1}

$E/R = 6215.7$ K^{-1}

$V_r = 0.24$ m^3

$V_j = 0.012$ m^3

$T_{cw} = 293.15$ K

$\Delta H = 8000$ kcal/kmol and

$C_{a0} = 31.29$ kmol/m^3.

C.2 Derivation of the Explicit Model Based Control Law

This model is linearized about the steady-state values of $T_r = 318.15$, $C_a = 12.5$, and $T_j = 313.15$ to obtain a discrete state space representation.

$$\begin{cases} x_{t+1} = Ax_t + Bu_t + B_d d_t \\ y_t = Cx_t \end{cases} \tag{C.4}$$

subject to the following constraints:

$$\begin{aligned} y_{\min} \le y_t \le y_{\max} \\ u_{\min} \le u_t \le u_{\max} \end{aligned} \tag{C.5}$$

where $x_t \in R^n$, $u_t \in R^m$, and $y_t \in R^p$ are the state, input and output vectors respectively at time t, subscripts *min* and *max* denote lower and upper bounds respectively. The state variables, x_t, correspond to $(C_a - 12.5)$ and $(T_r - 318.15)$ and input variable, u_t correspond to the manipulating variable T_j. The output variable y_t represents the measured variables T_r and C_a and d_t represents the input disturbance which is feed flow rate F. The sampling time considered is 20 seconds. The discrete state-space matrices A, B, C and B_d are as follows:

$$A = \begin{bmatrix} 0.9937 & -0.0226 \\ 0.0036 & 0.9554 \end{bmatrix}$$

$$B = \begin{bmatrix} -0.0008 \\ 0.0647 \end{bmatrix}$$

$$C = \begin{bmatrix} 1 & 0 \\ 0 & 1 \end{bmatrix}$$

$$B_d = \begin{bmatrix} 0.0523 \\ -0.0060 \end{bmatrix}$$

C.3 Results

The parametric control law is derived for a prediction and control horizon of 10, consisting of 19 critical regions, i.e. by partitioning the space of state variables, in which a unique explicit expression in terms of state variables is defined. The critical regions are shown in Figure C.3. For example, region 2, is defined by the following state inequalities:

$$27.7161\ C_a - 0.05\ T_r \leq 399.937$$

$$-0.401913\ C_a - 9.83647\ T_r \leq -3130.55$$

$$-0.401913\ C_a \leq -4.02391$$

$$0.401913\ C_a + 9.83647\ T_r \leq 3152.6$$

while its associated control function for the first time interval $T_j(1)$ is given by:

$$T_j(1) = -0.443395C_a - 10.8517T_r + 3771.17$$

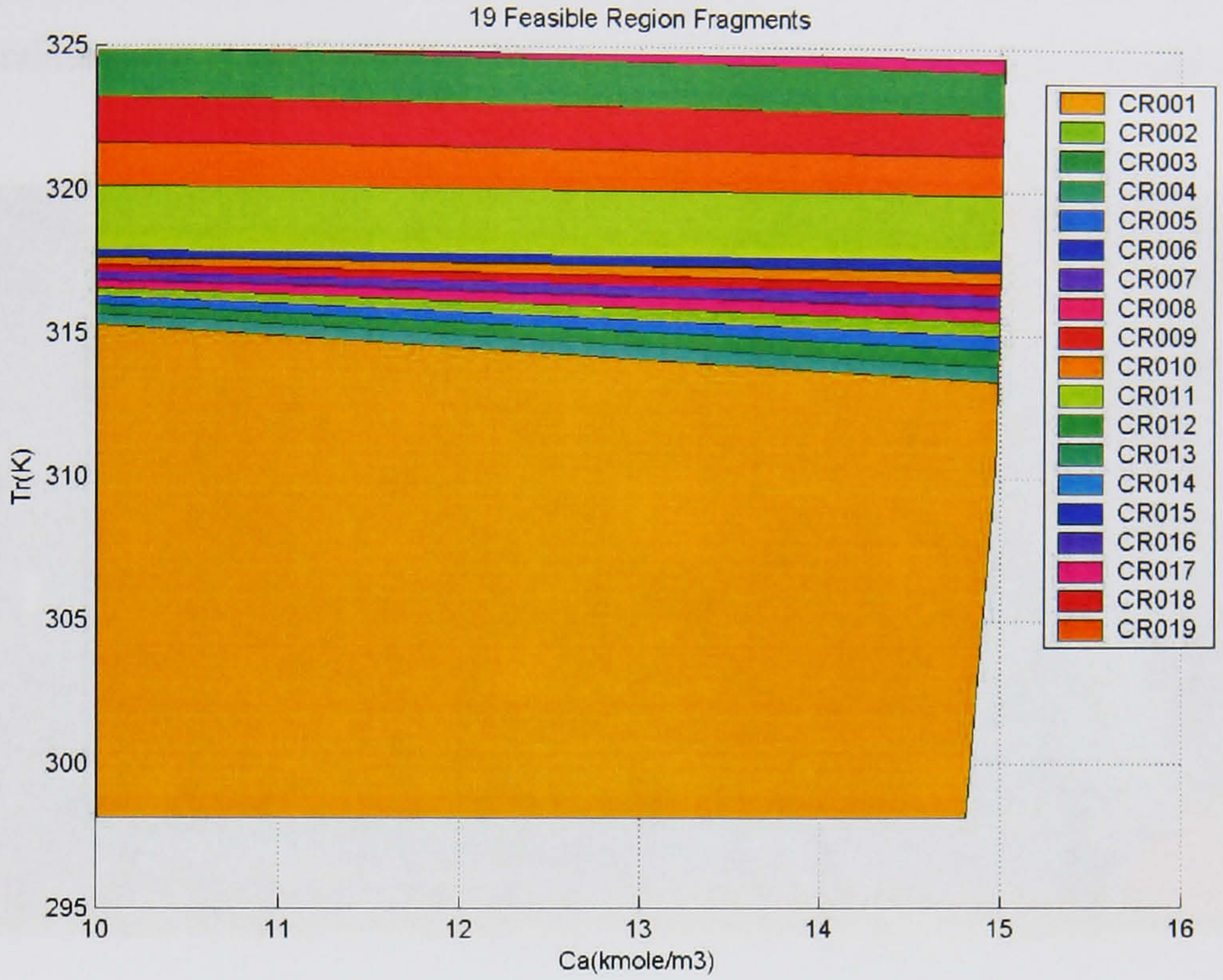


Figure C.3 Critical Regions stored on a microchip and also on a computer

C.4 Implementation of the Parametric Controller

These 19 control laws were stored on a FM-400 microchip (Figure C.4) and also on a computer, which is interfaced to the pilot plant using software PARAGON, 5.3 (Figure C.5). FM-400 has 512 K-bytes of Flash EEPROM and 512 K-bytes of static RAM; other specifications of FM-400 processor are available on www.cms.uk.com. The control law was executed by using the microchip and also by the computer containing the parametric controller. Similar controller performance for both the cases was observed and is shown in Figure C.6. The oscillations around the set point, T_r = 318.15 K (45°C), are observed due to the presence of disturbances and nonlinearity. As shown in Figure C.6, the parametric controller performs well and brings the state to the desired steady state set point starting from a non-steady state point. Note that the steady state and non-steady state values of 45°C and 51°C are derived based upon the model and the data given in Section C.1. Similarly, some other steady state and

non-steady state values for a different set of data have also been reported by Pinheiro and Kershenbaum (1999). The performance of PI controller is also shown. Note that the parametric controller incorporates the model of the plant and the system constraints and it is easy to implement on a simple software and hardware platform.

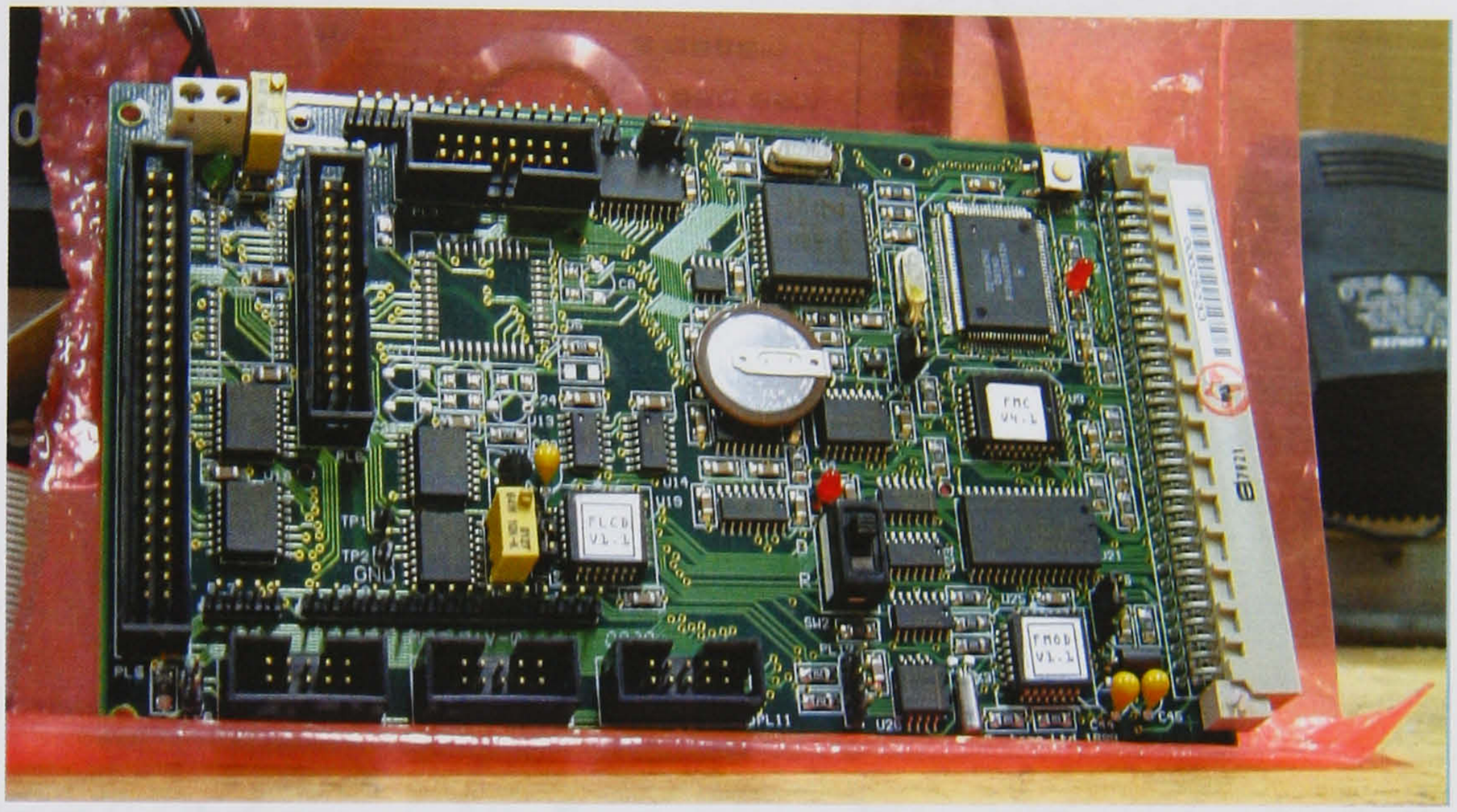


Figure C.4 The microchip containing the parametric controller

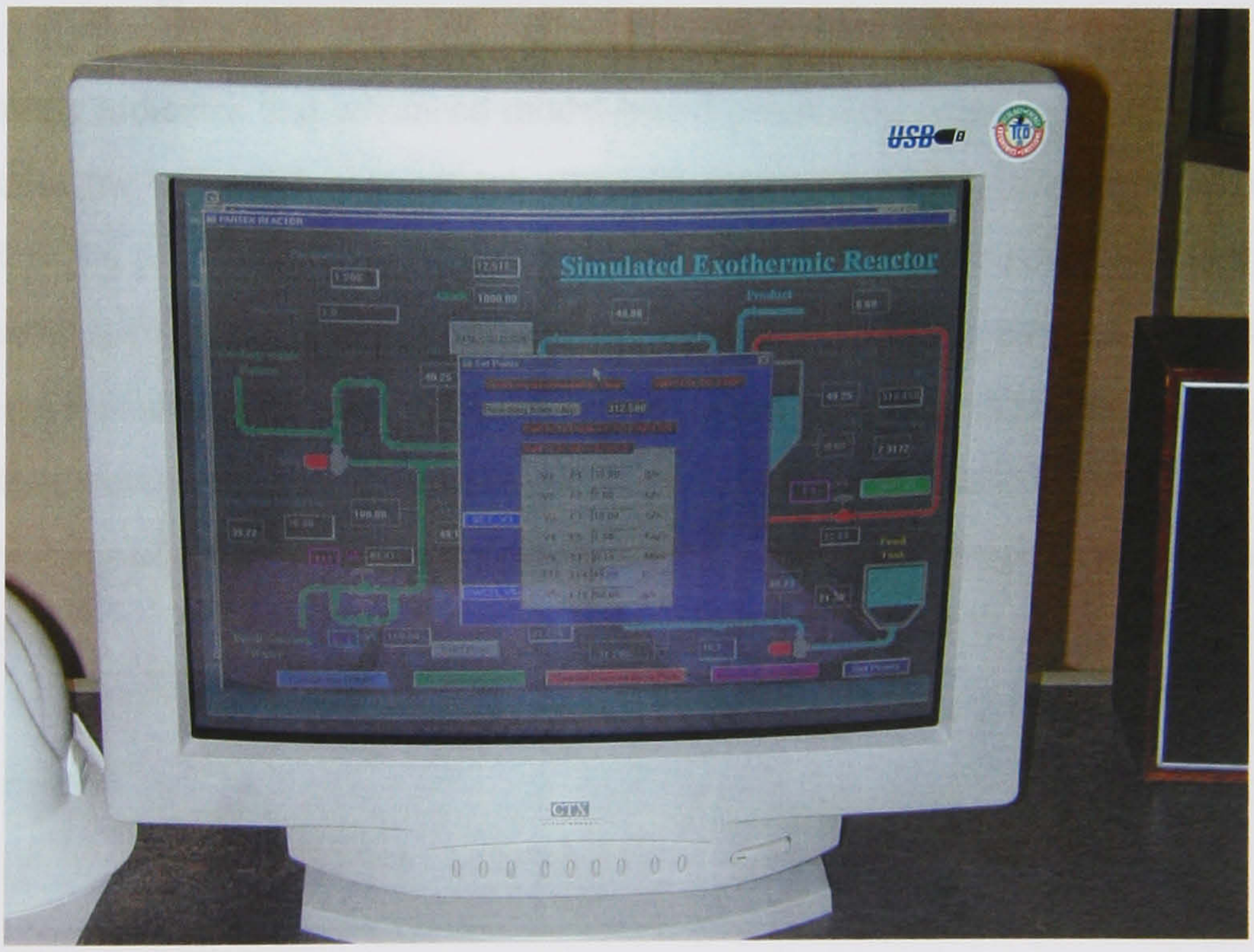


Figure C.5 Current Control Software

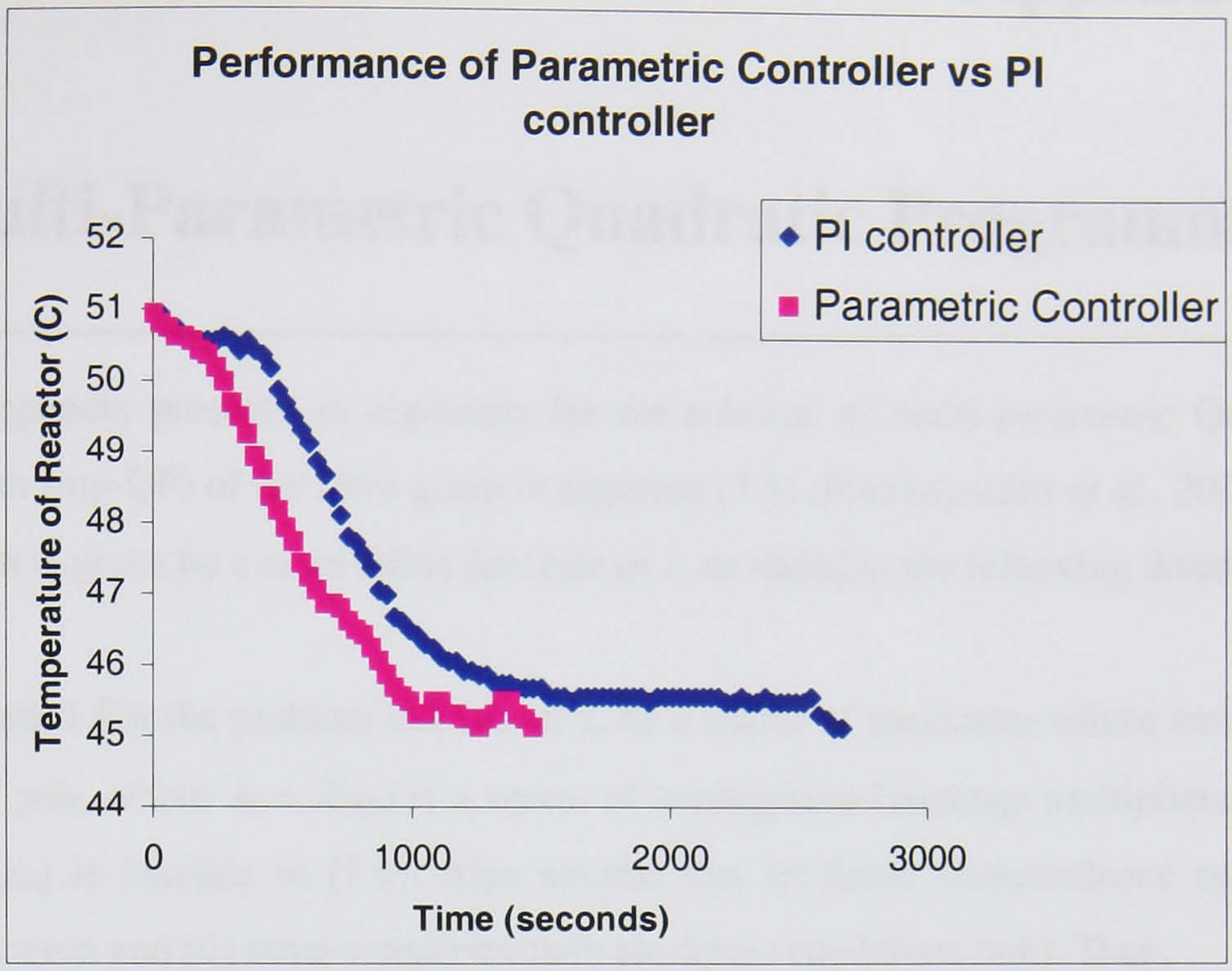


Figure C.6 Performance of the Parametric and PI Controller in the pilot plant

Concluding Remarks

This study indicates that advanced model-based parametric controllers are a profound candidate for industrial applications since (i) they incorporate in their structure the model of the plant and the system constraints and (ii) they can be easily implemented on simple software or a hardware platform. This testing of the parametric controller also provides a step towards extension of using these controllers for other applications including insulin delivery for people with type 1 diabetes, discussed in chapter 3 and 4 and delivery of anesthetics for people being operated under surgery, as discussed in chapter 5.

Appendix D

Multi-Parametric Quadratic Programming

This appendix presents an algorithm for the solution of multi-parametric Quadratic Program (mp-QP) of the form given in equation (3.6) (Pistikopoulos *et al.*, 2002). The solution is given by z as an affine function of x, as stated in the following theorem.

Theorem 1 For the problem in (3.6) let x_0 be a vector of parameter values and (z_0, λ_0) a KKT pair, where $\lambda_0 = \lambda(x_0)$ is a vector of nonnegative Lagrange multipliers, λ, and $z_0 = z(x_0)$ is feasible in (3.6). Also assume that (i) linear independence constraint qualification and (ii) strict complementary slackness conditions hold. Then,

$$\begin{bmatrix} z(x) \\ \lambda(x) \end{bmatrix} = -(M_0)^{-1} N_0 (x - x_0) + \begin{bmatrix} z_0 \\ \lambda_0 \end{bmatrix} \tag{D.1}$$

where,

$$M_0 = \begin{pmatrix} H & G_1^T & \cdots & G_q^T \\ -\lambda_1 G_1 & -V_1 & & \\ \vdots & & \ddots & \\ -\lambda_p G_q & & & -V_q \end{pmatrix}$$

$$N_0 = \left(Y, \lambda_1 S_1, \cdots, \lambda_p S_p\right)^T$$

where G_i denotes the ith row of G, S_i denotes the ith row of S, $V_i = G_i z_0 - W_i - S_i x_0$, W_i denotes the ith row of W and Y is a null matrix of dimension $(s \times n)$.

See Pistikopoulos *et al.* (2002) for the proof. The space of x where this solution, (D.1) remains optimal is defined as the Critical Region (CR^0) and can be obtained as follows. Let CR^R represent the set of inequalities obtained (i) by substituting $z(x)$ into the inequalities in (3.6) and (ii) from the positivity of the Lagrange multipliers, as follows:

$$CR^R = \{Gz(x) \leq W + Sx(t), \lambda(x) \geq 0\}, \tag{D.2}$$

then CR^0 is obtained by removing the redundant constraints from CR^R as follows:

$$CR^0 = \Delta\{CR^R\}, \tag{D.3}$$

where Δ is an operator which removes the redundant constraints – for a procedure to identify the redundant constraints, see Gal (1995). Since for a given space of state-variables, X, so far we have characterized only a subset of X i.e. $CR^0 \subseteq X$, in the next step the rest of the region CR^{rest} , is obtained as follows (Pistikopoulos et al., 2002):

$$CR^{rest} = X - CR^0. \tag{D.4}$$

The above steps, (D.1 – D.4) are repeated and a set of $z(x)$, $\lambda(x)$ and corresponding CR^0s is obtained. The solution procedure terminates when no more regions can be obtained, i.e. when $CR^{rest} = \varnothing$. For the regions which have the same solution and can be unified to give a convex region, such a unification is performed and a compact representation is obtained. The continuity and convexity properties of the optimal solution are summarized in the next theorem.

Theorem 2 For the mp-QP problem, (3.6) the set of feasible parameters $X_f \subseteq X$ is convex, the optimal solution, $z(x) : X_f \mapsto R^S$ is continuous, convex and piecewise quadratic.

See Pistikopoulos *et al.* (2002) for the proof. Based upon the above theoretical developments, an algorithm for the solution of an mp-QP of the form given in (3.6) to calculate U as an affine function of x and characterize X by a set of polyhedral regions, CRs, has been developed which is summarized in Table D.1.

Table D.1 Solution Steps of the mp-QP Algorithm

Step 1	For a given space of x solve (3.6) by treating x as a free variable and obtain $[x_0]$.
Step 2	In (3.6) fix $x = x_0$ and solve (3.6) to obtain $[z_0 , \lambda_0]$.
Step 3	Obtain $[z(x), \lambda(x)]$ from (D.1).
Step 4	Define CR^R as given in (D.2).
Step 5	From CR^R remove redundant inequalities and define the region of optimality CR^0 as given in (D.3).
Step 6	Define the rest of the region, CR^{rest}, as given in (D.4)
Step 7	If no more regions to explore, go to the next step, otherwise go to Step 1.
Step 8	Collect all the solutions and unify a convex combination of the regions having the same solution to obtain a compact representation.

Appendix E

Multiparametric Mixed-Integer Linear Programming

This appendix presents an algorithm for the solution of multiparametric Mixed Integer Linear Programs (mp-MILP) of the following form (Dua and Pistikopoulos, 2000):

$$\begin{aligned} & J\left(x(t)\right) = \min_{\pi_c, \pi_d} \phi_1^T \pi_c + \phi_2^T \pi_d \\ \text{s.t.} \quad & G_c \pi_c + G_d \pi_d \le S + Fx(t) \end{aligned} \tag{E.1}$$

where ϕ_1 and ϕ_2 are constant vectors, π_c and π_d are continuous and discrete variables respectively and G_c, G_d, S and F are constant vectors and matrices of appropriate dimension.

An initial feasible π_d is obtained by solving the following MILP:

$$\begin{aligned} & \min_{\pi_c, \pi_d, x(t)} \phi_1^T \pi_c + \phi_2^T \pi_d \\ \text{s.t.} \quad & G_c \pi_c + G_d \pi_d \le S + Fx(t) \end{aligned} \tag{E.2}$$

where $x(t)$ is treated as a vector of free variable to find a starting feasible integer solution. Let the solution of (E.2) be given by $\pi_d = \bar{\pi}_d$.

Fix $\pi_d = \bar{\pi}_d$ in (E.1) to obtain a multiparametric LP problem of the following form:

$$\begin{aligned} & \hat{J}\left(x(t)\right) = \min_{\pi_c} \phi_1^T \pi_c + \phi_2^T \pi_d \\ \text{s.t.} \quad & G_c \pi_c + G_d \bar{\pi}_d \le S + Fx(t) \end{aligned} \tag{E.3}$$

The solution of the multiparametric LP (Gal, 1995) subproblem in (E.3) which represents a parametric upper bound on the final solution is given by (i) a set of parametric profiles, $\hat{J}(x(t))^i$, and the corresponding critical regions, CR^i, and (ii) a set of infeasible regions where $\hat{J}(x(t))^i = \infty$.

For each critical region, CR^i, obtained from the solution of the multiparametric LP subproblem in (E.3), an MILP subproblem is formulated as follows:

$$\begin{aligned} & \min_{\pi_c, \pi_d, x(t)} \phi_1^T \pi_c + \phi_2^T \pi_d \\ \text{s.t.} \quad & G_c \pi_c + G_d \pi_d \le S + Fx(t) \\ & \phi_1^{\mathrm{T}} \pi_c + \phi_2^{\mathrm{T}} \pi_d \le \hat{J}(x(t))^i \\ & \pi_d \ne \overline{\pi}_d \\ & x \in CR^i \end{aligned} \tag{E.4}$$

The integer solution, $\pi_d = \overline{\pi}_d^{\,1}$, and the corresponding *CR*s, obtained from the solution of (E.4), are then recycled back to the multiparametric LP subproblem – to obtain another set of parametric profiles. Note that the integer cut, $\pi_d \ne \overline{\pi}_d$, and the parametric cut, $\phi_1^{\mathrm{T}} \pi_c + \phi_2^{\mathrm{T}} \pi_d \le \hat{J}(x(t))^i$, are accumulated at every iteration.

If there is no feasible solution to the MILP subproblem (E.4) in a CR^i, that region is excluded from further consideration and the current upper bound in that region represents the final solution.

The set of parametric solutions corresponding to an integer solution, $\pi_d = \overline{\pi}_d$, which represents the current upper bound are then compared to the parametric solutions corresponding to another integer solution, $\pi_d = \overline{\pi}_d^{\,1}$, in the corresponding *CR*s in order to obtain the lower of the two parametric solutions and update the upper bound. This is achieved by using the procedure by Acevedo and Pistikopoulos (1997). Based upon the above theoretical developments, the steps of the algorithm are stated in Table E.1.

Table E.1 Solution Steps of the mp-MILP Algorithm

Step 0	Initialization: Define an initial region of $x(t)$, CR, with best upper bound $\hat{J}^*(x(t)) = \infty$, and an integer solution $\overline{\pi}_d$.
Step 1	Multiparametric LP Problem: For each region with a new integer solution, $\overline{\pi}_d$: (a) Solve multiparametric LP subproblem (E.3) to obtain a set of parametric upper bounds $\hat{J}(x(t))$ and corresponding critical regions, CR. (b) If $\hat{J}(x(t)) \le \hat{J}^*(x(t))$ for some region of $x(t)$, update the best upper bound function, $\hat{J}^*(x(t))$, and the corresponding integer solutions, $\overline{\pi}_d^*$. (c) If an infeasibility is found in some region CR, go to Step 2.
Step 2	Master Subproblem: For each region CR, formulate and solve MILP master problem in (E.4) by (i) treating $x(t)$ as a variable bounded in the region CR, (ii) introducing an integer cut, $\pi_d \neq \overline{\pi}_d$, and (iii) introducing a parametric cut, $\phi_1^{\mathrm{T}}\pi_c + \phi_2^{\mathrm{T}}\pi_d \le \hat{J}(x(t))^i$. Return to Step 1 with new integer solutions and corresponding CRs.
Step 3	Convergence: The algorithm terminates in a region where the solution of the MILP subproblem is infeasible. The final solution is given by the current upper bounds $\hat{J}^*(x(t))$ in the corresponding CRs. The $\pi_c(x(t))$ and $\pi_d(x(t))$ corresponding to $\hat{J}^*(x(t))$ are then used to obtain $u(x(t))$.